Haemophilus influenzae survival and biofilm formation in a complex physical, chemical and multi-species environment

Alexandra Tikhomirova

(B.Sc. (Biomedical Science) Hons.)

A thesis submitted in the fulfillment of the requirements for the degree of Doctor of Philosophy from the University of Adelaide

(May, 2016)

Discipline of Microbiology and Immunology
Faculty of Science

School of Biological Sciences

The University of Adelaide

Adelaide, South Australia, Australia

Table of Contents

Declaration

This work contains no material which has been accepted for the award of any other degree or diploma in any university or other tertiary institution to **Alexandra Tikhomirova** and, to the best of my knowledge and belief, no material previously published or written by another person, except where due reference has been made in the text.

I give consent to this copy of my thesis, when deposited in the University Library, being made available for loan and photocopying, subject to provisions of the Copyright Act 1968.

I also give permission for the digital version of my thesis to be made available on the web, via the University's digital research repository, the Library catalogue, the Australasian Digital Theses Program (ADTP) and also through web search engines, unless permission has been granted by the University to restrict access for a period of time.

Alexandra Tikhomirova,

Adelaide, May, 2016.

Acknowledgements

Most importantly, I would like to thank my supervisor, Dr. Stephen Kidd, for his support throughout the past 4 years, for his inspirational and creative approach to science, his advice and guidance, and consistent confidence, both in me, and in a project which seemed so difficult to accomplish. I would like to also thank him also for introducing me to the world of microbiology, and being a life-long inspiration in this area.

Secondly, I would like to thank my co-supervisor Prof. James Paton for his assistance, with the project – a contribution without which it could not be accomplished.

I would also like to thank Dr. Peter Zilm for his help with assembling and manufacturing the flow cell apparatus, and for his timely advice related to methodologies and practical approaches to technical issues.

I am also very grateful to Long Bui, for being a great friend in the lab and always helping out when problems arose, to Donald Jiang, for helping out in the beginning stages of the project, and to all the past lab members for their assistance, company and friendship: Nadiah Ishak, Gregory Sequeira, Tamara Alhamami, and DeeKang Ren.

I would also like to express my gratitude to all research officers in James Paton's Lab, Renato's Lab and Chris's Lab: firstly to Dr. Claudia Trappetti for her enormous help in the most difficult times, and to Dr. Lauren McAllister for her vast knowledge and help with the most difficult aspects of bioinformatics and the many technical issues arising in this, as well as Dr. Adam Potter, Dr. David Ogunniyi, Dr. Layla Mahdi, Dr. Richard Harvey, Dr. Alistair Standish, Dr. Elizabeth Tran, Dr. Miranda Ween and my lab friends Pratiti Nath, Mabel Lum, Min Teh, Broke Herdman, Zarina Amin, and Victoria Lewis who were always very nice to work alongside and willing to share their experiences.

I would also like to acknowledge the Channel 7 Children's Research Foundation for providing extensive support, which made it possible to expand this project and perform deeper investigations than would otherwise have been possible.

Lastly, I would like to thank my family, my friends and those closest to me, for always being there.

Abstract

H. influenzae is an opportunistic human pathogen capable of occupying a range of niches in the respiratory tract. Both during health and disease processes, *H. influenzae* must adapt to the conditions present in the microniches it encounters and correspondingly alter its lifestyle in the presence of non-optimal conditions. The niches encountered by *H. influenzae* in the human host include the presence of chemical stress such as ROS and RCS compounds, as well as a diverse range of pH conditions ranging from pH 7-9, and the presence of other members of the microflora, such as *Streptococcus pneumoniae*.

In this thesis, we have identified that there are strain-specific components related to the adaptation of *H. influenzae* to specific conditions. We have identified that different *H. influenzae* isolates employ different mechanisms to adapt to the presence of diverse, and often stress-inducing conditions. One adaptation mechanisms employed by *H. influenzae* is the adoption of a sessile biofilm lifestyle. We have shown that there is a strain-specific response of *H. influenzae* isolates in their biofilm formation to the presence of different nutrient conditions, and to the presence of ROS and RCS such as formaldehyde, methylglyoxal and H_2O_2. We have also shown that in different nutrient conditions, there is a different requirement for eDNA in the EPS matrix of individual strains.

In addition, we have identified a role of the nickel import system *nikKLMQO-nimR* of *H. influenzae* in its biofilm formation. We have shown that when this system is absent, or when *H. influenzae* is in a nickel limited environment, the *H. influenzae* cells display an increased biofilm formation. This biofilm formation response was accompanied by a global transcriptomics response, which displayed global changes in metabolic pathways.

Further to these findings, we have shown that there are strain-specific differences in *H. influenzae* adaptation to different pH conditions. These differences were expressed both as differences in biofilm formation, and differences on the transcriptomics level.

Another significant finding was that the pH played an important role in the inter-species interactions of *H. influenzae* and *S. pneumoniae*. In a batch culture system in stationary phase at a lower initial pH of 7.4, *S. pneumoniae* was able to convert *H. influenzae* into a VBNC

state. However, *H. influenzae* was able to survive in a culturable state in co-culture in log phase, or when a higher initital pH was used. We have also shown that in co-culture, there were significant transcriptomics changes both in *H. influenzae* and *S. pneumoniae*, including an induction of stress response genes in *H. influenzae*, and a down-regulation of sugar utilisation genes in *S. pneumoniae*.

Importantly, we have shown that in a continuous flow cell system, *H. influenzae* and *S. pneumoniae* exist in a different lifestyle and different transcriptomics profile than in a batch culture system, both in mono- and co-culture. In this system, the 2 species were able to co-exist without the reduction in culturability in either of the species. We have also shown that the transcriptomic profile in co-culture in a flow cell system is different to what was observed in the batch system, with one of the major findings being the up-regulation of sugar utilisation genes in *S. pneumoniae*, suggesting the potential metabolic relationship between *H. influenzae* and *S. pneumoniae*.

We have investigated this finding further, and have indeed demonstrated that nutrient availability and carbon source impact the *H. influenzae/ S. pneumoniae* interactions. In a flow cell system containing a nutrient-limited CDM media with glucose, *H. influenzae* was able to survive equally in mono- and co-culture. However, *S. pneumoniae* was unable to grow in mono-culture, and in co-culture displayed 3 phenotypes: a wild-type phenotype at 24 h, an undetectable state until 336 h, and a small colony variant state at 336 h. *S. pneumoniae* did not significantly impact the *H. influenzae* transcriptome in co-culture in either the undetected or SCV state, but did subtly modify the *H. influenzae* transcriptome upon transition to different time-points of growth, or different nutrient conditions. We have also preliminarily identified transcriptomic changes in *S. pneumoniae* at 64 h and 336 h, which correspond to a persister-cell like state observed in other bacterial species.

Overall, we have identified that environmental factors significantly impact the ability of *H. influenzae* to survive and to adopt lifestyles pertaining to these environments, in a strain-specific manner. We have shown that these adaptations are often accompanied by global transcriptomics changes. We have also identified that the inter-species interactions between *H. influenzae* and *S. pneumoniae* are highly complex and their outcome depends on a multitude of environmental conditions.

List of Publications

The work presented in this thesis has contributed to a range of publications listed below.

- **Tikhomirova A**, Kidd SP. The outcome of *Haemophilus influenzae* and *Streptococcus pneumoniae* inter-species interactions depends on pH, nutrient availability and growth phase. *International Journal of Medical Microbiology*. *In Press.*

- **Tikhomirova A**, Jiang D, Kidd SP. A new insight into the intracellular nickel levels for the stress response, surface properties and twitching motility by *Haemophilus influenzae*. 2015. *Metallomics*. 8:650-61.

- Ishak N, **Tikhomirova A**, Bent SJ, Ehrlich GD, Hu FZ, Kidd SP. There is a specific response to pH by isolates of *Haemophilus influenzae* and this has a direct influence on biofilm formation. 2014. *BMC Microbiology*. 14:47

- **Tikhomirova A**, Kidd SP. *Haemophilus influenzae* and *Streptococcus pneumoniae*: living together in a biofilm. 2013. *Pathogens and Disease*. 69:114-26

List of Abbreviations

CDM	chemically defined medium
CFU	colony forming unit
COM	chronic otitis media
COPD	chronic obstructive pulmonary disease
CV	crystal violet
DNA	deoxyribonucleic acid
eDNA	extracellular DNA
EPS	extracellular polymeric substance matrix
h	hour(s)
HI	heart infusion
H_2O_2	hydrogen peroxide
LB	Luria-Bertani
LOS	lipooligosaccharide
min	minute(s)
ml; µl	milliliter; microlitre
mRNA	messenger RNA
NET	neutrophil extracellular trap
NTHi	non-typeable *Haemophilus influenzae*
OD	optical density
OM	otitis media
PCR	polymerase chain reaction
RCS	Reactive Carbonyl Species

RNA	ribonucleic acid
ROS	Reactive Oxygen Species
RNASeq	RNA sequencing
rpm	revoloutions per minute
SCVs	small colony variants
SEM	scanning electron microscopy
Tfp	type IV (four) pili
VBNC	viable but non-culturable
v/v	volume/volume
WT	wild-type
w/v	weight/volume

List of Figures

Chapter 1

Chapter 3

Chapter 6

Appendix 1

Appendix 2

List of Tables

Chapter 1

Chapter 2

Chapter 3

Chapter 6

Title: *H. influenzae* survival and biofilm formation in a complex physical, chemical and multi-species environment

Chapter 1.

Background and Introduction

Overview

This Chapter presents the background and current knowledge of *H. influenzae* survival in a complex environment. This includes *H. influenzae* biofilm formation in chronic disease, and both environmental and genetic factors influencing this biofilm formation. *H. influenzae* growth and survival in a complex multi-species environment, in the context of the Gram-positive pathogen *S. pneumoniae* is also described. Current research investigating *H. influenzae/S. pneumoniae* multi-species biofilm information, as well as environmental and molecular factors influencing their biofilm formation and co-existence are explored.

1.1.1 *H. influenzae* exists in a complex multi-species environment.

Haemophilus influenzae is commensal bacterial species that inhabits the nasopharynx of healthy humans, and asymptomatic nasopharyngeal carriage in healthy children has been documented to range up to 80% for *H. influenzae* (LaCross *et al*.,2013). However, *H. influenzae* is not the only species to colonise the nasopharyngaeal niche; indeed it is often found to co-colonise this niche with other bacterial species, including *Streptococcus pneumoniae*, *Staphylococcus aureus* and *Moraxella catarrhalis*. One of the most common species known to co-colonise the nasopharyngaeal niche with *H. influenzae* is the Gram positive species *S. pneumoniae*. Asymptomatic nasopharyngaeal carriage for *S. pneumoniae* has been documented to be at least 20% (Bogaert *et al*., 2004). Despite this asymptomatic carriage, both bacterial species have the capacity to migrate from this anatomical niche and, in doing so, to cause various diseases. This includes transit to the bronchi to cause bronchitis (Bresser *et al*.,2000; Priftis *et al*., 2013), to the lungs to cause pneumonia (Berk *et al*., 1982; Weiss *et al*., 2004), to the middle ear to cause otitis media (OM; Hall-Stoodley *et al*., 2006), to the blood to cause septicaemia (Goetghebuer *et al*., 2000) and across the blood–brain barrier to cause meningitis (Goetghebuer *et al*., 2000). For *H. influenzae*, a vaccine exists against the encapsulated type b of *H. influenzae*, which had been the predominant cause of invasive diseases such as meningitis and septicaemia (Adam *et al*., 2010). Since the introduction of this vaccine, there has been a decline in invasive diseases caused by the vaccine type (Adams *et al*., 1993; Peltola, 2000; Leung *et al*., 2012; Georges *et al*., 2013). However, the other serotypes of encapsulated *H. influenzae* (a, c, d, e and f; Waggoner-Fountain *et al*., 1995; Urwin *et al*.,1996; Murphy *et al*., 1999; Adderson *et al*., 2001) as well as the multitude of nontypeable unencapsulated strains (also known as the **n**on**t**ypeable ***H****aemophilus* ***i****nfluenzae* or NTHi; Falla *et al*., 1993; Murphy *et al*., 1999) still pose a threat, particularly for the development of diseases of the respiratory tract such as OM (Ribeiro *et al*., 2003). Importantly, a majority of strains colonizing the paediatric nasopharynx consist of NTHi strains, carriage itself posing a high risk of development of respiratory tract infection due to these NTHi (Spinola *et al*., 1986).

There also exists a range of vaccines against some *S. pneumoniae* serotypes. The polysaccharide vaccine consists of purified polysaccharides from 23 serotypes of *S. pneumoniae* (specifically, 1, 2, 3, 4, 5, 6B, 7F, 8, 9N, 9V, 10A, 11A, 12F, 14, 15B, 17F, 18C, 19A, 19F, 20, 22F, 23F and 33F; Nuorti & Whitney, 2010) and does offer protection from pneumococcal bacteraemia and pneumonia in adults (Shapiro *et al*., 1991; Cornu *et al*., 2001; Melegaro & Edmunds, 2004). However, it is less immunogenic than the conjugate 7- or 13-valent vaccines (Åhman *et al*., 1998). In the conjugate vaccines, the polysaccharides are conjugated to diphtheria toxin, which is highly immunogenic and generates a more robust immune response (Åhman *et al*., 1998). Importantly, however, while both vaccines offer protection from carriage and invasive disease caused by the vaccine serotypes (Fenoll *et al*., 2009; Isaacman *et al*., 2010; Ho *et al*., 2011; Egere *et al*., 2012; Alonso *et al*., 2013), over 90 serotypes of *S. pneumoniae* (van der Linden *et al*., 2013) have been described, and the majority of these are not included in the polysaccharide or conjugate vaccines. Hence, both *H. influenzae* and *S. pneumoniae* still pose a threat to human health due to colonization and therefore disease is still a possible outcome of infection by non-vaccine serotypes. Currently, the specific molecular factors and signals that cause the transit from a commensal colonization of the nasopharynx to an invasion of sterile sites of the respiratory tract remain incompletely defined, although host factors such as the anatomy of the eustachian tubes (Stenström*et al*., 1991; Bylander-Groth & Stenström, 1998), age (Teele *et al*., 1989) and immune competence (Engel *et al*., 2001; Faden, 2001) seem to play a role. Importantly, to cause invasive disease, these bacteria must be able to adapt to the specific conditions of the microniche they transit to in the lung, middle ear or cerebrospinal fluid. This includes adaptation to the niche-specific pH, nutrient availability and antimicrobial compounds.

In addition, both bacterial species must have the capability to persist within the site after initial colonization. This includes expression of appropriate adhesins and the ability to evade the host immune response (Fig. 1.1). It is known that for both bacterial species, a key feature of their colonization, survival and persistence, as well as the disease outcome when they become established in a particular niche, is their ability to form a biofilm.

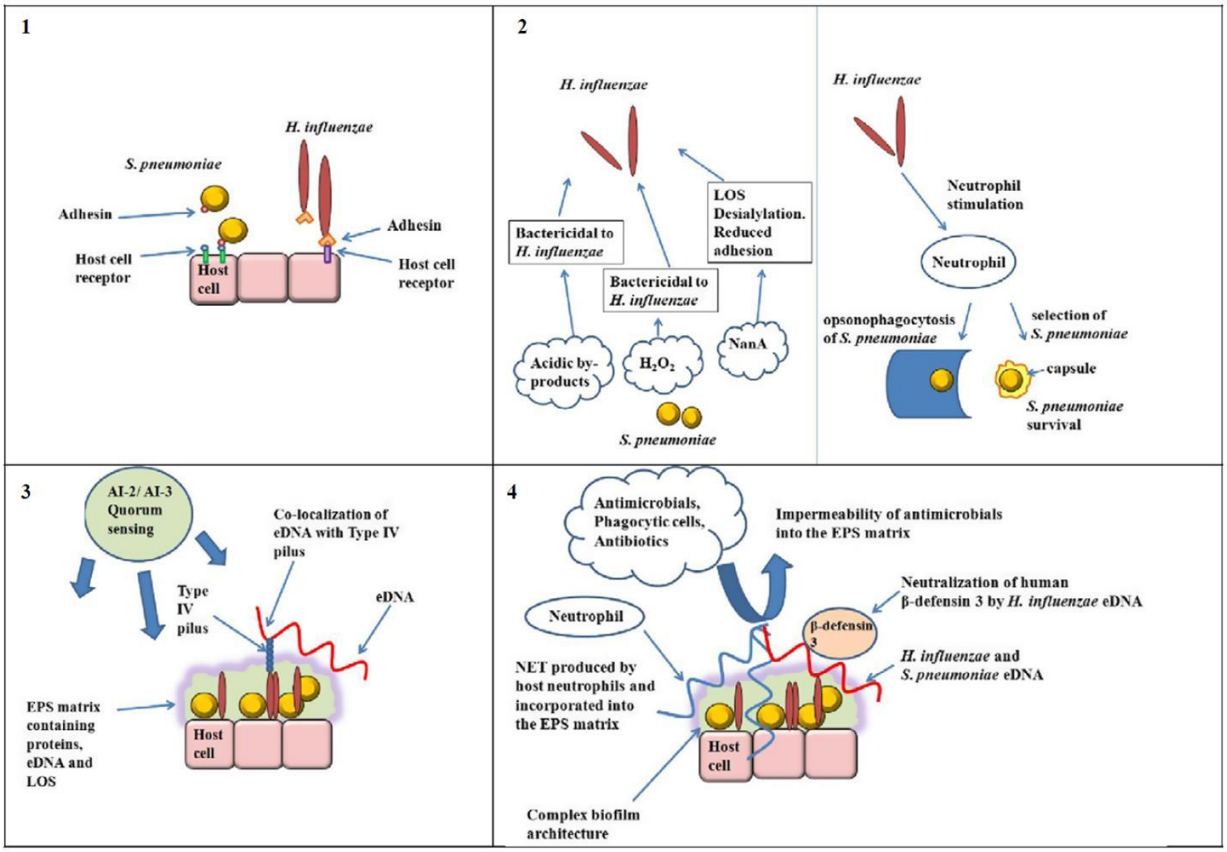

Fig. 1.1. The expected stages of *Haemophilus influenzae* and *Streptococcus pneumoniae* multi-species biofilm development. Stage 1 – adaptation and initial adhesion: the first step in the formation of a multi-species biofilm involves adaptation to the niche pH, nutrient availability, immune mediators, as well as initial adhesion to host surfaces. Stage 2 – adaptation to interspecies stresses and strain selection: this involves adaptation to the presence of stresses imposed by the other species including chemical stresses, pH stress and immune-mediated stress. The strains that are selected for in the interspecies interactions are those that can coexist and may be those that are able to facilitate production of a more extensive protective EPS matrix.

Stage 3 – multi-species biofilm formation and maturation: this involves quorum sensing via AI-2 or AI-3 to sense a multi-species environment and subsequent expression of EPS matrix components such as type IV pili, eDNA and lipooligosaccharide (LOS) to facilitate cohesion, adhesion and biofilm structure. Importantly, interactions between EPS matrix components such as eDNA and the Tfp may contribute to the stability, structure and intra-organization of the

biofilm. Stage 4 – utilizing the EPS matrix to resist host-mediated stress: this involves resisting antibiotic and antimicrobial stresses due to the formation of an extensive and protective EPS matrix. This may also involve exploiting the host immune response to enhance the EPS matrix and remain protected from immune-mediated clearance, for instance, by incorporating host NET structures into the biofilm EPS matrix, as well as the nonspecific binding of host antimicrobials to EPS matrix components.

1.1.2. Co-existence within the multi-species biofilm as a mode of bacterial persistence.

In recent years, it has been proposed that the biofilm lifestyle of both *S. pneumoniae* and NTHi is responsible for the persistence of these bacteria in the chronic forms of OM (Hall-Stoodley *et al*., 2006) and chronic rhinosinusitis (Cope *et al*., 2011).

The mono-species biofilm formation of both *S. pneumoniae* and *H. influenzae* has been described in both *in vitro* and *in vivo* settings (Reid *et al*., 2009; Weimer *et al*., 2010; Cope *et al*., 2011; Carruthers *et al*., 2012). More importantly, however, **f**luorescence ***i**n **s**itu* **h**ybridization (FISH) techniques have shown that both *S. pneumoniae* and *H. influenzae* are present in middle ear tissues excised from chronic OM patients (Hall-Stoodley *et al*., 2006). The persistence of these species within a biofilm provides a vast array of phenotypes that allow for both bacterial adaptation to a host niche and for the persistence of these species in a niche for a prolonged period. Specifically, residence within a biofilm drives global changes in gene and protein expression profiles, which has many effects on cell physiology and in part this leads to an increased resistance to antimicrobial agents, as well as expression of cell surface appendages such as the type IV pili, lipopolysaccharide or lipooligosaccharide and the release of biomolecules such as extracellular DNA (eDNA), which all promote adhesion and cohesion properties of biofilm cells, thereby increasing persistence (Table 1.1). Therefore, the existence of bacterial cells within a biofilm may both protect the bacterial cells from exogenous stress and allow them to persist for prolonged periods within the host. However, it is not known whether

the existence within a multi-species biofilm, in comparison to a mono-species biofilm is more advantageous for *H. influenzae* or *S. pneumoniae*, and whether it poses additional adaptation strategies or a different biofilm cell physiology compared to the one achieved in a mono-species biofilm.

In addition, although *H. influenzae* and *S. pneumoniae* are known and coexist within a biofilm in many chronic diseases of the respiratory tract, the nature of the interplay between these pathogens and the effect of co-infection on disease outcome has not yet been extensively studied. There are, however, significant factors that seem to have been determined to function in this interplay.

Table 1.1. The systems with an increased expression in the biofilm state compared to the planktonic state for *Haemophilus influenzae* and *Streptococcus pneumoniae* mono-species biofilms and in the co-culture biofilm where increased expression compares the expression of genes in the co-culture biofilm compared to the mono-species biofilms.

Factors upregulated	Genes involved	Function
Factors upregulated in the *H. influenzae* monospecies biofilm compared to the planktonic state		
Type IV pilus	*pilA-D comABCDEF* (Bakaletz *et al.*, 2005; Carruthers *et al.*, 2012)	Adhesion to host cells, twitching motility, colocalization with eDNA (Jurcisek & Bakaletz, 2007)
eDNA	Unknown; possibly involvement of quorum-sensing *luxS* for release (Jurcisek & Bakaletz, 2007)	Maintenance of biofilm structure and stability (Jurcisek & Bakaletz, 2007) Neutralization of host antimicrobials (Jones *et al.*, 2013)
Sialylated lipooligosaccharide	*lic3*A, *siaA*, *lsgB* (Jones *et al.*, 2002)	Adhesion to host cells, maintenance of biofilm architecture (Swords *et al.*, 2004)
Phosphorylcholine decorated lipooligosaccharide	*licABCD* (Weiser *et al.*, 1997)	Reduced induction of host innate immune response (West-Barnette *et al.*, 2006)
Outer membrane protein P5	*p5* (Webb & Cripps, 1998)	Adhesion (Gallaher *et al.*, 2006)
Outer membrane protein P6	omp *p6* (Chang *et al.*, 2011)	Adhesion (Gallaher *et al.*, 2006)
Hap	*hap* (Fink & St. Geme, 2003)	Adhesion (Webster *et al.*, 2006)
HMW1	*hmw*1A (Barenkamp & St Geme, 1994)	Adhesion (Webster *et al.*, 2006)
HMW2	*hmw*2A (Barenkamp & St Geme, 1994)	Adhesion (Webster *et al.*, 2006)
IgA1 protease	Iga (Poulsen *et al.*, 1992)	Proteolysis of secretory forms of IgA1 antibodies, involvement in microcolony formation (Webster *et al.*, 2006)
Factors upregulated in the *S. pneumoniae* monospecies biofilm compared to the planktonic state		
eDNA	LuxS-mediated *lytA* autolysis implicated in eDNA release (Romao *et al.*, 2006)	Adhesion, cohesion and biofilm structure (Moscoso *et al.*, 2006; Hall-Stoodley *et al.*, 2008)
CbpA	*cbpA* (Sanchez *et al.*, 2011)	Adhesion to laminin receptor (Huang & Jong, 2009; Sanchez *et al.*, 2011)
PsrP	*psrP* (Sanchez *et al.*, 2011)	Host cell and intraspecies adhesion (Sanchez *et al.*, 2011) Adhesion to keratin 10 (Shivshankar *et al.*, 2009)
ChoP	*licD2* (Zhang *et al.*, 1999)	Adhesion to host PAFR (Cundell *et al.*, 1995; Sanchez *et al.*, 2011)
Factors upregulated in the *H. influenzae*/*S. pneumoniae* multispecies biofilm compared to the monospecies biofilms		
H. influenzae type IV pilus	*pilABCD comABCDEF* (Bakaletz *et al.*, 2005; Carruthers *et al.*, 2012)	Possibly adhesion, cohesion and biofilm structure (Cope *et al.*, 2011)
S. pneumoniae H_2O_2 production	*spxB* (Spellerberg *et al.*, 1996)	Possibly to compete with *H. influenzae* for nutrients or space or to mediate *H. influenzae* lysis and eDNA release (Cope *et al.*, 2011)

1.1.3. The NTHi and *S. pneumoniae* multi-species biofilm: The basis for the chronicity of OM

OM is an inflammatory disease of the middle ear, affecting over 70% of children before 3 years of age (Teele *et al*., 1989; Berman, 1995). OM poses a serious risk of progression to systemic disease (Klein, 2000) as well as impaired hearing (Hunter *et al*., 1996), which in children can progress to speech delay (Shriberg *et al*., 2000) and impaired cognitive development (Williams & Jacobs, 2009). The major aetiological agents of OM are the bacterial pathogens *S. pneumoniae*, *H. influenzae* and *M. catarrhalis* (Hall-Stoodley *et al*., 2006). While OM is commonly treated with antibiotics (Dowell *et al*., 1999) or tympanostomy tube placement (Gebhart, 1981), chronic (COM) or recurring (ROM) forms of OM are often unresponsive to these treatments (Williams *et al*., 1993; Ojano-Dirain & Antonelli, 2012).

The opportunistic pathogens *S. pneumoniae* and *H. influenzae* (NTHi in most cases) are significant contributors to the pathogenesis of acute OM (AOM). Recently, FISH techniques demonstrated the presence of biofilms harbouring both NTHi and *S. pneumoniae* on middle ear membrane tissue from COM patients (Hall-Stoodley *et al*., 2006; Thornton *et al*., 2011).

A biofilm is a bacterial lifestyle in which the cells reside adhered to a substratum and to each other and are encased in a self-produced extracellular polymeric substance matrix (EPS matrix; Sutherland, 2001; Flemming & Wingender, 2010; Hoa *et al*., 2010). An important feature of bacterial biofilms is their persistent nature and their insensitivity to immune mediators and clinically used antimicrobial agents (Domenech *et al*., 2013a, b). These features can be explained both by the physiology of the biofilm-resident cells themselves and by the physical properties of the EPS matrix components. The presence of an EPS matrix allows for biofilm persistence by physically limiting the diffusion of antimicrobial compounds into the biofilm (Høiby *et al*., 2010), thus allowing for the increased persistence of biofilm-resident cells. Additionally, the biofilm-resident cells themselves have been shown to undergo changes in gene expression profiles upon transition from planktonic to biofilm state (Prigent-Combaret *et al*., 1999; Becker *et al*., 2001; Sauer & Camper, 2001; Sauer *et al*., 2002). The switch in gene expression that defines biofilm-resident cells seems to have global effects on

cellular functions. This includes changes not only in the surface components expressed, but also in the metabolic and biosynthetic pathways for maintaining intracellular conditions such as pH and redox balance (Schembri *et al*., 2003). Often, these global physiological changes include a physiological state with an increased recalcitrance to antimicrobial agents (Mah & O'Toole, 2001), which contributes to an increased persistence. The biofilm nature of COM explains the difficulty in treatment of COM with antibiotics (Williams *et al*., 1993; Segal *et al*., 2005; Rovers *et al*., 2006), as biofilm communities display increased recalcitrance to antibiotics and explains the resistance to tympanostomy tube placement (Post, 2001), as both pathogens are able to re-establish the biofilm on the tympanostomy tube.

1.1.4. The *H. influenzae* and *S. pneumoniae* biofilm lifestyle

Residence within a biofilm for both *H. influenzae* and *S. pneumoniae* involves global changes in gene expression and physiology to enable them to adapt to the environmental conditions and persist in the host. However, while it is a multi-species biofilm that contributes to the pathogenesis of chronic OM, to date, the biofilms of both species have been studied primarily in mono-culture.

It is known that in a biofilm, one major phenotypic cellular changes is that of a production of an EPS matrix (Branda *et al*., 2005; Flemming & Wingender, 2010). The composition of the matrix differs between bacterial species, but generally includes lipids, proteins and nucleic acids (Flemming & Wingender, 2010). The EPS matrix has been shown to reduce the permeability of the biofilm matrix to antimicrobial compounds, as well as contributing to the adhesion and cohesion of the cells to the host cells and to each other (Branda *et al*., 2005; Flemming & Wingender, 2010). Various adhesion factors have been shown to be upregulated in the *H. influenzae* and *S. pneumoniae* biofilms (Table 1.1). In this context, there may be features of the host tissue, the middle ear mucosa for instance, that permit adhesion and biofilm development (and in particular, multi-species biofilm development) or there may be features of the bacterial survival strategies that mean the properties and stresses of a specific niche act to

signal for the bacterial cells to switch to a biofilm (and in particular, a multi-species biofilm). In addition, the biofilm mode of life involves global changes in the expression of genes that are not involved in the EPS matrix and rather may be involved in the response to low nutrient levels, which may vary throughout the biofilm, as well as oxidative stresses or local pH stress (Schembri *et al*., 2003; Beenken *et al*., 2004).

Importantly, changes in the expression of genes and their protein products have been observed from the planktonic to the biofilm state for both *H. influenzae* and *S. pneumoniae*. The *S. pneumoniae* biofilm cells have been shown to have an increased adhesion by up to 12× compared with their planktonic counterparts (Sanchez *et al*., 2011). This was due to a reduced expression of capsular polysaccharide which exposed bacterial cell surface proteins and an increased expression of phosphorylcholine which is known to bind to the host receptor PAFr and increased expression of protein CbpA which binds to Laminin receptor on host cells and PsrP which binds keratin 10 (Sanchez *et al*., 2011). eDNA has also been shown to form a part of the *S. pneumoniae* EPS matrix (Moscoso & Claverys, 2004; Moscoso *et al*., 2006; Hall-Stoodley *et al*., 2008). Additionally, it was recently shown that eDNA–protein complexes play a role in the EPS matrix. Thus, the lysozyme LytC protein was shown to bind to the eDNA in *S. pneumoniae* biofilms (Domenech *et al*., 2013a, b). A novel polysaccharide component to the *S. pneumoniae* EPS matrix which was distinct from the capsule has also been identified (Domenech *et al*., 2013a, b). A clear part of the switch in lifestyle is that an upregulation of the gene expression of some stress response genes was observed in the biofilm of *S. pneumoniae* compared with the planktonic state. Specifically, there was an upregulation in the expression of stress-related chaperonins and proteases including GroEL, class I heat shock proteins, the universal stress family proteins, thioredoxin, 2 Clp proteases and 3 transposases, as well as 18 hypothetical proteins (Sanchez *et al*., 2011). Hence, it appears that stress response plays a role in the maintenance of *S. pneumoniae* in the biofilm state; the profile of transcriptionally active genes defines that lifestyle and this certainly indicates that in a biofilm lifestyle, the cell is predisposed to a stress response state.

Webster *et al*. (2006) showed an involvement of the lipooligosaccharide of *H. influenzae* in the mono-species biofilm as well as the proteins Hap, HMW1 and HMW2. The secreted IgA protease was also associated with the EPS matrix; however, it was primarily localized at the outer regions of the matrix, corresponding to a role in protection from the host immune response

via degradation of the secretory forms of IgA1 (Webster *et al*., 2006). A study by Gallaher *et al*. (2006) investigated numerous proteins associated with the *H. influenzae* EPS matrix and found the involvement of outer membrane proteins 5 and 6 (OMP5 and OMP6), as well as various proteins implicated in biofilms of other bacteria such as GroEL, KasA/FabB, UspA and peroxiredoxin; however, their precise function in the *H. influenzae* EPS matrix have not been thoroughly investigated. In addition, both eDNA and the type IV pilus (Tfp) have recently been identified as aspects of the *H. influenzae* EPS matrix and were shown to contribute to the stability and structure of the biofilm (Jurcisek & Bakaletz, 2007).

While genes expressed in the biofilm for each species allow adaptation to and persistence within the host environment, little is known about the genes expressed in a multi-species biofilm. In the case of a multi-species biofilm, adhesion genes in the EPS matrix would also be required to facilitate cell–cell cohesion between the two different species that possess different cell surface appendages and proteins. In addition, the architecture of the multi-species biofilm would need to facilitate the spatial localization of cells that would allow for the survival of both species. This would involve complex sub-localizations depending on nutrient and oxygen requirements, as well as protection from external stresses and intra-biofilm stresses such as the waste of 'self-species' cells and the waste or toxic by-products of the other competing species. An overview of the sequence of events proposed to occur in multi-species biofilm development is given in Fig. 1.1 Currently, little is known about the genes expressed in the multi-species biofilm; however, in part, the genes expressed would rely on the nature of the interaction between *H. influenzae* and *S. pneumoniae* (Fig. 1.1). To date, despite several studies in this regard, it remains unclear as to whether this interaction is synergistic, antagonistic or both. It is worthy at this juncture to collate the data from what is known and analysing the supposed conflicts.

1.1.5. Mutual protection and stability in the multi-species biofilm

The colocalization of NTHi and *S. pneumoniae* has suggested a synergistic interaction between the two organisms. Indeed, some studies have demonstrated that the coexistence in a multi-species biofilm provides advantages to one or both of these species. One advantage is the passive protection from antibiotic therapy seen in the multi-species biofilm. Weimer *et al*. (2011) showed that the β-lactamase-producing NTHi strain 86-028NP was able to protect both planktonic and biofilm-resident *S. pneumoniae* from amoxicillin treatment in the chinchilla middle ear. This finding demonstrates the importance of sharing a diverse gene bank within the multi-species community of the respiratory tract where gene expression has repercussions not only for one bacterial species, but the whole microbiome of the resident environment. However, this study demonstrated that β-lactamase production by *H. influenzae* was not the only method of *S. pneumoniae* protection against amoxicillin. In fact, the β-lactamase-deficient strain 86-028NP *bla* was able to protect biofilm *S. pneumoniae* from amoxicillin. In addition, the co-culture 86-028NP *bla* strain could be isolated from bullar homogenate biofilms, whereas the mono-culture inoculated 86-028NP *bla* was unable to survive on its own. Hence, while β-lactamase production played a role in interspecies synergy, the formation of a multi-species biofilm by even β-lactamase-deficient strain was shown to be beneficial in protection from antibiotics for both species. While the reason for such protection was not further analysed, most likely the protection was due to the formation of an extensive matrix of EPS in the formation of a multi-species biofilm; the EPS matrix is known to limit the physical diffusion of antimicrobials into close proximity with the biofilm-resident cells.

A recent study by Cope *et al*. (2011) also demonstrated synergy between *H. influenzae* and *S. pneumoniae*. Specifically, both species reached higher cell densities in co-culture compared with mono-culture, and in polymicrobial biofilms, they were shown to modulate the expression of each other's virulence genes, resulting in persistent biofilm (Cope *et al*., 2011). Specifically, it was shown that in a co-culture biofilm setting, physical contact of *H. influenzae* with *S. pneumoniae* resulted in an upregulation of *pilA* expression by the *H. influenzae* (Table 1). The *pilA* of *H. influenzae* is known to encode the major subunit of

the Tfp (Bakaletz *et al*., 2005), an important appendage in adhesion and biofilm stability of the mono-species biofilm. Hence, this indicates that in co-culture, genes may be expressed that facilitate biofilm formation, and which perhaps may benefit both species in the biofilm.

Overall, a stable and robust biofilm would be beneficial to both species due to the possibility of passive protection from antimicrobial substances and due to an extensive EPS matrix to promote adhesion to host surfaces and protection from antimicrobial substances. However, a multi-species biofilm would also have the greater benefit in the wider diversity of the biofilm genome, where the genetic reservoir would harbour genes from not only different strains, but also different species. It has been shown that *in vivo S. pneumoniae* can uptake genes from lysed cells within the biofilm and that the competence for genetic uptake is 10^7-fold higher in the biofilm state than in the planktonic state (Marks *et al*., 2012). Thus, the potential for uptake of genes by different species within the biofilm would be high and would allow for an increased interspecies genetic transfer and diversity, which could impact both treatment outcomes and progression of the disease.

1.1.6. Biocide Production: An antagonistic interaction, or for the greater common good?

In contrast to the aforementioned interactions, there have been some studies that have demonstrated not synergistic, but competitive interactions with contradictory competition outcomes. Specifically, the H_2O_2 generated by *S. pneumoniae* was toxic to NTHi (Pericone *et al*., 2000). However, it is worth noting that Cope *et al*. (2011) showed that the *spxB* of *S. pneumoniae* responsible for H_2O_2 production was upregulated in the co-culture *S. pneumoniae* – *H. influenzae* biofilm (Table 1.1). Hence, it could be that the toxic H_2O_2 production plays a competitive role in the multi-species biofilm or, in contrast, that H_2O_2 production plays a more complex role. Specifically, H_2O_2 could locally reduce *H. influenzae* viable cells, which could result in cell death and subsequent release of nutrients and other cellular components such as genomic DNA. Indeed, such a release of

nutrients could serve to benefit both species within the biofilm, providing that a subset of viable *H. influenzae* cells was still present. Additionally, released DNA could serve multiple roles in a multi-species biofilm; if taken up by competent cells in the biofilm, it could increase genetic diversity of both species, it could be utilized as a nutrient or contribute to the EPS matrix increasing biofilm adhesion or cohesion.

1.1.7. Competition for nutrients, attachment space and optimal conditions

As both species possess individual genomes and utilize unique metabolic pathways, it is likely that as well as the metabolic production of H_2O_2 by *S. pneumoniae*, there exists a myriad of biological factors that may impact the growth of one of the species. These factors include metabolic by-products produced by one of the species, which can be beneficial or detrimental to the other species. The metabolic by-products generated are in turn dependent on the environmental conditions, nutrient availability and physical conditions of the environment.

Recently, it has been observed that in a batch co-culture model of *S. pneumoniae* and *H. influenzae* growth, *S. pneumoniae* was able to outcompete *H. influenzae* (Tikhomirova et al. 2015). This effect was not dependent on the strains used and was not a result of H_2O_2-mediated competition as an *spxB* isogenic mutant of *S. pneumoniae* also inhibited *H. influenzae* planktonic and biofilm growth. Importantly, this growth inhibition effect was time dependent, where *H. influenzae* cell death occurred only after the entering of both species into stationary phase. This growth inhibition effect appeared to be a result of a pH change occurring in the *S. pneumoniae* growth after reaching stationary phase (Tikhomirova et al. 2015). Hence, it appears that by modifying the pH of the immediate environment during certain growth stages, *S. pneumoniae* can diminish the viability of *H. influenzae*. Hence, *H. influenzae* may be more adapted for survival and potentially biofilm formation in an environment where pH is elevated. This is supported by the finding that the type IV pili important for *H. influenzae* biofilm formation were expressed in a chemically defined medium at pH 8.5–9.0, but not 7.2 (Bakaletz *et al*., 2005). The pH of the middle ear environment has not been extensively studied; however, it has been shown that the pH of middle ear effusions of OM patients with chronic secretory forms of OM extends to a basic pH that ranges from pH

7–9 (Nuutinen *et al*., 1993; Wezyk & Makowski, 2000). If *S. pneumoniae* lowers the pH during a multi-species infection, *H. influenzae* must have mechanisms to regulate the pH to maintain a neutral or basic pH of the environment. One pH regulatory mechanism in *H. influenzae* is urease. The *H. influenzae* urease is a nickel-dependent enzyme, which is involved in catalysing the hydrolysis of urea to ammonia and carbon dioxide (Mobley *et al*., 1995). In other bacteria, the urease functions to raise the pH of the environment, allowing bacterial survival at low pH environments (Ferrero & Lee, 1991; Stingl *et al*., 2002). In a chinchilla model of OM, it has been demonstrated that the *ureH*, a homologue of a gene requires for expression of an active urease in *Helicobacter pylori*, was upregulated in the chinchilla middle ear (Mason *et al*., 2003). Additionally, in human chronic obstructive pulmonary disease, antibodies against *H. influenzae* urease increased with exacerbations of the disease, indicating urease expression in chronic diseases of the respiratory tract (Murphy & Brauer, 2011). The *ure* operon was also found to be more prevalent in *H. influenzae* isolates from OM or COPD than from isolates obtained from throats of healthy individuals (Zhang *et al*., 2013). It would be likely that if *S. pneumoniae* growth dramatically reduces the pH of the environment (Tikhomirova et al. 2015), then for a co-culture growth within the middle ear, acidification of the environment would be prevented or shifted to a more alkalizing state that would facilitate survival, type IV pili expression and a multi-species biofilm formation. Hence, in chronic forms of OM that involve multi-species infections, *H. influenzae* may require urease or other systems to maintain the pH at a neutral or slightly basic state, which is consistent with the clinical observations for the presence of urease.

1.1.8. Exploiting the host immune system to out-compete a competitor

In addition to H_2O_2-mediated competition of *S. pneumoniae* with *H. influenzae*, there have been reports of immune-mediated competition between these two species. Shakhnovich *et al*. (2002) have shown that *S. pneumoniae* produces a neuraminidase capable of desialylating the sialic acid – decorated on the lipooligosaccharide structures of *H. influenzae*. It has been hypothesized that *in vivo*, such desialylation could lead to a reduction in *H. influenzae* viability due to the decrease in sialic acid association with complement factor H and, thus, an increase in complement-mediated removal of *H. influenzae* from the host. It is important also to note that sialic acid was shown to be central in *H. influenzae* biofilm formation (Swords *et al*., 2004) and that mutants deficient in *siaB* produced only asialylated lipooligosaccharide and formed reduced biofilm in a continuous flow system, and that this led to a reduced persistence and colonization in the gerbil OM model (Swords *et al*., 2004). In the chinchilla OM model, NTHi mutants deficient in sialyltransferases *siaA* and *lsgB* also displayed an atypical biofilm phenotype where, while a biofilm was formed, it contained mostly nonviable bacteria (Jurcisek *et al*., 2005).

However, the opposite – that is, the domination of *H. influenzae* over *S. pneumoniae* via immune-mediated competition of *H. influenzae* with *S. pneumoniae* – has also been shown. Lysenko *et al*. (2005) showed that NTHi was dominant in a mouse model through its stimulation of opsonophagocytic killing of *S. pneumoniae*. In other animal studies, NTHi had an improved colonization of the rat nasopharynx when *S. pneumoniae* was previously established, seemingly through mediating immune competition with *S. pneumoniae* (Margolis *et al*., 2010). Importantly, the immune-mediated competition of *H. influenzae* with *S. pneumoniae* was specific to particular *S. pneumoniae* strains (Margolis *et al*., 2010). However, the factors that govern these strain-specific interactions remain unclear. It had been suggested that because NTHi directed the opsonophagocytosis response against *S. pneumoniae*, encapsulated *S. pneumoniae* strains would prevail in a co-culture setting, and the capsular type and thickness would determine the survival of *S. pneumoniae* in this setting (Lysenko *et al*., 2010). It is well known that *S. pneumoniae* has a phase-variable capsular expression that is linked to colony morphology determined by the opaque or transparent colony phenotype (Kim & Weiser, 1998; Kim *et al*., 1999).

Specifically, *S. pneumoniae* is able to switch from expression of high levels of capsular polysaccharide, which is determined by the opaque colony phenotype, to lower levels of capsular polysaccharide expression and the transparent morphology (Kim & Weiser, 1998; Kim *et al*., 1999). It could be suggested by the mathematical model of Lysenko *et al*. (2010) that in a co-culture setting, opaque strains expressing higher levels of capsular polysaccharide would predominate. However, this theory is contradicted by several findings. Firstly, capsule expression was shown to be reduced in mono-species *S. pneumoniae* biofilm models (Hall-Stoodley *et al*., 2008), and reduced capsular expression mutants displayed augmented biofilm formation (Muñoz-Elías *et al*.,2008; Qin *et al*., 2013). Likewise, expression of a capsule by capsular *S. pneumoniae* strains has been associated with a reduced biofilm formation as compared to nontypeable strains (Moscoso *et al*., 2006). This suggests that capsular expression may not be favoured in the biofilm lifestyle of *S. pneumoniae*. Most importantly, however, in a chinchilla OM co-infection model, there was shown to be an increased proportion of translucent *S. pneumoniae* types within the multi-species biofilm (Weimer *et al*., 2010).
Hence, the indication is that there is selection for strains that have a capacity for survival in co-culture and in the multi-species biofilm, mediated through yet to be identified determinants that are not necessarily related to capsular type or capsular expression.

1.1.9. The EPS Matrix and inter-species interactions

While specific factors that impact the interspecies interactions have not yet been identified, it is likely that synergistic relationships may be established by strains that would benefit the mutual biofilm. It is known that the EPS matrix plays a vital role in biofilm stability, protection against antimicrobial compounds and adhesion to host cells – factors that would benefit both species in a host environment. Therefore, it could be suggested that strains that would benefit the mutual biofilm could be those that are able to establish an extensive EPS matrix structure or strains where the EPS matrix components could synergistically interact with the EPS matrix components of the other species. To date, some studies support this hypothesis. Cope *et al*.

(2011) showed that the NTHi *pilA*, which encodes the Tfp, was upregulated in the *S. pneumoniae*/NTHi multi-species biofilm. Previously, it was shown that in the NTHi mono-species biofilm, the type IV pili increased biofilm stability (Jurcisek *et al*., 2007) and mediated twitching motility (Bakaletz *et al*., 2005). NTHi type IV pili also bind DNA (Aas *et al*.,2002) and were colocalized with eDNA (Jurcisek & Bakaletz, 2007) in a mono-species biofilm formed in the chinchilla middle ear. The type IV pili DNA-binding role is key to mature NTHi biofilm formation as a complex mature biofilm structure could be formed via twitching motility-directed migration of individual cells along eDNA (Allesen-Holm *et al*., 2006). It is important that both *S. pneumoniae* (Moscoso *et al*., 2006) and NTHi (Jurcisek & Bakaletz, 2007) are known to release eDNA into their own EPS matrix but the role and interactions of type IV pili and eDNA in the multi-species biofilm remain unclear. The evidence suggests that they are important and may function in strain-specific selection.

1.1.10. Molecular factors of the communication; inter/intra-species interplay.

To initiate and maintain formation of a biofilm, resident cells must be able to regulate expression of appropriate genes that may facilitate biofilm formation or promote survival in the presence of strain-specific selection forces. The environmental basis for bacteria switching into their biofilm state is complex and the factors responsible for this are not fully understood, although the physical, chemical and biological conditions of the immediate environment such as nutrient starvation, pH stress and oxygen levels likely play a role in inducing biofilm formation.

It is important to note, that the biofilm lifestyle, as mentioned previously, may act as a protective structure for the bacterial cells. Therefore, in the presence of stress, or damaging antimicrobial agents, biofilm formation may be favoured in order to assume a lifestyle which may protect the cells from the presence of damaging compounds. Indeed, some potentially damaging compounds

have been shown to induce biofilm formation of *H. influenzae* and *S. pneumoniae*. In *H. influenzae*, sub-inhibitory levels of β-lactam antibiotics have been shown to increase biofilm formation in a strain-dependent manner (Wu et al. 2014). Addition of glucocorticosteroids to *H. influenzae* was also shown to induce biofilm formation (Earl et al. 2015).

It is also known that potentially damaging environmental factors, including volatile pollutants, can also stimulate biofilm formation, and it has recently been shown that cigarette smoke condensate augmented biofilm formation of *S. pneumoniae* (Mutepe *et al*., 2013).

In NTHi, it has also been shown that some environmental conditions pertaining to the host environment, including a higher pH of 8.0, and a lower oxygen tension, induced biofilm formation (Osgood et al. 2015). This is particularly relevant to disease, as the pH of the middle ear during chronic OM has been identified to have a basic pH range from pH 7-9.

Hence, as a biofilm offers protection from antimicrobial compounds, the presence of some antimicrobial compounds has been shown to induce biofilm formation, stimulating a protected lifestyle in both *H. influenzae* and *S. pneumoniae*. However, it is known that in addition to protecting biofilm resident cells from exogenous stresses, a biofilm lifestyle can be characterised by a reduced metabolic rate compared to the planktonic lifestyle – this has been shown in *S. aureus*, where metabolic gene expression in the biofilm reduced with time (Resch et al. 2005). Although the biofilm is heterogenous in terms of factors such as nutrient availability and cell distribution (Stewart and Franklin 2008), there is a potential that residence of bacterial cells within a biofilm could facilitate survival in the presence of unfavourable conditions, such as during low nutrient levels, by allowing the existence in a more metabolically quiescent or metabolically altered state.

Supporting this hypothesis, it has been shown that a knockout in the *H. influenzae* nickel uptake system *nikKLMQO–nimR* displayed an increased biofilm formation, which was attributed to a change in the surface properties of the cell (Ng & Kidd, 2013). Specifically, the mutant cells, which were unable to import nickel, were more negatively charged and hydrophobic compared with the wild type, which stimulated cell–cell aggregation and biofilm formation. Hence, it is likely that for *H. influenzae*, the environmental conditions that determine a requirement for nickel and the local concentration of nickel can modulate biofilm formation propensity (Ng & Kidd, 2013).

It is important that for many bacterial species, cell density-dependent quorum-sensing signals are vital in the formation of mono-species biofilms (Merritt *et al*., 2003; Yoshida *et al*., 2005). For both *H. influenzae* and *S. pneumoniae* mono-species biofilms, quorum sensing appears to be an important initiation factor.

In many bacterial species, the quorum-sensing signal autoinducer-2 (AI-2) encoded by the *luxS* gene, is vital for inducing biofilm formation (Merritt *et al*., 2003; Yoshida *et al*., 2005; González Barrios *et al*., 2006). AI-2 is produced as a by-product in the homocysteine synthesis pathway, where S-ribosylhomocysteine is converted to homocysteine via the action of the *luxS*-encoded S-ribosylhomocysteine lyase (Walters *et al*., 2006). The by-product of this reaction is 4,5-dihydroxy-2,3-pentadione (DPD); however, as this compound is highly unstable, it is able to spontaneously cyclize, forming several furanone ring structures, including AI-2 (Walters *et al*., 2006). The action of AI-2 involves a density-dependent sensing by a cell surface uptake system or a two-component regulatory system. In *H. influenzae*, the AI-2 uptake receptor was found to be RbsB (Armbruster *et al*., 2011). However, it is also important to note that in enterrohaemorrhagic *Escherichia coli* (EHEC), an alternate QS system involving the autoinducer AI-3 has also been shown to be affected by *luxS* (Walters *et al*.,2006), and interestingly, in *H. influenzae*, the QseB/QseC 2 component regulatory system was found to be a homologue of the EHEC QseB/QseC AI-3 sensing system (Ünal *et al*., 2012). Hence, in the majority of studies investigating AI-2-mediated quorum sensing via analysis of *luxS* knockouts, the phenotype of both AI-2 and AI-3 mutant strains could be mistaken for a purely AI-2 lacking phenotype. Importantly, in *S. pneumoniae*, while *luxS* has been shown to be important for biofilm formation, a homologue of the AI-2 receptor or the AI-3 receptor has not yet been determined, which may be due to sequence diversity of the receptor (Rezzonico & Duffy, 2008). While for both species, the precise downstream signalling events for AI-2 or AI-3 sensing are not yet known, certainly the ultimate result is the regulation of quorum-sensing-dependent genes. Both *H. influenzae* and *S. pneumoniae* encode *luxS*, which was shown to be important for formation of a mono-species biofilm in both species (Moscoso *et al*., 2006; Vidal *et al*., 2011, 2013). In *H. influenzae*, *luxS* was shown to modify the lipooligosaccharide moieties on the bacterial surface, which was thought to account for the reduction in biofilm formation in a *lux*S mutant (Armbruster *et al*., 2009). In *S. pneumoniae*, *lux*S controls transcription of *lytA*, an autolysin implicated in biofilm formation (Vidal *et al*., 2011), and

possibly involved in lysis-induced eDNA release into the EPS matrix (Romao *et al*., 2006), as well as early and late competence genes of the *com* competence quorum-sensing system (Trappetti *et al*., 2011; Vidal *et al*., 2011), which are implicated in competence and competence-dependent fratricide and associated DNA release (Steinmoen *et al*., 2002; Vidal *et al*., 2013). Hence, AI-2-mediated quorum sensing may be involved in initiating biofilm formation by establishing the EPS matrix in *S. pneumoniae* strains capable of eDNA release, possibly through coregulation of the *com* genes.

In the context of a multi-species biofilm, it is likely that the presence of the other bacterial species is also sensed, inducing formation of a multi-species biofilm. Currently, a specific sensing pathway whereby one species is able to sense the presence of another, especially in the context of *H. influenzae* and *S. pneumoniae*, has not been established. Importantly, although both species encode *lux*S, AI-2 production may be sensed by strains that may not produce AI-2, as has been observed with *M. catarrhalis* in the *M. catarrhalis/H. influenzae* multi-species biofilm (Armbruster *et al*., 2010). It could be that each bacterial species is also able to sense the AI-2 produced by the other species as well as the self-produced AI-2 and that coordinated production of AI-2 by both species is responsible for a quicker switch to the biofilm lifestyle or the more efficient formation of a robust biofilm.

Importantly, the expression of *luxS* itself may be dependent on more global environmental signals. For example, it has been shown in *S. pneumoniae* that extracellular iron Fe(III) stimulated *luxS* expression, and, in turn, increased the biofilm formation (Trappetti *et al*.,2011). It is possible that not only extracellular iron, but also environmental factors signalling of the presence of the other species may be sensed resulting in *luxS* expression, more efficient interspecies sensing and subsequent biofilm formation.

1.1.11. *H. influenzae* and *S. pneumoniae* working together to avoid the host immune response.

In the presence of external signals, which are currently unclear, *H. influenzae* and *S. pneumoniae* are able to sense each other's presence in the niche and initiate polymicrobial biofilm formation. This would involve expression of appropriate adhesins for such a multi-species biofilm. It is known that in the multi-species biofilm, residents are offered protection from host immune mediators and antimicrobial agents due to reduced permeability into the biofilm. However, such anti-immunity biofilm properties are sometimes more diverse and may depend on the nature of the EPS matrix components. For instance, it has recently been shown that in the NTHi biofilm, eDNA as an anionic molecule, can bind to the cationic β-defensin three antimicrobial peptide, thus deactivating it (Jones *et al*., 2013). It is important that if both *H. influenzae* and *S. pneumoniae* are together able to release higher levels of eDNA into the biofilm matrix, the antimicrobial action of the eDNA could be augmented allowing for a longer persistence of the biofilm. Another mechanism of biofilm-related host defence resistance is neutrophil extracellular trap (NET) utilization. It is known that host neutrophils produce NETs that are comprised of double-stranded DNA, histones and elastase (Yousefi *et al*., 2009). These structures have microbicidal activity due to entrapping bacterial cells within the DNA matrix and killing them by granular components (Brinkmann *et al*., 2004). However, it has been shown that NTHi biofilms can exist in a viable state within the NET structures, and such survival has been correlated to a higher bacterial load during experimentally induced OM (Hong *et al*., 2009). Hence, it does appear host NETs, derived as an immune response to infection, are actually utilized by bacterial communities to maintain persistence. It has also been shown that the NTHi cells are able to induce the formation of NETs, possibly due to signalling of NTHi lipooligosaccharide through the TLR4 (Juneau *et al*., 2011). It has been shown that the *S. pneumoniae* protein α-enolase also stimulates the formation of NETs (Mori *et al*., 2012). While this study showed that the α-enolase actually increased the bactericidal function of NETs, this was shown in human blood, where bacteria are normally present in the planktonic form. Hence, in an environment where biofilm formation is favoured, such as the

middle ear, the α-enolase activity may promote persistence rather than bacterial clearance. Hence, bacterial infection can promote NET formation, which under certain conditions may augment persistence. While the function of a multi-species infection in NET formation and function has not been investigated, it is likely that in the context of biofilm formation in the middle ear, *H. influenzae* and *S. pneumoniae* can exploit the host immune response to facilitate a more protected biofilm lifestyle.

1.1.12. The multi-species biofilm and future therapeutic approaches.

In disease situations, *H. influenzae* and *S. pneumoniae* form a multi-species biofilm; however, the nature of this interaction is only starting to be understood. The review of the literature collates research from different perspectives and shows that the current research suggesting the relationship between these pathogens may be strain-specific and may depend on multiple and possibly strain-specific factors (Fig. 1.1). Synergistic interactions may be enhanced in strains with an ability to generate a structured EPS matrix. Evidence is emerging that type IV pili associations with eDNA function in the EPS matrix and could lead to strain selection within the multi-species biofilm. In the future, transcriptomic and proteomic analyses of the multi-species biofilms may help to establish the stress response and EPS-component genes that are involved in generating and maintaining the multi-species *H. influenzae/S. pneumoniae* biofilm. It is also important to note that the effects of strain or serotype replacement of either *S. pneumoniae* or *H. influenzae* as a result of vaccine use and novel vaccine development on multi-species interactions remain unknown. Such alterations in microbial ecology of the nasopharynx could potentially be either detrimental or beneficial for interspecies interactions and could thus either reduce or augment the risk of COM. Such a risk would need to be noted when introducing new vaccines directed against the common otopathogens *H. influenzae* and *S. pneumoniae*. Understanding the interactions between these species will enable selection of drugs that may inhibit these interactions and thus their capacity to form a multi-species biofilm

as a means of survival. The upregulation of *pilA* in the biofilm, for instance, suggests the possible involvement of the type IV pili in biofilm formation. Administering a Tfp blocker may reduce the multi-species biofilm formation. Means of dispersing the biofilm structure in COM patients by targeting the structures that allow its formation may assist in the administration of other therapeutic agents such as antibiotics, which may otherwise not be able to permeate into the biofilm. In addition, if *S. pneumoniae* pH-mediated competition is important in the multi-species biofilm clinically, then administering a urease inhibitor may reduce the ability of *H. influenzae* to survive in the multi-species community and contribute to the multi-species biofilm formation. Further studies will likely expose new targets for drug design that may be involved in the multi-species biofilm formation. In addition, it is important to note the strain variation present among the *H. influenzae* and *S. pneumoniae* isolates, which may determine the differences in their interspecies interactions and also in the molecular factors utilized to facilitate these interactions. So, while new molecular targets for COM therapy will be identified, future therapy should focus on diagnosing the disease based on the specific isolates involved and administering therapeutic agents based on the classification of the strains involved. Another aspect that is open for investigation in OM therapy of the future should be the prognosis of OM development; specifically, any strain-specific therapy that is utilized should optimally involve screening of nasopharyngeal communities to analyse the probability of strain replacement and the development of subsequent OM cases. This will allow the optimal selection of therapy on an individual basis.

1.2 Aims of this Thesis.

The overarching aim of this thesis, was to determine the molecular mechanisms allowing *H. influenzae* to adapt to, and survive in complex environments relevant to its host niches.

The first aim of this thesis was to establish *H. influenzae* adaptation to various nutrient conditions, pH levels, and to the presence of damaging stress compounds, and to analyse the *H. influenzae* biofilm formation response in these environments.

The second aim, was to identify *H. influenzae* adaptation to host-relevant environments by analyzing in detail its global transcriptomics response pertaining to the change in environmental conditions.

The final aim of this study was to analyse the *H. influenzae* adaptation to and co-existence with *S. pneumoniae*. This involved an in-depth analysis of planktonic and biofilm-state interactions of both species in different growth models and environmental conditions, as well as a full transcriptomics characterization of both species during these interactions.

Cumulatively, the work described in this thesis has allowed us to enhance our understanding of the *H. influenzae* adaptation, survival and lifestyle modification processes in a complex chemical and multi-species environment. Importantly, we have identified various molecular factors involved in the *H. influenzae* adaptation to a range of environmental conditions, as well as molecular factors involved in mediating *H. influenzae* and *S. pneumoniae* interactions. We have identified that the *H. influenzae* response to different environmental conditions is complex and multifactorial, and that it is further complicated by the interactions dynamic observed in the presence of *S. pneumoniae*.

Chapter 2

Materials and Methods

Overview

This Chapter describes the bacterial strains, reagents as well as experimental conditions used throughout the body of this thesis.

These experimental procedures relate to the analysis of planktonic growth and biofilm formation of a range of *H. influenzae* strains in varying environmental conditions as well as the establishment of these growth environments. The establishment of mixed-culture growth assays of *H. influenzae* and *S. pneumoniae* in batch and continuous flow cell conditions are also described. The procedures involving harvesting and purifying bacterial RNA from both *H. influenzae* and *S. pneumoniae* cells are also documented, as is the bioinformatics procedure used to obtain transcriptomics data from the samples.

2.1. Bacterial strains used

To identify biofilm formation potential of *H. influenzae* strains, a set of 65 clinical isolates and the laboratory *H. influenzae* strain RdKW20 was used, which included both encapsulated strains, and NTHi strains (Table 1.1). A full list of wild-type and modified *H. influenzae* and *S. pneumoniae* strains used throughout this study, is presented in Table 1.1.

Table 2.1. Complete list of wild-type and modified *H. influenzae* and *S. pneumoniae* strains used in this study, including information about capsular type, disease source and genetic modification of strains.

Strain	**Capsular Type**	**Disease source**	**Modification**
***H. influenzae* strains**			
Rd KW20	Serotype D non-capsular	Blood isolate; laboratory strain	Non-capsular
86-028NP	NTHi (non-typeable)	OM	-
162	NTHi	OM	-
285	NTHi	OM	-
375	NTHi	OM	-
432	NTHi	OM	-
477	NTHi	OM	-
486	NTHi	OM	-
1008	NTHi	OM	-
1124	NTHi	OM	-
1158	NTHi	OM	-
1159	NTHi	OM	-
1180	NTHi	OM	-
1181	NTHi	OM	-
1200	NTHi	OM	-
1207	NTHi	OM	-
1231	NTHi	OM	-
1232	NTHi	OM	-
1247	NTHi	OM	-
1268	NTHi	OM	-
1292	NTHi	OM	-
86-0272MEE (MEE)	-	OM	-

86.027NP (NP)	-	Nasopharynx	-
C486	NTHi	OM	-
C505	NTHi	OM	-
C1344	NTHi	OM	-
Eagan	Serotype B	CSF	-
HI667	NTHi	OM	-
NT001	NTHi	-	-
NT002	NTHi	-	-
NT003	NTHi	-	-
NT004	NTHi	-	-
NT005	NTHi	-	-
NT006	NTHi	-	-
NT007	NTHi	-	-
NT008	NTHi	-	-
NT009	NTHi	-	-
R1527	Serotype F	CSF	-
R1831	Serotype F	Blood or CSF	-
R2866	NTHi	Blood	-
R3022	NTHi	Healthy child	-
R3023	NTHi	Healthy child	-
R3140	NTHi	OM	-
R3141	NTHi	OM	-
R3157	NTHi	OM	-
R3264	NTHi	Healthy child, middle ear	-
R3265	NTHi	Healthy child	-
R3327	Serotype D	Blood	-
R3363	Serotype E	-	-
R3368	Serotype e	Healthy child	-
R3567	NTHi	Blood	-
R3570	NTHi	Blood	-
R3579	NTHi	Blood	-
R3601	NTHi	Blood	-
R539	-	-	-
R540	-	-	-
R541	-	-	-
R542	-	-	-
R543	-	-	-
R547	Serotype D	Throat	-
R874	-	-	-
RM7004	-	-	-
981	NTHi	OM	-
R2846	NTHi	OM	-
723	NTHi	OM	-
BS139	-	OM	Naturally *comA-F-; pilT-*

BS171	-	OM	Naturally *comA-F-; pilT-* -
Modified *H. influenzae* strains			
RdKW20 *nikQ-*	Serotype D	Blood origin	*nikQ-*
86-028NP *nikQ-*	NTHi	OM origin	*nikQ-*
R2866 *nikQ-*	NTHi	Blood origin	*nikQ-*
***S. pneumoniae* strains used**			
D39	Serotype 2	Blood	-
11	Serotype 3	OM	-
11 SCV	Serotype 3	OM	Small colony variant developed after prolonged growth in a flow-cell co-culture in CDM+glucose conditions
Modified *S. pneumoniae* strains			
D39 *lytA-*	Serotype 2	OM origin	*lytA-*
D39 *spxB-*	Serotype 2	OM origin	*spxB-*
D39 *glpO-*	Serotype 2	OM origin	*glpO-*
D39 *blpY-*	Serotype 2	OM origin	*blpY-*

2.2. Growth media used for bacterial growth and biofilm formation assays and throughout experimental procedures.

For the biofilm formation assays of *H. influenzae* strains, as well as throughout experimental procedures analyzing *H. influenzae* growth at different pH levels, and *H. influenzae* and *S. pneumoniae* co-culture interactions, 2 types of growth media were used: HI media and CDM.

HI media (Oxoid) was used a media rich in carbon source, and has been previously described as a growth medium for *H. influenzae*. HI media was prepared as 3.7% (w/v) HI powder (Oxoid) and dissolved in MiliQ water, and subsequently autoclaved at 121ºC for 15min. The pH of the growth medium after preparation and autoclaving was approximately pH 7.2. Where appropriate, the pH was adjusted to 6.8 with HCl , or to pH 7.4 and 8.0 with NaOH or KOH. Due to the growth requirements of *H. influenzae* for hemin and NAD, the HI media was supplemented with10 µg/ml Hemin (0.1% w/v hemin, 0.1% w/v L-histidine) and β-NAD (2 µg/ml).

For sub-culturing of *H. influenzae*, as for plating in order to determine CFU/ml, solid HI media agar was used. For solid HI agar, 1.5% (w/v) agar was added to HI media solution, autoclaved at 121ºC for 15min, and subsequently supplemented with 10% (w/v) Levinthal blood, prepared as previously described (Irino et al. 1988). For sub-culturing *S. pneumoniae*, HI media was supplemented with defibrinated horse blood (Oxoid) at a 1/10 ratio, and gentamycin at a concentration of 5µg/ml. HI media supplemented with defibrinated horse blood and gentamycin was also used as a selection growth media for selection of *S. pneumoniae* strains in co-culture.

The chemically defined medium (CDM) used for the assays has been previously described to be appropriate for *H. influenzae* cell culture (Coleman et al. 2003). For CDM containing glucose or lactose as the carbon source, glucose or lactose was added to the growth medium at a

concentration of 2g/L, respectively, and the growth medium was sterilized by filter sterilization through a 0.2μm Millipore filter.

2.3. Bacterial growth and storage conditions

All bacterial strains used were stored at -80ºC as 30% glycerol stocks. Fresh colonies were taken from glycerol stocks and streaked onto HI agar plates, after which the plates were incubated overnight at 37ºC at 5% CO_2 in a SANYO CO_2 incubator.

For storage, all bacterial strains were grown in HI media to mid-long phase (OD_{600}=0.3), and centrifuged at 4000rpm for 10 min. The cell pellet was then resuspended in 2ml of HI media with 30% glycerol and stored in 2ml tubes (Eppendorf). Cells were stored at -80ºC in a SANYO Ultra-Low Freezer - 80 MDF-U73V.

2.4. *H. influenzae* biofilm formation screening assay

To identify strains possessing biofilm formation capabilities, mono-species biofilm assays of *H. influenzae* were performed, using the O'Toole and Kolter microtitre plate biofilm assay as previously described (O'Toole and Kolter 1998; Greiner et al. 2004). Cultures of *H. influenzae* strains were grown to an OD_{600} of 0.6 and diluted into HI media or CDM at a 1:10 ratio. The bacterial suspensions were then inoculated into a 96 well plate for 16 h, and incubated at 37°C with 5% CO_2. An OD_{600} measurement was taken at 6 h and 16 h to quantify growth. Subsequently, media was removed, and the biofilm was stained with 0.1% crystal violet for 1 h, after which the plates were rinsed with sterile water and air dried. The CV was resuspended in 30% acetic acid, and an OD_{600} reading was taken to quantify biofilm formation. The biofilm

formation value was normalized to growth by calculating the value of (after CV staining OD_{600}/OD_{600} growth value).

For biofilm formation screening assays utilizing *H. influenzae*, either HI or CDM media was used. Initially biofilm formation assays were performed in the absence of stress in either media. Subsequently, growth curves were performed using a small subset of *H. influenzae* strains in order to determine sub-lethal concentrations of stress compounds formaldehyde, H_2O_2 and mtethylglyoxal which would reduce *H. influenzae* growth compared to conditions of absence of stress, but would still allow growth in their presence.

In HI media, the optimal sub-lethal concentrations of stress were determined to be 0.0137% for formaldehyde (Sigma-Aldrich), 0.016% for H_2O_2 (Sigma-Aldrich), and 0.6% methylglyoxal (Sigma-Aldrich). In CDM, the optimal sub-lethal concentrations of stress were determined to be 0.002% for formaldehyde (Sigma-Aldrich), 0.005% for H_2O_2 (Sigma-Aldrich), and 0.008% for methylglyoxal (Sigma-Aldrich). After determining these optimal sub-lethal concentrations of stress compounds, further large-scale biofilm screening of 65 clinical *H. influenzae* isolates was performed in the presence of these concentrations in the presence of stress.

2.5. Batch culture growth assay: Determining bacterial planktonic and biofilm cell numbers by CFU/ml.

To determine bacterial planktonic and biofilm cell numbers as CFU/ml, initially a batch culture growth assay was performed. Bacterial cells were taken from HI agar plates and inoculated into 10 ml HI media, and grown with moderate aeration (with shaking at 100 rpm) to mid-log phase (OD_{600}-0.3). Subsequently, the culture was diluted into fresh HI media at a 1/20 dilution and 200µl was inoculated into a 96-well plate (Microtest U-bottom, polystyrene, non-tissue culture treated plates, Falcon). Three replicate wells were inoculated for each conditions/strain used. The plate was covered with a breather easy sealing membrane (Sigma-Aldrich), and were grown in a Biotek (ES260) microtitre plate reader at 37ºC. To obtain growth curves, OD_{600} readings were taken every 30 min. After 14-16 h of incubation, the plate was removed from the microtitre plate

reader. To obtain planktonic CFU/ml cell counts, 20 µl of each cell culture was taken from the microtitre plate and diluted into 180 µl of sterile PBS. Serial dilutions were performed in the following manner from 10^{-1} to 10^{-8} and 20 µl of each dilution was plated onto a HI agar plate, and the HI plates were incubated overnight at 37ºC at 5% CO_2. Colonies were counted and CFU/ml calculated (CFU/ml = (number of colonies × $10^{\text{Dilution factor}}$)/0.02). To determine the biofilm growth levels, firstly the planktonic cells present in the wells were removed. Subsequently, the biofilms were washed three times with 200µL of either LB growth media or HI media, after which 100 µL of HI media was added to each biofilm-containing well. The cells were then detached by sonication for 3 seconds (Soniclean sonicating waterbath, a protocol established to disrupt bacterial attachment and aggregation), followed by removal of 20 µL from each well and performing serial dilutions from 10^{-1} to 10^{-8} and plating onto HI agar plates.

2.6. Biofilm formation assays in the presence of DNAseI

In order to analyse the biofilm formation of a set of *H. influenzae* isolates in the presence of DNAseI, a biofilm formation assay was set up in HI or CDM media, where the media was supplemented with DNAseI to a final concentration of 166 µg/ml. The cells were incubated in the presence of DNAseI for 16 h, after which the OD_{600} of the cells was measured, and the planktonic cells were removed, and the biofilm stained with CV and quantified for biofilm formation.

2.7. Screening the *H. influenzae* isolates for the presence of *pilA*.

In order to identify the presence of the *pilA-pilB* segment in *H. influenzae* isolates, a PCR reaction was established using the primers *pilA* FOR – 5' –CGTTGCCAACAAAGGCTTAAT-3', and *pilB* Seg1REV – 5' –GAAATGCTTGTTGCTGATTTTC-3'. *H. influenzae* cell lysates were prepared by resuspending a *H. influenzae* cell pellet in 200µl of sterile PBS and heating at

95ºC for 20 min. Subsequently, the solution was centrifuged at 13,000 rpm for 1 min, after which the supernatant containing the *H. influenzae* DNA was used as the DNA template for the PCR reaction. For this PCR reaction, an annealing temperature of 52ºC was used, and the extension time used was 1 min. The DNA polymerase used for all reactions was the Phusion HF DNA polymerase (NEB), and the reaction components and conditions were performed as in the instruction manual of the product manufacturer.

To check for the presence of the expected 1.3 kb band, indicating the presence of the *pilA-pilB* segment, the PCR reaction product was loaded onto a 1% agarose gel and run for 45 min at 100mV.

2.8. Chromosomal inactivation of *nikQ* and *gloA* from 86-028NP

A 1.5 kb DNA fragment containing the putative *nikQ* from 86-028NP strain (annotated as *cbiQ*; NTHI1421) and flanking DNA sequences was amplified by PCR from *H. influenzae* 86-028NP using the following primers: 1421-KOF (50-CTGCTCTGCGATATGATACG-30) and 1421-KOR (50-CTGTGGGGTTACGTCGTTTA-30). PCR was carried out using 96 ºC for 10 min, then 30 cycles of 96 ºC for 30 s, 55 ºC for 30 s and 72 ºC for 3 min, followed by a final extension step of 72 ºC for 10 min. PCR products were purified (QIAquick PCR purification Kit, Qiagen, USA) and cloned into pT7Blue Perfectly Blunt Cloning Vector (Novagen, USA), creating the plasmid pT7Blue::*nikQ*-KO. This plasmid was linearized by digestion with BglII (New England Biolabs, USA), digesting the DNA within the *nikQ* gene. This was then treated with Mung Bean Nuclease (NEB, USA) to remove the single-stranded DNA overhangs. The kanamycin resistant gene cassette from pUC4Kan was isolated by digestion with HincII and extracted from a 1% agarose gel using a QIAquick gel extraction kit (Qiagen, USA). This cassette has no promoter or terminator and does not affect transcription or create a polar effect. The kanamycin resistant cassette was phosphorylated and cloned into the digested pT7Blue-T::*nikQ*-KO clones. The orientation of the insert was determined and then the construct with the kanamycin resistance open reading frame (ORF) in the same orientation as the NTHI1421 were selected. The

pT7Blue::*nikQ*-KO::*kan* was linearized with BglI and transformed into *H. influenzae* 86-028NP as described by Herriott et al. (1970). 23 Mutants were created by double cross-over and recombinant colonies were selected on BHI plates with 20 mg/ml kanamycin.

Site-specific recombination of *nikQ*::*kan*R was confirmed by PCR using a primer within the primers NTHI1421-koSCR-F (50-GTGTGATACCAAGACGTTC-30) and a primer located on the *H. influenzae* chromosome and outside the sites used to generate the original construct, NTHI1421-KOSCR-R (50-TGGTGCAGTGCTTGCTGT-30). The resulting PCR product was purified and sequenced to confirm the correct insertion. The *gloA* gene from 86-028NP (NTHI0441) was inactivated using the same protocol. The initial PCR used the primers: NTHI*gloA*-KO-For: GATTTACCGCCTCAGGAG and NTHI*gloA*KO-Rev: CTTTACGCCAGTGCGTTCA. The kanamycin resistant cassette was cloned into a NruI restriction site within the *gloA* gene. The resulting kanamycin resistant strains were confirmed as the result of a correct recombination event by PCR using the primers: NTHI*gloA*-check-For: ATTCAAGCACTTGAAGCG and NTHI*gloA*-check-Rev: GCCAAAAGGGTGGAAGG.

In strain R2866, the *nikQ* gene was inactivated by transforming into competent R2866 cells sheared chromosomal DNA extracted from 86-028NP *nikQ*::kanR. The resultant *kanR* transformants were screened for the correct insert using the same primers as used for 86-028NP.

2.9. Cell aggregation assay

Broth cultures of selected *H. influenzae* strains were grown overnight in BHI at 37 ºC and 220 rpm. The overnight cultures were adjusted to a similar optical density (OD_{600nm}) by dilution with BHI broth (OD of 0.7). The cultures were then left stationary at room temperature. Every 1 h, 200 µl was taken from the culture–air interface and the OD_{600nm} measured.

Assays were performed in triplicate and each experiment was performed at least three times. To further assess the aggregation of the cells, phase contrast microscopy was used to examine the cells. The samples taken in the aggregation assay were mounted on glass slides with a coverslip and viewed with an Olympus IX-70 microscope and phase contrast optics using 40x oil immersion objective. Samples throughout these experiments; from the overnight aggregation assay, and from the samples taken, were also plated onto BHI plates to assess their viability.

2.10. Metal content in *H. influenzae* strains

To quantify intracellular metal content (nickel, cobalt, magnesium, manganese, iron and zinc) in the wild type *H. influenzae* 86-028NP and its *nikQ* mutant, ICP-MS (Inductively-Coupled Plasma Mass Spectrometry, Adelaide Microscopy) was performed. These strains were grown in broth culture overnight and then collected by centrifugation (8000x g, 20 min). The harvested cells were washed three times with EDTA (1 mM) to ensure extracellular metal content was removed and then resuspended in 2 ml filtered MilliQ water. A 1 ml aliquot was allowed to dry overnight (80ºC) and the dried weight measured. To the remaining 1 ml, concentrated (69%) nitric acid was added. The samples were then diluted to a concentration of 2% nitric acid and then analysed by ICP-MS.

2.11. Determination of the surface charge; zeta potential

Overnight cultures were grown for 6 h at 37 ºC, 220 rpm. Bacteria were pelleted (3200x g for 10 min) , washed twice in 5 ml of 15 mM sodium chloride (pH 6.5) and finally resuspended in buffer at specific pH. The zeta potential was measured using a zeta particle size analyzer (Malvern, UK); 1 ml cell samples were added to ZetaSizer Nano series folded capillary cell (Malvern, UK). Each sample was measured 30 times and an average calculated and each sample was performed in triplicate.

2.12. Urease assays

Qualitative analysis of urease activity was assayed as described previously (Young et al. 1996). Fresh overnight cultures of *H. influenzae* were inoculated into 5 ml HI broth and grown to an OD_{600nm} 0.4. For comparison between strains, an equal number of cells were plated onto HI agar plates and incubated at 37 1C, 5% CO2 for 18 h. The cultures were overlaid with the urease activity solution (0.01% w/v phenol red, 0.3 M urea, 0.5% w/v agarose) and left for one minute. Urease activity was indicated by the red colour of the phenol red, indicative of a pH > 6.5.

Quantitatively, urease activities were assayed as follows. An overnight culture of cells grown in HI were pelleted and resuspended in lysis buffer (5 ml PBS with 330 mg lysozyme and 130 mg sodium deoxycholate). DNaseI (1.6 mg) was added and cell debris was removed by centrifugation. Increasing amounts of the clarified lysate supernatant were added to 200 µl of substrate solution (50 mM urea in PEB: 100 mM sodium phosphate, 10 mM EDTA, pH 7.5). The mixtures were incubated at room temperature for 30 min before adding 400 µl phenol nitroprusside and 400 µl alkaline hypochlorite. After incubation at 50ºC for 1 h, absorbance values at 625 nm were measured. A blank for the activity was generated using cell extracts that were deactivated by boiling at 100 ºC for 5 min. The final amount of NH_4Cl generated from the assay was calculated by creating a calibration curve of NH_4Cl concentrations (1000, 500, 250, 125, 62.5, 31.25 mM). The total protein was measured for each sample and the results were calculated as mg of NH_4Cl generated per mg total protein per minute (units per mg). To assess the inactivation of urease activity by flurofamide fresh overnight cultures of *H. influenzae* were assayed for urease activity in the presence of 0, 2.5, 5, 10, 20 and 50 mM flurofamide. The activities were 4.22 ±0.366 Units per mg total protein, 3.80 ±0.322, 1.66 ±0.223, not detectable (ND), ND, and ND, respectively. As with previous reports, urease activity was not detectable with 10 mM flurofamide, this concentration was used throughout the study. Whenever flurofamide was used, quantitative assays were performed to confirm no urease activity was present.

2.13. Twitching motility assays

There is noted variability in *H. influenzae* motility assays; we therefore took two different approaches and repeated assays with several biological replicates (Harvey et al. 2009; de Bernonville et al. 2014; Filloux and Ramos 2014). Briefly, overnight cultures were inoculated as a standard 10^7 CFU onto 0.8% agar (CDM). The plates were allowed to grow for 24–48 h and the zone of growth through the agar created by twitching motility was visualized (this could be measured). Further to this the initial inoculum was stabbed into the media and the resultant zones of twitching motility were assessed by removing the agar and staining the bacteria adherent to the polystyrene petri dish by staining with crystal violet (1% w/v). Each assay included four replicates and the assays were performed at least three times.

2.14. Strains used for co-culture assays

The *H. influenzae* strains used for co-culture experiments were Rd KW20, 86-028NP (a non-typeable strain, NTHi), R3157 (a NTHi OM isolate).

The *S. pneumoniae* D39 (wild-type) strain, and its D39 *lytA*$^-$, D39 *spxB*$^-$, D39 *glpO*$^-$ mutant strains have been described previously (Berry et al., 1989; Mahdi et al., 2012). Additionally the wild-type strain 11 (an otitis media isolate of serotype 3) was used (McAllister et al., 2011).

2.15. Construction of a *blpY* gene knock out strain in *S. pneumoniae* D39.

The *blpY* gene was deleted from *S. pneumoniae* D39 and replaced with a spectinomycin resistance cassette by transformation with a linear DNA fragment constructed by overlap extension PCR as previously described (Horton et al. 1992).

The primer pairs used to amplify regions 5’ and 3’ to the *blpY* gene were *blpY* F – “TCATATAGTGGATAGGTCT”,

blpY Spe R – "TATGTATTCATATATATCCTCCTCAGAAATCCTCCCTCATTTCT" and

blpY Spe F –"AAATAACAGATTGAAGAAGGTATAAAGGCTTGCTTTTCAGCCAT", *blpY* R – "AGCGAGGTTACAAGAAGACT".

The spectinomycin resistance cassette was amplified using the primer pairs

Spec F – "GAGGAGGATATATATGAATACATA" and

Spec R – "TTATACCTTCTTCAATCTGTTATTT".

Subsequently, all 3 PCR fragments were combined and amplified in an overlap PCR reaction to create a DNA fragment comprising the *blpY* 5' and 3' regions flanking the spectinomycin resistance cassette. The *S. pneumoniae* D39 strain was transformed with this construct and selected for spectinomycin resistance, with the successful inactivation of *blpY* being confirmed by PCR.

2.16. Pre-culture conditions used for co-culture assays

S. pneumoniae strains were sub-cultured on HI (Oxoid) agar supplemented with defibrinated horse blood and gentamycin, and incubated overnight at 37ºC/5% CO_2.

H. influenzae strains were sub-cultured on HI agar supplemented with 10% w/v Levinthal blood, incubated overnight at 37ºC/ 5% CO_2. Both species were grown in HI media supplemented with10 µg/ml Hemin (0.1% w/v hemin, 0.1% w/v L-histidine) and β-NAD (2 µg/ml). While the respiratory tract is not known to be a nutrient rich environment, preference was given to HI media for growth analyses rather than a defined media. Firstly, genome analyses have shown that *S. pneumoniae* possesses a higher number of carbohydrate utilisation genes than other members of the respiratory tract microflora, suggesting an adaptation to a multispecies environment where multiple carbon sources are present (Buckwalter and King 2012). Before an initial growth and transcriptomic analysis of the two species, we could not predict either the metabolic pathways

utilised by each species in such an environment, or the consequences of any potential metabolic sharing. Hence, we used a nutrient-rich HI media to globally analyse and gain a comprehensive understanding of the growth and interactions between species in an environment containing various carbon sources.

For further co-culture analyses where CDM with glucose or lactose was used as the growth medium, pre-culture was also performed in CDM containing the appropriate carbon source.

2.17. Co-culture growth analysis in batch culture.

For co-culture growth analyses utilizing HI media, *H. influenzae* was pre-cultured in supplemented HI media, with shaking at 100 rpm, until an OD_{630} of 0.3 was reached. Likewise, *S. pneumoniae* was pre-cultured statically in HI media, until an OD_{630} of 0.3 was reached. Subsequently, cultures were diluted 1/10, and 100 µl of each culture were then added to 100 µl of the 1/10 dilution of the alternate species (for co-culture growth), or an equal volume of supplemented HI media (for mono-culture growth). Cultures were grown statically at 37ºC in a 96-well microtitre plate covered with a Breatheasy membrane (Sigma –Aldrich), and incubated in a microtitire plate reader (Biotek) whereby growth OD_{630nm} readings were obtained every 30 min. (The resulting growth curve established the growth phenotype of cultures before performing a more detailed analysis and determining CFU/ml). After 6 h or 16 h of growth, planktonic and biofilm mono and co-cultures were collected, and 20 µL of appropriate serial dilutions of the cultures were plated onto HI agar or selective blood agar plates containing gentamycin (for selecting for *S. pneumoniae*) at a concentration of 5 µg/ml.

For co-culture growth analyses in CDM, *H. influenzae* was pre-cultured in Chemically Defined Media (CDM), containing glucose or lactose at a concentration of 2 g/L. Pre-culture was achieved with shaking at 100 rpm, until an OD_{630} of 0.25 (determined as the mid-log phase of growth in CDM) was reached. Likewise, *S. pneumoniae* was pre-cultured statically, until an OD_{630} of 0.15-0.2 (determined as the mid-log phase of growth in CDM) was reached. Subsequently, the cultures were diluted 1/10 and added to 100 µL of the 1/10 dilution of the alternate species (for co-culture growth), or an equal volume of media (for mono-culture

growth). Cultures were grown statically at 37ºC in a 96-well microtitre plate in a Biotek microtitrer plate reader. After 16 h of growth, mono and co-cultures were collected, diluted and plated onto HI agar or selective blood agar plates containing gentamycin (selecting for *S. pneumoniae*) at a concentration of 5 µg/ml.

For co-culture growth analysis of the *S. pneumoniae* SCVs and *H. influenzae* in HI media, *H. influenzae* was pre-cultured in HI media, with shaking at 100rpm until an OD_{630} of 0.3 was reached. *S. pneumoniae* SCV was also pre-cultured, statically, until it reached an OD value of 0.3. Subsequently, both cultures were diluted 1/10, and 100µl of each culture was added to an equal volume of HI media, or the other species.

2.18. Co-culture growth in the flow cell system

A flow cell chamber was constructed to permit a constant in-flow of media into the chamber using a peristaltic pump and an equal out-flow. For growth in the flow cell system, three individual flow cell chambers of a volume of approximately 30 ml were sterilised by autoclaving and subsequently connected with sterile silicone tubing to inlet chambers containing supplemented HI media, and outflow waste containers. To induce flow, the silicone tubing connecting the inlet media and the flow cell chambers was connected to a peristaltic pump. After each chamber was filled with supplemented HI media and inoculated with 2 ml that contained 1 ml of a 1/10 dilution of an OD_{630} of 0.3 culture of *H. influenzae* and *S. pneumoniae* for co-culture, or 1 ml of either species supplemented with 1 ml supplemented HI media for the mono-culture analysis. After inoculation, cultures were left for 1 h to adapt to flow cell chamber conditions without flow, after which, flow at a rate of 3 ml/h, was applied. For growth experiments utilizing HI and CDM+lactose/+glucose media, samples were taken at 24 h intervals and samples from selected time-points were then assessed for CFU/ml, sampled for RNA extraction and examination using Scanning Electron Microscopy (SEM).

2.19. Statistical Analysis

All experiments were performed in triplicates and repeated at least twice. The presented data on figures represents collated data from 2 independent experiments with 6 replicates in total. Error bars represent the standard deviation from the mean for the replicates used in the experiment.

For statistical analysis of the CFU/ml growth data of *H. influenzae* and *S. pneumoniae* growth in mono- and co-cultures, an unpaired Student T-test (two-tailed) was used. Statistically significant results are presented as * $p<0.05$, ** $p<0.01$, *** $p<0.001$, or **** $p<0.0001$.

2.20. RNA extraction

For RNA extraction of strains Eagan and R3264 (at pH 6.8 and 8.)), cells were directly added to Phenol/ Ethanol solution. The composition of phenol/ethanol solution is; 5% v/v Phenol (pH 4.3) and 95% v/v ethanol. The ratio used is 2/5 of the total cell culture volume: phenol/ ethanol. This was left on ice for 2 hours before being centrifuged for 5 min. (4°C/4000×g) and the supernatant discarded. The cell pellet was kept at −80°C until RNA extraction.

For cells analysed in experiments pertaining to co-culture conditions as well as for cells used in the comparison of Rd KW20 and Rd KW20 *nikQ*-, cells collected from batch culture and flow cell experiments were transferred directly to an equal volume of RNA Protect bacterial reagent (Qiagen), vortexed, incubated for 5 min at room temperature, and centrifuged (4,000 x *g* for 10 min). The resulting cell pellet was stored at -80ºC.

For the RNA extraction of Eagan, R3264, Rd KW20 *nikQ*- and its wild-type, RNA was extracted with the Qiagen RNeasy kit, as described by the manufacturer.

For the RNA extraction of all cultures pertaining to batch and flow cell mono- and co-culture analyses, a combination of the hot phenol extraction method and a commercial RNA extraction kit (Qiagen, RNeasy Mini Kit) were utilised to achieve greatest RNA yield. Firstly, the cell pellet was resuspended in 400 µl of hot (65ºC) phenol-chloroform mix, and placed at 65ºC for 5 min.

Subsequently, 400 µl of hot (65ºC) NAES (50mM Sodium acetate pH 5.1; 1% SDS) was added to the cell pellet/phenol chloroform mix. The mixture was mixed, and incubated at 65ºC for 5 min. The mixture was then placed on ice for 1 min, and centrifuged at 10,000 x *g* for 2 min. After centrifugation, the upper aqueous phase was removed and resuspended in 400 µl of hot (65ºC) phenol-chloroform for 5 min, after which it was placed on ice for 1 min, and subsequently, centrifuged at 10,000 x *g* for 2 min. The upper aqueous phase was removed and further RNA extraction from the lysate was performed with the Qiagen RNeasy Kit as described by the manufacturer with omission of the lysis step.

2.21. Transcriptomics analysis

The RNA quality of the samples was confirmed with the Agilent 2100 Bioanalyzer (according to Agilent RNA 6000 Nano kit standard protocol). For each sample three biological replicates of cell growth, harvesting and RNA extractions was performed. The replicate RNA was pooled and supplied to the Adelaide Cancer Genomic Research Facility (Adelaide, Australia) or the AGRF (Australian Genome Research Facility, Australia) for library preparation and sequencing (RNAseq) using either the Ion Proton platform (Ion Torrent, Life Technologies) or the Illumina platform . The resulting data from the RNAseq was provided in fastq files format. For alignment of the genomes, the reference genomes of Rd KW20 (for *H. influenzae* Genbank: NC_000907) and OXC141 (a serotype 3 strain of *S. pneumoniae*, Genbank: NC_017592, for *S. pneumoniae*) were used. First, the fastq files were aligned to the reference genomes, using bowtie2 in the local mode. The resulting sam files were then converted to bam file format, and then to the bed file format. Subsequently, the bed files were aligned to the reference genomes in gff format to create a bed file format containing read numbers aligned to genes. The statistical analysis was performed with the DESeq package in R, to identify the genes with a $\log_2$ fold change>2 that was statistically significant with p-values controlled at <0.05 or 0.1 where specified.

2.22. Scanning Electron Microscopy (SEM).

For SEM, the bacterial cell culture at a volume of 2-3 ml was filtered through a 0.2 μm Millipore filter. Subsequently, the cells on the filter were fixed in SEM fixative solution (4% paraformaldehyde and 1.25% glutaraldehyde in Phosphate Buffer Solution and 4% sucrose, pH 7.2). Samples were then treated with 2% osmium tetroxide, after which samples were dehydrated using ethanol and then with hexamethyldisilazane (HMDS). All the samples were then mounted on stubs, coated with platinum and visualized using Field Emission Scanning Electron Microscope (Philips XL30, Adelaide Microscopy).

Chapter 3

Biofilm formation of *H. influenzae* is determined by a combination of strain-specific factors and environmental conditions.

Overview

In this Chapter, we have shown that the biofilm formation of *H. influenzae* was highly strain-specific and was influenced by the growth media used, as well as by the presence of ROS or RCS compounds.

The strain-specificity of biofilm formation was unrelated to the disease source of the strain or to the presence of the *pilA* gene, however, the presence of eDNA was shown to play a role in the biofilm formation of some strains.

In addition, we have shown that the enhanced biofilm formation of a *nikQ* mutant of *H. influenzae* unable to import nickel, is related to a global transcriptomics response related to the alteration of cell surface structures, and modification of intracellular metabolism. We have also identified the presence of the *nikKLMQO-nimR* operon in a biofilm forming strain 86-028NP, and have shown the importance of nickel in the increased aggregation and biofilm formation, as well as its role in the decrease of twitching motility of this strain.

3.1. Introduction.

3.1.1. The role of environmental stresses in *H. influenzae* biofilm formation.

While it is known that *H. influenzae* can form a biofilm, and that it is this biofilm which is involved in causing chronic opportunistic infections of the airways including OM (Hall-Stoodley et al. 2006; García-Cobos et al. 2014) and chronic rhinosinusitis (Sanderson et al. 2006), little is known about the mechanisms leading to biofilm formation.

Bacterial cells within a biofilm are often resistant to exogenous antibiotics and inflammatory agents, and this has been attributed in part to an altered physiological and metabolic rate of biofilm cells, as well as to the presence of an extensive extracellular polymeric substance (EPS) matrix, which has been shown to provide protection for cells within a biofilm against exogenous antimicrobial compounds (Davies 2003). Hence, a biofilm lifestyle can allow for a bacterial community to persist and remain protected from exogenous harmful compounds. As a biofilm lifestyle has been shown to protect the bacterial cells from environmental stresses, including antimicrobial compounds (Williams et al. 1993), sensing sub-lethal levels of stress could allow the bacteria that are able to induce the biofilm lifestyle to do so, and hence remain in a protected environment and promote their survival. Previous studies have shown that other bacterial species, such as *Staphylococcus epidermidis* induce biofilm formation upon sub-lethal levels of antimicrobial stress (Rachid et al. 2000). In addition, a recent study has demonstrated that the presence of sub-inhibitory levels of β-lactam antibiotics increases *H. influenzae* biofilm formation in a strain-dependent manner (Wu et al. 2014). A higher pH of 8.0, and a lower oxygen tension was also shown to induce NTHi biofilm formation (Osgood et al. 2015).

It has also recently been shown that the addition of glucocorticosteroids was able to influence *H. influenzae* biofilm formation, and enhance the resistance of the biofilm to antibiotic treatment (Earl et al. 2015).

In addition to therapeutically-administered antibiotics, which can acts a stressors and induce biofilm formation, there is a range of antimicrobial compounds occurring naturally in the human host, which can acts as stressors for the bacterial cells, and induce protective mechanisms such as biofilm formation. Reactive oxygen species (ROS) and reactive carbonyl species (RCS) are examples of chemical stresses that are relevant to the *H. influenzae* lifestyle within the human host. Importantly, both ROS and RCS are damaging to cellular proteins and nucleic acids (Cabiscol et al. 2010; Voulgaridou et al. 2011). ROS include compounds such as the superoxide and H_2O_2 produced by host neutrophils and macrophages as a response to bacterial infection (Hampton et al. 1998; Dahlgren and Karlsson 1999). ROS can also be generated by aerobic metabolism of other bacterial species of the human nasopharynx, as well as endogenously by the *H. influenzae* aerobic metabolism (Pericone et al. 2000). It is important to note that studies into other bacteria have shown that these exact stresses do stimulate biofilm formation; for example, *S. aureus* was shown to enhance biofilm formation in the presence of the ROS H_2O_2, the reactive nitrogen species GSNO, and RCS including methylglyoxal and malonaldehyde (Kulkarni et al. 2012; Bui et al. 2015).

RCS include molecules such as reactive aldehydes methylglyoxal, acrolein and formaldehyde, which have a potential to induce damage to cellular proteins and DNA (Voulgaridou et al. 2011). Formaldehyde is such a reactive aldehyde, and is present as an environmental contaminant (Clarisse et al. 2003), and may also be produced in the nasopharynx by eukaryotic cytochrome p450-dependent mono-oxygenases (Dahl and Hadley 1983). Methylglyoxal is another RCS, which is known to be produced as a by-product of bacterial metabolism from dihydroxyacetone phosphate through the action of methylglyoxal synthase (Ferguson et al. 1998).

H_2O_2 is a ROS which is known to be produced by host neutrophils and macrophages as a response to infection (Dahlgren and Karlsson 1999) and is also produced by the nasopharyngeal commensal *S. pneumoniae* as a result of SpxB activity during its growth (Pericone et al. 2000). As *H. influenzae* and *S. pneumoniae* share a niche, *H. influenzae* is likely to encounter H_2O_2 as a result of its interactions with *S. pneumoniae*.

Therefore, as a result of the *H. influenzae* occupation of the complex nasopharyngeal environment, it would be susceptible to encounter multiple ROS and RCS both as a result of its own metabolism, as well as from contact with these exogenous agents as host or microbiome factors, or as environmental contaminants. However, to date, the impact of these ROS and RCS on *H. influenzae* biofilm formation have not been studied.

3.1.2. The role of the EPS matrix in the biofilm formation of *H. influenzae*.

The EPS matrix is a vital element of the biofilm, facilitating biofilm stability and shear force resistance, adhesion and cohesion properties (Flemming and Wingender 2010). It is likely that strains capable of forming a more robust EPS matrix are at an advantage within the community for their biofilm formation and indeed are selected for within the biofilm.

The components of the EPS are generally known to include proteins, polysaccharides and extracellular DNA. The exact nature of these varies between and even within the EPS of the biofilm formed by a bacterial species. However, the EPS matrix components of the *H. influenzae* biofilm are largely unknown.

Recently, both type IV pili and extracellular DNA (eDNA) have been identified in mono-species biofilms of *H. influenzae* in a chinchilla model of OM *in vivo* (Jurcisek et al. 2007). In the *H. influenzae* mono-species biofilm, type IV pili were shown to increase adhesion, and biofilm stability in the *H. influenzae* biofilm, as well as playing a role in twitching-motility (Bakaletz et al. 2005; Jurcisek et al. 2007; Carruthers et al. 2012). In addition, *pilA*, encoding the major subunit of the type IV pili was shown to be up-regulated in the *H. influenzae/S. pneumoniae* multi-species biofilm, and therefore particularly interesting in the context of this work (Cope et al. 2011).

The type IV pili are also known for their ability to bind DNA (van Schaik et al. 2005), and in *H. influenzae* biofilms, type IV pili were found to co-localise with eDNA strands (Jurcisek and Bakaletz 2007). An eDNA-binding role for type IV pili could impact the structure and intra-organisation of the biofilm. It has been demonstrated that for *P. aeruginosa* biofilms, both type IV pili and eDNA allow for a formation of a complex structured biofilm (Barken et al. 2008). *H. influenzae* has been shown to harbour eDNA in the EPS biofilm matrix, and this component is a vital structural component of the mono-species biofilms, as well as having proposed roles as a nutrient source, an adhesin (Das et al. 2010), and a source of genetic variation for naturally competent cells (Ehrlich et al. 2010). In addition, the presence of eDNA has been shown to be vital for the efficient self-organisation of cells within the biofilm (Gloag et al. 2013). While type IV pili and eDNA have been studied in the context of the *H. influenzae* mono-species biofilm, it

remains unclear what role these EPS matrix components play in the strain-specificity of the *H. influenzae* biofilm formation. It is possible, that the nature or levels of the presence of particular elements in the biofilm may be the basis for strain-specific selection. We hypothesized, that the strain-specificity of biofilm formation could be related to the presence, or temporal regulation of the expression of EPS-related genes. We further hypothesised, that the biofilm forming ability of a strain that is able to release increased amounts of eDNA into the biofilm matrix would be greater compared to a strain which is unable to release large amounts of eDNA. These hypotheses were a focus for this study, as the large scale screen of *H. influenzae* biofilm formation in different conditions (Fig. 3.1-3.8), was performed by a crystal violet (CV) staining assay. Crystal violet is able to stain all components of the biofilm, including the cells and the EPS matrix. Unlike cell-counting quantification of biofilm formation, this technique allows for determining of the total biofilm formation, without distinguishing the EPS matrix from the cells. Therefore, we hypothesized, that the high biofilm forming strains may be forming a high level of biofilm, in part, due to the formation of an extensive EPS matrix.

3.1.3. The role of nickel in *H. influenzae* biofilm formation.

In this Chapter, we show that there is a strain-specificity in the ability of *H. influenzae* to form biofilm, and that this strain-specificity was also dependent on the environmental conditions and on the presence of chemical stress. In addition, biofilm formation is a multifactorial process, also dependent on the presence of an EPS matrix. While it is known that the adaptation of a strain to environmental conditions pertinent to its niche may induce or repress biofilm formation, little is known about the intracellular events which stimulate this switch in lifestyle. While we did not investigate the genetic variability between the 65 clinical isolates tested, it is known that specific genetic components play a role in the ability of a cell to survive in specific environmental conditions, and to induce biofilm formation. Previously, it has been shown that in *H. influenzae*, nickel uptake and the nickel uptake system *nikKLMQO-nimR*, has a role in the regulation of cell-cell aggregation and biofilm formation, as well as playing vital role in the adaptation of *H. influenzae* to exogenous stress (Ng and Kidd 2013). The *nikKLMQO-nimR* system was

previously shown to be involved specifically in the import of nickel into the cell, and was shown to be induced in low exogenous levels of nickel, as well as at low exogenous pH. Such a pH dependent role for the nickel uptake system was linked to the requirement of nickel as a cofactor by the urease enzyme; an enzyme involved in maintaining intracellular pH of *H. influenzae*. Importantly, however, the role of nickel in the *H. influenzae* cell, and subsequently the *nikKLMQO-nimR* system in *H. influenzae* appeared to have a broader role, unrelated specifically to low pH levels. The role of nickel and the nickel uptake system in *H. influenzae* served rather a multifactorial purpose, controlling the homeostatic balance between maintenance of cellular functions and control of pH in permitting conditions in the presence of nickel, and facilitating a lifestyle switch to biofilm formation in unfavourable conditions, in the absence of nickel. Specifically, mutants in *nikQ* or the nickel uptake operon regulator *nimR*, showed an equal ability to grow compared to the wild-type, however they also displayed an increased cell-cell aggregation and biofilm formation compared to the wild-type. This phenotype was shown to be unrelated to the inactivation of nickel-cofactored enzymes GloA and/or urease, as a result of reduced nickel levels. It was however shown, that the increased biofilm formation phenotype was related to a change in the overall cell-surface charge of the nickel-deficient cells. Specifically, the cells deficient in *nikQ* were more electronegatively charged and also more hydrophobic compared to the wild-type. Further analysis also uncovered the presence of differences in the lipooligosaccharide (LOS), and the outer membrane proteins (OMP) of the *nikQ* mutant strain compared to its wild-type counterpart. These results suggested, that in an environmental condition when nickel is limited, *H. influenzae* did not display a growth defect, but instead adapted to the limiting environmental conditions to adopt a lifestyle favouring biofilm formation. However, while this lifestyle was shown to incorporate a change in cell-surface structures including LOS and OMP, and resulting in a net increased hydrophobicity and electronegative charge, the specific molecular and regulatory events governing this phenotype were not yet known. In addition, this study did not investigate whether there were additional global changes in the metabolism of these cells. Importantly, in other bacterial species, biofilm formation was also linked to global changes in lifestyle (Waite et al. 2005; Resch et al. 2006; Post et al. 2014), including global changes in metabolic processes. Therefore, a global transcriptomic-based study would be essential in order to uncover the molecular events governing the phenotype of biofilm formation in the nickel-deficient *H. influenzae*.

3.2. Results

3.2.1. Biofilm formation is strain-dependent and related to the growth medium utilised

When the biofilm formation of 65 *H. influenzae* isolates grown in CDM in the absence of stress, was measured, differences were found in the relative ability of these strains to form a biofilm. The amount of biofilm determined as high was equal or greater than the biofilm formation observed for the laboratory Rd KW20 strain (biofilm formation index >2). In CDM media, strains which formed a high amount of biofilm were Rd KW20, NT006, R3157, R3327, R3567, R2866 and R2846 (Fig. 3.1; Table 3.1).

In contrast, using the rich media HI media with no stress, a larger number of strains formed high levels of biofilm. These strains included Rd KW20 and isolates 1124, 1231, NP, C505, 667, NT001, NT005, R2866, R3327, R3363, R3567, R3570, R3601, R542, R2866, 176 and 86-028NP (Fig. 3.2; Table 3.1).

Strains which consistently displayed high biofilm formation in both CDM and HI in these assay conditions included Rd KW20, R3327, R3567, R2866 and R2846.

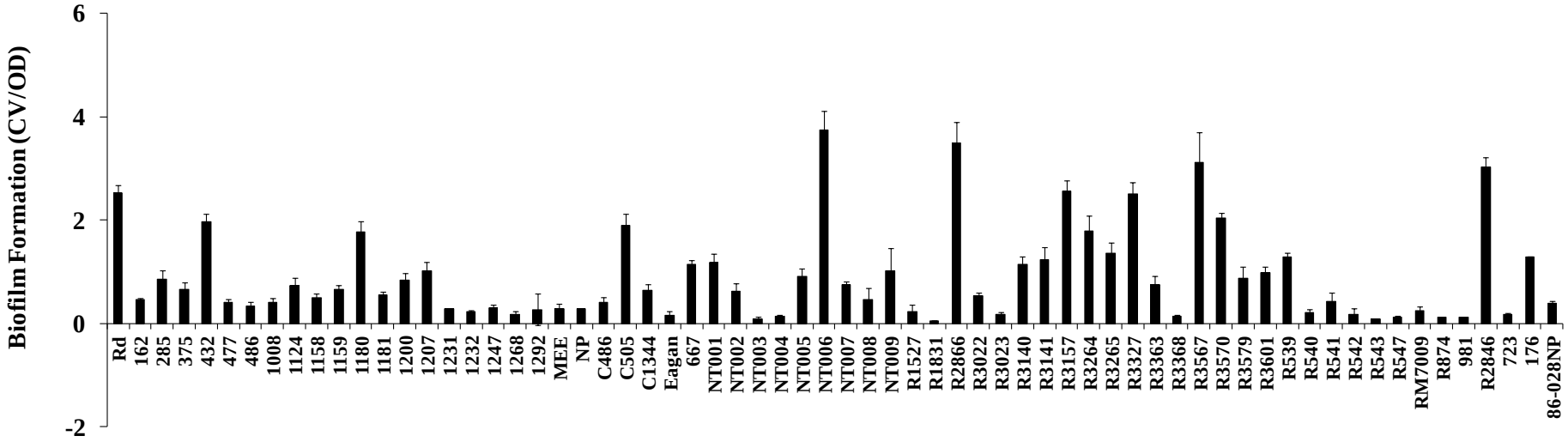

Fig. 3.1. The biofilm formation of *H. influenzae* is strain dependent in CDM. The relative biofilm formation of *H. influenzae* laboratory strain Rd KW20 (Rd) and 65 clinical isolates in CDM in the absence of stress showed a high strain-specific variation. The level of biofilm formation did not correlate to the specific disease origin of the strain or to a capsular type.

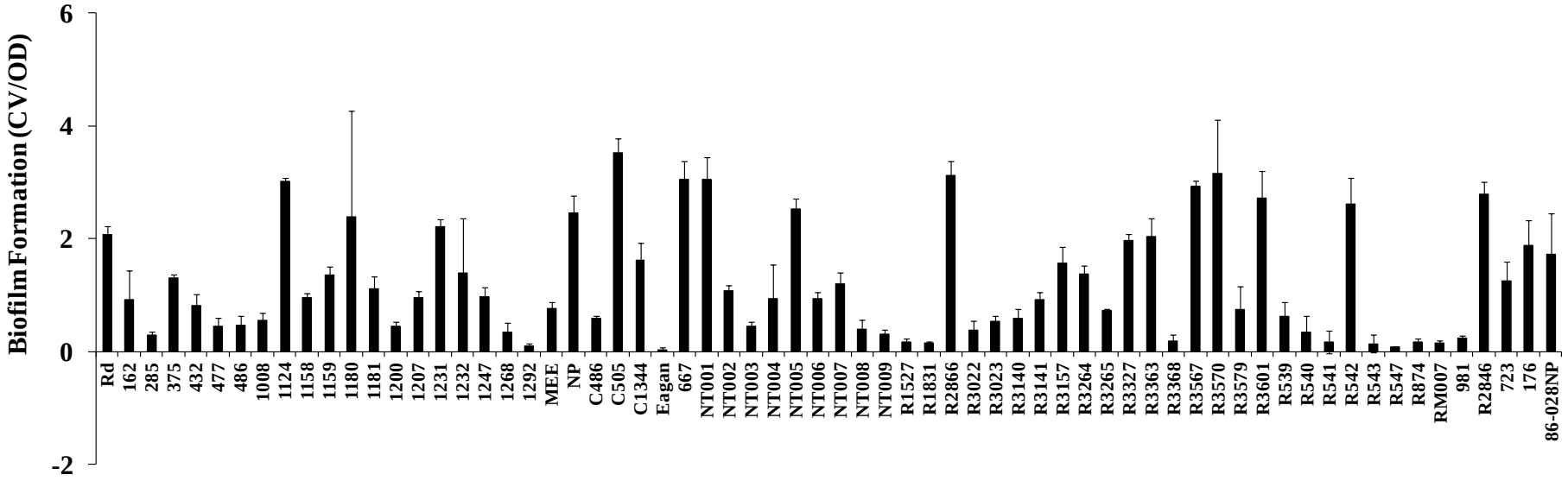

Fig. 3.2. The biofilm formation of *H. influenzae* is strain-dependent in HI media. The relative biofilm formation of *H. influenzae* laboratory strain Rd KW20 and 65 clinical isolate strains of *H. influenzae* in HI media in the absence of stress showed a high strain-specific variation. The level of biofilm formation did not correlate to a specific disease origin or capsular type.

Table 3.1 Showing strains with high biofilm formation in CDM/ HI media in the absence of stress, and the strain origins and capsular types of these strains.

CDM	Capsular type; strain origin	HI	Capsular type; strain origin
Rd KW20	D; blood	Rd KW20	D; blood
NT006	NT; N/K	1124	NT; OM
R3157	NT; OM	1231	NT; OM
R3327	D; blood	NP	N/K; NP
R3567	NT; blood	C505	NT; OM
R2866	NT; blood	667	NT; OM
R2846	NT; OM	NT001	NT; N/K
		NT005	NT; N/K
		R2866	NT; blood
		R3327	D; blood
		R3363	E; N/K
		R3567	NT; blood
		R3570	NT; blood
		R3601	NT; blood
		R542	N/K; N/K
		R2846	NT; OM
		176	NT; OM
		86-028NP	NT; OM

3.2.2. The presence of formaldehyde stress can enhance or reduce biofilm formation in a strain and growth-medium dependent manner.

In CDM, in the presence of a sub-lethal concentration of formaldehyde, some strains induced their biofilm formation. These strains included isolates 432, 1180, C505, 667, NT005, NT007, R3140, R3157, R3264, R3265, R3567, R3570, R3601 R2846 and 176 (Fig. 3.3; Table 3.2). Importantly, the laboratory strain Rd KW20 and the non-typeable strain NT006 showed a reduced biofilm formation in the presence of formaldehyde (Fig. 3.3; Table 3.2).

In HI media, the kinetics of biofilm formation differed. Most strains showed a reduction or no change in biofilm formation. Strains that showed an increase in biofilm formation were C1344, R2866, R3157, R3567 and R2846 (Fig. 3.4; Table 3.2). Of these strains only R3157, R2846 and R3567 also showed an increase in biofilm formation in CDM media. This result suggests that the clinical isolate strains may greatly differ in their response to environmental stresses, particularly regarding biofilm formation, and that the response of the strains to the nutrient composition of the media may further alter their response to stress. Strains which decreased their biofilm production upon the presence of formaldehyde in HI media included strains 1124, 1231, NT005, NT003, NT002, NT007, 1158, 1159, 1181 and the laboratory strain Rd KW20 which showed a slight reduction in biofilm formation (Fig. 3.4; Table 3.2).

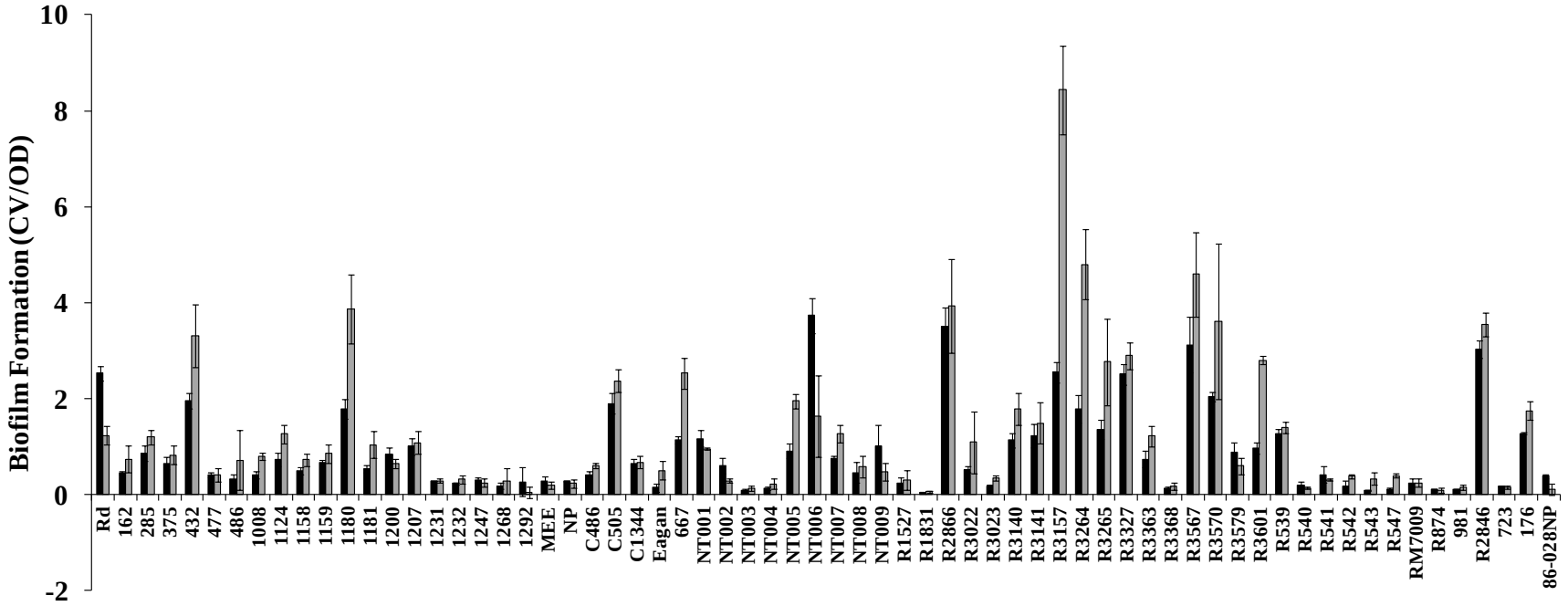

Fig. 3.3. The biofilm formation of *H. influenzae* strains in CDM is induced or repressed by formaldehyde in a strain-specific manner. The relative biofilm formation is shown for *H. influenzae* laboratory strain Rd KW20 (Rd), and 65 clinical isolate strains in CDM (black bars) or CDM with 0.002% formaldehyde (grey bars). The *H. influenzae* biofilm formation response to formaldehyde appeared to be strain specific, but did not correlate to a specific disease origin or capsular type.

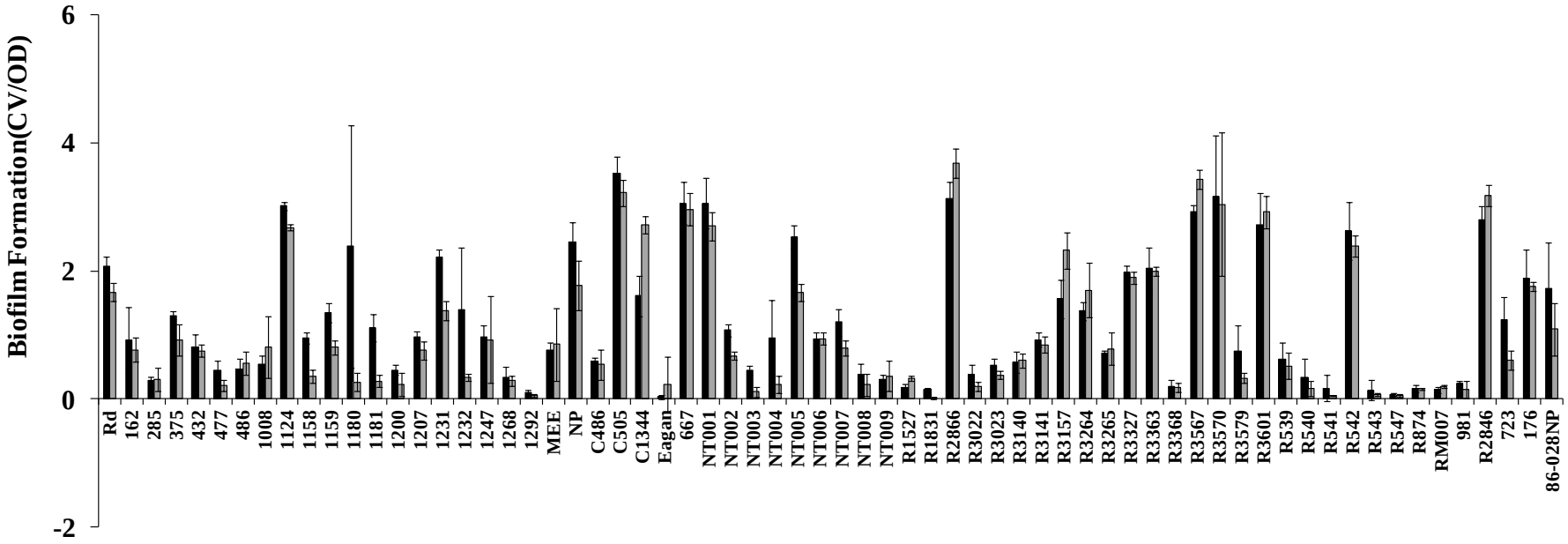

Fig. 3.4. The biofilm formation of *H. influenzae* is induced or repressed by formaldehyde in a strain-dependent manner in HI media. The relative biofilm formation is shown for the *H. influenzae* laboratory strain Rd KW20 and 65 clinical isolate strains in HI media (black bars), and HI media with 0.0137% formaldehyde (grey bars). The *H. influenzae* biofilm formation response to formaldehyde in HI media is strain-dependent, but does not correlate to a specific disease source or capsular type.

Table 3.2. Showing strains which increased or decreased biofilm formation in the presence of formaldehyde in CDM or HI media, and the capsular type and strain origin of these strains.

CDM Increase in biofilm formation with stress	**Capsular type; strain origin**	**HI**	**Capsular type; strain origin**
432	NT; OM	C1344	NT; OM
1180	NT; OM	R2866	NT; blood
C505	NT; OM	R3157	NT; OM
667	B; throat or NT	R3567	NT; blood
NT005	NT; N/K	R2846	NT; OM
NT007	NT; N/K		
R3140	NT; OM		
R3157	NT; OM		
R3264	NT; healthy child		
R3265	NT; healthy child		
R3567	NT; blood		
R3570	NT; blood		
R3601	NT; blood		
R2846	NT; OM		
176	NT; OM		
CDM Decrease in biofilm formation with stress			
Rd KW20	D; blood	1124	NT; OM
NT006	NT; N/K	1231	NT; OM
		NT005	NT; N/K
		NT003	NT; N/K
		NT002	NT; N/K
		NT007	NT; N/K

	1158	NT; OM
	1159	NT; OM
	1181	NT; OM
	Rd KW20	D; blood

3.2.3. The presence of H_2O_2 stress can enhance or reduce biofilm formation in a strain and growth-medium dependent manner.

In the presence of sub-lethal levels of H_2O_2, in CDM most strains displayed a reduction or no change in biofilm formation. Strains which showed a decrease in biofilm formation included strains 667, 1200, NT005, NT006, NT007, NT009, R3327, R3579, R539 and 176 (Fig. 3.5; Table 3.3). Strains 375, R3264 and C1344 showed an increase in biofilm formation in the presence of H_2O_2 in CDM (Fig. 3.5; Table 3.3).

In HI media in the presence of H_2O_2, strains R2866, R3264, R3567 and R2846 showed an increase in biofilm formation, while almost all strains showed a reduction or no change (Fig. 3.6; Table 3.3).

The increase in R3264 biofilm formation with H_2O_2 was consistent in both HI and CDM.

These results suggest that while H_2O_2 is a stress, for most strains it does not induce biofilm formation. Rather, a biofilm reduction is most common. While a biofilm could protect strains from the damaging effects of H_2O_2, strains may employ other mechanisms of H_2O_2 detoxification, or physiological changes which could protect from the stress.

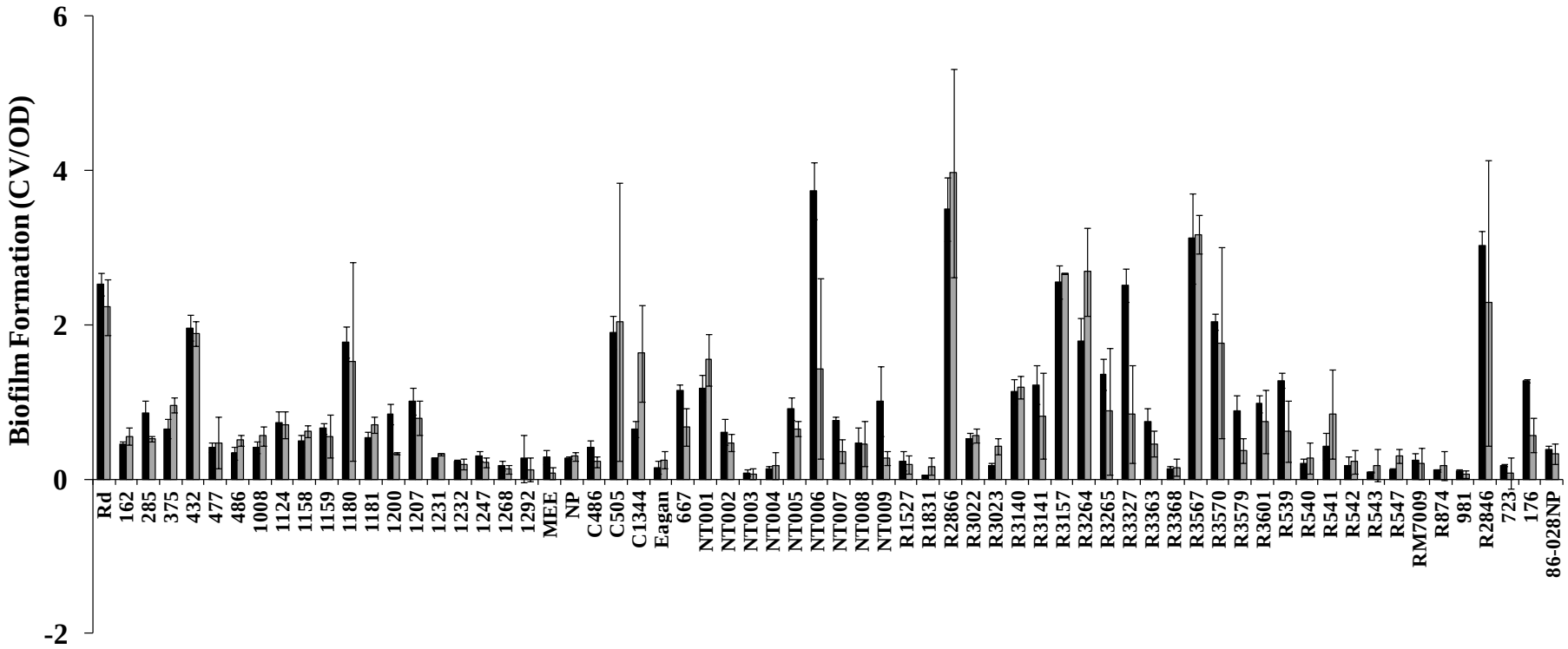

Fig. 3.5. The biofilm formation of *H. influenzae* in CDM is induced or repressed by H_2O_2 in a strain-dependent manner. The relative biofilm formation of the *H. influenzae* is shown for the laboratory strain Rd KW20 and 65 clinical isolate strains in CDM (black bars), or CDM with 0.005% H_2O_2 (grey bars). The *H. influenzae* biofilm formation response to H_2O_2 is strain specific, but does not correlate to a specific disease origin or capsular type.

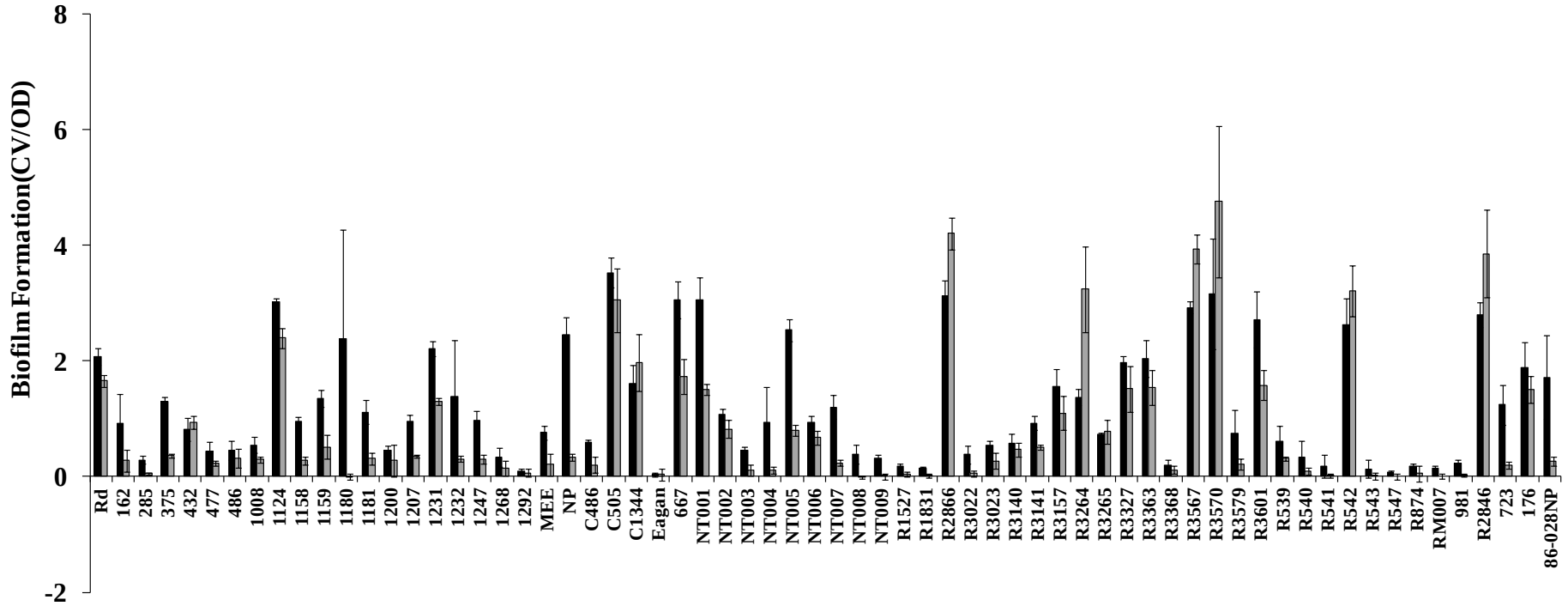

Fig. 3.6. The biofilm formation of *H. influenzae* in HI media is induced or repressed by the presence of H_2O_2 in a strain-dependent manner. The relative biofilm formation is shown for the *H. influenzae* laboratory strain Rd KW20 (Rd), and 65 clinical isolate strains in HI media (black bars), and 0.016% H_2O_2 (grey bars). The *H. influenzae* biofilm formation response to H_2O_2 in HI media is strain-specific, but is not associated to a particular disease origin or capsular type of the strain.

Table 3.3 Showing strains which increased or decreased biofilm formation in the presence of H_2O_2 in CDM or HI media, and the capsular type and strain origin of these strains

CDM Increase in biofilm formation	**Capsular type; strain origin**	**HI Increase in biofilm formation**	**Capsular type; strain origin**
375	NT; OM	R2866	NT; blood
R3264	NT; healthy child	R3264	NT; healthy child
C1344	NT; OM	R3567	NT; blood
		R2846	NT; OM
CDM Decrease in biofilm formation			
Rd KW20	D; blood	375	NT; OM
667	NT; OM	1124	NT; OM
1200	NT; OM	1158	NT; OM
NT005	NT; N/K	1159	NT; OM
NT006	NT; N/K	1181	NT; OM
NT007	NT; N/K	1207	NT; OM
NT009	NT; N/K	1231	NT; OM
R3327	D; blood	1247	NT; OM
R3579	NT; blood	MEE	N/ K; OM
R539	N/K; N/K	NP	N; K; NP
176	NT; OM	667	NT; OM
		NT001	NT; N/K
		NT005	NT; N/K
		NT007	NT; N/K
		R3601	NT; blood
		723	NT; OM
		86-028NP	NT; OM
		Rd KW20	D; blood

3.2.4. The presence of methylglyoxal can enhance or reduce biofilm formation in a strain and growth medium dependent manner.

In CDM with methylglyoxal, some strains did show a difference in biofilm formation compared to their biofilm formation in CDM media. Strains that showed an increase in biofilm formation in the presence of methylglyoxal included Rd KW20, and clinical isolates 162, 375, 1180, 1181, 667, NT007, R3140, R3264, R3570, R3567, R3601, R541 (Fig. 3.7; Table 3.4). Only strain R2846 showed a reduction in biofilm formation with methylglyoxal, while most strains showed no difference in their biofilm formation (Fig. 3.7; Table 3.4).

Biofilm formation in HI media with methylglyoxal did not show significant differences in the ability of strains to form biofilm, with generally large variation and error (Fig. 3.8).

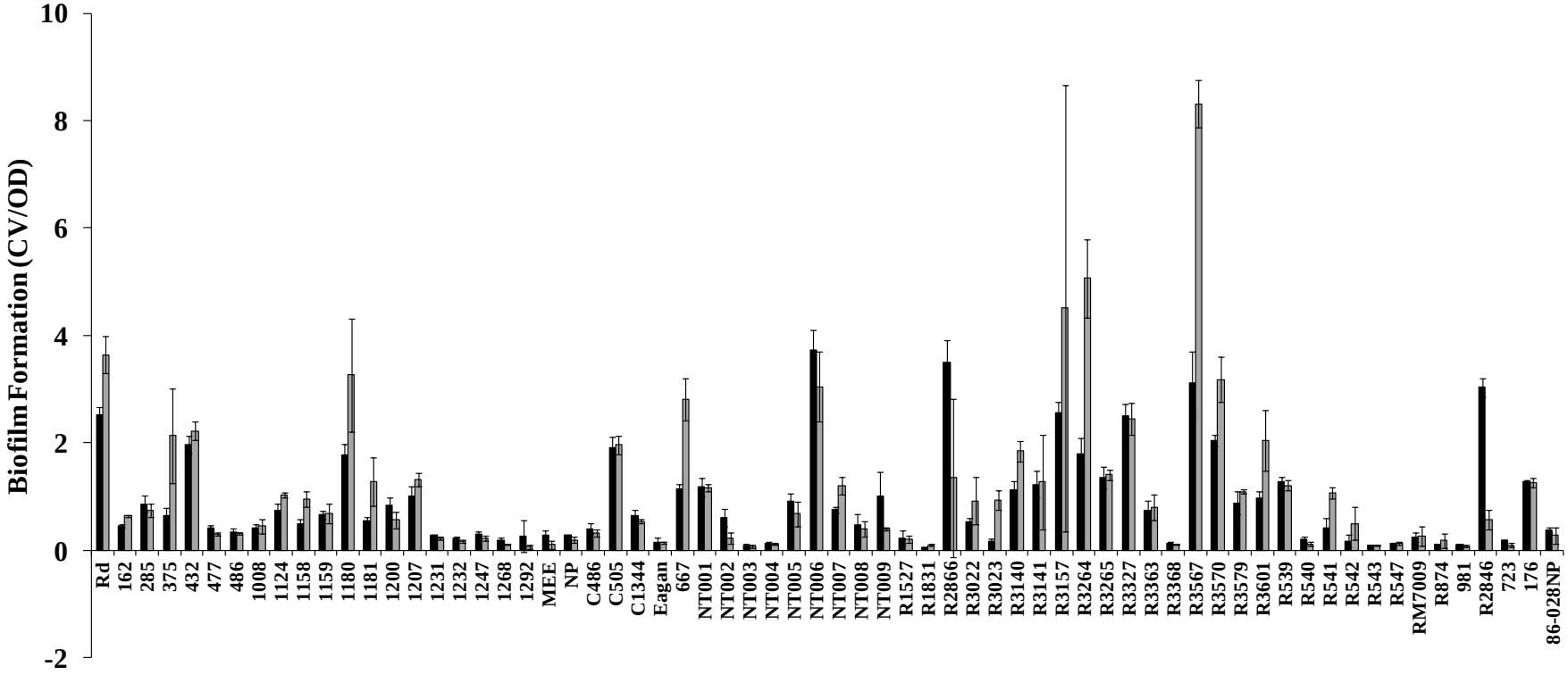

Fig 3.7. The biofilm formation of *H. influenzae* strains in CDM is induced or repressed by methylglyoxal in a strain-dependent manner. The relative biofilm formation is shown for *H. influenzae* laboratory strain Rd KW20 (Rd), and 65 clinical isolate strains in CDM (black bars) or CDM with 0.008% methylglyoxal (grey bars). The *H. influenzae* biofilm formation response to methylglyoxal appears to be strain-specific, but does not correlate to a specific disease source or capsular type.

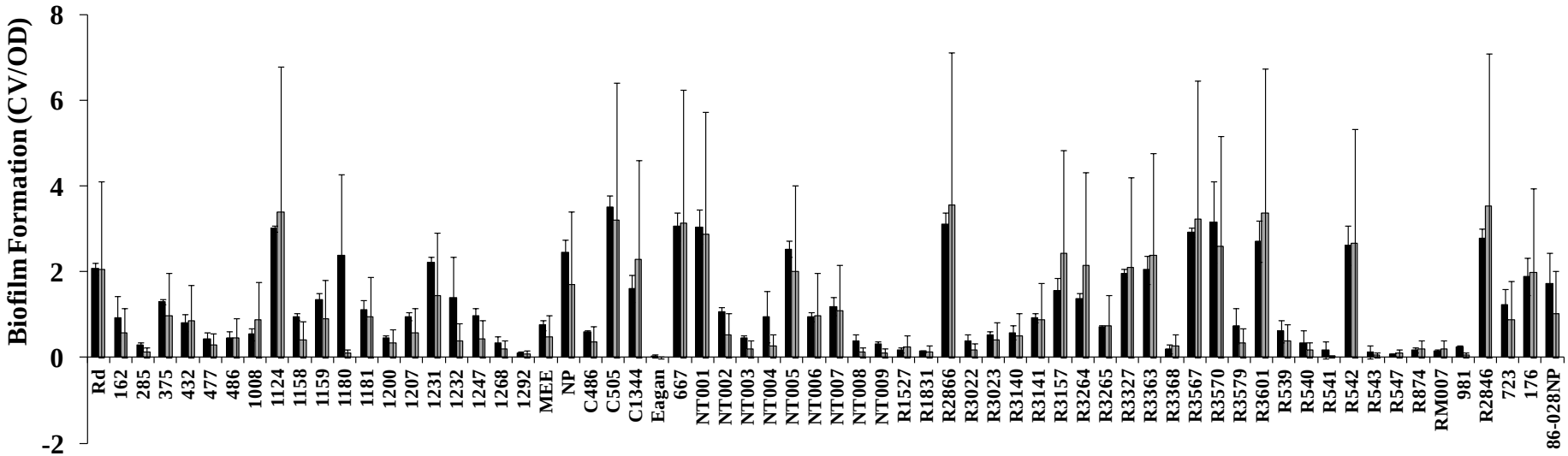

Fig. 3.8. The biofilm formation of *H. influenzae* does not appear to be significantly induced or repressed by methylglyoxal in HI media. The relative biofilm formation is shown for the *H. influenzae* laboratory strain Rd KW20 (Rd) and 65 clinical isolate strains in HI media (black bars), and HI media with 0.6% methylglyoxal (grey bars). Due to the large variation and error for *H. influenzae* biofilm formation in the presence of methylglyoxal in HI media, no conclusion about a significant difference in biofilm formation in these conditions can be made.

Table 3.4 Showing strains which increased or decreased biofilm formation in the presence of methylglyoxal in CDM media, and the capsular type and strain origin of these strains

CDM	**Capsular type; strain origin**
Increase in biofilm formation	
162	NT; OM
375	NT; OM
1180	NT; OM
1181	NT; OM
667	NT; OM
NT007	NT; N/K
R3140	NT; OM
R3264	NT; healthy child
R3570	NT; blood
R3601	NT; blood
R541	N/K; N/K
R3567	NT; blood
CDM Decrease in biofilm formation	
R2846	NT; OM

3.2.5. *H. influenzae* biofilm formation is dependent on eDNA

As shown in (Fig. 3.1-3.8), there was a vast strain variation in the ability of *H. influenzae* isolates to form a biofilm. This strain variation could be related to both specific genetic and regulatory events specific to the isolates, which could determine the induction or repression of biofilm formation under certain conditions. One essential element of biofilm formation, which could determine the ability of a strain to form biofilm, or the amount of biofilm that is formed, is the EPS and the specific elements of this extracellular matrix. The EPS matrix has been shown to contribute to the biofilm adhesion and cohesion properties, as well as to the complexity of the biofilm structure and intra-organisation (Flemming and Wingender 2010). A known and important factor in *H. influenzae* biofilm EPS matrix has previously been shown to be eDNA (Jurcisek and Bakaletz 2007).

In order to determine the role of the EPS matrix component eDNA in the biofilm formation of *H. influenzae* strains, the biofilm formation assay of a select number of strains was performed both in HI and CDM in the presence of DNAse I. These strains included those which formed moderate-high levels of biofilm, both in CDM and HI media. We hypothesized that if eDNA was involved in forming the EPS matrix of a particular strain, or present in greater amounts, then administration of DNAse I would prevent the development of a mature and structured biofilm, resulting in a greater reduction in biofilm compared to a strain which is not as dependent on the presence of eDNA in its EPS matrix.

The results showed that in HI media, the addition of DNAse I caused a slight reduction in the biofilm formation for strains Rd KW20, 86-028NP, R3157 and R2866, but not for strain C505 (Fig. 3.9).

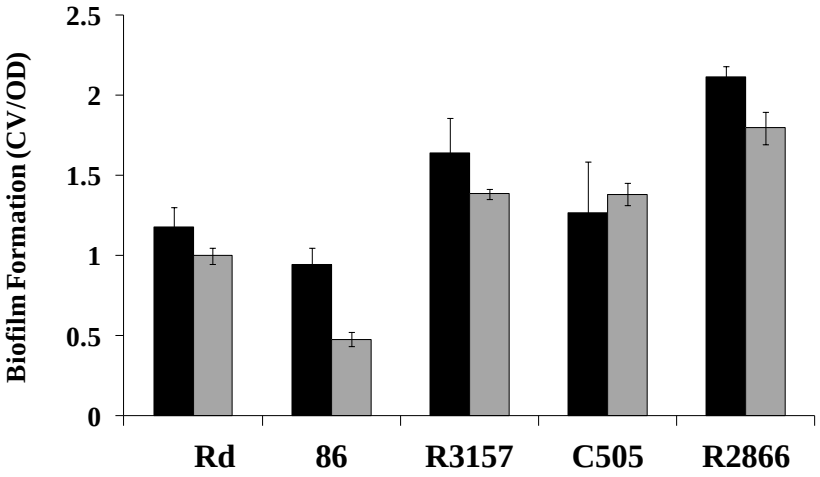

Fig. 3.9. The biofilm formation of *H. influenzae* in HI media is reduced by the presence of DNAse I in a strain-dependent manner. The biofilm formation of *H. influenzae* laboratory strain Rd KW20 (Rd) and clinical isolates 86-028NP (86), R3157, C505 and R2866 are shown in the absence of DNAseI (black bars), and the presence of DNAse I (grey bars). In the presence of DNAse I, biofilm formation was slightly reduced for strains Rd KW20, 86-028NP, R3157 and R2866, but not for C505.

In CDM, DNAse I presence reduced the biofilm formation of R3157, C505 and R2866, but not for Rd KW20 or 86-028NP (Fig. 3.10). The biofilm reduction which occurred in CDM was greater than the biofilm reduction observed in HI media (Fig. 3.10).

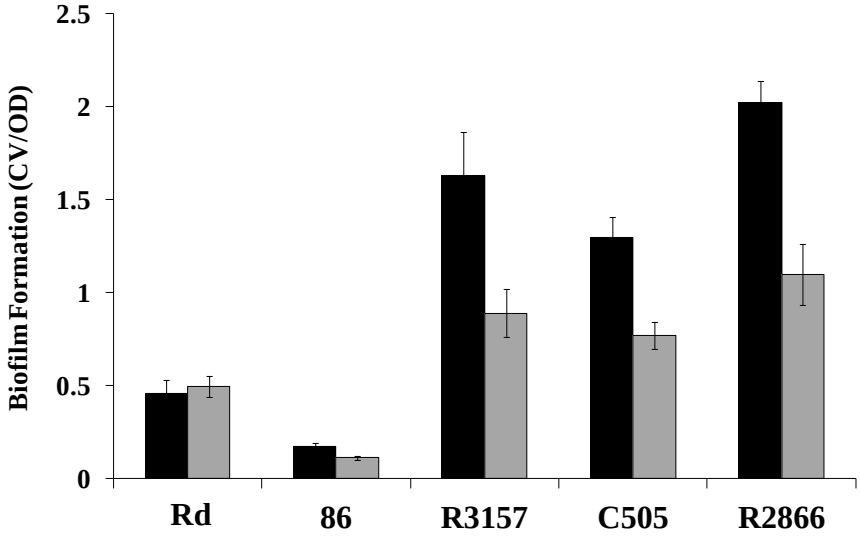

Fig. 3.10. The biofilm formation of *H. influenzae* in CDM media is reduced by the presence of DNAseI in a strain-dependent manner. The biofilm formation of *H. influenzae* laboratory strain Rd KW20 (Rd) and clinical isolates 86-028NP (86), R3157, C505 and R2866 are shown in the absence of DNAse I (black bars), and in the presence of DNAseI (grey bars). In the presence of DNAse I, biofilm formation was reduced for strains R3157, C505 and R2866, but not for Rd KW20 or 86-028NP.

These results indicated that eDNA may have different roles in the biofilm matrix for specific strains, and that even for the same strain, the importance and role of eDNA may be varied, depending on the nutrient medium used, and the environment biofilm formation occurs in.

3.2.6. The Genetics of Type IV pili in *H. influenzae* biofilm formation.

In *H. influenzae,* type IV pili have been shown to increase adhesion and biofilm stability in the *H. influenzae* biofilm (Carruthers et al. 2012). They have also been shown to physically associate with eDNA in the *H. influenzae* biofilm (Jurcisek and Bakaletz 2007). Hence, the expression of the type IV pili could enhance the adhesion and cohesion of cells in the biofilm, as well as binding to other components of the EPS such as the eDNA. An increased EPS matrix could in turn stain more profusely in the CV assay, showing a high biofilm formation.

Although the type IV pili assembly and function are encoded by many genes of the *pil* and *com* operons (Carruthers et al. 2012), the absence of the *pilA* gene encoding the major pilus subunit, would certainly render the pilus non-functional. Therefore, we screened a small subset of strains for the presence of *pilA* by performing a PCR using primers encompassing all of *pilA* and a segment of *pilB*, the subsequent gene in the *pil* operon, with the expected PCR product approximating 1.3kb.

The results showed that the tested strains Rd KW20, 86-028NP, 162, 285, 375, 432, 477, 486, 1008, 1124, 1158, 1159, 1180, 1200, 1232, 1247, 1268, 1292, MEE harboured the *pilA-pilB* gene segment. No band was present for strains 1181, 1207, 1231 or NP (Fig. 3.11; 3.12).

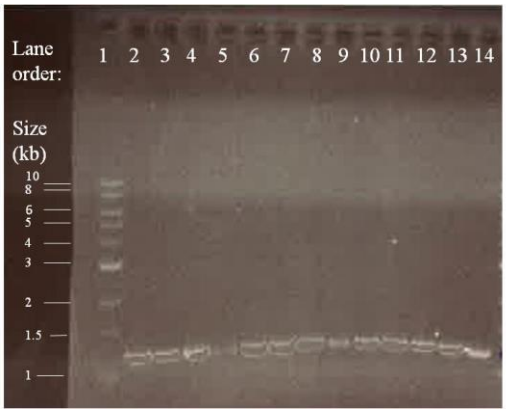

Fig. 3.11. *H. influenzae* isolates possess the *pilA-pilB* gene segment encoding the type IV pilus major subunit. Photo of agarose gel electrophoresis, showing the results of screening 13 *H. influenzae* isolates for the presence of *pilA*. Lane order displayed (Lane 1-14): 1kb ladder, *H. influenzae* strains: Rd KW20, 86-028NP, 162, 285, 375, 432, 477, 486, 1008, 1124, 1158, 1159, 1180. All strains displayed a band of approximately 1.3kb, spanning the 450 bp ORF of *pilA* and approximately 850bp of the 1.3kb *pilB* ORF.

Fig. 3.12. *H. influenzae* isolates 1181, 1207, 1231 and NP do not possess the *pilA-pilB* gene segment encoding the type IV pilus major subunit. Photo of agarose gel electrophoresis, showing the results of screening of 12 *H. influenzae* isolates for the presence of *pilA*. Lane order displayed (Lane 1-14): 1kb ladder, *H. influenzae* isolates: Rd KW20, 86-028NP, 1181, 1200, 1207, 1231, 1232, 1247, 1268, 1292, MEE, NP, 1kb ladder.

3.2.7. The role of nickel transport in *H. influenzae* biofilm formation.

In this Chapter, we have shown that there is a strain-specificity in the ability of *H. influenzae* to form a biofilm, and this strain-specificity was also dependent on the presence of stress and environmental conditions. In addition, we have shown that biofilm formation is a multifactorial process, also dependent on the presence of elements of the EPS matrix. While it is known that the adaptation of a strain to environmental conditions pertinent to its niche may induce or repress biofilm formation, little is known about the intracellular events which stimulate this switch in lifestyle. While we did not investigate the genetic variability between the 65 clinical isolates tested, it is known that specific genetic components play a role in the ability of a cell to survive in the presence of stress, and to induce biofilm formation. These genetic components can be either directly related to the biofilm structure – such as those encoding type IV pili and other components of the EPS matrix, or indirectly related – such as genes involved in stress response, and global gene regulation. Some genetic factors have also been shown to play multiple roles within the cell, and to be involved in regulating different aspects of the cell's physiology and adaptation mechanisms. Indeed, one system of *H. influenzae* known to have pleiotrophic roles within the cell is the nickel uptake system (*nimR-nikKLMQO*). This system consists of the NimR regulator and the *nikKLMQO* genes, specifically involved in nickel import into the cell (Kidd et al. 2011). As nickel is a known co-factor for urease, an enzyme involved in acid tolerance, it was hypothesized that these nickel import system genes would be important for urease activity, maintaining intracellular pH and the cell's response to changes to extracellular pH changes. Indeed, *nimR* and *nikQ* deficient mutants in Rd KW20 have shown a reduced acid tolerance compared to the wild-type, as well as reduced urease activity. This confirmed the role of nickel in the acid tolerance response of *H. influenzae* (Kidd et al. 2011). However the roles of the nickel uptake genes appeared to have a broader function. Specifically, the *nimR* and *nikQ* mutants displayed an increased aggregation and biofilm formation compared to the wild-type Rd KW20 (Ng and Kidd 2013). In addition, these cells were more hydrophobic and negatively charged; importantly, these changes were not attributed solely to the loss of function of urease, or to the loss of function of glyoxalase I (GloA) – the only known nickel-cofactored enzymes in *H.*

influenzae (Ng and Kidd 2013). Hence, it was proposed that in conditions when the cell is unable to import nickel, or in an environment where nickel levels are low, *H. influenzae* adopts a biofilm-formation lifestyle. However, the intracellular or transcriptomic events which occur in *H. influenzae* upon nickel depletion and thereby stimulate cell surface changes and biofilm formation were unknown. Hence, to further investigate changes which occur in the nickel depleted *nikQ* mutant in Rd KW20, RNA sequencing was performed (refer to section in Materials and Methods) in the Rd KW20 *nikQ* mutant and compared to the genome-wide expression in the wild-type Rd KW20. **This work is described in the publication (Tikhomirova, A; Jiang D; Kidd SP, 2015. A new insight into the role of intracellular nickel levels for the stress response, surface properties and twitching motility by *Haemophilus influenzae*. Metallomics.)** (Shown in full in Appendix 2).

Table 3.5. Key genes differentially expressed in Rd KW20 *nikQ*- compared to Rd KW20.

Gene/s	Description	Change[a]
Genes up-regulated in *nik* mutant		
Metabolic pathways		
HI0243/HI0242	HHE/heme binding	3.9
HI0357/*thiE*	thiamine biosynthesis	3.1-3.3
pyrD	dihydroorotate dehydrogenase	2.6
neuA	CMP-sialic acid synthase	2.5
HI0152	acetyl carrier protein	2.3
folP-2	folic acid biosynthesis	2.2
Membrane/transporters		
nikKLM	Ni^{2+} uptake	2.6-3.2
hitB	iron uptake	3.1
HI1697/HI1695	LOS biosynthesis	2.4-2.6
bolA	cell morphology	2.3
nanK	sialic acid metabolism	2.3
HI0894	RND efflux pump	2.2
sapC	peptide transporter	2.2
dctM	TRAP transporter	2.2
Stress response		
htpG, dnaJK, hslVU, groES, groEL, clpB	molecular chaperones, protein folding	3.2-6.1
hsdMRS	restriction system	3.3-4.2
htrA, hflKC	proteases	2.0-2.4
Gene regulation		
vapA	toxin-antitoxin system	3.0
HI0420	RHH regulator	3.0
sprT	regulator of *bolA*	2.1
Genes down-regulated in *nik* mutant		
Metabolic pathways		
dmsABC	DMSO reductase	2.3-7.2
nrfDC	nitrate reductase	2.4-3.4
glpAB	anaerobic glycerol metabolism	3.2
bisC/yecK	biotin co-factored reductase	2.0-3.2
frdD	fumarate reductase	2.9
acpP	acyl carrier protein	2.8
gdhA	glutamate dehydrogenase	2.6
malQ	amylomaltase	2.4
bioD (HI1445)	biotin biosynthesis	2.4
napG	nitrate reductase	2.2
mdh	malate dehydrogenase	2.2
fumC	fumarate hydratase	2.2
pfl	pyruvate-formate lyase	2.2

gapdH	glyceraldehyde-3-phospohate DH	2.1
gpmA	phosphoglyceromutase, pyvuvate	2.1
Membrane/transporters		
HI1078/79/80	PAAT (amino acid) transporter	2.1-3.5
HI1154	Na^+/dicarboxylate symporter	3.7
modA	Mo uptake	3.3
nikO	Ni^{2+} uptake	3.3
dppA	heme uptake	2.8
pal	OMP P6	2.6
pilC	pilin biosynthesis	2.3
Gene regulation		
HI0093	sugar di-acid regulator	2.5
oxyR	oxidative stress regulator	2.1
trpR	trp operon repressor	2.0

[a] – Fold change is $\log_2$ fold change. Selected genes are presented and grouped within a role or category and values are summarized accordingly.

The results of this study showed that several classes of genes were up-regulated in the *nikQ*- compared to the wild-type Rd KW20 (Table 3.5). A class of stress response enzymes including molecular chaperones involved in protein folding, as well as a restriction system and proteases were up-regulated in the *nikQ* mutant. This was expected, given the role of these enzymes in aiding protein folding, a known event in the conditions of acid stress. Other up-regulated genes included membrane associated genes and transporters, including genes involved in LOS biosynthesis, as well as metabolism-related genes, which included heme binding proteins. The up-regulation of a range of membrane associated genes and LOS biosynthesis genes, suggests the global changes in the expression of cell-surface associated components in the *nikQ*- strain, which are expressed phenotypically as a more electronegatively charged cell. While not all of the roles of the up-regulated metabolic genes are evident, several heme binding and 1 iron uptake genes were up-regulated. It has been shown for *H. influenzae* previously, that iron plays an important role in biofilm formation (Vogel et al. 2012). Therefore, the up-regulation of genes involved in importing iron (or heme/iron complexes) into the cell, supports the observation that biofilm formation is induced in the *nikQ*- strain, and that this biofilm induction may be a more global process than solely the modification of cell-surface structures. In addition, in the *nikQ*- strain, a

number of central metabolic genes were down-regulated, as were a number of anaerobic metabolic pathways. While this was not investigated further, this could indicate that the metabolism of the cells is being switched to a lower metabolic rate, which has previously been characterized for biofilm growing cells.

Therefore, it was shown that in the *nikQ*- strain of Rd KW20, global changes pertaining to cell surface structures as well as stress response and metabolism, were occurring. However, Rd KW20 is a known laboratory strain and therefore may not represent the global role of nickel in a strain directly associated with disease. Therefore, in order to expand the study to a more relevant model, the nickel uptake locus of the OM isolate 86-028NP was studied.

A locus in 86-028NP was identified that was homologous *to nikKLMQO* from Rd KW20: NTHI1418-1422 (currently annotated as *cbiK*, NTHI1419, *cbiM*, NTHI1421 and *cbiO*; we have putatively renamed these *nikKLMQO*). We initially showed they did form an operon (this was using RT-PCR, data not shown). We generated a knock-out strain, 86-028NP *nikQ*. The wild type and *nikQ* mutant 86-028NP strains were grown with different levels of exogenous nickel, and the intracellular metal concentrations were measured (by ICP-MS). The results showed that the *nikQ* mutant was incapable of importing nickel (Table 3.6). If an excess of nickel was added (2 mM) to the growth media there was an increase in intracellular nickel in the *nikQ* mutant strain; an indication that at elevated concentrations nickel was able to be transported into the cell through other pathways (Table 3.6).

Table 3.6. Intracellular metal concentrations in *H. influenzae* 86-028NP compared to its *nikQ* mutant (metal ion concentrations are given at 10^8 atoms per CFU; the normalized total g dry weight has been converted to viable cell numbers; colony forming units, CFU.

Strain + exogenous metal added	Ni	Co	Mg	Mn	Fe	Zn
86-028NP	11.46 ± 0.28	0.03 ± 0.001	77.98 ± 14.92	0.54 ± 0.01	12.78 ± 0.33	21.48 ± 1.66
86-028NP + 0.1 mM Ni	92.57 ± 9.75	0.04 ± 0.001	97.55 ± 9.89	0.62 ± 0.01	30.05 ± 1.64	31.84 ± 1.23
86-028NP + 0.25 mM Ni	279.9 ± 31.92	0.08 ± 0.002	139.55 ± 33.22	0.65 ± 0.02	33.28 ± 2.38	43.55 ± 2.59
86-028NP + 0.2 mM Co	2.28 ± 0.39	3.22 ± 0.41	69.15± 11.50	0.76 ± 0.02	32.15 ± 1.22	33.41 ± 2.33
86-028NP + 0.5 mM Co	67.49 ± 8.90	18.28 ± 2.44	68.44 ± 14.11	0.66 ± 0.02	38.94 ± 2.91	38.66 ± 2.76
86-028NP *nikQ*	ND*	0.04 ± 0.001	1911.67± 423.22	707.54 ± 43.14	33600.11 ± 1245.98	10032.64 ± 986.22
86-028NP *nikQ* + 0.1 mM Ni	392.33 ± 28.77	54.47 ± 11.21	16329.12 ± 3553.65	2150.95 ± 166.54	32110.40 ± 1102.34	2518.34 ± 145.55
86-028NP *nikQ* + 0.25 mM Ni	103.45 ± 6.72	12.97 ± 4.13	1354.01 ± 128.33	12.11 ± 5.26	458.17 ± 54.67	505.78 ± 34.98
86-028NP *nikQ* + 0.2 mM Co	ND	438.59 ± 74.26	19456.22 ± 3215.78	488.43 ± 98.09	501.23 ± 45.88	7204.22 ± 494.59
86-028NP *nikQ* + 0.5 mM Co	ND	138.91 ± 51.48	21085.66 ± 1873.99	818.35 ± 123.45	589.147 ± 49.88	5607.22 ± 675.22

We then grew the wild type 86-028NP strain and its *nikQ* mutant in CDM (media we had assessed by ICP-MS as being limited in nickel, Table 3.6) and compared their growth profile (Fig. 3.13A). The *nikQ* mutant grew poorly compared to its wild type. Addition of nickel (Fig. 3.13B) rescued this growth defect, whereas the addition of other metal ions (cobalt, zinc, magnesium, manganese and iron) had no affect on growth (for cobalt, see Fig. 3.13C).

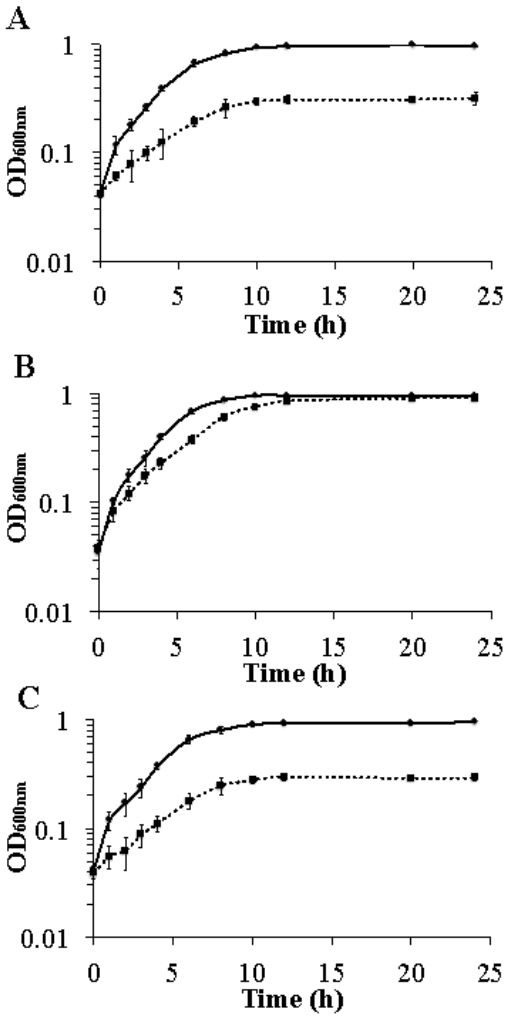

Fig. 3.13. A growth defect in the *H. influenzae* 86-028NP *nikQ* mutant strain can be specifically restored by nickel. The growth of 86-028NP strain (solid line) and its isogenic *nikQ* mutant (dotted line) was assessed in (A) HI broth, (B) with exogenous nickel added (0.2mM), and (C) with exogenous cobalt (0.1mM) added. Values are an average of triplicates and error bars represent the standard deviation.

As we had previously observed the *nikQ* mutant of Rd KW20 to have altered surface properties relative to the wild-type, it was necessary to establish whether this was the case with the *nikQ* mutant of 86-028NP. To assess whether the resultant limited intracellular nickel levels in the *nikQ* mutant strain affected the surface properties, we measured surface charge by determining

the electrophoretic mobility and calculating the zeta potential (Table 3.7). The nickel limited cells (*nikQ* mutant) were more negatively charged than the wild type cells and importantly we showed that the addition of nickel to levels we knew entered the cell, restored the *nikQ* mutant to wild type properties.

Table 3.7. The electrophoretic mobility (EM) and subsequently calculated zeta (ζ) potential for 86-028NP and the *nikQ* mutant grown in HI broth and HI broth with nickel added.

Strain + exogenous metal	z-potential (mV)	EM(mmcm/Vs)
86-028NP	-39.3 ± 3.70	-2.99 ± 0.345
86-028NP + 0.1mM Ni^{2+}	-37.8 ± 4.14	-2.91 ± 0.299
86-028NP + 0.25mM Ni^{2+}	-36.9 ± 3.99	-2.84 ± 0.432
86-028NP *nikQ*	-44.1 ± 4.14	-3.21 ± 0.379
86-028NP *nikQ* + 0.1mM Ni^{2+}	-38.3 ± 3.86	-2.94 ± 0.444
86-028NP *nikQ* + 0.25mM Ni^{2+}	36.8 ± 2.15	-2.81 ± 0.369

In addition, we measured the surface charge across pH conditions to identify the pI (or isoelectric point, IEP) of the bacterial cells (Fig. 3.14). The *nikQ* cells displayed a much lower IEP, indeed not reaching an IEP in the pH range we measured compared to the wild-type cells.

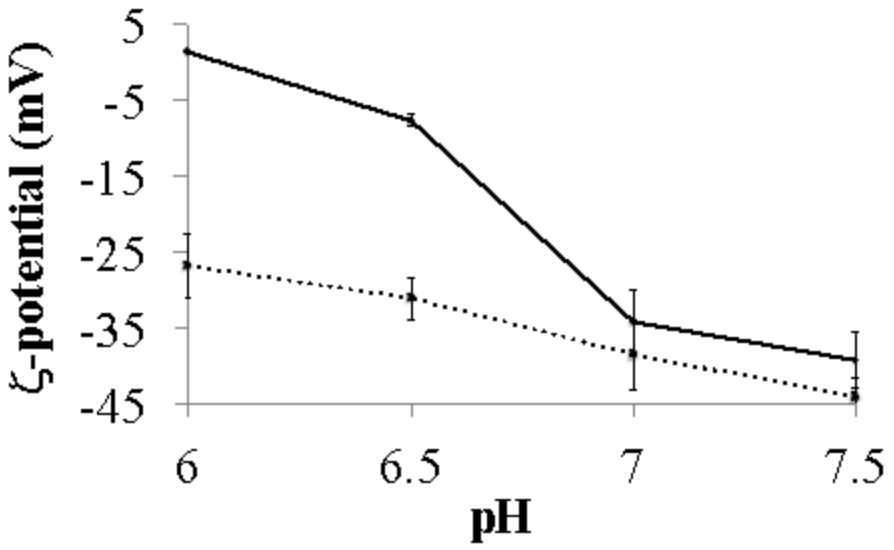

Fig. 3.14. *H. influenzae* 86-028NP *nikQ* cells are more negatively charged than their wild-type counterparts. The y-axis shows the zeta (ζ) potential as mV measured at a range of pH values for the 86-028NP wild-type cells (solid line) and its *nikQ* mutant (dotted line). The values are an average of triplicates and the error bars represent the standard deviation.

Surface charge is related to the presence, absence or the chemistry of surface structures. Cells that are altered in these characteristics and become more negatively charged are known to be related to a sessile lifestyle. The alteration in the surface charge of the 86-028NP *nikQ* mutant cells did result in an increased cell–cell aggregation (Fig. 3.15) compared to wild type cells.

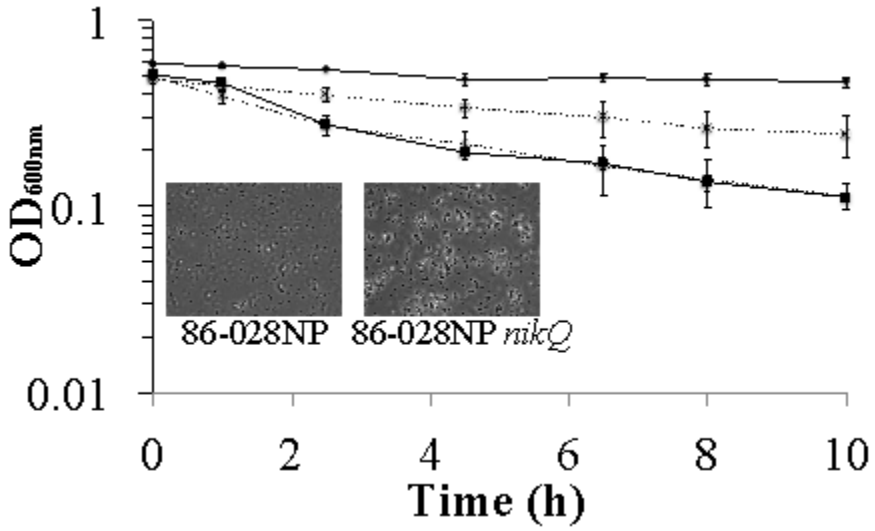

Fig. 3.15. The *H. influenzae* 86-028NP *nikQ* strain displays an enhanced cell–cell aggregation phenotype. The wild type Rd KW20 (crosses, solid line) and 86-028NP (crosses, dotted line) strains were grown in HI and the ability of the cells to aggregate was assayed (y-axis shows the OD600nm) and compared to the Rd KW20 *nikQ* (square, solid line) and 86-028NP *nikQ* (squares, dotted line) mutants. The insert shows phase contrast micrographs of 86-028NP cells (left panel) and the cell–cell aggregation in its *nikQ* mutants (right panel). The experiments were performed in triplicates, the values are an average and the error bars represent the standard deviation.

Cell-cell aggregation is linked to the first stages of bacterial biofilm formation. We therefore assayed the 86-028NP wild type and *nikQ* mutant cells for biofilm formation and noted an increase in biofilm in the *nikQ* mutant (Fig. 3.16). Adding nickel reduced the biofilm formation, but not the addition of other metal ions (Fig. 3.16A). By adding nickel in increasing amounts (to levels we had quantified were capable of increasing the intracellular nickel, Table 3.6) resulted in a corresponding increased effect on the biofilm formation (Fig. 3.16B).

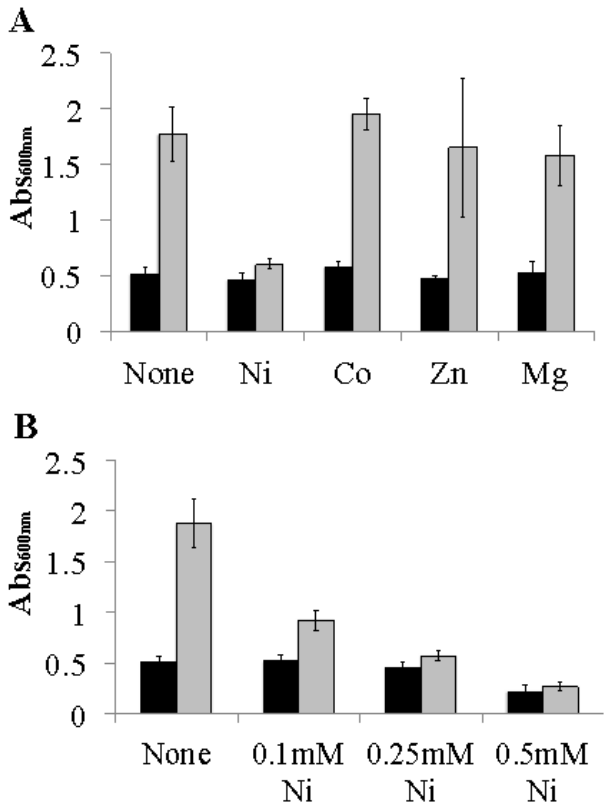

Fig. 3.16. The intracellular nickel in *H. influenzae* 86-028NP is linked to the cell's biofilm formation. (A) Biofilm was assayed for the 86-028NP wild type strain (black bars) and for its *nikQ* mutant (grey bars) from bacterial growth in HI broth and then with the addition of nickel (Ni), cobalt (Co), zinc (Zn) and magnesium (Mg); at concentrations described in the Materials and methods. (B) The effect of exogenously added nickel on 86-028NP (black bars) and its *nikQ* mutant (grey bars) was analysed over range of nickel concentrations. The Abs_{600nm} values (y-axis) are an average of triplicate experiments (each with numerous replicates) and the error bars represent the standard deviation.

Nickel has been documented as a co-factor for different enzymes; it is essential for the function of urease and GloA, two enzymes present in *H. influenzae*. In the *nikQ* mutant there is no urease activity (Fig. 3.17A). We have also assayed for GloA activity and the *nikQ* mutant has little or no activity compared to the wild type (data not shown). The *nikQ* mutant was also more sensitive to decreasing pH (Fig. 3.17B). This is unsurprising as the nickel *nikQ* imports is essential for urease activity. Interestingly, we used conditions that concurrently removed the activity of both these known nickel co-factored enzymes from 86-028NP (a *gloA* mutant and the addition of

flurofamide, a urease inhibitor). Compared to these conditions the *nikQ* cell was still more sensitive to pH (Fig. 3.17C). The *nikQ* mutant was also significantly more sensitive to oxidative stress (Fig. 3.17C). We have additionally used a strain that is naturally urease negative; the blood isolate R2866. Genome analysis of this strain shows that it is urease-negative because the entire urease locus has replaced by a single non-homolgous gene, *mtrF*, expressing an antibiotic resistant membrane protein. In this strain we have similarly generated a *nikQ* mutant and observed an increase in sensitivity to oxidative stress (Appendix 1: Fig. S1).

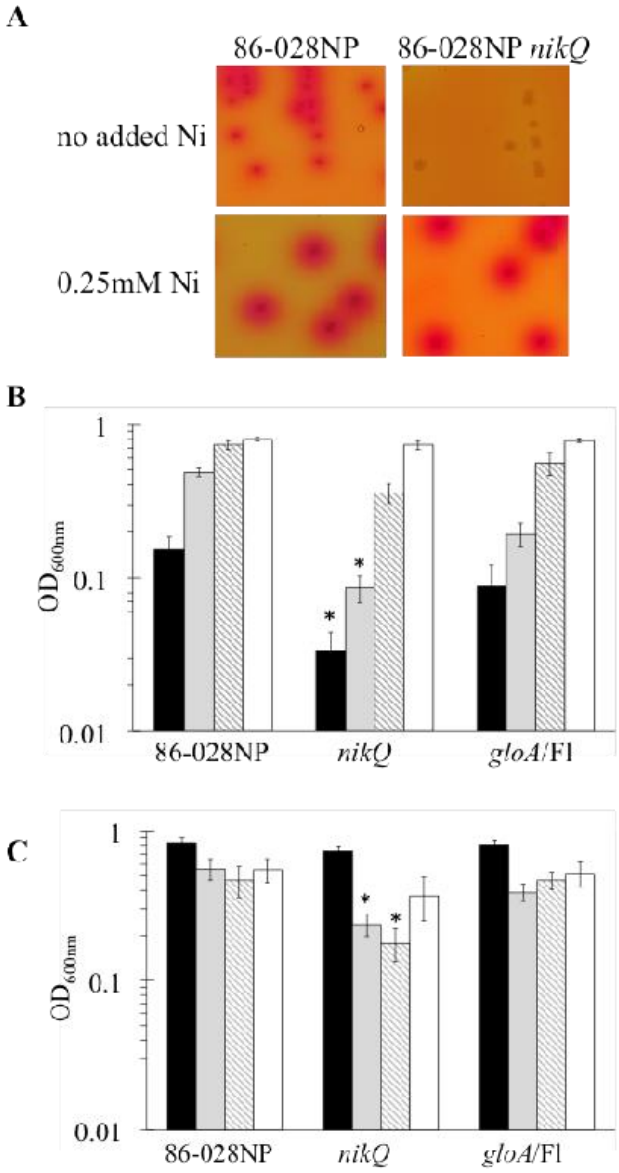

Fig. 3.17. The *H. influenzae* 86-028NP strain imports nickel for urease activity and other functions in stress response. (A) Urease assays on HI agar plates with no added nickel (top

panel) indicated that the *nikQ* mutant strain has no urease activity but with added nickel (bottom panel) the urease activity was restored to wild type levels. (B) Growth was assessed (OD_{600nm}, y-axis) at pH 5.2 (black bars), 5.6 (grey bars), 6.0 (crossed bars) and 6.4 (white bars) for the wild type 86-028NP, *nikQ* mutant strain and a *gloA* mutant strain with addition of the urease inhibited (flurofamide, Fl). (C) Growth was assessed (OD_{600nm}, y-axis) for the wild type 86-028NP, *nikQ* mutant strain and a *gloA* mutant strain with the urease inhibited (flurofamide, Fl) grown in HI broth (black bars) and then with menadione (grey bars), hydrogen peroxide (crossed bars), and GSNO (white bars). Flurofamide treated samples were checked for urease activity with quantitative assays. Values are an average of triplicates, errors are the standard deviation. Statistical significance was calculated by Student t-test *$p \leq 0.001$.

Correlating to a sessile lifestyle, and the associated the cell–cell aggregation together with the RNAseq data, we formed a hypothesis that the *nikQ* mutant strain would be less motile than its wild type cells. We used different assays to observe motility (Fig. 3.18) and we clearly showed that the *nikQ* mutant (in either Rd KW20 or 86-028NP) was less motile than wild type cells (Fig. 3.18A). The addition of nickel increased the motility (Fig. 3.18B and C); other metal ions had little or no effect (data not shown).

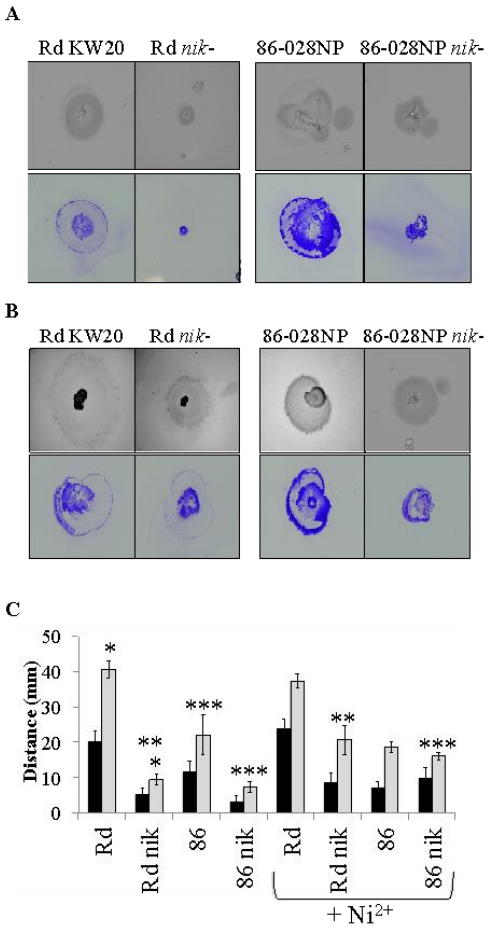

Fig. 3.18. ***H. influenzae*** **motility is influenced by nickel concentrations.** (A) Twitching motility was assayed with two methods (described in Materials and methods) for Rd KW20, its *nikQ* mutant and strain 86-028NP and its *nikQ* mutant. (B) The assay was repeated with nickel (0.25 mM) added into the media. (C) The inner and outer zones of colony migrations were measured and the values plotted. Values are an average of experimental triplicates and error bars are the standard deviation. Statistical significance was calculated by Student t-test *$p \leq 0.001$.

Overall, low intracellular nickel levels were shown to induce a global transcriptomic response in *H. influenzae*, including an up-regulation of genes related to surface structures, as well as heme/iron import and global metabolic pathways pertinent to a biofilm formation lifestyle. In addition, it was shown that the clinically relevant OM strain 86-028NP also harboured the

nikKLMQO-nimR operon, and that in 86-028NP the inactivation of the nickel import system was associated with a more electronegative cell charge, increased cell-cell aggregation and biofilm formation, and a reduced twitching motility.

3.3. Discussion

An analysis of 65 clinical isolates of *H. influenzae* for their biofilm forming ability in different media and in the presence of different stresses determined that there is a vast variation in the biofilm formation of the different strains, which can be influenced by a suite of environmental factors.

Different *H. influenzae* strains had different abilities to form biofilm when grown in CDM compared to rich HI media. The anatomical niches relevant to *H. influenzae* survival do vary in terms of nutrient availability, and hence this switch between niches (for example, during the transition from the nasopharynx to the middle ear) may also influence the switch to a biofilm lifestyle for some strains. While there was a variation in the amount of biofilm formed by respective strains, a cut-off point was used for reference – a "high" biofilm forming strain was defined as one forming the same amount of biofilm or more than the reference Rd KW20 strain (biofilm formation index >2). In CDM, Rd KW20, and 5 clinical isolates showed a high biofilm formation. These included a serotype d blood isolate and 4 non-typeable strains, 2 of which had an OM origin, and 2 of which were sourced from the blood. Contrary to our expectation, there was no correlation in the ability of a strain to form high levels of biofilm and its disease origin.

In HI Media, in the absence of stress, 18 strains showed a high biofilm formation. These included the laboratory strain Rd KW20, 7 non-typeable OM isolates, 4 non-typeable and 1 serotype d blood isolates, and 5 strains of unknown origin. Like the situation in CDM, there appeared to be no correlation of the disease origin of the strain to its biofilm formation. It is interesting that strains which consistently had a high biofilm formation in both HI and CDM media included 4 blood isolates (1 type d and 2 non-typeable), and only 1 non-typeable OM isolate. While biofilm formation is defined as a sessile bacterial community attached to a surface, the biofilm formation process itself consist of several stages (Sauer 2003), including initial adhesion and aggregation, irreversible adhesion, subsequent biofilm maturation and eventual dispersal from the biofilm matrix. The temporal correlation of these biofilm formation stages and factors in these stages that can promote or repress the development of more invasive disease, are not fully understood. While biofilm formation in *H. influenzae* has been associated with a persistent and less invasive infectious process relevant to OM (Weimer et al. 2010), this is not

the case for all bacterial species or strains. For some bacterial species, the biofilm lifestyle has also been associated with the expression of various virulence determinants. For example, an *E. coli* strain displaying increased virulence (O104:H4), had highest expression of virulence genes *in vivo*, when co-expressing genes associated with autoaggregation and biofilm formation (Safadi et al. 2012). Likewise, in *S. pneumoniae*, host norepinephrine caused an up-regulation of virulence gene expression, and a concurrent increase in biofilm formation (Sandrini et al. 2014). Therefore, it may be possible that initiation of certain stages of biofilm development may also be required for invasive disease. Such a situation would explain why blood isolates were consistent in their high biofilm formation. In addition, biofilm formation has been linked not only to a lifestyle pertaining to OM, but also to nasopharyngeal colonisation. It is possible, that strains with an increased ability to persist within the nasopharynx form extensive biofilm. It is also possible, that such persistent strains have an increased ability to cause invasive disease – including sepsis, due to their persistence in carriage, and potential out-competition of other strains in the carriage phase.

In the presence of stresses, different strains of *H. influenzae* induced or reduced their biofilm formation. However, this was highly dependent on the media used. It should be noted there are clear limitations to the assay used and while we have normalised the biofilm formed against cell growth, there may be other bacterial physiological factors affected by the media and the presence of stress that also influence bacterial biofilm. We had previously determined the non-lethal level of each of the stresses used but even this may have varying effects across the number of strains we used. In the presence of formaldehyde in CDM, 15 strains induced biofilm formation, whereas 1 strain showed a reduction in biofilm formation upon addition of formaldehyde, and the remaining strains appeared unaffected. Interestingly, the strains that induced biofilm formation varied in their capsular type and disease origin. While most of the strains which increased their biofilm formation were non-typeable and sourced from OM cases, there was some variation – strains R3570 and R3601 were both sourced from the blood, although non-typeable, and strain 667 was a serotype b strain isolated from the throat.

In HI media, 5 non-typeable strains increased biofilm formation in formaldehyde included 3 OM isolates and 2 blood isolate strains. The strains which reduced their biofilm formation in the

presence of formaldehyde in HI media were all non-typeable OM isolates, except the laboratory strain Rd KW20.

Importantly, strains R3157 (with OM origin), R2846 (with OM origin) and R3567 (with blood origin) consistently showed an increase in biofilm formation in the presence of formaldehyde regardless of the media used.

Overall, these results indicate that the capsular type of the strain and its disease origin do not necessarily determine its capacity to form biofilm in different environmental conditions. Rather, there may be a more complex genetic or transcriptomic response to the presence of formaldehyde that determines biofilm formation capacity. A finer transcriptomics response would also likely be temporal, and may not be evident in a batch culture experiment achieved in 24 h.

In CDM, in the presence of methylglyoxal 12 strains increased their biofilm formation. The majority of these strains were non-typeable, with an OM origin, however 2 non-typeable strains had a blood origin, and 1 strain was recovered from a healthy child. In HI media no definitive trend in biofilm formation with methylglyoxal was identified, due to a large variation in biofilm formation values in the presence of methylglyoxal.

In the presence of H_2O_2, few strains increased their biofilm formation, while most strains showed a reduction in biofilm formation, and some showed no difference. In CDM 3 strains increased their biofilm formation – all were non-typeable, with 2 having an OM origin, and 1 originating from a healthy child. In HI media, 4 strains induced biofilm formation in the presence of H_2O_2, and these included non-typeable isolates sourced from the blood and 2 non-typeable isolates sourced from OM. Strains that reduced their biofilm formation in H_2O_2 also varied in their disease origin. In CDM, these strains included the laboratory strain Rd KW20 and a number of non-typeable OM isolates, however 2 blood isolates were also present – one a non-typeable strain, and the other a type d strain. In HI media, strains which reduced biofilm formation in the presence of H_2O_2 included Rd KW20, and 16 strains (predominantly non-typeable OM strains, with some strains of unknown origin) as well as 1 non-typeable blood isolate.

In the presence of H_2O_2, the only strain to consistently induce biofilm formation in both HI and CDM was R3264 – a non-typeable strain isolated from a healthy child.

Overall, the origin of the strains and their biofilm formation response to different nutrient conditions or the presence of chemical stress, did not seem to correlate. This suggests that the biofilm formation response is complex, and highly strain specific. This response is highly dependent on the environmental conditions, and in addition, may be dependent on host factors, which were not incorporated into this *in vitro* large-scale screen, and the capacity of the assay. In addition, the relationship between colonisation, biofilm formation and transition to invasive disease, is not well understood. In fact, in some bacteria, biofilm formation and the expression of virulence factors are linked. It is possible, that strains with an increased biofilm formation may have an increased persistence in the host, and in appropriate environmental conditions can cause more invasive disease; this could explain the high biofilm forming ability or biofilm induction of some blood isolates in this study. However, further studies would be needed to investigate this.

While we did not investigate the mechanisms responsible for the enhancement or reduction of biofilm formation upon exposure to ROS and RCS, several potential mechanisms were investigated in other bacterial species. It is known that quorum sensing through the AHL signal in Gram-negative bacteria, or through AI-2 in Gram-negative and Gram-positive bacteria, was shown to influence biofilm formation. In some bacterial species, including *E. coli* and *S. pneumoniae*, quorum sensing was shown to induce biofilm formation (González Barrios et al. 2006; Vidal et al. 2011), whereas quorum sensing repressed biofilm formation for other species such as *Vibrio cholerae* (Hammer and Bassler 2003). Recent data has shown that the quorum sensing signal AI-2 produced via *luxS* is able to induce biofilm formation in *H. influenzae* (Armbruster et al. 2009), although previous results suggested that it did not play a role in biofilm formation (Daines et al. 2005). Importantly, ROS were shown to influence quorum sensing for some bacterial species. Specifically, ROS could inhibit *S. aureus* autoinducer signalling *in vitro* and *in vivo* (Rothfork et al. 2004). However, an enhancement of quorum sensing upon exposure to ROS is also possible, as it has been demonstrated that the oxidation of AHL increased its biological activity (Frey et al. 2010). In addition, it has recently been shown for *M. avis*, that the AI-2 signal previously associated with quorum sensing, induced an oxidative stress response in the bacterial cell, triggering biofilm formation in a similar manner to H_2O_2, suggesting the involvement of AI-2 in the oxidative stress response rather than purely quorum sensing (Geier et al. 2008).

Another possible mechanism for the induction or repression of biofilm formation in the presence of stress could be a global stress response mechanism modulated by a global transcriptional regulator. In fact, a number of genes have been identified, which are important for both biofilm growth and resistance to oxidative stress. One example is the global transcriptional regulator OxyR, a transcriptional regulator mediating oxidative stress response in many bacterial species (Antelmann and Helmann 2011). This transcriptional regulator forms a disulfide bond upon activation by H_2O_2, leading to the expression of genes under its regulation. In *E. coli*, OxyR has been shown to be involved in biofilm formation via leading to the expression of the Ag43 adhesin (antigen 43) involved both in intercellular and surface adhesion (Danese et al. 2000), an observation corroborating the link between oxidative stress response and biofilm formation.

In view of the high variability in the biofilm formation of *H. influenzae*, it was also likely that there was a variation in the involvement of surface elements of the EPS matrix in the biofilms of these strains. It has been previously shown for *H. influenzae*, that eDNA and type IV pili were involved in the biofilm formation *in vivo* (Jurcisek and Bakaletz 2007). Therefore, we were interested to investigate whether these EPS matrix factors played a role in the biofilm formation of *H. influenzae* strains, and whether they accounted for some of the strain-specificity observed.

The results obtained from the biofilm formation assays performed in the presence of DNAse I, indicate the involvement of eDNA in the biofilm formation processes of some *H. influenzae* strains. For these assays, strains with a moderate-high biofilm formation potential were used. The response of these strains to the presence of DNAse I differed, depending on the growth media used. In HI media, only strains 86-028NP, a non-typeable OM isolate and R2866, a non-typeable blood isolate, showed a reduction in biofilm formation in the presence of DNAse I, indicating the involvement of eDNA in the biofilm formation of these two strains. In CDM, all strains except Rd KW20 and 86-028NP showed a reduction in biofilm formation. Importantly, in CDM the reduction in biofilm formation was greater than in HI media, potentially indicating a more significant role for eDNA in the biofilms formed in CDM compared to HI media. While all strains used in the DNAse I experiment formed moderate-high levels of biofilm in CDM and HI media, the results suggest that eDNA did not play an equal role in the biofilms formed by these strains. The fact that Rd KW20 and 86-028NP were affected in their biofilm formation by DNAseI in HI media, but not CDM may be explained by the fact that in this assay more biofilm

was formed by these strains in HI media. Strains R3157 and R2866, however, formed a high level of biofilm both in HI and CDM media, but were more affected by DNAse I presence in CDM. One explanation for this could be that the composition of the EPS matrix differs between the media used, and the environmental conditions utilised. For example, a comparison of *Salmonella enterica* serovar Typhimurium biofilm formation on glass and gallstones identified different compositions of the EPS matrix, as well as different roles of EPS matrix components in each condition (Prouty and Gunn 2003). These assays utilised not only different support matrix for the biofilm formation (i.e. glass or gallstones), but also a different growth media for each condition utilising Luria Bertani broth for growth on gallstones, and tryptic soy broth for growth on glass. Overall, such an observation supports our findings that indicate different roles for eDNA in biofilms formed in different growth media. Another explanation for the intra-strain variability in the involvement of eDNA in biofilm formation in different media conditions, could be that although the relative amount of biofilm stained by the CV was similar between both types of media, the temporal development of the biofilms was different, depending on the media used. Indeed, it is known that some components of the biofilms of other species are temporally regulated, and may be required only in early stages of biofilm development, or in later stages of biofilm maturation (Waite et al. 2005; Grande et al. 2014).

As type IV pili were previously shown to be important in the *H. influenzae* biofilm, it was important to determine whether the low biofilm formation of some strains could be explained by the absence of the type IV pili (in this case simply measured as a genetic absence of the major pilin subunit-encoding *pilA* gene). Importantly, screening of a subset of strains for the presence of the *pilA* gene identified the presence of *pilA* in 18 strains. Some of these strains, including Rd KW20 and 86-028NP, formed significant biofilm, whereas the majority did not. Two of the strains which did not produce a band correlating to the 1.3 kb expected fragment (1231 and NP) formed significant biofilm in HI media (but not CDM). Hence, in some conditions, these strains were still capable of forming biofilm. Again, this supports the observation that the presence of the *pilA-pilB* gene segment is not sufficient to determine a strain's biofilm forming capacity. This was partially expected, as not only the type IV pili, but many more EPS matrix components are involved in *H. influenzae* biofilm formation, including proteins, eDNA and carbohydrates such as LOS and sialic acid (Swords et al. 2004; Jones et al. 2013; Wu et al. 2014). In addition, true type IV pilus expression and functionality is determined by a much larger genetic subset

than *pilA* alone and indeed the transcriptional activation and repression is likely to be complex. For *H. influenzae*, it has been determined that the products of the *pilABCD* and *comABCDEF* operons are required for proper type IV pilus function (Carruthers et al. 2012). In addition, it has been shown in other bacterial species, that type IV pilus expression and function is under the control of different transcriptional pathways and indeed global regulators – for example, in *P. aeruginosa*, the global catabolite repressor control protein (CRP), which plays a role in carbon metabolism, also has a role in controlling *pilA* expression and type IV pilus twitching motility (O'Toole et al. 2000). The role of such global regulators in the expression and functionality of the type IV pilus in *H. influenzae* has not been determined, and therefore, opens the potential for a wider set of genes and global response pathways for the regulation of type IV pilus functionality. Therefore, the identification of *pilA* does not necessarily indicate a functional type IV pilus, and may not fully determine the role of the type IV pilus in the biofilm forming ability of these strains. Detailed analysis of type IV pili is not in the scope of this study.

Screening a range of clinical isolates for their biofilm formation in different environmental conditions, and in the face of stress revealed that there were differences in the ability of strains to form a biofilm. In addition, it was determined that eDNA did play a role in the biofilm EPS biofilm matrix, but that its role was strain-specific and dependent on the environmental conditions used for biofilm formation.

In addition, we have also shown that genetic determinants required for the adaptation of *H. influenzae* to different environmental conditions are also involved in aspects of biofilm formation. Specifically, we have shown that the *nimR-nikKLMQO* nickel uptake system plays a role in biofilm formation. This system was previously shown to be essential for the acid tolerance response of *H. influenzae* due to the role of nickel as a cofactor for urease (Kidd et al. 2011). In addition, it has been shown that the *H. influenzae nikQ* knockout strain in the Rd KW20 laboratory strain of *H. influenzae* was unable to import nickel and had a more electronegative surface charge and a higher aggregation and biofilm formation compared to the wild-type (Ng and Kidd 2013). We have shown that the *nikQ* mutant strain in Rd KW20 globally changed its gene expression pattern compared to the wild-type cells (Tikhomirova et al. 2015). This included the up-regulation of stress response genes such as chaperones involved in protein re-folding, as well as the up-regulation of heme/iron import and the up-regulation of several

membrane associated proteins and LOS biosynthesis genes. The up-regulation of the stress response genes (*dnaK*, *dnaJ*, *groES/L*, and *clpB*) could be explained by the reduced functioning of urease in the absence of nickel, and hence the higher degree of acid associated stress and damage to cellular DNA and proteins. The up-regulation of heme/iron import, however, could indicate the induction of biofilm formation in this strain, as iron has previously been shown to be involved in the biofilm formation of *H. influenzae* (Vogel et al. 2012). In addition, the up-regulation of cell-surface associated proteins and appendages (including LOS, sialic acid metabolism and pilin genes), supports the hypothesis of a global change in the expression of cell surface molecules to facilitate cell-cell interactions, and acquire globally a net negative change and hydrophobicity (Ng and Kidd 2013). Interestingly, in the *nikQ* mutant, there was a down-regulation of anaerobic metabolic genes including *dmsABC*, *nrf*, *glpAB*. There was also a surprising down-regulation of *oxyR*. The OxyR regulon has been studied in various bacteria, including NTHi, and while for *E. coli*, when OxyR is in a reduced state it represses itself, this did not seem to be the case in microarray analysis in an NTHi study (Harrison et al. 2007; Chiang and Schellhorn 2012). This does not rule out the redox state of the cell being altered in the *nikQ* mutant. The possibility could be that the *H. influenzae* cell is responding to the depleted levels of nickel as a signal for conditions to switch lifestyles and thereby affecting different pathways that are required for growth in this state. It is interesting that here was a also a down-regulation of central metabolic genes in the *nikQ*- strain, including *gdhA*, *mdh*, *fumC*, *pfl*, *gapDH*, and *gpmA*. Such global changes resulting in the own-regulation of anaerobic and central metabolism genes, suggested global metabolic change in the absence of nickel, which together with an up-regulation of cell-surface structures, could be explained by the cell's adoption of a metabolically dormant state, more suitable for sessile biofilm growth. Such metabolically-dormant cells have previously been reported in biofilms, and are considered to account, in part, for an increased antimicrobial tolerance in the biofilm (Kim et al. 2009).

To further study the role of nickel and the nickel uptake system in *H. influenzae*, a clinical OM isolate of *H. influenzae*, strain 86-028NP, was used. The *nikKLMQO-nimR* locus was also identified in the otitis media isolate strain 86-028NP. This strain has been shown to be different to Rd KW20 on a genetic level, and has been shown to form biofilms *in vivo*. The loss of *nikQ* resulted in a nickel depleted 86-028NP strain. It is worth noting that while the *nikQ* mutant had

undetectable levels of nickel (Table 3.6) there were also changes in the levels of other metal ions, such as iron. However, the other metal ions (as mentioned above) did not rescue the growth defect seen in the *nikQ* mutant suggesting a degree of nickel dependence on the physiological changes. It does still suggest a potential that that the loss of nickel uptake has broad consequences on the cell such as an increased level of iron, and it is these broader consequences which contribute to the cellular changes we observed. One of these changes included the *nikQ* mutant to have an increased cell-cell aggregation and more electronegative change compared to the wild-type cell. Cell–cell and cell–surface interactions have long been studied in the context of the surface properties (Schembri et al. 2002; van Merode et al. 2006; Andrews et al. 2010; Bonifait et al. 2010). Changes in the bacterial surface structures and the exact chemical nature of the bacterial surface results in various outcomes. The role of surface charge has been described by adapting the DLVO (Dejagiun, Landau, Verwey, Overbeek) theory to bacterial adhesion to a surface. This theory describes the interactions between non-biological lyophobic colloids, where the particle adhesion is determined through van der Waal interactions and interactions due to electric double layers (electrostatic interactions). The theory has been extended to include short range Lewis acid–base interactions. The DVLO theory has subsequently provided an understanding of various forms of bacterial adhesion (Poortinga et al. 2002; Rosenberg 2006). Under normal physiological conditions bacterial surfaces have a net negative charge, but they are known to be significantly variable due to environmental conditions but more importantly, due to changes in their macromolecular components. Bacterial surface structures such as pili/fimbriae, fibrils, surface proteins, and lipopolysaccharides/lipooligosaccharide (LPS/LOS) do have a capacity to vary in their chemical composition and nature, such as their size or content. These changes can include the addition or removal of hydrophobic amino acids or extracellular polymeric substances (EPS) which can contain glyocoproteins, polysaccharides or even attached acids such as sialic acid or uronic acids. These surface factors when in solution will be charged and therefore the presence and nature of these surface appendages will alter the bacterial cell charge (Tashiro et al. 2010). The surface charge of a bacterial cell can be determined by measuring its electrophoretic mobility (EM) and subsequently the electro-kinetic potential or zeta potential of the cell per s (Poortinga et al. 2002). The pH at which the EM is zero is the isoelectric point (IEP) and this represents the balance between anionic and cationic acid–base groups on the bacterial surface and is directly coupled to the molecular nature of the surface

structure of a bacterial cell. In this study, we found that the zeta potential/EM was more negative in the *nikQ* mutant of 86-028NP than the wild type. The surface charge of the 86-028NP *nikQ* mutant did not reach zero using a logical range of pH values. When nickel was added in excess (to a concentration we had calculated did result in nickel being able to enter the cell) to these cells, the charge returned to the wild type values. It is worth noting that *E. coli* cells with a isoelectric point less than 2.8 (as with the *nikQ* mutant) have been shown to be covered with more anionic polysaccharides, while if the isoelectric point increases over 4.0 (such as the wild type) the bacterial surface is more proteinaceous (Rijnaarts et al. 1999). More negatively charged bacterial cells have also been linked to higher cell–cell aggregation phenotypes and biofilm formations (van Merode et al. 2006; Bonifait et al. 2010). The *nikQ* mutant did aggregate, displaying an increased aggregation compared to the wild-type 86-028NP cells, and this aggregation was achieved through cell–cell interactions (Fig. 3.15).

We therefore assessed the biofilm formed by the *nikQ* mutant compared to its wild type (Fig. 3.16). Consistent with the discussion above, the *nikQ* mutant did form more biofilm than the wild type. This was directly linked to the cellular nickel levels – the addition of other metal ions had little or no affect on the biofilm. The key feature of cells that transit into a biofilm state compared to those actively growing planktonically, is a switch in numerous pathways, in the global systems driving the cell functions and defining its lifestyle. This includes the metabolism (the pathways for energy generation, biosynthesis of essential cellular components and maintenance of redox state), the surface presentation (the adhesins present and the chemical nature of those) and also well documented is the change in expression of stress response pathways. Our initial transcriptomics revealed that the genes with differential expression in the Rd KW20 *nikQ* mutant as compared to the wild type, collectively defined a change in lifestyle in the *nikQ* cells; its metabolism, its surface structures and the stress response. Perhaps consistent with the down-regulation of *oxyR* in Rd KW20 *nikQ*-, and the indication of the cellular state, the 86-028NP *nikQ* mutant was more sensitive to oxidative stress (Fig. 3.17). This switch in lifestyle is shown by an increased biofilm and decreased motility by the *nikQ* strain. There are few reports documenting the molecular mechanism for the environmental switch for motility in *H. influenzae*. Certainly Bakaletz et al. have variously described the involvement of different operons (*com* and *pil* operons) in the biosynthesis of *H. influenzae* type IV pili and this has been

shown to have a role in biofilm and separately in twitching motility (Bakaletz et al. 2005; Jurcisek and Bakaletz 2007; Heijstra et al. 2009). There are difficulties in clearly characterizing this type IV pili and twitching motility in laboratory conditions. This is associated with as yet unidentified strain specific factors as well as the environmental factors that induce expression of type IV pili. Twitching motility assays are variable and prone to significant error. We used two independent assay methods and several biological replicates and repeated the assay on three occasions, to be sure of the results. Consistent with a broad change in the *nikQ* strain's lifestyle we clearly observed a twitching motility phenotype that was significantly reduced in *nikQ* and then recovered by the addition of nickel. Not only is this important in further showing the pleiotropic effects of nickel to the cell but it also gives a new insight into the coupling of environmental signals to *H. influenzae* motility.

Our data has shown that *H. influenzae* does change its whole cell profile, under conditions where it does not import the correct level of nickel. Interestingly this was also seen by sensitivity in the 86-028NP *nikQ* strain to lowering pH and then to oxidative stresses. This was both nickel dependent and through an effect that went further than is attributable to GloA or urease (Fig. 3.17). It is an interesting consideration that the stress response genes are up-regulated in the Rd KW20 *nikQ* mutant and the *nikQ* mutant strain in 86-028NP was actually more sensitive to exogenous attack by stresses that those genes would protect against; that is, acidic conditions and oxidative stress. This is consistent with some other bacterial biofilm states; in *Vibrio cholera*e increases in the secondary metabolite, c-di-GMP, results in biofilm formation and repression of RpoS and in this state it is more sensitive to oxidative and other stresses (Wang et al. 2014). Also in *Pseudomonas* the protection of the biofilms cells from antimicrobials (oxidative or antibiotic stress) seems to be mainly through the development of the extracellular matrix; the biofilm cells without this coat can be more sensitive (Tseng et al. 2013). Nickel is essential in some pathogenic bacteria for their survival within the host. Nickel has been shown to have a core role for *H. influenzae* and this goes beyond the functions for the known enzymes that use nickel as a co-factor. In the host, variations in the level of nickel alter the host-pathogen environment. For example, an increase in nickel causes immune cells to increase their production of certain inflammatory cytokines (TNF-a, IL-1b and IL-6) (Taira et al. 2008) and nitric oxide (NO) (Chakrabarti et al. 2001; Taira et al. 2008) as well as leading to an elevation in oxidative stress

(Chakrabarti et al. 2001). Studies using animal models and human cell lines have shown that invading bacteria increase the local nickel levels and this is associated with a decrease in the production of antimicrobial agents and the ability to remove bacteria (Taira et al. 2008). In view of the environmental and host-related conditions which may create an environment limited in nickel, the alterations which occur in *H. influenzae* as a result of a nickel-limitation are important in understanding bacterial persistence and virulence. We demonstrated that in conditions in which nickel cannot be properly imported, *H. influenzae* switches its lifestyle; it changes its stress response gene expression, its surface structures and it forms a biofilm and reduces motility.

H. influenzae biofilm formation is a complex, multifactorial process. This process is both highly strain specific, and also specific to subtle micro-environmental conditions. Overall, we could not relate the differences in biofilm formation between the different strains to a certain disease profile or capsular type. There was no correlation of phenotype and isolate source. However, we identified that environmental conditions, including the media composition as well as the presence of ROS and RCS stress, did impact the existing strain specificity, either enhancing or repressing biofilm formation. In addition, we have shown that the EPS matrix plays a role in the biofilm formation of *H. influenzae*; the role of the EPS matrix in biofilm formation was also highly strain-specific and dependent on the environmental conditions in which biofilm formation occurred. Finally, we have shown that the presence of nickel impacts *H. influenzae* biofilm formation, and that in the absence of nickel, *H. influenzae* is able to induce a biofilm formation lifestyle determined by a global transcriptomic change.

Chapter 4.

The strain specificity of *H. influenzae* biofilm formation and survival in co-culture is related to subtle genetic and transcriptomics differences pertaining to the strain's adaptation to environmental conditions.

Overview

In this Chapter, we analyse in detail the adaptation to different environmental pH conditions, the biofilm formation and transcriptomics profile of 2 *H. influenzae* clinical isolates – the blood isolate Eagan, and the OM isolate strain R3264. We have shown that the transcriptomics profile reflects the adaptive mechanisms of these strains to different pH conditions.

In this chapter, we also show that different *H. influenzae* strains have different abilities to co-exist with the otitis media pathogen *Streptococcus pneumoniae* in permissive conditions (pH 8.6), but display a ubiquitous response of non-culturability in co-culture in non-permissive conditions (pH 7.4).

4.1 Introduction

Previous results (Chapter 3) have shown inter-strain differences in the ability of a set of 65 clinical *H. influenzae* isolates to form biofilm in different environmental conditions, suggesting the potential of variation at the genetic level to influence the adaptation of a strain to stress and result in biofilm formation. These biofilm formation and stress adaptation differences were not evidently associated with the disease source or capsular type, a phenomenon which has been previously reported (Obaid et al. 2015), and hence it was hypothesised that they are related in fact to specific genetic inter-strain differences. Indeed, it has previously been shown that there are significant genetic differences between *H. influenzae* strains Rd KW20 and the OM isolate 86-028NP (Munson et al. 2004; Harrison et al. 2005). These differences included 280 ORFs in 86-028NP which were absent from the genome of Rd KW20, and 169 ORFs present in Rd KW20 which were absent from strain 86-028NP. Some of the genes unique to 86-028NP were identified as involved in protection against ROS (*tsaA*), HMW proteins involved in adhesion and possibly biofilm formation, *tnaA* involved in protection against pH stress and a family of virulence associated transporters. In addition, a study comparing Rd KW20 and 12 clinical NTHi strains also found a high level of genetic variation between strains (Hogg et al. 2007). On average each clinical isolate had 127 insertions (>90kb) not found in Rd KW20, and 147 deletions. Overall, these studies suggested the existence of a *H. influenzae* supragenome, where the number of genes exceeds those found in any individual *H. influenzae* strain.

The high level of variation between *H. influenzae* strains also suggests the potential of different adaptation mechanisms to a particular niche or microniche within the human host. Such differences in adaptation, however, are likely to manifest in not only phenotypic or genetic differences, but also in more subtle regulatory and transcriptomics differences. We hypothesised, that strains with even minor differences in biofilm formation phenotype and disease source, would demonstrate significant transcriptional differences upon growth or adaptation to an environment. To investigate this hypothesis, we performed RNA sequencing to uncover transcriptional differences between a NTHi biofilm forming strain (R3264) and a type b strain (Eagan).

4.2 Results

4.2.1. The growth of different strains of *H. influenzae* with changing pH.

The growth of 11 strains (Appendix 2: Table S1) of *H. influenzae* was assessed over a range of pH values; pH 6.8, 7.4 and 8.0 as the physiological pH is known to vary among host organs, tissues and niches. Even within a particular body site there can be spatial and temporal changes in pH as a consequence of specific events (Nuutinen et al. 1993). Despite this uncertainty in the precise nature of the pH value associated with host-pathogen microenvironments, it is clear that there are distinct differences between the primary site of colonization (nasopharynx) and the various sites of infection, including the lower respiratory tract, the blood and the middle ear. As an example, the blood can be within the pH range of 6.8-7.4 and the middle ear is usually considered to be around pH 8.0, with the middle ear effusion in chronic OM patients ranging from pH 7-9. (Nuutinen et al. 1993; Wezyk and Makowski 1999). We assessed the pH response of a small set of isolates of *H. influenzae* that were known to colonise either the blood or the middle ear. We grew the bacteria (in liquid cultures, see Methods) at pH 6.8, 7.4 and 8.0 and plotted their growth curves (Appendix 1: Fig. S1) and from this we calculated mean growth rates (Table S4.1 and Appendix 1: Fig. S2). There were no clear patterns, and the observed changes represented only slight variations. The equivocal differences in growth at different pH levels does not exclude the possibility that the cells are responding differently, such as with an alternative lifestyle (biofilm formation).

4.2.2. The formation of biofilm by *H. influenzae* as a consequence of changing pH.

Given that colonization by *H. influenzae* within various host niches, such as the middle ear, is linked to their induction of a biofilm, and increased pH is characteristic of these environments, we assessed the possibility that biofilm induction is a consequence of increased pH. It has been previously suggested that for *H. influenzae* the biofilm formation is induced at pH 8.0 (Bakaletz et al. 2005). We assayed for biofilm formation at pH 6.8, 7.4 and 8.0 (Appendix 1: Fig. S3). These screening assays were performed by counting planktonic cells (as described in Methods) followed by washing and then releasing the biofilm cells, and counting colonies (to calculate colony forming units per ml; CFU/ml). In some strains, such as isolate R3264, there was significant induction of biofilm at pH 8.0 (Appendix 1: Fig. S3). Other strains, including Eagan, did not form biofilm at any pH. To compare in detail contrasting isolates from this screening of *H. influenzae*, Eagan (a capsular, blood isolate) and R3264 (a NTHi middle ear isolate) were selected for further analysis (Fig. 4.1), more biological and experimental replicates.

Planktonic cell growth was assessed and then biofilm cell numbers were enumerated. Eagan grew equally well at pH 6.8 and 8.0, as did R3264, but Eagan did not form any biofilm at either pH 6.8 or 8.0 whereas R3264 produced a significant biofilm at pH 8.0, and within the context of this assay there was an increase in biofilm formation at pH 8.0 (Fig. 4.1B). These results are consistent with what is generally accepted and known with regard to *H. influenzae* pathogenesis; that the capsular strains cope with increased pH by continuing planktonic growth while a NTHi isolate that colonizes the middle ear switches to a biofilm mode of growth (Anderson et al. 1998; Ehrlich et al. 2002; Hall-Stoodley et al. 2006).

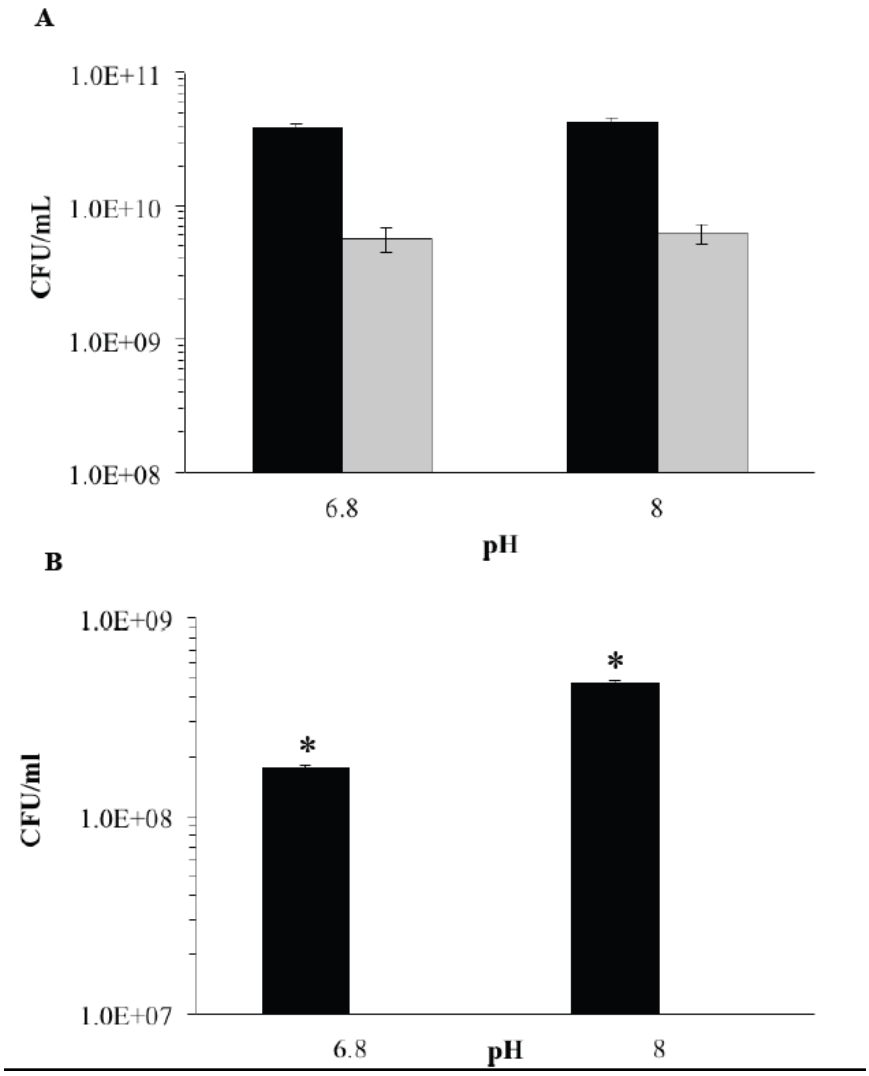

Fig 4.1. The effect of pH on the (A) growth and (B) biofilm formed by *H. influenzae* isolates Eagan and R3264. The cells of strain R3264 (black bars) and Eagan (grey bars) from planktonic growth at pH 6.8 and then 8.0 were assessed. Similarly, the (B) biofilm cells were collected and cell numbers enumerated. Error bars are the standard deviation, *$p < 0.001$ (Student t-test).

4.2.3. Transcriptional analyses of Eagan and R3264 under different pH.

Given the definite, growth-style, variations in response to a shift in pH from 6.8 to 8.0 between Eagan and R3264, we were interested in determining the underlying transcriptional differences that varied between Eagan and R3264. We therefore used RNAseq to analyse the whole cell transcriptome at pH 6.8 and 8.0 for the planktonic growth of both Eagan and R3264 (Fig. 4.2).

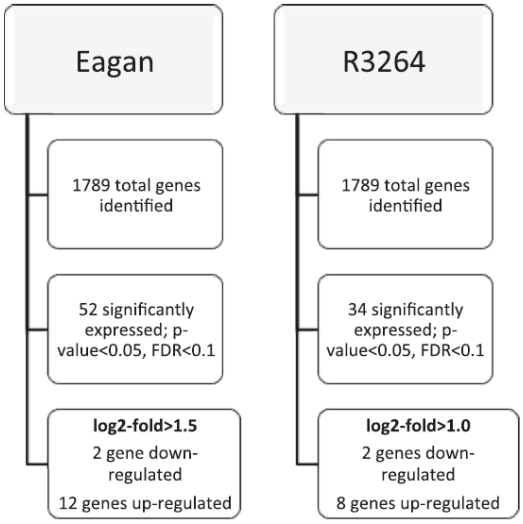

Fig. 4.2. An overview of RNASeq results for *H. influenzae* strains Eagan and R3264 grown at pH 6.8 and 8.0. RNA was collected from planktonic growth of strains Eagan and R3264 when grown at pH 6.8 and 8.0 and the whole genome expression was compared. The numbers of genes differentially expressed under these conditions is shown.

The shift from pH 6.8 to 8.0, while biologically relevant and certainly impacting bacterial style of growth (Fig. 4.2), is still a subtle change and it was not expected to generate a large set of cellular pathways with changed expression patterns. Genes that were differentially expressed in Eagan (Table 4.1 and Appendix 1: Fig. S4) revealed predominantly an up-regulation of two gluconate:H+ symporters (HI1015 and HI0092) and the associated gluconate (or sugar acid) metabolic genes (HI1010-1015, see Fig. 4.3) and a potential glycerate kinase (HI0091) that links into glycolysis. It is worth noting that these genes/pathways are genetically unlinked, adding to

validity of the response. In addition to the HI1015/*gntP* symporter, the HI1010-1015 genes include homologs to a sugar epimerase, aldolase and isomerases that are within the first stages of the pentose phosphate pathway (PPP). The first gene (HI1010) is a potential 6-phosphogluconate dehydrogenase that generates ribulose-5-phosphate. This links directly into the PPP and other energy and biosynthetic pathways (outlined in Fig. 4.3). The GntP symporter family of transporters also imports H+, as part of the survival response associated with an increased environmental pH (Table 4.1).

Table 4.1. Genes differentially expressed in *H. influenzae* Eagan at pH 8.0 compared to pH 6.8.

Genes up-regulated at pH 8.0 compared to 6.8

Metabolic genes

Gene	Log_2 fold	*p*-value	FDR	Comment
HI1010	2.21	$5.12x10^{-10}$	$1.02x10^{-7}$	6-phosphogluconate dehydrogenase
HI1011	2.20	$6.83x10^{-10}$	$1.22x10^{-7}$	Similar to YgbK
HI1012	2.04	$3.06x10^{-8}$	$3.64x10^{-6}$	Sugar isomerase
HI1013	1.88	$3.04x10^{-7}$	$2.86x10^{-5}$	Hydroxypyruvate isomerase
HI1014	1.52	$2.33x10^{-5}$	$1.54x10^{-3}$	Sugar epimerase
HI1015	1.12	$1.18x10^{-3}$	$4.70x10^{-2}$	GntP family, gluconate:H+ symporter
HI0091	1.74	$5.98x10^{-7}$	$5.33x10^{-5}$	hypothetical protein; homologous to GlxK, glycerate kinase
HI0092	2.14	$1.49x10^{-9}$	$2.41x10^{-7}$	GntP family, gluconate:H+ symporter

Iron uptake genes

Gene	Log_2 fold	*p*-value	FDR	Comment
HI0995	1.53	$1.72x10^{-5}$	$1.23x10^{-3}$	OMP, iron-binding
hitA	2.21	$1.69x10^{-10}$	$3.77x10^{-8}$	Iron uptake,

hxuB	1.65	$1.54x10^{-6}$	$1.25x10^{-4}$	hemopexin utilization protein
hxuC	1.70	$8.04x10^{-7}$	$6.83x10^{-5}$	TonB-dependent heme receptor
Genes of unknown function				
Gene	Log_2 fold	*p*-value	FDR	Comment
HI1427	1.54	$6.87x10^{-6}$	$5.33x10^{-4}$	hypothetical protein
Genes down-regulated at pH 8.0 compared to 6.8				
Gene	Log_2 fold	*p*-value	FDR	Comment
HI1349	-2.31	$5.58x10^{-11}$	$1.42x10^{-8}$	ferritin
HI1385	-1.55	$2.27x10^{-5}$	$1.54x10^{-3}$	FtnB; non-heme ferritin

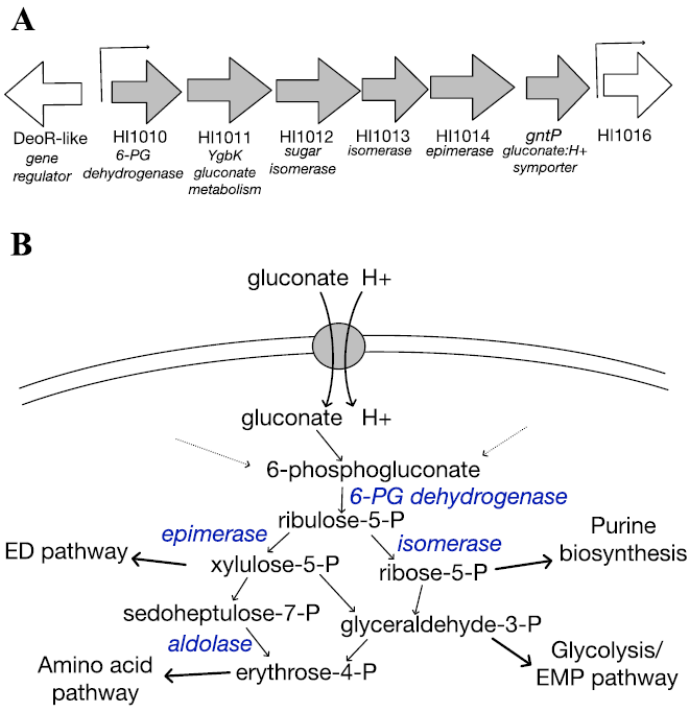

Fig. 4.3. The pathway uniquely induced in *H. influenzae* Eagan at pH 8.0. (A) Genes HI1010-1015 (block arrows, grey) were all induced in *H. influenzae* Eagan at pH 8.0. In silico analysis identified 2 promoters across this region of the genome (indicated by line arrows) and HI1010-HI1015 forms a single operon. (B) These HI1010-1015 genes encode a gluconate:H+ symporter, a putative 6-phospohogluconate dehydrogenase and a range of sugar isomerases and epimerases that would link gluconate to the PPP and other metabolic pathways (the putative roles for these genes are shown in blue).

It is interesting to note that our bioinformatic analyses have identified an operator/promoter upstream of HI1010 (Fig. 4.3) with a putative DeoR binding site; HI1010 is divergent to a DeoR-like gene. While not within the scope of this project it is known in other bacteria that DeoR-like regulators variously control pathways directing sugar metabolism and are connected to the PPP. Also, the bioinformatics analyses indicate that the HI1010-1015 genes are on a single transcriptional unit, forming an operon. Traditionally, high concentrations of glucose are thought to be oxidized extracellularly by membrane-bound dehydrogenases, whereas under low glucose conditions, oxidized glucose is imported and phosphorylated within the cell to 6-phosphogluconate (Cohen 1951) which feeds into either the Entner-Dourdooff (ED) pathway or the PPP (Eisenberg and Dobrogosz 1967) for energy. In addition, gluconate can act as an

exogenous carbon source and therefore be taken up as a direct mode of growth. It has been shown in some contexts that such metabolism is related to bacterial growth in the host-pathogen environment, such as with *E. coli* colonization of the mouse large intestine (Sweeney et al. 1996; Sweeney et al. 1996) where gluconate is also important in the growth and pathogenesis of other pathogens (Patra et al. 2012). Some bacteria possess multiple gluconate uptake systems (Izu et al. 1997; Porco et al. 1997), such as those characterized in *E. coli*, where there are four (Peekhaus et al. 1997). Not all of these are necessarily primary gluconate transporters, with some acting on other sugar acids that are able to be utilized by the same permeases. At least one of these has been shown to be likely to preferentially import fructuronate and not gluconate (Utz et al. 2004). In *E. coli* and other bacteria these transporters are regulated through different transcriptional pathways controlled by sugar-utilizing systems and signals; such as the sensing of the presence of gluconate by GntR, or as in a cAMP-dependent catabolite repression system/s, by the global transcriptional regulator CRP (Izu et al. 1997; Letek et al. 2006; Frunzke et al. 2008). There is an emerging consensus that the regulation and role of these sugar acid metabolic systems is broader than originally thought. Recently it has been shown that in *E. coli*, the hexuronate utilizing pathways are regulated by a complex interplay of regulatory systems including induction under osmotic stress conditions (Klein et al. 2011). What is clear from our results is that there are two homologous gluconate transport systems in *H. influenzae* Eagan that both are upregulated at pH 8.0. The media used throughout our studies was rich in glucose and other carbon and energy sources (and the media was the same between pH 6.8 and 8.0; changes in carbon availability and the subsequent regulatory systems is therefore not a reason for these genes being upregulated at pH 8.0 compared to 6.8). It is worth noting that there are other genes responsible for these steps in the PPP in the genomes of *H. influenzae*, however these genes are not physically linked on an operon as with HI1010-1015. The indication is that in the Eagan strain the HI1010-1015 operon is uniquely regulated based on pH and it feeds into the PPP functioning under increased pH. The duplication of genes for steps in the PPP is not unusual, there are homologs of these *H. influenzae* genes (HI1011-1015) in several bacteria that have a similar duplication. In *Pectobacterium carotovorum* the homologs to HI1011-1015 are *vguABCD* and these function in gluconate metabolism and have an as yet uncharacterized role in the pathogenesis of this plant pathogen (Mole et al. 2010). Interestingly, the sugar acid metabolism pathways can also feed into cell wall composition or modifications. Glucuronic acid can be

incorporated into the inner core of the lipopolysaccharide (LPS) in *E. coli* and these potential modifications are a response to environmental stresses, specifically those associated with envelope stress, such as pH, and this response is controlled by several regulatory pathways (Klein et al. 2011; Klein et al. 2013). We demonstrated that as the pH increases to 8.0, the Eagan isolate induced two gluconate permeases, one being part of an operon with gluconate metabolism genes, these likely providing the proteins and enzymes linked into energy production (through the ED or PPP pathways) but also potentially providing other cellular alterations for coping with the stress (modifying the LOS, for instance).

In contrast, the NTHi R3264 isolate did not induce the HI1010-1015 operon at pH 8.0. Consistent with this isolate inducing its biofilm formation at pH 8.0, it induced various, genetically unlinked iron acquisition genes (Table 4.2; the iron uptake genes *hitAB, tbp1-tbp2* and *hxuB* were all upregulated and the iron storage ferritin gene was down-regulated).

Table 4.2. Genes differentially expressed in *H. influenzae* R3264 at pH 8.0 compared to pH 6.8.

Genes up-regulated at pH 8.0 compared to 6.8				
Iron uptake genes				
Gene	Log_2 fold	*p*-value	FDR	Comment
hitA	1.76	$9.65x10^{-12}$	$2.46x10^{-9}$	Iron uptake ABC, periplasmic domain
hitB	1.31	$8.77x10^{-7}$	$1.11x10^{-4}$	Iron uptake ABC, permease domain
tbp2	1.54	$2.92x10^{-5}$	$2.74x10^{-3}$	Iron-binding OM receptor
tbp1	1.49	$3.53x10^{-7}$	$5.26x10^{-5}$	Transferrin binding protein
hxuB	1.02	$8.62x10^{-5}$	$7.32x10^{-3}$	Heme-hemopexin utilization protein.
Metabolic genes				
Gene	Log_2 fold	*p*-value	FDR	Comment
glpB	1.08	$5.35x10^{-5}$	$4.77x10^{-3}$	Glycerol metabolism
Genes of unknown function				
Gene	Log_2 fold	*p*-value	FDR	Comment
HI0997	1.34	$8.95x10^{-4}$	$5.51x10^{-2}$	hypothetical protein

HI1427	1.31	$4.17x10^{-7}$	$5.72x10^{-5}$	Transmembrane protein
Genes down-regulated at pH 8.0 compared to 6.8				
Gene	Log_2 fold	*p*-value	FDR	Comment
HI1349	-1.23	$5.14x10^{-6}$	$5.10x10^{-4}$	Ferritin
ahpD	-1.72	$1.24x10^{-7}$	$2.01x10^{-5}$	Stress response.

In multiple bacterial species iron acquisition pathways have been linked to the development of the biofilm lifestyle; such that if these pathways are removed or iron is unavailable it depletes their biofilm-forming ability (Chhibber et al. 2013; Rumbo-Feal et al. 2013). Likewise in studies on NTHi biofilm formation and biofilm maturation, the iron uptake has been shown to be essential (Mason et al. 2003; Mason et al. 2005; Harrison et al. 2013; Szelestey et al. 2013). It should be noted that in our comparative analyses of R3264 and Eagan at pH 8.0 we showed that Eagan did not form significant amounts of biofilm. As a comparison of their profile of growth pathways at pH 8.0 and then for R3264 at 6.8 (when R3264 cells forms less biofilm), the transcriptional switch in the planktonic R3264 cells at pH 8.0 compared to 6.8 is an indication of their response to this environmental condition and mechanisms that predispose the cells to biofilm formation as well as allowing a direct comparison to the Eagan planktonic cells at pH 8.0. The R3264 cells at pH 8.0 that are in the biofilm were therefore excluded from our comparison; these by definition would be greatly different (probably including the type IV pili or other adhesins) and not a clear comparison to the non-biofilm forming Eagan cells. It was not our aim to compare planktonic against biofilm cell but the response to increased pH, conditions we know shift the R3264 cells to a biofilm-forming state. It is worth noting that there were iron-associated genes up-regulated in Eagan at pH 8.0 but not to the extent observed in R3264.

Importantly, these results have shown that there are phenotypic and transcriptomic differences in the adaptation of different *H. influenzae* strains to environmental conditions, their survival and biofilm formation. In further chapters of this thesis we show in detail (Chapter 5), that pH is also a vital determining factor in the ability of some *H. influenzae* strains to survive in co-culture with *S. pneumoniae* (both in planktonic and biofilm form) (Tikhomirova et al. 2015). Therefore, it was important to establish whether strains Eagan, and R3264, which have had their pH response analysed more deeply at a transcriptomics level, as well as several other clinical isolates of *H.*

influenzae for which there is some known genetic information, have different abilities to survive in co-culture with *S. pneumoniae*.

4.2.4 Strain variation does not significantly alter the ability of *H. influenzae* to survive in co-culture with *S. pneumoniae* at pH 7.4.

Initially, it was important to assess the planktonic growth of these clinical isolates in mono-culture, and in co-culture with *S. pneumoniae* at pH 7.4, a pH at which Rd KW20 and the control clinical isolate strain 86-028NP did not survive (further examined in Chapter 5). Further experiments led us to hypothesise that this result may actually be the entry of *H. influenzae* into a VBNC (Viable But Non-Culturable) state, rather than its cell death (as discussed in Chapter 5). To investigate whether there was a difference in the abilities of clinical isolates to survive in co-culture with *S. pneumoniae*, we repeated the static growth assays described in Chapter 5, where mono- and co-cultures of *H. influenzae* strains (Rd KW20, R3264, 86-028NP) and *S. pneumoniae* (strain 11), were grown in static conditions, in HI media for 14 h at pH 7.4.

Results showed, that at a pH of 7.4 there were no significant differences between the growth of Rd KW20, 86-028NP, Eagan or R3264, however, in co-culture with *S. pneumoniae* strain 11, none of these strains was able to survive after 14 h (Fig. 4.4). This result indicates that in co-culture at pH 7.4, the drop in pH may be extreme, and the inhibition of culturability for *H. influenzae* may be a broad effect relevant for all of the *H. influenzae* strains tested. It may be that this is a condition of extreme stress for *H. influenzae* and hence, genetic and transcriptomics inter-strain variation does not impact on this phenomenon.

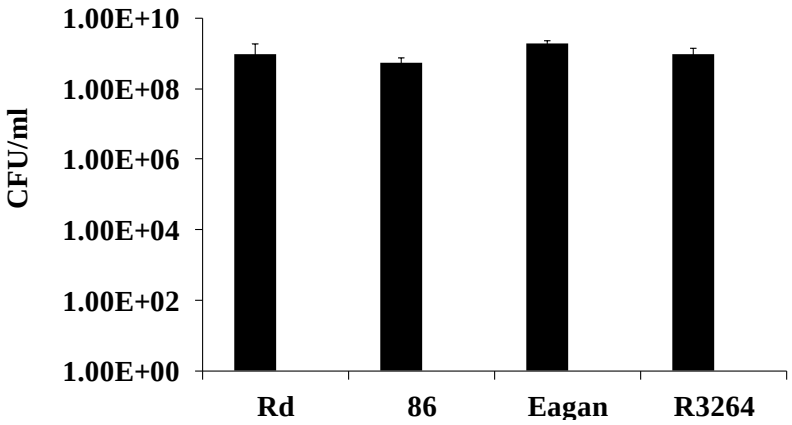

Fig 4.4. *H. influenzae* strains Rd KW20, 86-028NP, Eagan and R3264 are all non-culturable in the presence of *S. pneumoniae* (at pH 7.4). The planktonic mono-culture growth of *H. influenzae* Rd KW20 and clinical isolates 86-028NP, Eagan and R3264 at pH 7.4 after 14 h is displayed (black bars). The mono-cultures of the strains are shown in black bars. The co-culture of all strains at pH 7.4 was below the detection limit of the assay, therefore is not seen in the graph.

It is worth noting, that *S. pneumoniae* strain 11 did not significantly reduce its culturability in co-culture with *H. influenzae* isolates at pH 7.4 (Fig. 4.5). Although it appeared to have a slightly higher culturability in mono-culture and with strain R3264 than with Rd KW20, 86-028NP or Eagan, this difference is very slight and may not be of physiological significance, unlike the complete reduction of *H. influenzae* culturability in co-culture.

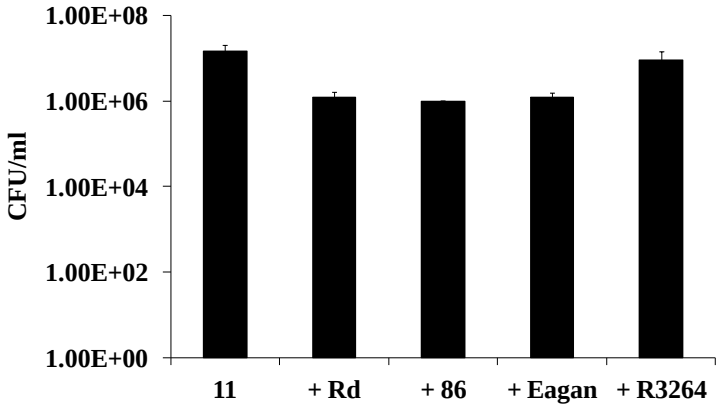

Fig 4.5. *S. pneumoniae* strain 11 has comparable growth in mono-culture and in the presence of *H. influenzae* strains Rd KW20, 86-028NP, Eagan and R3264 (at pH 7.4). The planktonic growth is shown for *S. pneumoniae* strain 11 in mono-culture, and in co-culture with *H. influenzae* strain Rd KW20 and *H. influenzae* clinical isolates 86-028NP, Eagan and R3264 at pH 7.4.

4.2.5. Strain variation displays differences in the ability of *H. influenzae* isolates to survive in co-culture with *S. pneumoniae* at pH 8.6.

Further to the fact that none of the *H. influenzae* isolates showed a difference in their response to co-culture with *S. pneumoniae* at pH 7.4, we decided to analyse their ability to planktonically grow and form a biofilm with *S. pneumoniae* at a higher pH. Previously, we have demonstrated that strain Eagan is unable to form a biofilm at pH 6.8 and 8.0, and strain R3264 was able to increase biofilm formation at pH 8.0. In addition, we have shown that at pH 8.0, *H. influenzae* is able to be cultured from the *S. pneumoniae* co-culture, however, still experiences a reduction in culturability relative to its mono-culture (these studies are shown in Chapter 5) (Tikhomirova et al. 2015). Therefore, we hypothesised that the use of a higher pH than 8.0, which would still be

physiologically relevant, would be more appropriate to test finer differences in the inter-strain variation of *H. influenzae* isolates' response to *S. pneumoniae* co-culture, and that at this higher pH, the biofilm forming, and thus more biologically relevant, strain R3264 could demonstrate differences in its ability to survive in co-culture relative to the non-biofilm forming strain Eagan.

Once again, we repeated the static growth and biofilm formation assay of mono- and co-cultures of *H. influenzae* strains (Rd KW20, 86-028NP, R3264, as well as 2 more clinical isolates, strains BS139 and BS171, which are predicted based on genetic analysis not to possess a functional type IV pilus), and *S. pneumoniae* (strain 11), in static conditions, in HI media for 14 h, but at pH 8.6.

Performing *H. influenzae/ S. pneumoniae* co-culture experiment at pH 8.6 revealed that there were some inter-strain differences in the ability of *H. influenzae* strains to grow in co-culture.

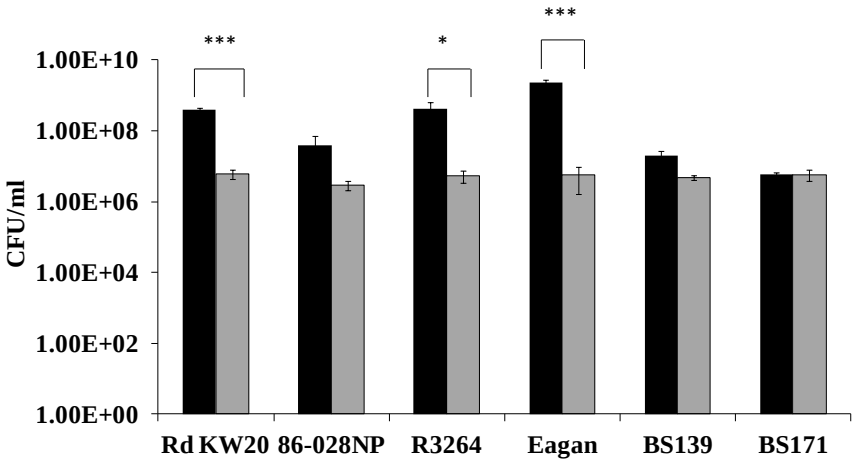

Fig 4.6. *H. influenzae* strains Rd KW20, 86-028NP, R3264, Eagan have equal abilities to survive in the presence of *S. pneumoniae*, while strains BS139 and BS171 display lower levels of growth and greater adaptation to *S. pneumoniae* co-culture (at pH 8.6). The planktonic mono- (black bars) and co-culture (grey bars) growth of *H. influenzae* Rd KW20 and clinical isolates 86-028NP, R3264, Eagan, BS139 and BS171 with *S. pneumoniae* strain 11 at pH 8.6 is shown. For strains Rd KW20, R3264 and Eagan there is a statistically significant difference in the ability to survive in co-culture compared to mono-culture. The difference for

86-028NP is not significant, although close to $x10^1$ difference, and is low and non-significant for BS139 and BS171.

Strain Rd KW20, 86-028NP, R3264 and Eagan displayed a significant (10^1-10^2 times) reduction in culturability in co-culture compared to mono-culture (Fig. 4.6), with Eagan displaying the greatest reduction in culturability. (It is noteworthy that the reduction in culturability of 86-028NP was not statistically significant, but still equal to a 10^1 times reduction, and therefore is regarded as a biologically significant reduction in cell numbers for the purposes of this discussion). This correlated to what was seen for strain Rd KW20 in co-culture at pH 8.0 (see Chapter 5). However, strain BS139 and BS171 displayed a slightly different phenotype. Both strains had lower CFU/ml values in mono-culture compared to the other strains, and altered co-culture phenotypes. Strain BS139 showed a reduction in culturability in co-culture, however, this reduction was less significant than what was observed for strains Rd KW20, 86-028NP, R3264 and Eagan. Strain BS171 did not show a reduction in culturability in co-culture.

Results of biofilm formation for these strains showed similar results (Fig. 4.7). Strains Rd KW20, 86-028NP, R3264 and Eagan showed a reduction in biofilm formation in co-culture with *S. pneumoniae* from 10^1 - 10^2 (Fig. 4.7). However, strain BS139 did not show a reduction in biofilm formation in co-culture, and strain BS171 did not form any biofilm in co-culture, although it did form biofilm in mono-culture. Importantly, both BS139 and BS171 had lower biofilm formation even in mono-culture compared to strains Rd KW20, 86-028NP, R3264 and Eagan. Importantly, both strains were deficient in *pilT* and *comA-F* genes and were predicted to be deficient in a functional type IV pilus.

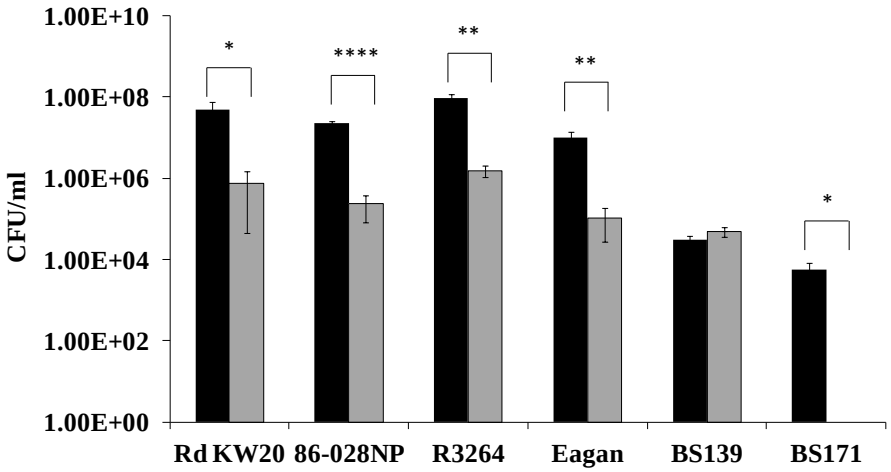

Fig 4.7. *H. influenzae* strains Rd KW20, 86-028NP, R3264, Eagan and BS171 are reduced in their ability to form biofilm in the presence of *S. pneumoniae*, while the biofilm forming ability of BS139 remains unaffected (at pH 8.6). Biofilm mono-(black) and co-cultures (grey bars) of *H. influenzae* Rd KW20 and clinical isolates 86-028NP, R3264, Eagan, BS139 and BS171 with *S. pneumoniae* strain 11 are shown at pH 7.4. The biofilm formation in co-culture with *S. pneumoniae* was significantly different for all strains except BS139.

It is important to note that at pH 8.6, there were no differences in the ability of *S. pneumoniae* strain 11 to grow planktonically or form a biofilm in the presence of *H. influenzae* strains (Fig. 4.8).

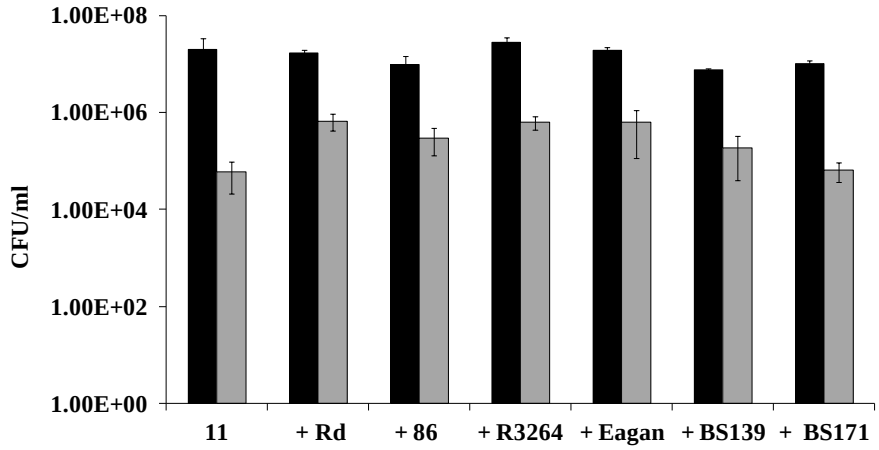

Fig. 4.8. The planktonic growth and biofilm formation is not significantly different for *S. pneumoniae* growth in mono-culture or in co-culture with various *H. influenzae* isolates (at pH 8.6). The planktonic (black) and biofilm (grey) growth of *S. pneumoniae* strain 11 is shown in mono-culture (11), and in co-culture with *H. influenzae* strain Rd KW20 and clinical isolates Rd KW20, 86-028NP, R3264, Eagan, BS139, BS171.

4.2.6. The *nikQ* gene is required for the ability of *H. influenzae* to survive in the presence of *S. pneumoniae*.

It has been shown that the Rd KW20 *nikQ*- strain, which is unable to import nickel had an increased biofilm formation and changes in cell surface properties (Kidd et al. 2011; Ng and Kidd 2013; Tikhomirova et al. 2015). It has also been shown that the *nikQ*- mutant in the biofilm forming strain 86-028NP, displayed transcriptomics differences compared to the wild-type, including an upregulation of genes associated with increased biofilm formation – such as the LOS biosynthesis genes (Tikhomirova et al. 2015).

In addition, the MerR like regulator (*nimR*) and the nickel import system genes (*nikKLMQO*) have been shown to be important in acid tolerance (Kidd et al. 2011). This system was activated upon depleted nickel levels or decreased extracellular pH. The likely reason for this is that nickel is a cofactor the urease enzyme which is involved in acid stress response in many bacteria (Kidd et al. 2011).

As we have shown the involvement of acidic by-products in the interactions of *H. influenzae* and *S. pneumoniae*, it was important to establish the role of the nickel import system in these interactions given the involvement of the pH factor as a variable in these interactions.

To establish the involvement of the nickel import system in the *H. influenzae/S. pneumoniae* interactions, we performed a co-culture assay with the *H. influenzae nikQ*- strain and the *S. pneumoniae* strain 11, in HI media for 14 h, at pH 7.4 and pH 8.0. The results showed that the Rd KW20 *nikQ*- strain was non-culturable in the presence of *S. pneumoniae*, both in the planktonic and biofilm state (Fig. 4.9)

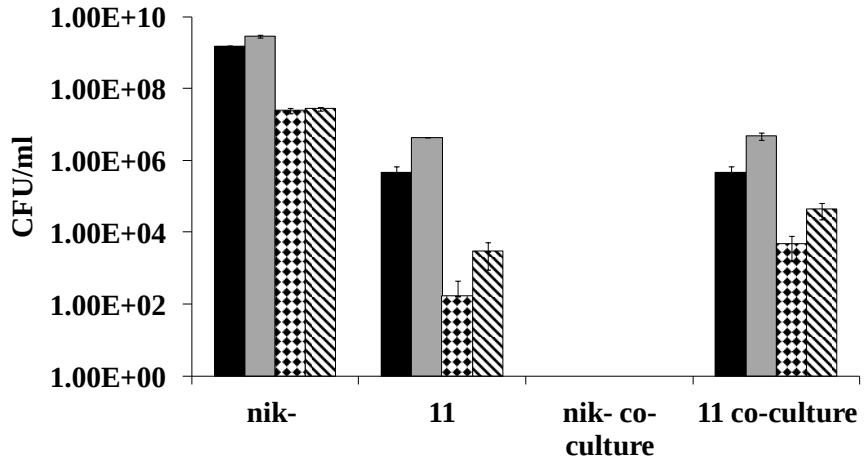

Fig. 4.9. *H. influenzae* Rd KW20 *nikQ*- (nik-) is non-cuturable in co-culture with *S. pneumoniae* at pH 7.4 and 8.0. The planktonic growth of *H. influenzae nikQ* ¯ (nik-) and *S. pneumoniae* strain 11 is shown at pH 7.4 (black bars), 8.0 (grey bars), and biofilm growth is shown at pH 7.4 (checked bars) and 8.0 (striped bars).

4.3 Discussion

Importantly, our results have shown that there are both physiological differences related to biofilm formation as well as significant transcriptional differences between 2 *H. influenzae* isolates sourced from different body sites, which reflected their ability to adapt to different environmental conditions.

H. influenzae can adapt to the physical and chemical properties that exist in different anatomical niches (such as the nasopharynx, lung, blood and the middle ear mucosa). Various strains of this pathogen adapt to these niches differently, such as by growing rapidly and planktonically or alternatively by forming a biofilm. The different niches are known to vary in a range of properties, the pH being one of these that subtly but significantly shifts from about neutral in the blood to pH 8.0 in the middle ear (Nuutinen et al. 1993; Wezyk and Makowski 1999). The pH does not remain constant within a niche and even in the blood there can various reasons for the pH to shift. While blood pH is tightly regulated at around pH 7.4, there are other parts of the body encountered by *H. influenzae* as a result of systemic infection starting in the blood that can include conditions that do reach pH 8.0. A capsular isolate taken from the blood (such as the strain Eagan) would therefore need to be able to exist in the pH range of 6.8-8.0 but in this context it is rarely associated with a biofilm. A NTHi isolate from the middle ear (R3264) would predominantly encounter pH 8.0 and its processes of colonization would occur at this pH (although once again the pH is thought not to be constant in this niche, but varying within a range of pH 7.0-9.0). In this niche as part of its colonization, the bacterial cell would form a biofilm. Indeed some studies have shown that biofilm is induced in the middle ear as a very likely consequence of the increased pH (this was presented as a function of the induction of type IV pili but does not exclude other pathways not examined in this study) (Bakaletz et al. 2005). In addition, the type IV pili genes are more likely to be highly regulated in the biofilm cells themselves and not the planktonic cells we analysed.

Not all *H. influenzae* isolates respond to the changes in physical and chemical properties between the niches that *H. influenzae* can occupy with the same capacity or in the same manner. We show that *H. influenzae* isolates respond differently to the subtle and yet physiologically relevant

changes in pH from 6.8 to 8.0. These changes are slight in regards to the observed growth rates but the changes are underpinned by lifestyle changes, such as modes of growth or biofilm formation. A capsular isolate (Eagan), continues to grow, with variation from pH 6.8 to 8.0 and does not form a biofilm while a NTHi isolate known to colonize the middle ear, does form a biofilm, increasing biofilm formation at pH 8.0. This is consistent with the established knowledge that the middle ear is more basic in its pH than the nasopharynx or the blood and NTHi colonize the middle ear by biofilm formation. While it was not unexpected that the NTHi isolate induced its iron uptake pathways during its growth at pH 8.0 as it cells become predisposed to forming a biofilm, it was a novel finding that the Eagan strain induced gluconate:H+ uptake and sugar acid/gluconate metabolic genes. This pathway was not induced in the biofilm-forming R3264 cells. This obviously provides a pathway for growth, through the link from gluconate to the ED and PPP energy production pathways, while at the same time providing a mechanism for maintaining pH homeostasis (importing H+). Our study has therefore identified clear differences between a capsular isolate and a NTHi isolate in their response to a relevant pH shift; these differences seem likely to be the basis for their mode of growth and survival within a specific niche.

Hence, overall, the results demonstrated that biofilm formation of a strain and its disease source can be linked to subtle transcriptomic differences between strains, which reflect the ability of a strain to adapt to and survive in a particular micro-environement.

We hypothesised, that some of these subtle adaptation differences resulting in transcriptomics changes, could also play a role in the ability of *H. influenzae* to interact and survive in the presence of *S. pneumoniae*. As we had previously seen *H. influenzae* transit to a completely non-culturable state in co-culture at a pH of 7.4, we were interested whether this phenotype would be altered by the use of genetically diverse clinical isolates with known transcriptomics differences. However, the results showed that at pH 7.4, all *H. influenzae* strains transited to a completely non-culturable state. This suggests, that the pH change occurring in co-culture at pH 7.4, is extreme, and falls past a certain toxicity threshold ubiquitous to all strains.

The ability of *H. influenzae* strains to survive in co-culture at pH 8.6 was, however, different. Strains Rd KW20, 86-028NP, R3264 and Eagan reduced their culturability in co-culture equally,

(10^1-10^2). This is despite the subtle differences in gene regulation that were demonstrated between Eagan and R3264 in different pH environments. This result suggests that if there were differences in the adaptation of these strains to a co-culture environment, these were likely subtle transcriptional changes, and not perceptible as differences in the phenotype. The result suggests that the pH change caused by the presence of *S. pneumoniae*, even when a higher pH of 8.6 is used, is sufficient to cause a proportion of the *H. influenzae* population to enter a non-culturable state. This proportion of cells entering a non-culturable state was comparable between these strains, and again, suggests the effect was ubiquitous and not strain specific.

However, strains BS139 and BS171 displayed a different phenotype. Both strains showed a reduced end-point CFU/ml count in mono and co-culture compared to the other strains. However, strain BS139 did not show a large reduction in CFU/ml in co-culture (in planktonic or biofilm form), and BS171 did not show any reduction in the planktonic form, although it did not form biofilm in co-culture.

Therefore, it appears that strains BS139 and BS171 display a reduced growth compared to other strains, but are nevertheless more adapted to maintain a culturable state in the multispecies environment with *S. pneumoniae*. Interestingly, strain BS171 was non-culturable when in co-culture in a biofilm state, suggesting also that the biofilm formation phenotype in co-culture may not necessarily be directly linked to the phenotype seen in the planktonic state. Nevertheless, it does appear that these strains are more adapted to a multispecies environment. Importantly, some genetic determinants are known about these strains. Specifically both BS139 and BS171 are known to lack the Tfp pilus assembly/retraction ATPase *pilT*, as well as to lack the complete *comA-F* operon. Hence, these strains would not possess a functional Tfp, and would be expected to have a reduced biofilm formation (Bakaletz et al. 2005; Jurcisek et al. 2007; Carruthers et al. 2012). Indeed, the mono-species biofilm formation in these strains is reduced in comparison to the other (wild-type) *H.influenzae* strains. However, the co-culture biofilm formation of BS139 is similar to that of the other strains, and while BS171 does not form a co-culture biofilm, it was able to form some biofilm in mono-culture. Most likely, the reduced biofilm formation phenotype in these strains is related to a reduced growth rate. While we have not followed up the relationship of the absence of *pilT* and *comA-F* on the growth of these strains, there is a possibility that the lack of a functional Tfp would be related to growth rate. Such an effect would

be possible, if the Tfp was originally used for uptake of DNA and its use as a nutrient source. Indeed, Tfp has been shown to bind extracellular DNA in *H. influenzae* (Jurcisek and Bakaletz 2007), and in *E. coli* the homologs of the *H. influenzae com* genes were shown to be important for DNA uptake, when DNA was used as the sole carbon source (Palchevskiy and Finkel 2006). We have also shown a nutritional/metabolic relationship between *H. influenzae/S. pneumoniae* (see Chapter 5). Therefore, if Tfp was involved in nutrient acquisition, its absence could also alter the inter-species interactions between *H. influenzae* and *S. pneumoniae*.

However, as only the *pilT* and *com* genes have been sequenced for these strains, it cannot be said with confidence that these inter-strain differences are the result of only an absence of the type IV pili. As type IV pili are known to be involved predominantly in biofilm formation, and the results seem to suggest differences in the growth rate or metabolism of these strains, compared to Rd KW20 and the other isolates used, it is more likely, there are broader genetic and possibly transcriptomic differences accounting for such an altered phenotype of these strains. Nevertheless, these potential growth and metabolic variations appear to have enabled BS139 and BS171 to have an improved survival in the presence of *S. pneumoniae* compared to the other strains used.

Importantly, the role of genetic changes in *H. influenzae* was shown to play a role in its ability to survive in the presence of *S. pneumoniae*. Specifically, the role of the nickel import system, including the *nimR* regulator and the *nikKLMQO* was shown to play a role in these interactions. Previously, it has been shown that a mutant in *nikQ*, was unable to import nickel and displayed a change in cell surface properties and an increase in biofilm formation (Kidd et al. 2011; Ng and Kidd 2013). In addition, the inactivation of *nikQ* in Rd KW20 resulted in an altered transcriptomics profile, including the upregulation of LOS biosynthesis genes and iron uptake, both of which are associated with biofilm formation (Swords et al. 2004). We hypothesised that such an inactivation of nickel import could benefit *H. influenzae* in its multispecies interactions by promoting biofilm formation. However, the nickel import system has also been shown to play a role in acid tolerance (Ng and Kidd 2013). This is due to the role of nickel as a cofactor for urease, an enzyme known to be involved in acid stress (Scott et al. 1998; Murphy and Brauer 2011; Ng and Kidd 2013). As we have previously shown an increased acidity to be the cause of *H. influenzae* transition to a non-culturable state in the presence of *S. pneumoniae*, we

hypothesised that a strain lacking the nickel import system, would have a reduced ability to survive in the presence of *S. pneumoniae* due to impaired acid tolerance. Indeed, when we performed a static co-culture growth assay of the Rd KW20 *nikQ*- strain, we found that it could not be recovered from co-culture, both at pH 7.4 and pH 8.0. This suggests that the Rd KW20 strain in which the nickel import system was inactivated, had a reduced acid tolerance, and thus was unable to survive in the presence of *S. pneumoniae* even at a higher environmental pH of 8.0. Hence, in the case of *H. influenzae/S. pneumoniae* inter-species interactions, the primary function of *nikQ* and nickel uptake was to control intracellular pH, rather than the involvement in surface structure determination. In a broader interpretation, this result suggests that in environments where nickel is limited, *H. influenzae* may not be able to survive in the presence of *S. pneumoniae*. While we have identified *H. influenzae* to transit to a VBNC state in co-culture with *S. pneumoniae* as a result of lowered pH (see Chapter 5, REF), we have not identified this state in the *nikQ* mutant, rendering further study being required in order to confirm that the observed state is indeed a VBNC state, and not cell death. In addition, the environmental conditions causing for nickel limitation in the respiratory tract are not clearly defined, although variation in nickel levels is known to be affected by immune cell function.

Overall, we have shown that subtle transcriptomic differences account for the environmental adaptation of *H. influenzae* strains, and impact on their ability to form biofilm or grow planktonically, achieving optimal adaptation to their micro-niche. We have also shown that the interplay of specific strain-specific genetic components of *H. influenzae* has great effects on the ability of strains to adapt to environmental conditions such as pH, and correspondingly regulate gene expression and adaptation mechanisms relating to growth or biofilm formation. However, we have also shown that some environmental conditions are broader, rendering a ubiquitous response for a multitude of strains: such as the response of *H. influenzae* to *S. pneumoniae* at pH 7.4. Nevertheless, strains BS139 and BS171 did show a difference in co-culture survival at a less extreme pH 8.0, and appeared to have a lower growth rate and better adaptation to *S. pneumoniae*. The nature of such better-adapted interactions was not investigated, and was not necessarily related to the known genetic information about these strains. Importantly, the deletion of the nickel uptake component in Rd KW20 had an inhibitory effect on *H. influenzae/S. pneumoniae* interactions due to enhanced sensitivity of such a strain to acid stress. In the context of this Chapter, we have shown that while there are some broader environmental responses in

extreme conditions, the presence of genetic and sometimes even subtle transcriptomics differences, can play an important role in the bacterial adaptation to a particular niche, and subsequent events encompassing biofilm formation and existence in the multispecies environment.

Chapter 5

The Outcome of *H. influenzae* and *S. pneumoniae* inter-species interactions depends on pH, nutrient availability and growth phase.

Overview

The body of this Chapter has now been accepted to be published in the International Journal of Medical Microbiology (Tikhomirova et al. 2015) , and is arranged corresponding to the format of the International Journal of Medical Microbiology.

Using a defined and kinetic analysis, our study has shown that while co-existence of the two species occurs, *S. pneumoniae* is also able to convert *H. influenzae* to a non-culturable state. We determined that this process was dependent on growth phase and pH. To analyse the *H. influenzae/S. pneumonia*e interactions in more depth, we investigated the growth and transcriptional profile in a pH-defined batch culture model, as well as in a growth phase independent flow cell system. Transcriptomics has shown that there are changes in gene expression in each of the species when grown in co-culture, intriguingly inducing the *S. pneumoniae* bacteriocin transport genes, and phage-associated genes in both species. Importantly, we have shown vast changes in gene expression in a group of *S. pneumoniae* metabolic genes, including those encoding lactose utilisation, glycerol utilisation and sugar transport proteins; we have shown that the expression of these genes depends not only on the presence of *H. influenzae*, but also on the growth system utilised.

5.1 Introduction

H. influenzae and *S. pneumoniae* are common commensals of the healthy human nasopharynx, and between 20-70% of the population have been shown to carry these organisms asymptomatically (Bogaert et al. 2004; LaCross et al. 2013). However, susceptible populations, particularly children, are at risk of developing opportunistic infections caused by these organisms. One of the most common paediatric infections caused by these organisms is otitis media (OM), an inflammatory condition of the middle ear, and at least 70% of children will have experienced at least 1 episode of OM by 3 years of age (Berman 1995). While the introduction of the *H. influenzae* type b vaccine has reduced invasive disease caused by the type b encapsulated strains of *H. influenzae* (Peltola 2000; Adam et al. 2010), strains of other capsular serotypes as well as the nontypeable and unencapsulated strains still pose a major risk (Waggoner-Fountain et al. 1995; Murphy et al. 1999; Adderson et al. 2001). A similar situation has occurred for *S. pneumoniae* where the introduction of a polysaccharide-protein conjugate vaccine has reduced the incidence of disease caused by the vaccine serotypes (Fenoll et al. 2009; Isaacman et al. 2010; Ho et al. 2011), but disease incidence caused by the other serotypes has not reduced. Hence, OM remains a major problem in paediatric practice; this problem is exacerbated by the fact that OM can present as a chronic (COM) or reccurent (ROM) infection as well as an acute infection. COM forms are much more difficult to treat as they are often insensitive to antibiotic therapy, and may reoccur even after the placement of tympanostomy tubes (Williams et al. 1993; Ojano-Dirain and Antonelli 2012).

Recently, it was shown that *H. influenzae* and *S. pneumoniae* form a multispecies biofilm on the middle ear membrane, and it is this mixed-species biofilm which is responsible for the chronicity of OM (Hall-Stoodley et al. 2006). However, while it has been established that both species are capable of forming a multispecies biofilm, the precise interactions between *H. influenzae* and *S. pneumoniae* in the host and in the biofilm have not been well defined. Indeed research findings relating to the outcomes of this interaction are conflicting, as recently reviewed (Tikhomirova and Kidd 2013). Some previous studies have suggested that the interaction between *H. influenzae* and *S. pneumoniae* is of a

synergistic nature, whereby the formation of a multispecies biofilm would benefit both species, and protect them from host antimicrobials, shear forces and antimicrobial agents used in treatment. It was shown that a β-lactamase producing strain of *H. influenzae* could protect *S. pneumoniae* from β-lactam treatment (Weimer et al. 2011). In addition, the same study showed that the formation of a multispecies biofilm with a *bla*$^-$ strain of *H. influenzae* also had a protective effect on both the biofilm resident *S. pneumoniae* and the biofilm resident *H. influenzae bla*$^-$ cells, which alone were susceptible to beta-lactamase treatment. A synergistic interaction between the two species was also shown, where *H. influenzae* and *S. pneumoniae* reached higher cell densities in co-culture than in mono-culture, and were able to modulate each other's gene expression in the biofilm, likely to facilitate the formation of a robust biofilm beneficial for both species (Cope et al. 2011). Associated with this has been the demonstration that *H. influenzae* inhibitis autolysis and fraticide of *S. pneumoniae* and thereby *H. influenzae* improves the biofilm formation by *S. pneumoniae* (Hong et al. 2014), although this effect was only observed at later stages of culturing and suggested that bacteria in co-culture biofilms may have altered biofilm formation processes, as a previous study showed that in mono-cultures of *S. pneumoniae* autolysis promoted biofilm formation (Trappetti et al., 2011). In addition, this was an *in vitro* study and there is certainly some indication that this environment is quite different to the co-culture biofilm formation processes on epithelial cells (Krishnamurthy and Kyd 2014).

However, antagonistic as well as synergistic interactions have been shown between the two species. In fact, some studies have demonstrated competitive interactions whereby *S. pneumoniae* is able to outcompete *H. influenzae* via production of the bactericidal H_2O_2 (Pericone et al. 2000). Another study implicated *S. pneumoniae* domination over *H. influenzae* in the host via production of a neuraminidase and subsequent desialylation of *H. influenzae* LOS, resulting in an increased susceptibility of *H. influenzae* to host complement (Shakhnovich et al. 2002). Other studies have demonstrated the potential of *H. influenzae* to outcompete *S. pneumoniae* via stimulating the host opsonophagocytosis response against *S. pneumoniae* (Lysenko et al. 2005). Hence, the nature of the interactions between these species remains unclear. It is likely, that these interactions are dependent on a multitude of specific host, genomic, and environmental factors, and that the discrepancy

observed between studies is a result of the variation of one or more of these parameters. In addition, most studies have investigated the role of *H. influenzae*/*S. pneumoniae* interactions from the perspective of biofilm formation. However, few studies have looked at such interactions from the perspective of planktonic cells preceding biofilm formation. In order to elucidate further the nature of interactions between *H. influenzae* and *S. pneumoniae*, our study investigated the planktonic growth and biofilm formation in two distinct experimental settings: batch culture growth and in a continuous culture flow cell growth chamber. For this study, analysis of global gene expression of both species in mono-culture and co-culture was performed with RNASeq technology, in order to understand global transcriptional changes occurring in these species during their co-culture, and then both in a batch culture growth and the growth phase-independent flow cell model of growth. To our knowledge, this is the first study analysing global gene expression patterns in the *H. influenzae/S. pneumoniae* co-culture situation. Furthermore, we have shown the potential for both synergystic and antagonistic interactions between *H. influenzae* and *S. pneumoniae*, which is largely dependent on the growth environment. We have also shown that both species undergo vast changes in their transcriptional profile in response to the growth environment, and to the presence of the other species, and propose that these environmental parameters and transcriptional patterns determine the synergistic or antagonistic nature of the *H. influenzae/ S. pneumoniae* interactions.

5.2 Results and Discussion

5.2.1 *H. influenzae* survival in co-culture depends on growth phase

The current study aimed to further investigate elements which may be involved in the interspecies interactions between *H. influenzae* and *S. pneumoniae*, and to specifically determine the molecular factors that influence their co-existence.

For the initial analysis of the interactions between *H. influenzae* and *S. pneumoniae*, growth assays were performed in supplemented HI media in static aerobic conditions, and cells from mono and co-cultures of each species were collected at varying time-points in their growth phase. The growth kinetics in these conditions was initally monitored and compared (Fig. 5.1).

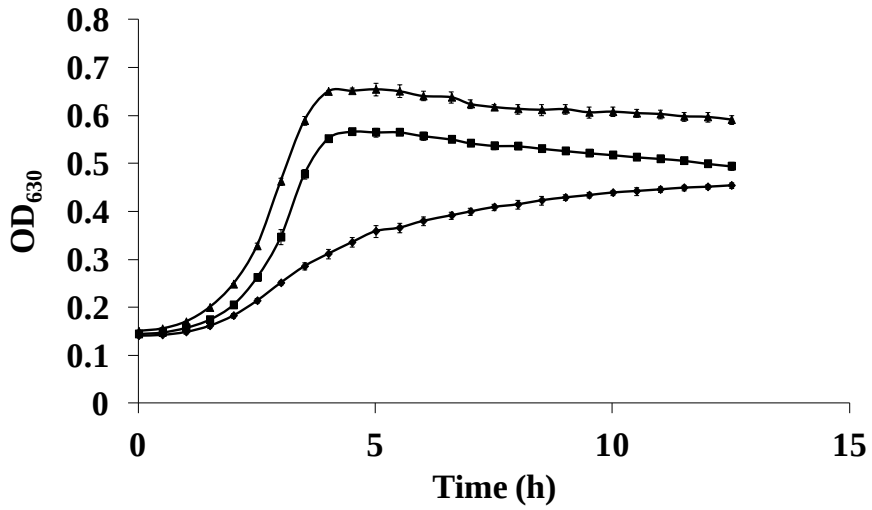

Fig. 5.1. Planktonic growth of *H. influenzae* Rd KW20 and *S. pneumoniae* D39. Growth curves based on OD_{630} values obtained from mono- culture growth of *H. influenzae* Rd KW20 (diamond marker), *S. pneumoniae* D39 (square marker) and their co-culture (triangle marker) over 14 h. There was a difference in the OD_{630} reached by *S. pneumoniae* and *H. influenzae*, with a higher OD_{630} reached by *S. pneumoniae*. In addition,

the growth curves presented display an increased growth rate of the co-culture compared to both the *H. influenzae* and *S. pneumoniae* mono-cultures in log phase up to 5 h, suggesting the survival of both *H. influenzae* and *S. pneumoniae* in co-culture.

Subsequently, planktonic and biofilm cell numbers were then quantified and assessed.
The results showed that both species were able to grow planktonically and form a biofilm equally well in co-culture and in mono-culture in late log phase (Fig. 5.2A). However, when cells were in a stationary phase, *S. pneumoniae* was able to completely out-compete *H. influenzae* (based on CFU/ml measurements) (Fig. 5.2B).

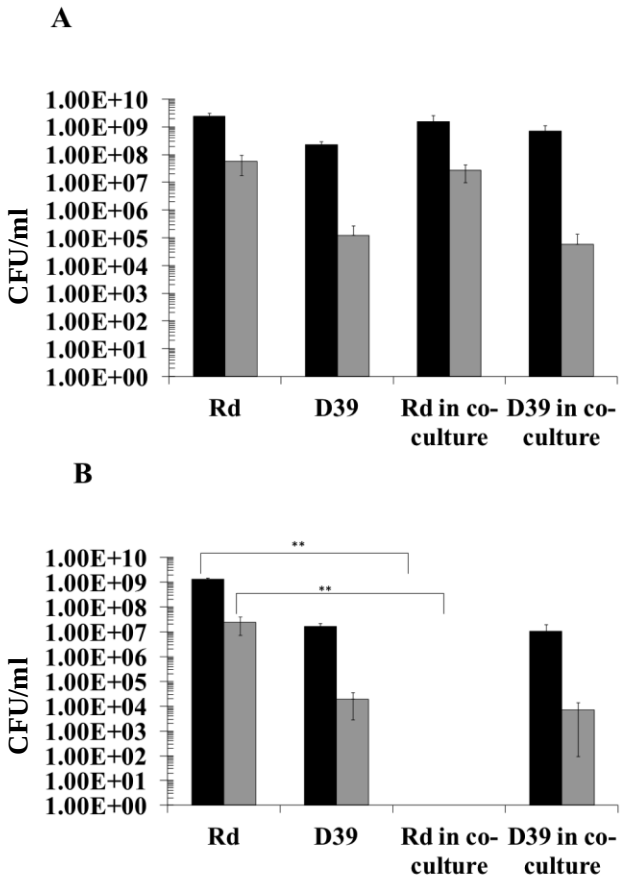

Fig. 5.2 *H. influenzae* is present in co-culture with *S. pneumoniae* at 6 h, but not at 14 h. CFU/ml values from *H. influenzae* Rd KW20 and *S. pneumoniae* D39 mono- and co-culture after (A) 6 h of growth or (B) 14 h of growth, in both the planktonic (black bars) and biofilm (grey bars) state.

Importantly, this effect was observed for both the laboratory strain of *H. influenzae* (Rd KW20) and OM clinical isolates 86-028NP and R3157, and was therefore seemingly not strain-specific (Fig. 5.3).

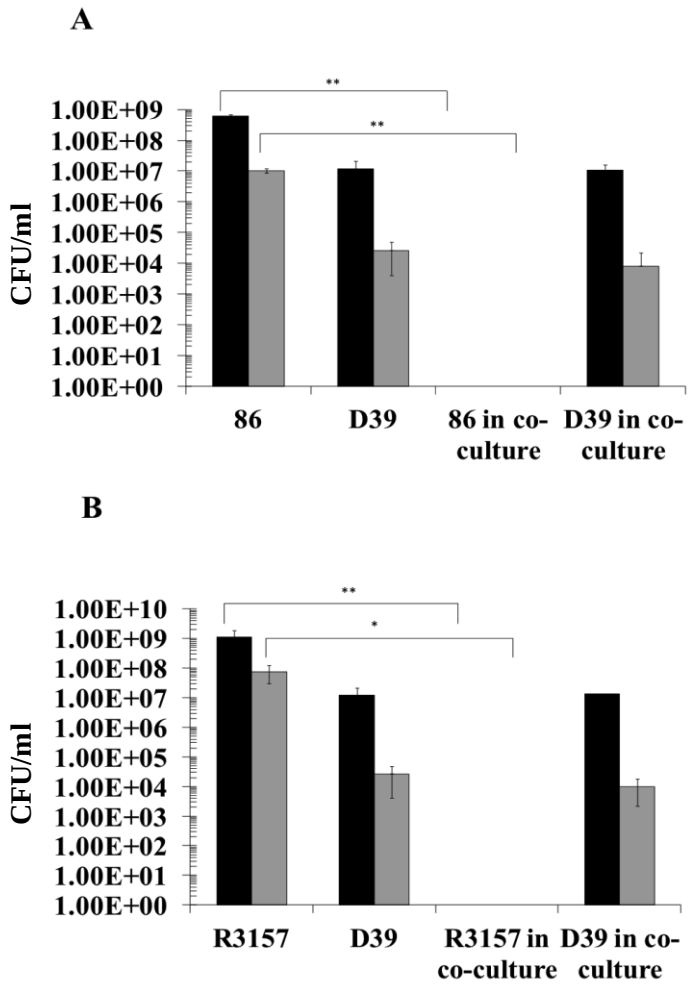

Fig. 5.3. *H. influenzae* clinical isolates 86-028NP and R3157 are not present in co-culture with *S. pneumoniae* at 14 h. CFU/ml values of *H. influenzae* clinical isolates (A) 86-028NP and (B) R3157 and *S. pneumoniae* D39 in both the planktonic (black bars) and biofilm (grey bars) state after growth in mono- and co-cultures for 14 h. The presence of *S. pneumoniae* D39 inhibited the viability of both *H. influenzae* clinical isolates, both in the planktonic and biofilm state. *S. pneumoniae* viability however remained equal for mono and co-culture conditions.

Likewise, co-culture of *H. influenzae* Rd KW20 with an OM clinical isolate of *S. pneumoniae*, strain 11, caused the same effect of *H. influenzae* cell number reduction in stationary phase, indicating the effect was not strain-specific for *S. pneumoniae* (Fig. 5.4). Hence, a fine threshold exists in the growth-phase of both species which could either allow or prevent *H. influenzae* culturability in the presence of *S. pneumoniae*.

5.2.2. *H. influenzae* survival in co-culture depends on pH.

We hypothesised, that the time-dependent killing of *H. influenzae* by *S. pneumoniae* could be explained by the production and accumulation of acidic by-products particular to the *S. pneumoniae* fermentative mode of growth. Hence, it could be an acidity of the growth medium leading to *H. influenzae* cell death. Further experiments showed that survival of *H. influenzae* in co-culture at stationary phase was possible, but depended on the pH of the growth medium; specifically, a higher starting pH of 8.0 allowed survival in co-culture, although with some reduction in cell numbers, whereas a pH of 7.4 did not allow for *H. influenzae* survival in co-culture (Fig. 5.4).

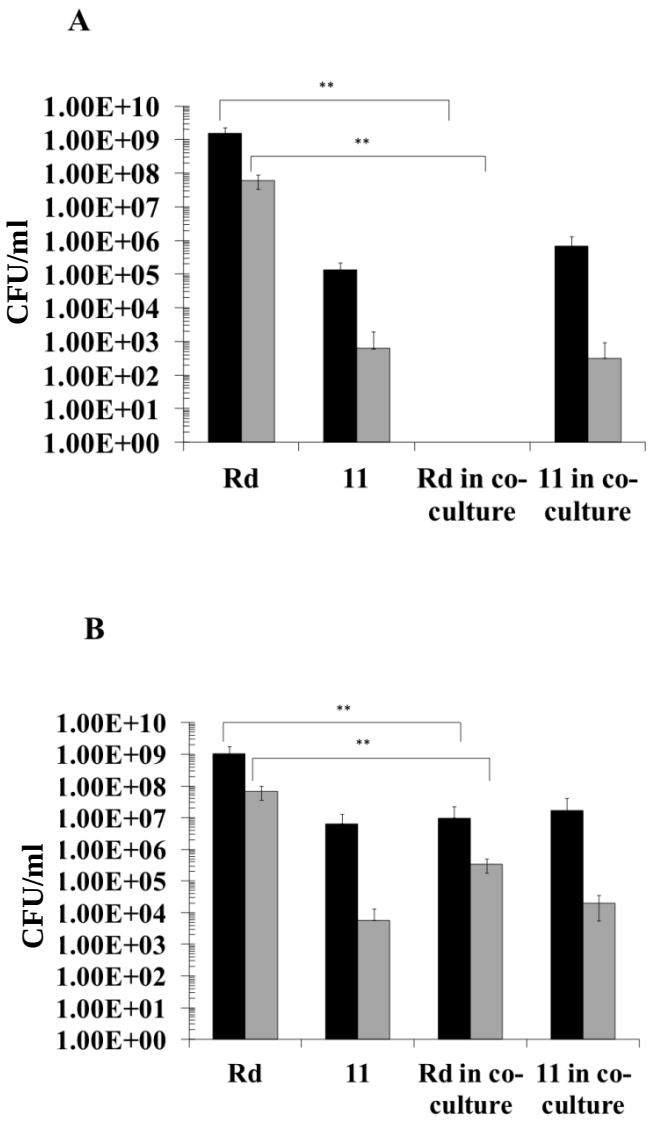

Fig. 5.4. *H. influenzae* can survive in co-culture with *S. pneumoniae* at 14 h when there is an initial pH of 8.0. CFU/ml of planktonic (black bars) and biofilm (grey bars) *H. influenzae* Rd KW20 and *S. pneumoniae* strain 11 cells at stationary phase of growth (14 h), in media of an initial pH of (A) 7.4 or (B) 8.0. *H. influenzae* Rd KW20 was able to grow and form a biofilm in a mono culture at pH 7.4 , but not in co-culture at the same pH. In contrast, at pH 8.0, Rd KW20 was able to grow and form a biofilm in co-culture, although its CFU/ml levels were significantly reduced relative to mono-culture.

The reason for the inability of *H. influenzae* to be cultured in co-culture at pH 7.4, specifically, was that the presence of *S. pneumoniae* in the culture medium caused a greater drop in pH of the *H.influenzae/ S. pneumoniae* co-culture (Fig. 5.5).

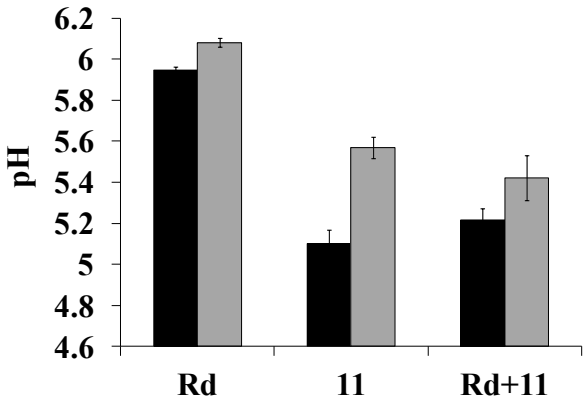

Fig. 5.5. The presence of *S. pneumoniae* causes the drop in pH of the *H. influenzae/ S. pneumoniae* co-culture. The end-point pH of *H. influenzae* Rd KW20 and *S. pneumoniae* strain 11 mono- and co-cultures obtained after 14 h of growth in HI media of pH 7.4 (black bars), and HI media of a pH of 8.0 (grey bars). The end-point pH is lower for *S. pneumoniae* and for the co-culture compared to the *H. influenzae* mono-culture, both at pH 7.4 and 8.0. However, the end-point pH in all situations is higher, when a starting pH of 8.0 is used.

While the nature of these acidic by-products produced by *S. pneumoniae* was not investigated in this study, the most likely acidic metabolites produced in large amounts by stationary phase would be the end-products of fermentation. In the case of homofermentation, this would be lactate (Martín-Galiano et al. 2005). In fact, the peak of *S. pneumoniae* response to acid stress has been shown to correspond with growth in stationary phase, when lactic acid levels accumulate (Martín-Galiano et al. 2005). The other possibility would be that the acidity was caused by end products of heterofermentation; acetate, formate and ethanol, of which acetate and formate are likewise both acidic compounds (Price et al. 2012). The switch from homofermentation to heterofermentation has been shown to be caused in other *Streptococci* and *Lactobacilli*

species by differing rates of sugar uptake and metabolism as well as oxygen availability (Price et al. 2012). While we have used a rich media for our studies, which opened a potential for the use of carbon sources other than lactate, it is known that the only carbon sources on which *S. pneumoniae* is strictly reliant on for energy are carbohydrates; the most studied sugars including lactose/galactose, maltose and sucrose all converge on the glycolysis pathway, and their fermentation would result in either homolactic fermentation or heterofermentation, depending on glycolytic flux and oxygen availability. The result of both types of fermentation would be the production of acidic by-products (lactate or acetate), which is what we observed (Price et al. 2012). It should be noted that the conditions of the respiratory tract would be limited in nutrients and the complex, rich medium used in this study is an initial *in vitro* analysis establishing key parameters for future analysis.

It is established that *S. pneumoniae* is able to induce expression of the *lytA* N-acetyl-muramoyl-L-alanine amidase responsible for *S. pneumoniae* cell lysis in stationary phase (Balachandran et al. 2001). As the *H. influenzae* cell death was observed in stationary phase, the expression of the pneumococcal *lytA* in stationary phase and subsequent cell lysis could release acidic metabolites into the growth medium. To determine whether *S. pneumoniae* cell lysis could be involved in *H. influenzae* killing, co-culture assays were performed in the the presence of choline chloride. Choline chloride is known to inhibit the noncovalent binding of *S. pneumoniae* choline binding proteins to the phosphorylcholine moieties of the *S. pneumoniae* cell wall through a conserved choline-binding domain. Some such known choline binding proteins include the murein hydrolases LytA, LytB and LytC, and it has been known for several years that the presence of choline chloride in growth medium acts as a cell lysis inhibitor for *S. pneumoniae* by inhibiting the autolysin protein LytA (Steinmoen et al. 2002). However, the addition of choline chloride did not restore survival of *H. influenzae* in co-culture, suggesting that the decrease in pH caused by *S. pneumoniae* was not a result of acidic by-products leaving lysed cells, but rather was due to metabolic by-products secreted by living cells (Fig. 5.6).

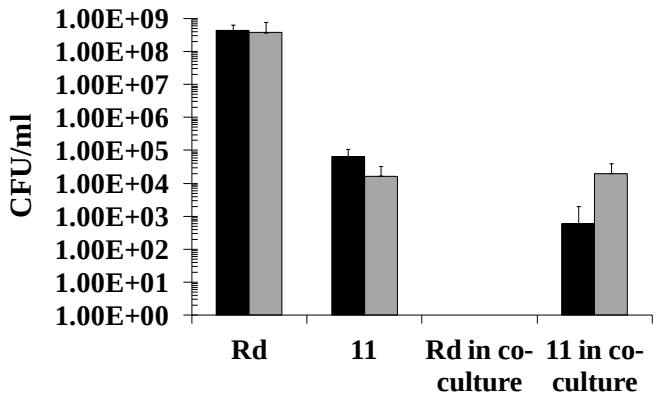

Fig. 5.6. *H. influenzae* reduction in co-culture with *S. pneumoniae* is not caused by intracellular components of lysed *S. pneumoniae* cells. The planktonic growth of *H. influenzae* Rd KW20, *S. pneumoniae* strain 11 in mono- and co-culture in normal conditions (black bars), and in the presence of 0.5% Choline (grey bars).

Interestingly, the pH of the middle ear effusion of chronic OM patients extends to a basic pH range of 7-9 (Wezyk and Makowski 2000). This suggests and perhaps corroborates our data, that the conditions of growth in the middle ear during chronic OM are optimal for the survival of both species.

To confirm that *H. influenzae* killing was the result of the lowering of the growth medium pH, *H. influenzae* growth in mono-culture was tested using a range of pH values including pH 7.4, 6.5, 5.8, 5.3 and 5.0. (Fig. 5.7). However, even when pH 5.0 was used (where the end-point pH achieved was 5.2), *H. influenzae* reduced in viability by only 100x, achieving an end-point of $1x10^7$ CFU/ml (Fig. 5.7). This is in contrast to the complete transition to an unviable state which occurred for *H. influenzae* in co-culture, where a final pH of 5.3 was obtained. This suggests that it was not solely the reduction in growth pH in co-culture which rendered *H. influenzae* unviable, but also the specific products produced by *S. pneumoniae*.

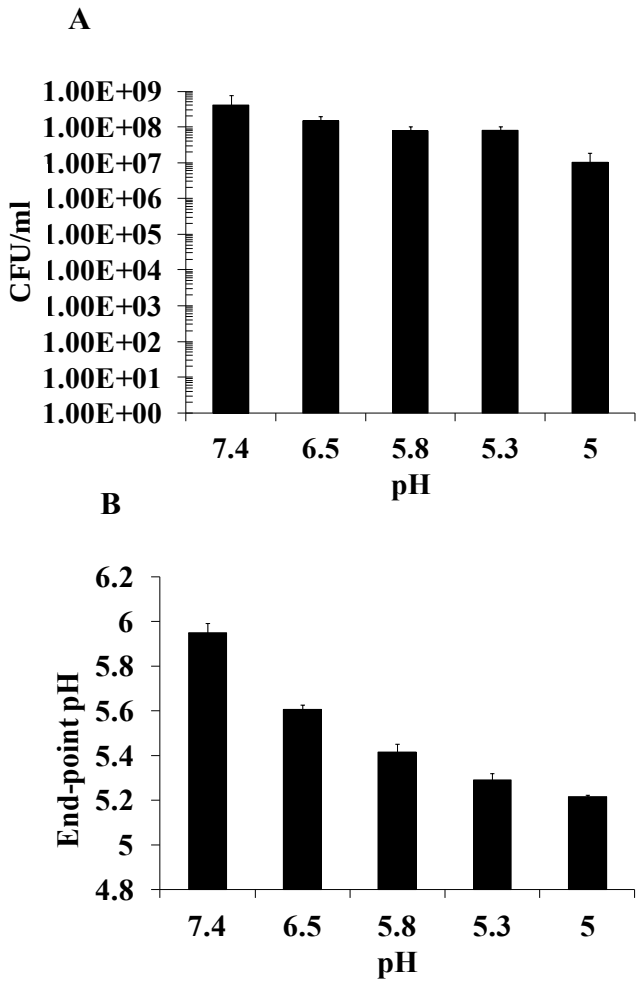

Fig. 5.7. *H. influenzae* Rd KW20 can grow and survive in a range of pH conditions in mono-culture, retaining viability. A) The planktonic CFU/ml of *H. influenzae* Rd KW20 in mono-culture after 14 h, when grown in HI media of varying pH values, and B) The end-point pH achieved from this mono-culture growth after 14 h. *H. influenzae* can survive at a pH as low as 5.0, increasing it to 5.2, and retaining planktonic cell counts of $1x10^7$ CFU/ml.

5.2.3. *H. influenzae* survival in co-culture does not depend on H_2O_2.

Based on previous studies, another mechanism which could account for *S. pneumoniae* mediated reduction of viable cell numbers of *H. influenzae* in stationary phase, could be the H_2O_2 production by *S. pneumoniae*. H_2O_2 is known to be produced by *S. pneumoniae* in microaerobic conditions, during the decarboxylation of pyruvate, an intermediate of carbohydrate metabolism, to acetylphosphate and the concurrent reduction of O_2 to H_2O_2 via the action of the pyruvate oxidase encoded by *spxB* (Carvalho et al. 2013). In addition, H_2O_2 is known to be produced via the action of α-glycerophosphate oxidase (*glpO*), via oxidation of α-glycerophosphate to dihydroxyacetone phosphate during glycerol metabolism (Mahdi et al. 2012). Hence, H_2O_2 production was likely to be occurring during growth in co-culture, either during carbohydrate or glycerol metabolism, and hence H_2O_2 levels could accumulate to a toxic threshold level for *H. influenzae* by stationary phase. To investigate whether this was the case, a co-culture assay was set up using the wild-type D39 strain, and an *spxB*$^-$ knock-out of D39, which is unable to produce H_2O_2 when glucose is used as the carbon source, and likewise a *glpO*$^-$ knock-out which is unable to produce H_2O_2 when fatty acids are used as the carbon source.

The results demonstrated that H_2O_2 was not involved in the competitive interactions of *S. pneumoniae* with *H. influenzae* as the use of *S. pneumoniae spxB*$^-$ and *glpO*$^-$ mutant strains in co-culture also displayed a competitive advantage with *H. influenzae* at stationary phase (Fig. 5.8).

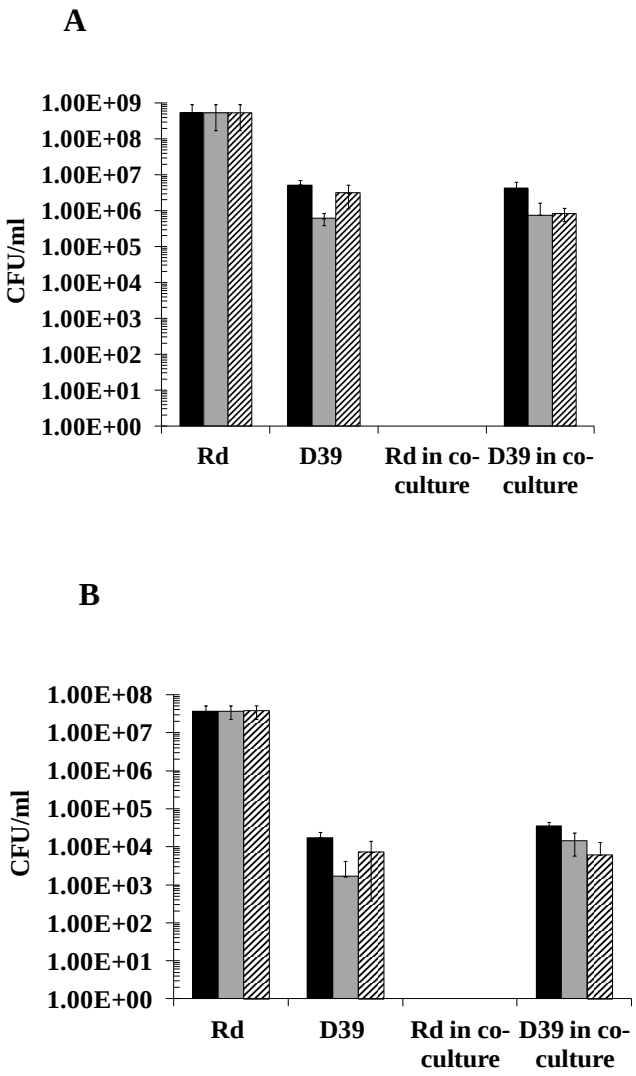

Fig. 5.8. *H. influenzae* was not present in co-culture with *S. pneumoniae* D39 *spxB*$^-$ and *glpO*$^-$ H_2O_2 deficient mutants at 14 h of growth. Showing CFU/ml values of (A) planktonic and (B) biofilm cells of *H. influenzae* Rd KW20 and *S. pneumoniae* strains D39 wild type (black), D39 *spxB*$^-$ (grey) and D39 *glpO*$^-$ (hatched) grown in mono- and co-cultures for 14 h. Rd KW20 was unable to survive in co-culture with the wild-type or mutant D39 strains, and there was no significant difference in the ability of the three *S. pneumoniae* strains to survive either in mono- or co-culture.

5.2.4. *H. influenzae* survival in co-culture does not depend on a soluble secreted factor

An alternate explanation for *H. influenzae* cell number reductions in co-culture could be a secreted soluble factor produced by *S. pneumoniae* accumulating by stationary phase.

To check whether a secreted factor caused this phenotype in the *S. pneumoniae* strain 11/ *H. influenzae* Rd KW20 co-culture, an experiment was performed where spent supernatants of *S. pneumoniae* (strain 11), *H. influenzae* Rd KW20 and their co-culture both at pH 7.4 and pH 8.0 were collected at stationary phase, filtered and inoculated with Rd KW20. Subsequently, the *H. influenzae* Rd KW20 supplemented with the spent supernatants was incubated statically at 37ºC for 14 h, after which the planktonic cells were collected and plated to determine the CFU/ml. This assay was done to determine whether a secreted soluble factor that was only produced at stationary phase, or only produced by *S. pneumoniae* in the presence of *H. influenzae*, was responsible for the killing phenotype. However, in this case, Rd KW20 was also unaffected by the presence of the spent supernatants, suggesting that a secreted soluble factor accumulating in stationary phase is not responsible for the killing phenotype (Fig. 5.9).

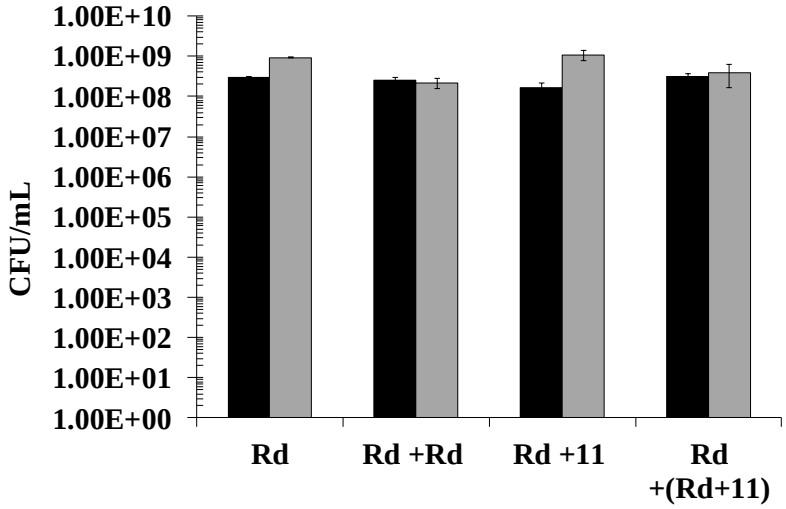

Fig. 5.9. The presence of spent supernatants from *H. influenzae* Rd KW20, *S. pneumoniae* strain 11 or their co-culture, did not reduce *H. influenzae* culturability in mono-culture. The planktonic growth of *H. influenzae* Rd KW20 at pH 7.4 (black) and pH 8.0 (grey), in mono-culture conditions (Rd), and supplemented with overnight supernatants of Rd KW20, *S. pneumoniae* strain 11, and the RdKW20 + 11 co-culture.

5.2.5. There are transcriptomic changes in *H. influenzae* in co-culture compared to mono-culture at pH 8.0.

To identify changes in whole cell gene expression occuring in co-culture, and to help identify the mechanisms involved in *H. influenzae* survival in permissive conditions but cell death in co-culture in restricted conditions, RNA was taken from *H. influenzae* mono-cultures grown at pH 7.4 and pH 8.0, and a *H. influenzae*/*S. pneumoniae* co-culture grown at pH 8.0 where survival of *H. influenzae* was still possible. In addition, RNA was taken from a *S. pneumoniae* mono-culture grown at pH 7.4, and a *S. pneumoniae/H. influenzae* co-culture was grown at pH 7.4, where *H. influenzae* was not present.

Importantly, no genes were significantly up- or down- regulated between the mono-cultures of Rd KW20 grown at pH 7.4 and pH 8.0 (data not shown), indicating that the *H. influenzae* cell death phenotype cannot be exlained by transcriptomic changes occuring as a result of growth at pH 7.4 compared to growth at pH 8.0.

Importantly, when the gene expression of Rd KW20 from co-culture growth at pH 8.0 was compared to the Rd KW20 from mono-culture growth at pH 8.0, transcriptomic changes were observed (Table 5.1).

Table 5.1. Up- and down-regulated *H. influenzae* Rd KW20 genes after growth in co-culture with *S. pneumoniae* strain 11 at pH 8.0 in a batch culture model, compared to mono-culture growth in batch culture. Results are displayed for genes with a $\log_2$ fold change ≥ 2, and a p-value ≤ 0.05.

*Gene HI1413 had a p-value slightly above 0.05, but was included in the analysis due to being part of the φ-Flu phage upregulated operon and a log2 fold change value ≥ 2.

Genes Upregulated Locus tag Gene Class:	**Gene**	**$\log_2$FoldChange**	**Function of Gene Product**
Bacteriophage			
HI1409	-	2.31	putative phage portal protein
HI1416	-	3.67	phage holin lambda
HI1413 *	-	2.33	phage lytic protein RZ1
HI1414	-	3.03	hypothetical membrane protein phage hypothetical protein
HI1488	-	2.68	mu-like prophage protein
HI1478	*muA*	2.92	transposase putative
Stress Response			
HI1053	-	3.03	similar to Alkylhydroperoxidase
HI0859	*clpB*	2.90	ATP-dependent *clp* protease
HI0053	-	2.62	zinc-type Alcohol dehydrogenase
HI0104	*htpG*	2.51	*htpG*, heat shock protein 90
HI1238	*dnaJ*	2.45	*DnaJ*, chaperone protein
HI0543	*groEL*	2.10	chaperonin *GroeL* - RNA degradation
HI1237	*dnaK*	2.143	DNA replication and hyperosmotic shock
HI1455	*msrA*	2.20	bifunctional methionine sulfoxide reductase subunits A/B
Dicarboxylate Transport			
HI0051-HI0052	-	2.58-2.97	putative TRAP-type C4 dicarboxylate transport protein
Ribose Transport			
HI0501-HI0504	*rbsA -rbsD*	2.0-2.87	ribose-transport system
Sialic acid metabolism			
HI0143	-	2.20	HTH-type transcriptional regulator
HI0144	*nanK*	2.04	catalyzes the phosphorylation of the N-acetylmannosamine (ManNAc) liberated from N-acetyl-neuraminic acid by the nanA protein

HI0871	*siaA*	2.03	LOS sialyltransferase
Metabolism			
HI1454	-	2.90	cytochrome C biogenesis protein
HI0043	-	2.33	membrane protein
HI0986	*leuA*	2.14	2-isopropylmalate synthase L-leucine biosynthesis
HI1453	*purL*	2.11	putative phosphoribosylformylglycinamidine synthase ,
HI1369	-	2.04	putative TonB dependent receptor
Downregulated Genes			
Locus tag			
Gene Class: Mu-like bacteriophage			
HI1505	-	-4.22	Mu-like gtp
HI1504	-	-3.49	bacteriophage Mu-1 protein
HI1512	-	-2.73	Mu-like prophage tail-tube protein
HI1508	-	-2.48	Mu like prophage protein gp36
HI1509	-	-2.35	Mu-like prophage protein gp37
HI1519	-	-2.35	hypothetical prophage protein
HI1513	-	-2.15	Mu like prophage protein gp41
HI1518	-	-2.09	Mu like prophage protein gp45
DNA-Associated			
HI1506	-	-2.84	unknown function, may bind nucleic acids
HI0062	*dksA*	-2.36	transcriptional regulator
Metabolic			
HI0222	*guaA*	-2.08	GMP synthase; involved in DNA/RNA synthesis
HI0221.1	-	-2.93	inosine-5'-monophosphate dehydrogenase-like protein

Some of the most highly up-regulated genes in co-culture were those encoding the holin and RZ1 lysin of the φ-Flu bacteriophage. The holin is responsible for forming a pore in the cell membrane, while the endolysin has a muralytic activity, causing degradation of the cell wall, and release of phage virions (Wang et al. 2000; Young et al. 2000). In the situation of the *H. influenzae/S. pneumoniae* co-culture, *H. influenzae* cell lysis could have a role in release of nutrients for *S. pneumoniae* at a stationary phase of growth. However, as these genes were up-regulated in co-culture at pH 8.0, where the *H. influenzae* population was largely still viable, these effects would be likely to affect a small portion of the population. Further study would be required to provide a more clear model for the specific role and function of these genes in the co-culture situation.

A suite of stress-response associated genes was also up-regulated in *H. influenzae* in the co-culture situation at pH 8.0 (Table 5.1) . These included an *ahpD* alkylhydroperoxidase, which could protect *H. influenzae* against *S. pneumoniae* generated H_2O_2, as well as four genes encoding protein chaperones and heat shock proteins which could aid re-folding of misfolded proteins caused by heat shock or other cellular stress such as low pH.

Genes involved in *H. influenzae* sialylation (*siaA*) (Jurcisek et al., 2005; Jones et al., 2002) and sialic acid metabolism (Olson et al., 2013) (*nanK*) were also up-regulated in co-culture. Sialylation of *H. influenzae* LOS allows for antigenic mimicry of *H. influenzae*, and thus reduces host complement-mediated opsonophagocytosis (Bouchet et al. 2003). In the co-culture situation *S. pneumoniae* is able to desialylate *H. influenzae* LOS (Shakhnovich et al., 2002). Hence, in a co-culture situation of desialylation, *H. influenzae* could be compensating for desialylated LOS by sialylation of LOS via *siaA*. As sialylated LOS have been shown to play a role in biofilm formation (Jurcisek et al., 2005), sensing the presence of *S. pneumoniae* may be stimulating *H. influenzae* to express cell-surface components that promote the formation of a multispecies biofilm. In addition, *H. influenzae* could be utilising available desialylated sialic acid residues as a metabolic source via the sialic acid metabolism genes such as *nanK*.

In addition, there was a down-regulation of the *dksA* transcriptional regulator in co-culture at pH 8.0, which may indicate global changes in gene expression regulation.

Altogether, the transcriptomics results of the batch culture at pH 8.0 (Table 5.1), suggested that *S. pneumoniae* caused a degree of stress for the *H. influenzae* cell. In turn, *H. influenzae* was able to induce stress-response systems, enabling protection from these stressful compounds. *S. pneumoniae*-mediated stress imposed on *H. influenzae* correlates to the observations of *H. influenzae* reductions in cell numbers, which occurred at pH 8.0.

5.2.6. At pH 7.4 in co-culture, *H. influenzae* enters a non-culturable state and alters its gene expression compared to mono-culture.

Importantly, comparison of *H. influenzae* Rd KW20 gene expression at pH 7.4 in batch mono-culture and batch co-culture revealed gene expression which occurred when *H. influenzae* cells appeared dead or non-culturable. Specifically, 56.15% of total reads in the co-culture situation mapped to the *H. influenzae* Rd KW20 genome, indicating the presence of *H. influenzae* mRNA in the co-culture, where no CFU/mL of *H. influenzae* were observed. The half-life of mRNA for *E. coli* has previously been reported to be 6.8 minutes (Selinger et al. 2003), and therefore, dead cells would be unlikely to harbour mRNA in such quantities. Hence, while *H. influenzae* was previously regarded as "killed", the presence of its mRNA might indicate the potential that the cells may be in a **V**iable **B**ut **N**on-**C**ulturable (VBNC) state previously reported for other species (Oliver, 2010; Li et al., 2014). For other bacterial species, this VBNC state was differentiated from the dead state by several observations; firstly, VBNC cells have an intact membrane, in contrast to dead cells, they are metabolically active and continue respiration (Besnard et al. 2000), VBNC cells continue gene transcription and mRNA production (del Mar Lleò et al. 2000; Coutard et al. 2005), and were shown to have continued uptake and incorporation of amino acids into proteins (del Mar Lleo et al. 1998). Our data supports each of these attributes and therefore it might indicate the potetial that the non-culturable *H. influenzae* cells in this study are in the VBNC state.

The SEM show that *H. influenzae* cells are intact (Fig. 5.11). In this non-culturable state in co-culture, *H. influenzae* had mRNA production and up-regulated a larger number of stress response genes than observed at pH 8.0. These included chaperones and catalase, suggesting the cells were under a high degree of stress, likely due to the combined damaging effect of a lowered pH and H_2O_2 (Table 5.2).

Table 5.2. Up- and down-regulated *H. influenzae* Rd KW20 genes after growth in co-culture with *S. pneumoniae* strain 11 at pH 7.4 in a batch culture model, compared to mono-culture growth at a pH of 7.4 in a batch culture model. Results are displayed for genes with a log2 fold change ≥ 2, and a **p-value ≤ 0.1.**

Upregulated Genes	**Gene Name**	**log_2FoldChange**	**Function**
Locus tag Stress Response			
Gene Class: Stress Response			
HI0017	*grcA*	5.20	autonomous glycyl radical cofactor GrcA
HI0542	*groES*	4.30	co-chaperonin GroES
HI0104	*htpG*	4.32	heat shock protein 90
HI0543	*groEL*	4.09	chaperonin GroEL
HI0053	-	3.95	zinc-type alcohol dehydrogenase
HI1238	*dnaJ*	3.60	chaperone protein DnaJ
HI0720	*htpX*	3.71	heat shock protein HtpX
HI0859	-	3.55	ATP-dependent Clp protease ATPase subunit
HI1237	*dnaK*	3.47	molecular chaperone DnaK
HI1349	-	3.25	starvation inducible DNA binding protein
HI0071	*grpE*	3.03	heat shock protein GrpE
HI0928	*hktE*	3.15	catalase
Metabolic			
Glycerol Metabolism			
HI0683 , HI0690, HI0691	*glpC, glpF, glpK*	3.19-2.55	sn-glycerol-3-phosphate dehydrogenase subunit C, glycerol uptake facilitator protein, glycerol kinase
Amino acid Biosynthesis			
HI0988, HI0986, HI0989	*leuA, leuC, leuD*	2.76-2.12	leucine biosynthesis genes ***pval 0.1-0.2**
Protease/ Peptidase			
HI0151	*hflK*	3.0	membrane protease subunit
HI0497, HI0496	*hslU, hslV*	3.17-2.76	ATP-dependent protease
Membrane Transport			
HI0043		2.69	putative membrane protein
HI0044		3.42	uncharacterised membrane protein
HI1383m	*pstS*	3.00	phosphate ABC transporter substrate-binding protein
HI1174		2.82	opacity protein – membrane porin
DNA and RNA related			
HI1478	*muA*	3.19	transposase
Other			
Carbon/metabolic processes			
HI1455	*msrA*	3.24	bifunctional methionine sulfoxide reductase subunits A/B
Phage associated			
HI1416	-	3.75	phage holin *** pval 0.12**

Downregulated Genes Locus tag	**Other metabolic genes of various functions**		
HI1434.1	*cspD*	-3.64	cold shock-like protein
HI0893	-	-3.29	TetR/AcrR family transcriptional regulator, multidrug resistance operon repressor
HI0036	-	-2.91	ABC transporter ATP-binding protein
HI0187a	*tatA*	-2.49	Sec-independent protein secretion pathway component TatA

In addition, genes involved in glycerol uptake and metabolism, amino acid biosynthesis and membrane transport were up-regulated, suggesting selective use of metabolic resources in co-culture. This up-regulation of metabolic genes once again supports the observation of VBNC cells, as dead cells not undergoing metabolic processes would not be expressing metabolism-associated genes, while VBNC cells have been observed to be metabolically active (Besnard et al. 2000). The ϕ-Flu phage gene encoding the holin was also up-regulated in co-culture, and, due to its up-regulation being also observed at pH 8.0 co-culture and the flow cell system, where *H. influenzae* was culturable, appears to be unrelated to cell survival/culturability, though probably involved in an aspect of interspecies interactions. A predicted transcriptional regulator was also down-regulated in the non-culturable co-culture in *H. influenzae*, suggesting that there are global changes in gene expression and regulation occurring in *H. influenzae* in co-culture in the non-culturable state. In addition to analysing gene expression in the VBNC state, we have also made an attempt to rescuscitate these cells into a culturable state. For this, the culture obtained after 14 h of growth in co-culture at pH 7.4, was diluted 1/10 and 1/25 into fresh HI media and incubated at 37ºC. The culture was collected and plated onto HI agar at 2 h, 5 h and 7 h time-points. However, at all time-points *H. influenzae* could not be detected. It is important to note, that for other bacterial species the conditions which allow for rescuscitation from the VBNC state vary and are often highly specific (Li et al. 2014). This is the first time that there has been documented a VBNC state for *H. influenzae*, and while we used a rich media for rescuscitation, the precise environmental conditions which may

facilitate this transition are not known, and this would need to be investigated further. It is also worth noting that the culturable *S. pneumoniae* was present in the co-culture with the VBNC *H. influenzae*, and hence, may have been repressing *H. influenzae* from subsequent resuscitation.

5.2.7. *S. pneumoniae* alters its transcriptional profile at pH 7.4 in co-culture.

Analysis of *S. pneumoniae* gene expression in batch co-culture compared to mono-culture (at pH 7.4), showed a down-regulation of metabolic genes involved in lactose metabolism, glycerol metabolism and sugar transport in co-culture (Table 5.3).

Table 5.3. Up- and down-regulated *S. pneumoniae* strain 11 genes during growth in co-culture at pH 7.4 with *H. influenzae* Rd KW20 during batch culture growth compared to mono-culture growth at pH 7.4 in batch culture. Results are displayed for genes with a $\log_2$ fold change ≥ 2, and a p-value ≤ 0.05.

Upregulated Genes **Locus tag** **Gene Class:**	**Gene**	**$\log_2$FoldChange**	**Function**
Bacteriophage			
SPNOXC_00280	-	5.62	hypothetical protein; prophage antirepressor
SPNOXC_00460	-	2.67	phage capsid protein
Bacteriocin			
SPNOXC_05010	*blpY*	3.38	putative bacteriocin ABC transporter / CAAX protease
SPNOXC_01490	-	2.01	bacteriocin ABC transporter
Metabolic			
SPNOXC_02650	-	3.03	ABC transporter ATP-binding protein. Spermidine/putrescine transport domain
SPNOXC_09160	-	2.27	4-oxalocrotonate tautomerase
SPNOXC_17950	-	2.39	putative sugar-specific permease, SgaT/UlaA family
DNA modification			
SPNOXC_04720	-	2.61	type I restriction-modification system R protein

SPNOXC_07990	-	2.79	restriction modification enzyme
Downregulated Genes			
Class: Metabolism			
Lactose/Galactose metabolism			
SPNOXC_10630-SPNOXC_10700	*lacA, lacB, lacC2, lacD2, lacE2, lacF, lacG2, lacT2*	-6.47- -2.68	galactose-6-phosphate isomerase subunit; galactose-6-phosphate isomerase subunit; tagatose-6-phosphate kinase 2; tagatose 1,6-diphosphate aldolase 2; PTS system, lactose-specific IIA and IIB components; 6-phospho-beta-galactosidase 2; transcription antiterminator
SPNOXC_16690	-	-3.66	alpha-galactosidase
SPNOXC_00970	-	-3.69	putative beta-galactosidase
SPNOXC_01020	-	-3.61	putative tagatose-6-phosphate aldose/ketose isomerase
SPNOXC_05930	-	-5.83	putative surface-anchored beta galactosidase
SPNOXC_16250	*galT*	-3.15	galactose-1-phosphate uridylyltransferase
SPNOXC_16260	*galK*	-3.23	galactokinase.
Sugar Transport			
SPNOXC_16660-SPNOXC_16680	*msmE - msmG*	-5.0- -4.51	raffinose/stachyose/melibiose transport system substrate-binding protein.
SPNOXC_01010	-	-4.15	PTS system fructose family transporter subunit IIA
SPNOXC_05920	-	-3.99	PTS system galactitol-specific family transporter subunit IIC
SPNOXC_00980-SPNOXC_00990	-	-3.4 --3.50	PTS system sorbose transporter
SPNOXC_14800	-	-3.26	sugar phosphotransferase system IIBC component
SPNOXC_01000	-	-3.83	PTS system, mannose-specific IID component
SPNOXC_14780	-	-3.44	putative transport system permease
SPNOXC_05910	-	-3.02	PTS system transporter subunit IIB
SPNOXC_05900	-	-2.69	PTS system transporter IIA component
SPNOXC_14790	-	-3.53	multiple sugar transport system substrate-binding protein
SPNOXC_10740	-	-2.23	PTS system transporter subunit IIA
SPNOXC_15150	*scrA*	-2.51	putative sucrose-specific phosphotransferase system (PTS), IIABC component
SPNOXC_01190 – SPNOXC_01210	-	-5.28 --4.491	putative aldouronate transport system
Glycerol metabolism			
SPNOXC_19270 – SPNOXC_19290	*glpF1, glpO, glpK*	-4.27 -4.78	glycerol uptake facilitator protein , glycerol kinase, alpha-glycerophosphate oxidase
Glycogen Biosynthesis			
SPNOXC_10290, SPNOXC_10260, SPNOXC_10270	*glgA-glgC*	-2.83 - -2.25	glycogen synthase; glucose-1-phosphate adenylyltransferase; 1,4-alpha glucan branching protein
SPNOXC_10280	-	-2.68	putative glycogen biosynthesis protein
Arginine degradation			

SPNOXC_18940 - SPNOXC_18960	*arcA-arcC*	-2.52—2.61	arginine deiminase, ornithine carbomoyltransferase, crbamate kinase
Other metabolic genes, including saccharide catabolism genes			
SPNOXC_16650	-	-5.21	sucrose phosphorylase
SPNOXC_01030	-	-4.48	putative aldose 1-epimerase
SPNOXC_14770	-	-3.96	putative transport system permease
SPNOXC_04620	-	-3.58	putative endo-beta-N-acetylglucosaminidase.
SPNOXC_14810	-	-4.25	putative N-acetylmannosamine-6-phosphate 2-epimerase
SPNOXC_14730	*nanH*	-3.72	putative N-acetylneuraminate lyase
SPNOXC_18880	-	-3.07	N-acetyl-beta-D-glucosaminidase
SPNOXC_15690	-	-2.65	beta-fructofuranosidase
SPNOXC_17830	*adhE*	-2.56	aldehyde-alcohol dehydrogenase 2
SPNOXC_00950	*strH*	-2.50	beta-N-acetylhexosaminidase
SPNOXC_18900	-	-2.43	putative glycosyl hydrolase
SPNOXC_18970	-	-2.21	C4-dicarboxylate anaerobic carrier protein.
SPNOXC_00730	-	-2.17	putative Co-A binding protein
SPNOXC_18930	-	-3.09	putative fucosidase
SPNOXC_16240	-	-3.39	thioesterase superfamily protein.
SPNOXC_16640	-	-3.06	putative polysaccharide repeat unit polymerase O antigen Wzy
SPNOXC_14720	-	-3.76	ROK family protein;sugar kinase/transcriptional regulator.
SPNOXC_18890	-	-2.78	ROK family protein;sugar kinase/transcriptional regulator
SPNOXC_03640	-	-2.68	cell-wall surface anchored protein
SPNOXC_18980	-	-2.85	putative peptidase
DNA modification.			
SPNOXC_05940	-	-2.97—3.44	hypothetical transposase

As *H. influenzae* displayed an up-regulation of glycerol utilisation genes in batch co-culture, it is possible that there is a sharing of resources, or a more complex metabolic relationship between the two species in batch co-culture. Interestingly, the down-regulation of lactose/galactose metabolism genes in co-culture has previously been documented for Group A *Streptococcu*s serotype M3 during co-culture with the respiratory pathogen *Moraxella catarrhalis* in batch culture (Verhaegh et al. 2013). Specifically, the down-regulated genes included *lacABCDF* and several PTS system sugar transporters (Verhaegh et al. 2013). The authors state that, as *M. cattarhalis* is typically unable to utilize exogenous carbohydrates, it is unclear whether a nutrient limitation in co-culture could lead to this gene down-regulation. However, the similar results obtained in our study, suggest that such a down-regulation of lactose and sugar utilisation genes in co-culture,

could actually be a *Streptococcus* sp. specific factor, ubiquitous to other Streptococcal species in co-culture with respiratory pathogens in batch culture conditions.

In addition to this vast down-regulation of metabolic genes, *S. pneumoniae* displayed an up-regulation of bacteriocin and phage genes in batch co-culture (Table 5.3), which were consistently up-regulated in the co-culture in both batch and flow cell conditions. Importantly, both in the batch co-culture and in the flow cell co-culture there was an up-regulation of the *blpY* gene encoding a bacteriocin transporter, and another gene also encoding a bacteriocin transporter. However, none of the *blp* genes encoding the bacteriocin itself (such as *blpMN or blpIJK* (Lux et al., 2007)) were up-regulated, indicating that bacteriocin production was constant. Therefore, the co-culture condition seems to favour *S. pneumoniae* transport and processing of a bacteriocin without increasing its production. In a co-culture situation, this could be avantageous for *S. pneumoniae*. Firstly, in view of the sharing of resources in co-culture, an increased export of bacteriocin could have the benefit of allowing a longer-term survival of a reduced *S. pneumoniae* population. Secondly, an increased export of bacteriocin could also have some bactericidal effects against *H. influenzae*. While the action of the *S. pneumoniae* bacteriocin against *H. influenzae* has never been investigated, it is possible, that the bacteriocins produced by *S. pneumoniae* would have an action not only against closely related species, but also against species with which they share a niche and resources. However, if this was to play a role, it would only be likely to target a portion of the *H. influenzae* population, and would not explain the phenotype of the *H. influenzae* non-culturable state observed in co-culture.

Indeed, a co-culture assay of an *S. pneumoniae* D39 *blpY* deletion strain showed that as with the wild-type *S. pneumoniae* strains, *H. influenzae* likewise did not display culturability in the co-culture situation (Fig. 5.10).

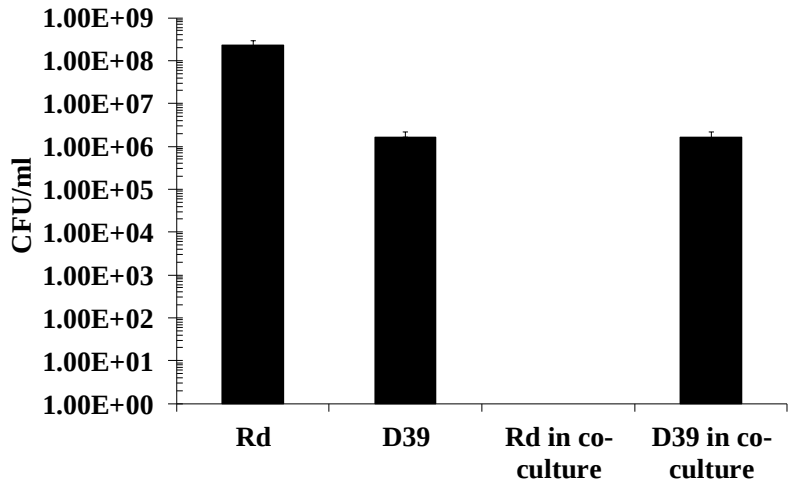

Fig. 5.10. Deletion of the *blpY* gene in *S. pneumoniae* D39 does not alter the *H. influenzae* culturability in co-culture with *S. pneumoniae*. The transcriptomic data has indicated the up-regulation of the bacteriocin transporter *blpY* in co-culture with *H. influenzae*, both in batch culture and in the flow cell system. To test whether *blpY* had a role in influencing the *H. influenzae/ S. pneumoniae* inter-species interactions, a deletion of *blpY* was constructed in *S. pneumoniae* D39, and a batch co-culture assay in HI media was established for 14 h. The planktonic mono-culture and co-culture growth of *H. influenzae* RdKW20 and *S. pneumoniae* D39 *blpY*- is shown (black bars). As with the wild-type *S. pneumoniae*, *H. influenzae* was not detected in co-culture with D39 *blpY*- by plate culture techniques, suggesting its presence in VBNC state.

S. pneumoniae phage genes, particularly the prophage antirepressor, were also shown to be up-regulated in co-culture (Table 5.3), both in batch co-culture and the flow cell co-culture at 64 h (Table 5.10). The antagonism of prophage repression could lead to the induction of prophage gene expression, potentially stimulating the lytic lifestyle of the phage. A potential benefit of prophage induction could be to release nutrients and DNA from cells via the phage mediated lysis, which could promote survival in a competitive polymicrobial environment (Carrolo et al. 2010). However, the functions of the prophage genes in these inter-species interactions would need to be further investigated in order to define their specific role in the inter-species environment.

5.2.8. *H. influenzae* displays phenotypic changes in co-culture at pH 8.0 and 7.4.

To further identify physical changes occurring in *H. influenzae* in co-culture, *H. influenzae* Rd KW20 and *S. pneumoniae* 11 mono and co-cultures were grown in batch culture (at pH 7.4 and pH 8.0), after which the planktonic cells were viewed under Scanning Electron Microscopy (SEM; Fig. 5.11).

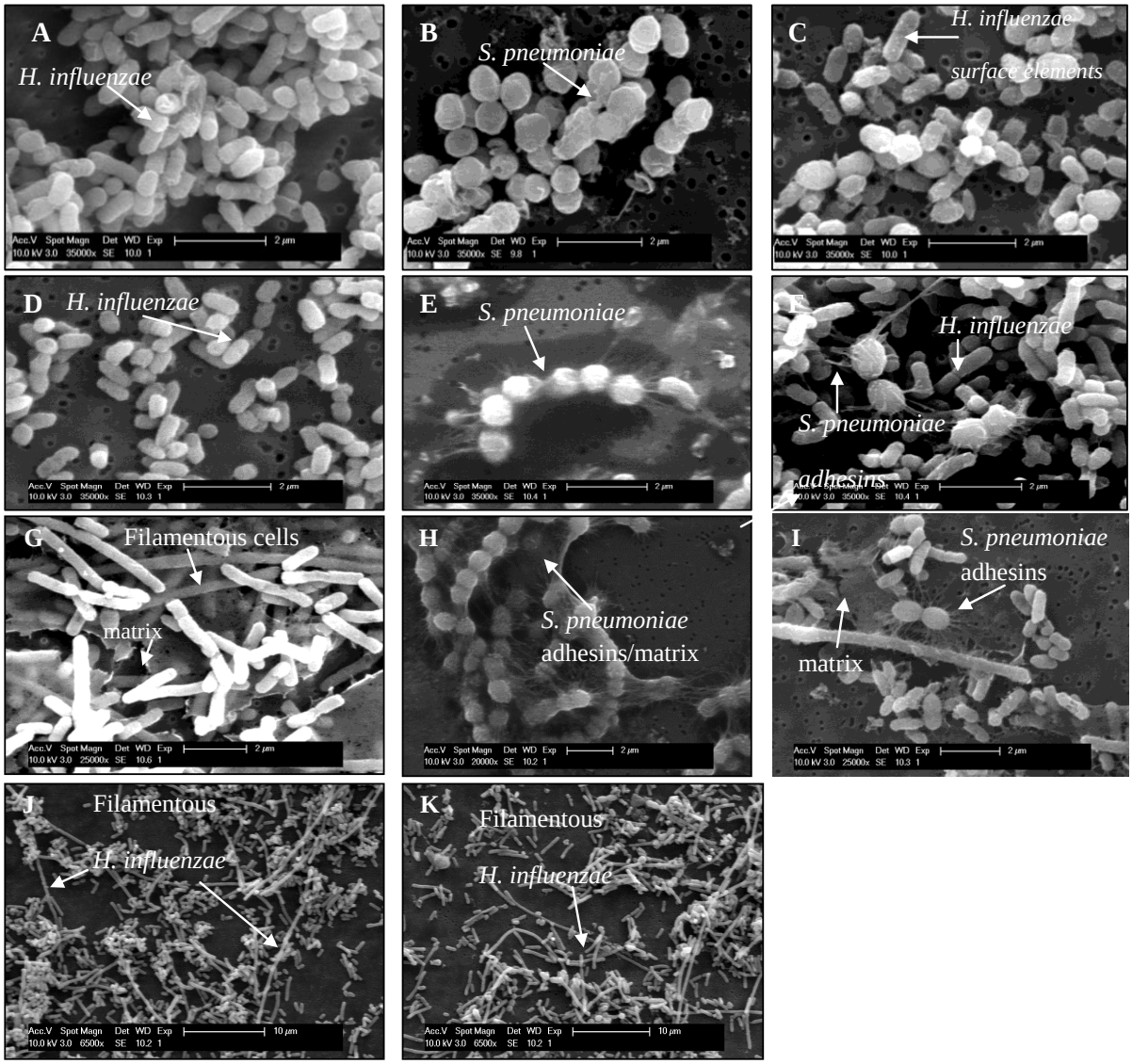

Fig. 5.11. Morphological changes occur in *H. influenzae* as a result of its existence in co-culture with *S. pneumoniae* or in the flow cell system environment. Field Emission Scanning Microscopy images (SEM) of *H. influenzae* Rd KW20 and *S. pneumoniae* strain 11 at pH 7.4 in batch mono-culture (A, B), and co-culture (C), and at pH 8.0 in batch mono-culture (D, E) and co-culture (F), respectively. Panel C reveals cell-surface structures of *H. influenzae* that are present in co-culture, but not in mono-culture at pH 7.4. Panel F shows *S. pneumoniae* adhesions and the absence of *H. influenzae* cell surface structures in co-culture at pH 8.0. SEM of *H. influenzae* and *S. pneumoniae* mono-cultures in the flow cell from growth at 40 h (G, H), and in co-culture (I). Both extracellular matrix and adhesion structures are present both in mono-cultures and in the co-culture in the flow cell system. *H. influenzae* also formed filamentous cells in the mono-culture and co-culture in the flow cell system *H. influenzae* grown in the flow cell system in mono-culture (J), and co-culture (K) respectively with a magnification of 6500x to show filamentous cell length. Filamentous cells present in the *H. influenzae* mono-culture and co-culture in the flow cell system reached up to 20μm in length.

Results of the SEM analysis showed that *S. pneumoniae* is able to cause physical changes in the *H. influenzae* cells in co-culture, inducing dot-like structure formations on the *H. influenzae* cell surface at pH 7.4 (Fig 5.11). These surface elements were only present on *H. influenzae* in co-culture, and were absent from the *S. pneumoniae* cells. While the nature of these structures is not confirmed, the transcriptomics data suggests that they could be surface structures or transport systems that were up-regulated in *H. influenzae* in co-culture. Importantly, these surface structures were absent from *H. influenzae* in co-culture at pH 8.0, suggesting they have a role in maintaining the non-culturable state of *H. influenzae*.

In contrast, *S. pneumoniae* formed extensive adhesin-like structures at pH 8.0 in mono- and co-culture, which were absent at pH 7.4 (Fig. 5.11). As these adhesin structures were shown to physically interact with *H. influenzae* in co-culture, it is possible that their presence could have a role in maintaining the culturable state of *H. influenzae* in co-culture at pH 8.0.

Hence, the SEM data suggests that the combination of adhesive elements as well as the absence of *H. influenzae* surface structures (Fig. 5.11) may mediate a lifestyle of *H. influenzae* and *S. pneumoniae* which bypasses competition and promotes co-existence.

5.2.9. *H. influenzae* survives in co-culture in a flow cell system.

Our data has shown that pH and growth phase impact on the outcome of co-culture. In order to analyse the *H. influenzae/S. pneumoniae* interspecies interactions in more detail, we used a system more closely representative of the host environment in the context of the mode of growth (continuous culture and not batch culture); a flow cell system. In contrast to the batch culture, *H. influenzae* was culturable, and was able to survive in co-culture in the flow cell system, at all time-points including 168 h without reductions in cell numbers relative to the mono-culture (Fig. 5.12). In addition, the pH in the flow chamber was measured and in these conditions was not lower than pH 6.0 for the co-culture (Fig. 5.12).

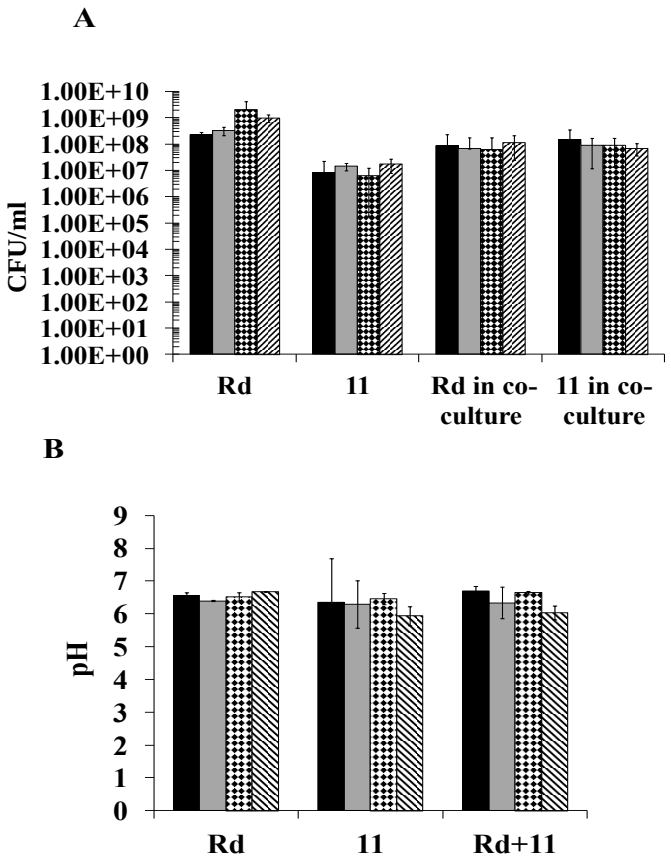

Fig. 5.12. Planktonic growth (CFU/ml), and end-point pH remain constant for both *H. influenzae* Rd KW20 and *S. pneumoniae* strain 11 in mono- and co-culture, when grown in a flow cell system. A) CFU/ml of *H. influenzae* Rd KW20 and *S. pneumoniae* strain 11 planktonic growth (CFU/ml) in the flow cell system at various time-points: 20 h (black bars), 40 h (grey bars), 64 h (checked bars), 168 h (hatched bars), and B) pH of *H. influenzae* Rd KW20 and *S. pneumoniae* strain 11 mono- and co-culture culture growth media during flow cell growth at 20 h (black bars), 40 h (grey bars), 64 h (checked bars) and 168 h (hatched bars).

These results indicated that the flow cell system, as a different environment, could stimulate the development of different interactions between *H. influenzae* and *S. pneumoniae* compared to the batch culture. In evidence, were the phenotypic differences observed for *H. influenzae* and *S. pneumoniae*, as well as their differential gene expression observed in the flow cell system.

Analysis of the gene expression patterns from the flow cell system allowed us to determine two major findings; 1) *H. influenzae* and *S. pneumoniae* alter their transcriptome upon the switch from batch culture to flow cell growth, and 2) *H. influenzae* and *S. pneumoniae* transcriptomes observed in co-culture in the flow cell system are different from the transcriptomes observed in mono-culture in the flow cell system.

5.2.10. There are changes in the cell morphology of *S. pneumoniae* and *H. influenzae* in the flow cell system.

The flow cell conditions are known to change environmental conditions central to the cell's physiology, including nutreint availability and oxygen tension. We therefore were interested in observing the cells in these conditions to establish the nature of their adaptation to the flow cell in mono-culture and co-culture, especially in the context that there was a change in the outcome of co-culture interactions. For these analyses, the planktonic mono-cultures and co-culture were collected from the flow cell system at various time points were viewed under SEM. The results showed that in both the mono-culture and the co-culture situations, both species formed aggregates encased in a fibrous extracellular material, suggesting potential initiation of biofilm formation processes (Fig. 5.11, Fig. 5.13).

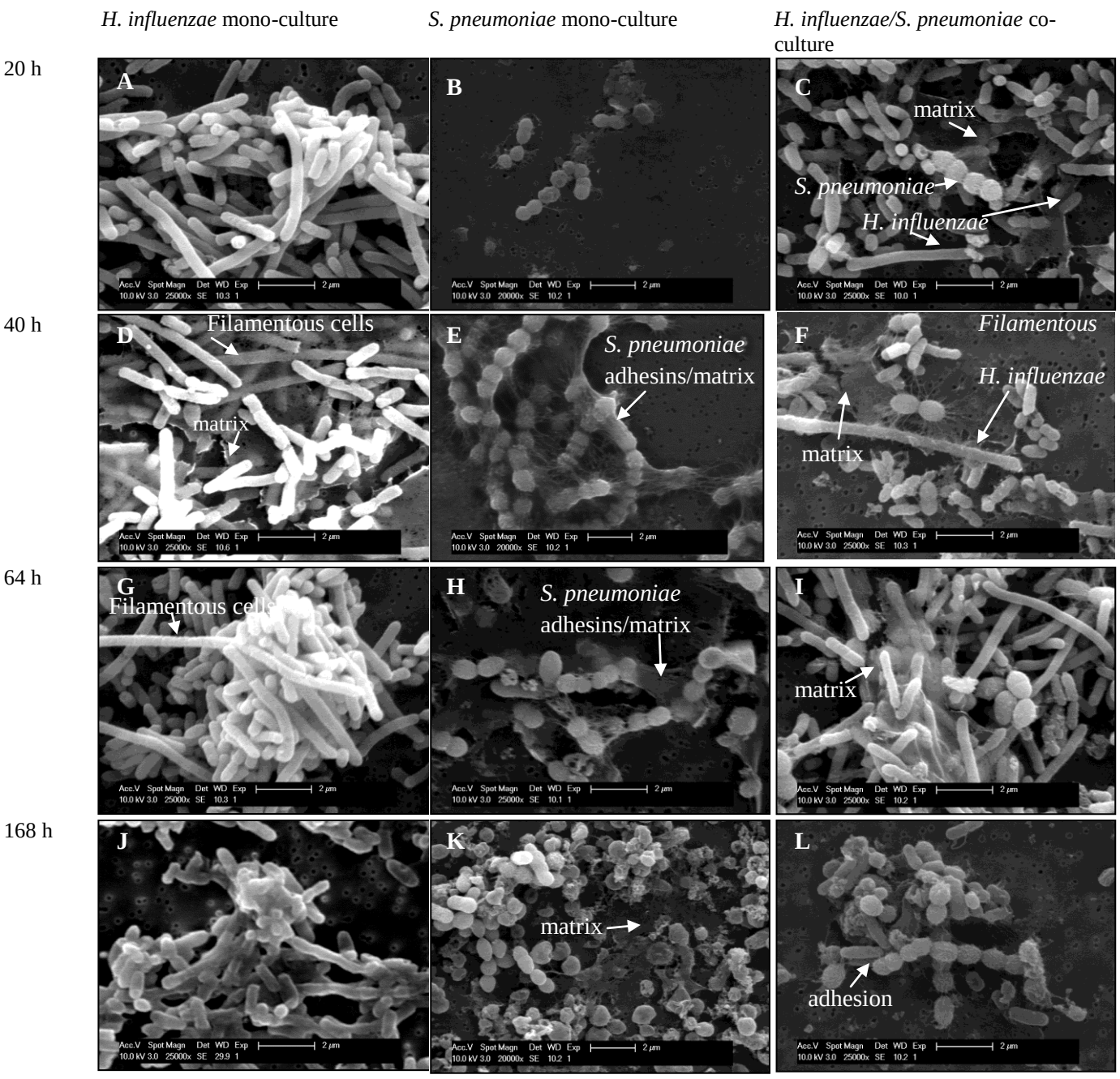

Fig. 5.13. Extracellular matrix formation and cell co-aggregation occurs in mono- and co-cultures of *H. influenzae* and *S. pneumoniae* in the flow cell system at various time-points; Filamentation of *H. influenzae* occurs in mono- and co-culture at various time-points in the flow cell system. Field Emission Scanning Microscopy (SEM) images

of planktonic *H. influenzae* Rd KW20 and *S. pneumoniae* strain 11 mono- and co-cultures after growth in the flow cell at 20 h (A, B, C), 40 h (D, E, F), 64 h (G, H, I) and 168 h (J, K, L). Images B, E and K are shown with a magnification of 20000x. All other images are shown using a magnification of 25000x (appropriate scale bars are provided). Fibrous extracellular material resemblant of a biofilm extracellular polymeric substance (EPS) matrix was seen for both *H. influenzae* and *S. pneumoniae* mono- and co-cultures at all time-points. Noticeably, cells of both species were shown to physically associate in co-culture, and this association was mediated by the EPS matrix adhering to both cell types. Filamentous *H. influenzae* cells were also seen in both mono- and co-culture.

In addition, *H. influenzae* was observed to form long, filamentous cells estimating up to 20 μm in length (compared to 1μm length cells in the batch culture state) in the flow cell system (Fig. 5.11, Fig. 5.13, Fig. 5.14). This occurred both in the mono-culture and in the co-culture situation, indicating that the environmental parameters of the flow cell facilitated cell filamentation. While it is unclear what role the filamentation played in the inter-species interactions, as the flow cell system is a more optimal representation of the host environment, the filamentous *H. influenzae* may also be a more accurate representation of the *H. influenzae* morphology and lifestyle during host infection processes. Filamentous *H. influenzae* have not previously been described in patient samples, but they were recently recovered from an experimental otitis media model (Leroy et al. 2007), suggesting their involvement in OM disease processes. It was important to establish this phenotypic adaptation to a flow cell system before investigating the gene expression response in these conditions.

H. influenzae mono-culture | *H. influenzae/ S. pneumoniae* co-culture

20 h

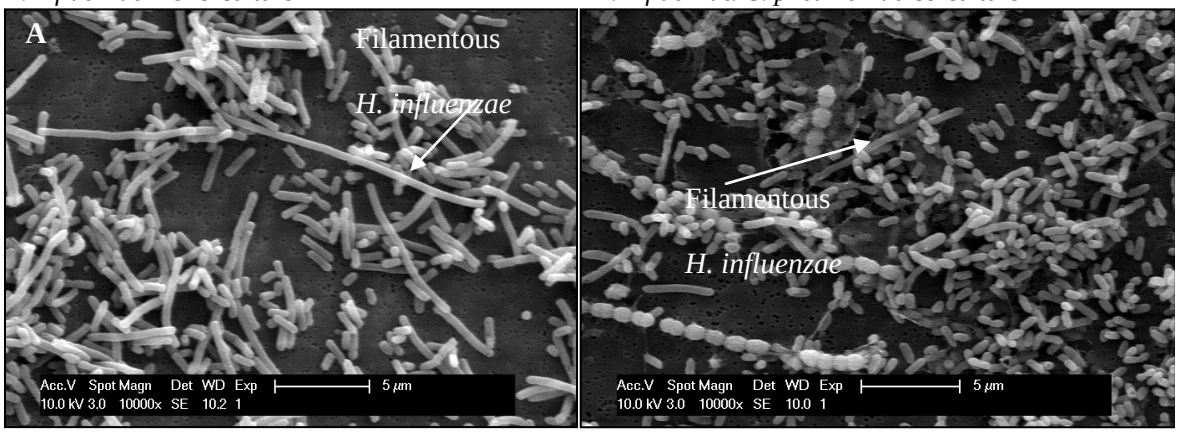

40 h

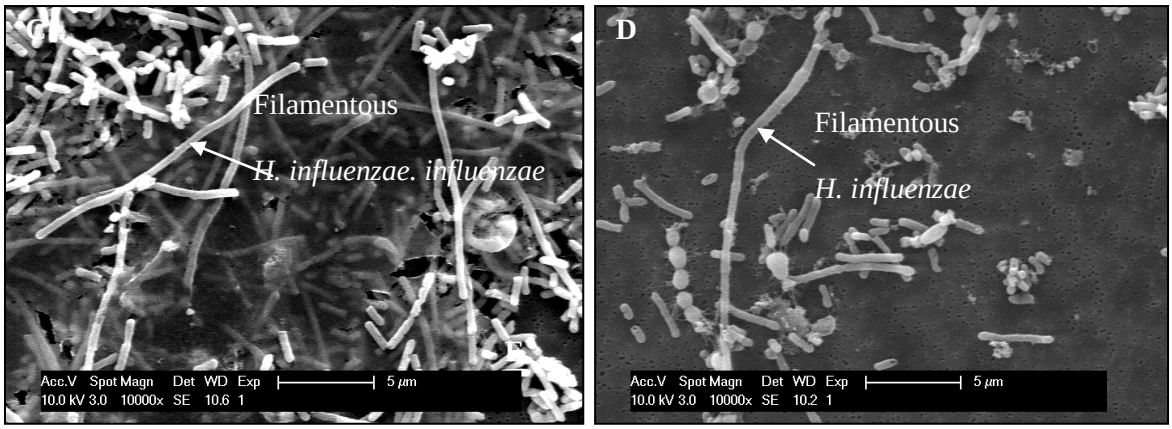

64 h

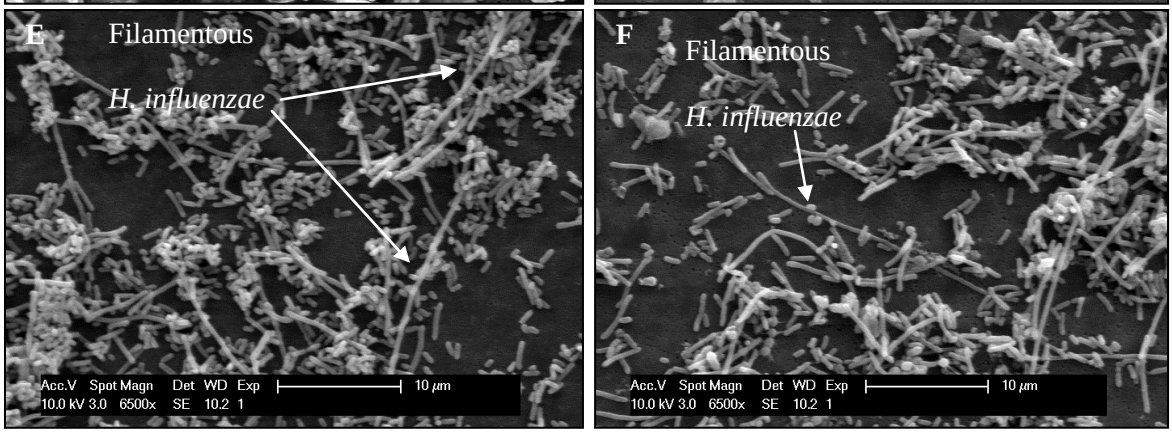

168 h

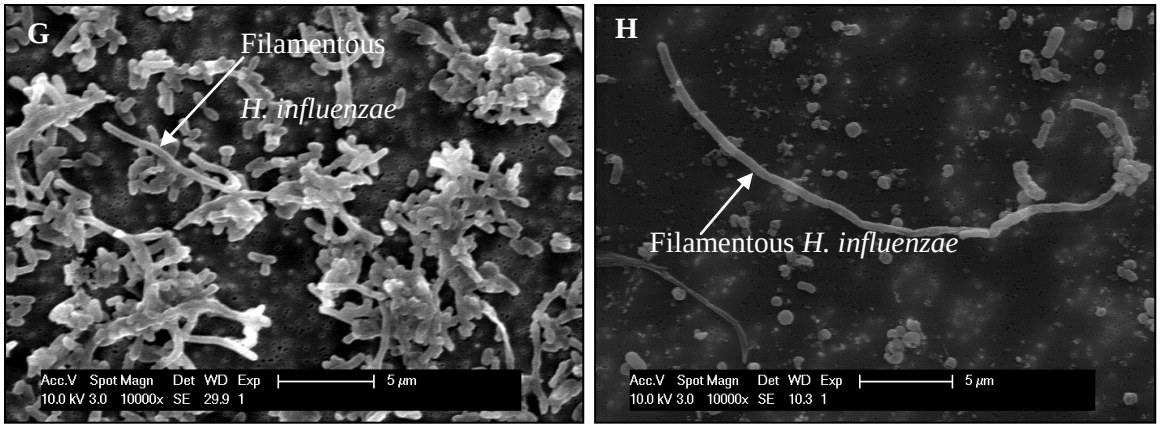

Fig. 5.14. *H. influenzae* cell filamentation occurs in a flow cell system in mono- and co-culture at various time-points. Field Emission Scanning Microscopy (SEM) images of examples of *H. influenzae* Rd KW20 filamentous cells (5-20µm) in planktonic mono- and co-culture at 20 h (A, B), 40 h (C, D), 64 h (E, F) and 168 h (G, H) in the flow cell system. 20 h, 40 h and 168 h images display cells at a magnification of 10000x, whereas 64 h images display cells magnified at 6500x. Filamentous cells were observed in *H. influenzae* mono- and co-culture at all time-points in the flow cell.

5.2.11. In the flow cell, *H. influenzae* alters its gene expression in mono-culture and in co-culture

When the *H. influenzae* batch mono-culture gene expression was compared to the *H. influenzae* flow cell mono-culture gene expression, it was found that at both 64 h and 168 h time-points there was an up-regulation of several gene classes (Table 5.4, Table 5.5).

Table 5.4. Up- and down-regulated *H. influenzae* Rd KW20 genes when grown in a flow cell in mono-culture at 64 h compared to *H. influenzae* grown in batch mono-culture at a pH of 7.4. Results are displayed for genes with a $\log_2$ fold change ≥ 2, and a p-value ≤ 0.05.

Up-regulated Genes Locus tag	**Gene name**	**$\log_2$FoldChange**	**Function**
Gene class: Iron Acquisition			
HI0262-HI0263	*hxuB-hxuC*	2.0-2.18	heme-hemopexin binding protein B, C
HI0131	*afuA*	2.11	iron (III) transport system substrate binding protein
Glycerol uptake and metabolism			
HI0683-HI0685	*glpA-glpC*	3.0-3.32	sn-glycerol-3-phosphate dehydrogenase subunit A-C
Thiamine metabolism			
HI0415		3.07	hydroxyethylthiazole kinase
HI1019	*tbpA*	2.41	thiamin ABC transporter substrate-binding protein
Other Metabolic Genes			
HI0354		2.58	putative hydroxymethylpyrimidine transport system ATP-binding protein
HI0185	*adhC*	1.98	alcohol dehydrogenase class III
HI0822	*mglB*	1.98	galactose ABC transporter substrate-binding protein and cell motility
HI0595	*arcC*	2.07	carbamate kinase
DNA modification			
HI1478	*muA*	2.63	muA phage transposase
Downregulated Genes			
HI1218	*lctP*	-2.93	L-lactate permease
HI1504		-2.18	bacteriophage Mu I protein

Table 5.5. Up- and down-regulated *H. influenzae* Rd KW20 genes when grown in a flow cell system in mono-culture at 168 h compared to *H. influenzae* grown in batch mono-culture at pH 7.4. Results are displayed for genes with a $\log_2$ fold change ≥ 2, and a p-value ≤ 0.05.

Gene	Gene name	$\log_2$FoldChange	Function
Upregulated Genes			
Gene class: Iron-acquisition			
HI0262-HI0264	*hxuA-hxuC*	2.57- 3.52	heme/hemopexin-binding protein A, B, C
HI0131	*afuA*	2.45	ferric ABC transporter protein
Glycerol metabolism			
HI0683-HI0685	*glpA-glpC*	3.20-3.69	sn-glycerol-3-phosphate dehydrogenase subunit A, B, C
Thiamine metabolism			
HI0415	-	3.70	thiamine metabolism hydroxyethylthiazole kinase
HI1019	*tbpA*	2.51	thiamine ABC transporter substrate-binding protein
HI0357	-	2.03	thiamine biosynthesis protein
HI0417	*thiE*	3.04	thiamine-phosphate pyrophosphorylase
HI0416	*thiD*	2.57	phosphomethylpyrimidine kinase
Metabolic			
HI0595	*arcC*	2.55	carbamate kinase
HI0091	-	2.56	glycerate kinase
HI1010	-	1.97	3-hydroxyisobutyrate dehydrogenase
HI0189	*gdhA*	1.99	glutamate dehydrogenase
HI0648	*mdaB*	2.03	modulator of drug activity B
HI0564	*asnA*	2.06	asparagine synthetase AsnA
HI0017	-	2.37	autonomous glycyl radical cofactor GrcA
HI0521	-	2.11	glycyl radical enzyme
HI1617	*aspC*	2.17	aromatic amino acid aminotransferase
HI1259	-	2.22	serine protease
HI1012	-	2.90	aldolase
HI1677.1	-	2.09	RNaseP
Electron transfer			
HI0343	*napD*	2.04	nitrate reductase assembly protein NapD
HI0346	*napH*	2.42	quinol dehydrogenase membrane subunit
Cellular transport			
HI0355	-	2.29	ABC transporter permease
HI0561	-	2.12	putative oligopeptide transporter
HI0822	*mglB*	2.64	galactose ABC transporter substrate-binding protein
HI0354	-	2.59	ABC transporter ATP-binding protein
HI0092	-	3.11	gluconate:H+ symporter, GntP family

HI0418	-	2.30	transporter
Phage associated			
HI1485	-	3.01	Mu like prophage
HI1478	*muA*	4.24	Mu like transposase
HI1483	-	3.14	Mu phage host-nuclease inhibitor - protein
HI1481	*muB*	2.85	DNA transposition protein
Downregulated Genes			
HI1218	*lctP*	-3.89	L-lactate permease
HI0550		-2.62	glycosyl transferase? lipooligosaccharide biosynthesis protein
HI1297	-	-2.42	hypothetical protein - holin-like protein
HI1298	-	-2.32	membrane protein - putative LrgB like protein
HI0235	-	-2.28	alternative ribosome-rescue factor A
HI1502.1;pseudo=true	-	-2.78	pseudogene

One of these gene classes up-regulated in the flow cell included heme-hemopexin-binding proteins, which are likely to function in importing iron complexes into the cell. In addition, glycerol uptake and degradation genes, and thiamine metabolism genes were up-regulated at both time-points in the flow cell. Therefore, it appears that in the flow cell system *H. influenzae* adopted an altered metabolism in order to adapt to low iron levels, and the available nutrient sources. Partly, this is confirmed by SEM imaging, which showed that in the flow cell system, *H. influenzae* adopts a different phenotype of cell filamentation and biofilm formation (Fig. 5.5). Previous studies have indicated that iron limitation results in *H. influenzae* cell filamentation (Vogel et al. 2012). The results of our study indicate that *H. influenzae* exists in an iron-limited environment in the flow cell and forms such filamentous cells in this environment.

While *H. influenzae* altered its gene expression upon transition from batch culture growth to flow cell growth, it also altered its gene expression upon transition from mono-culture growth in the flow cell system to co-culture growth in the flow cell system. Moreover, this change in gene expression appeared to be time-point specific (Tables 5.7, 5.6).

Table 5.6. Up- and down-regulated genes of *H. influenzae* Rd KW20 when grown in co-culture with *S. pneumoniae* strain 11 in a flow cell system for 64 h compared to *H. influenzae* grown in mono-culture in a flow cell system for 64 h. Results are displayed for genes with a $\log_2$ fold change ≥ 2, and a p-value ≤ 0.05.

Upregulated Genes **Locus tag**	**Gene Name**	**$\log_2$FoldChange**	**Function**
Gene Class: **Bacteriophage**			
HI1414	-	3.11	hypothetical protein - phage
HI1413	-	2.88	phage
HI1416	-	2.57	phage holin
HI1415	-	2.28	phage uncharacterised protein
Cell Structure			
HI0296	*hopD*	2.66	type 4 prepilin-like protein specific leader peptidase
HI0039	*mreD*	2.31	rod shape-determining protein MreD
Cell Transport			
HI0635	-	2.12	hemoglobin/transferrin/lactoferrin receptor protein
Downregulated Genes			
HI1674	*moaD*	-2.28	molybdopterin synthase small subunit

Table 5.7. Up- and down-regulated genes of *H. influenzae* Rd KW20 when grown in co-culture with *S. pneumoniae* strain 11 in a flow cell system for 168 h compared to *H. influenzae* grown in mono-culture in a flow cell system for 168 h. Results are displayed for genes with a $\log_2$ fold change ≥ 2, and a p-value ≤ 0.05.

Upregulated Genes Locus tag	**Gene Name**	**$\log_2$FoldChange**	**Function**
Cellular transport			
HI0051	-	4.07	putative TRAP transporter small permease protein
HI1030	-	2.48	TRAP-type C4-dicarboxylate transport system, small permease component
HI0052	-	3.62	hypothetical protein Substrate-binding domain of a sialic acid binding Tripartite ATP-independent Periplasmic transport system (SiaP) and related proteins
DNA-associated			
HI0980	*fis*	2.34	Fis family transcriptional regulator, factor for inversion stimulation protein
HI1349	-	2.59	starvation-inducible DNA-binding protein
HI1660	*nrdB*	1.97	DNA synthesis ribonucleotide-diphosphate reductase subunit beta
HI1659	*nrdA*	2.41	DNA synthesis ribonucleotide-diphosphate reductase subunit alpha
Cell division			
HI0668	-	1.93	cell division protein ZapB
Metabolic			
HI1053	-	2.87	uncharacterized homolog of gamma-carboxymuconolactone decarboxylase subunit
HI0591	*speF*	2.12	ornithine decarboxylase
HI1045	*dmsC*	2.27	anaerobic dimethyl sulfoxide reductase subunit C
HI1602	-	2.62	putative oxidoreductase
HI0053	-	3.97	zinc-type alcohol dehydrogenase
Downregulated Genes			
HI1483	*gam*	-2.53	Mu phage host-nuclease inhibitor protein
HI0910	*mutT*	-2.15	mutator protein: 8-oxo-dGTP diphosphatase
Metabolic			
HI0415	-	-2.09	thiamine metabolism hydroxyethylthiazole kinase
HI0669	*mioC*	-2.21	flavodoxin

At 64 h, the major changes upon transition to co-culture included an up-regulation of the φ-Flu bacteriophage genes (Table 5.6). These φ-flu phage genes were no longer up-regulated at the 168 h time-point, suggesting that this bacteriophage gene expression is a relatively early event in co-culture interactions (Table 5.7). As these bacteriophage genes were also up-regulated in batch co-culture, where *H. influenzae* reduced in viability or entered a non-culturable state, it is possible that the φ-Flu phage could be an initial stress response of *H. influenzae* to *S. pneumoniae*, and *H. influenzae* culturability could only be dependent on the expression of this phage in a threshold-dependent manner at early stages. At 168 h, transcriptomic changes in co-culture included an up-regulation of 3 TRAP transport proteins; 1 involved in dicarboxylate transport and 2 involved in sialic acid transport. DNA associated genes were also up-regulated including 2 DNA synthesis enzymes and 2 DNA-associated transcriptional regulators including the Fis family transcriptional regulator (Table 5.7). These results suggest that at 168 h in co-culture *H. influenzae* may be increasing the rate of cell division and metabolism, as well as globally changing the regulation of transcriptional pathways. Hence, at 168 h in co-culture, there are likely to be synergistic, rather than antagonistic interactions between the 2 species.

5.2.12. In the flow cell, *S. pneumoniae* alters its transcriptome in mono-culture and in co-culture.

S. pneumoniae was also shown to adopt a different transcriptional profile in the flow cell system compared to batch culture.

Table 5.8. Up- and down-regulated genes of *S. pneumoniae* strain 11 grown in mono-culture in a flow cell at 64 h compared to *S. pneumoniae* grown in mono-culture in batch culture at a pH of 7.4. Results are displayed for genes with a $\log_2$ fold change ≥ 2, and a p-value ≤ 0.05.

Upregulated Genes **Locus tag** **Gene class: Capsule synthesis**	**Gene Name**	**$\log_2$FoldChange**	**Function**
SPNOXC_03590	*Udg/ cap3A*	2.97	UDP-glucose 6-dehydrogenase Ugd.
SPNOXC_03600	*Cap3B*	2.37	serotype 3 capsule synthase
Iron acquisition			
SPNOXC_16040 – SPNOXC_16060	-	3.22-2.6	putative iron transport system *** for 2 genes pval 0.06**
Other metabolic genes			
SPNOXC_10590	*nrdH*	2.80	glutaredoxin-like protein
SPNOXC_16100	-	2.87	sortase-sorted surface anchored protein
Downregulated genes **Locus tag** **Gene class: Lactose /galactose metabolism**			
SPNOXC_10700, SPNOXC_10690, SPNOXC_10680, SPNOXC_10670, SPNOXC_10640, SPNOXC_10650, SPNOXC_10630, SPNOXC_10660	*lacA,lacB1,lacC2, lacD2, lacE2, lacF, lacG2, lacT2*	-4.93- -8.30	galactose-6-phosphate isomerase subunit, galactose-6-phosphate isomerase subunit LacB, tagatose-6-phosphate kinase 2, tagatose 1,6-diphosphate aldolase 2, lactose-specific phosphotransferase system (PTS), IIBC component 2, PTS system lactose-specific transporter subunit IIA, 6-phospho-beta-galactosidase 2, transcription antiterminator

			LacT 2
SPNOXC_05930	-	-8.82	putative surface anchored beta-galactosidase
SPNOXC_00970	-	-7.29	putative beta-galactosidase.
SPNOXC_16250	*galT*	-5.41	galactose-1-phosphate uridylyltransferase
SPNOXC_16260	*galK*	-4.79	galactokinase.
SPNOXC_16690	*aga*	-3.21	alpha-galactosidase.
Transporters			
SPNOXC_00980	-	-7.88	PTS system sorbose subfamily transporter subunit IIB
SPNOXC_10740	-	-6.13	PTS system transporter subunit IIA
SPNOXC_05900	-	-5.95	putative sugar phosphotransferase system (PTS), IIA component
SPNOXC_05920	-	-7.56	PTS system galactitol-specific family transporter subunit IIC
SPNOXC_01210	-	-7.50	extracellular solute-binding protein
SPNOXC_01000	-	-7.48	PTS system mannose/fructose/sorbose family transporter subunit IID
SPNOXC_00990	-	-7.24	PTS system sorbose-specific family transporter subunit IIC.
SPNOXC_01010	-	-7.20	PTS system fructose family transporter subunit IIA
SPNOXC_01200	-	-6.76	putative aldouronate transport system permease protein
SPNOXC_05910	-	-6.58	PTS system, galactitol-specific IIB component
SPNOXC_01190	-	-6.50	putative aldouronate transport system permease protein
SPNOXC_06280	-	-3.64	putative ABC transport system permease protein
SPNOXC_06300	-	-3.34	ABC transporter ATP-binding protein
SPNOXC_14520	-	-3.19	ABC transporter ATP-binding protein
SPNOXC_01390	-	-4.13	putative membrane protein
SPNOXC_16660	*msmG*	-4.06	multiple sugar-binding transport system permease protein
SPNOXC_14780	-	-3.88	putative transport system permease
SPNOXC_14800	-	-3.86	sugar phosphotransferase system (PTS), IIBC component
SPNOXC_15700	-	-3.80	putative aldouronate transport system substrate-binding protein
SPNOXC_14770	-	-3.75	putative transport system

			permease
SPNOXC_16670	*msmF*	-4.77	multiple sugar-binding transport system permease protein
SPNOXC_15710	-	-2.92	putative aldouronate transport system permease protein
SPNOXC_01400	-	-2.69	ABC transporter ATP-binding protein
SPNOXC_14740	-	-3.83	putative membrane protein
SPNOXC_16680	*msmE*	-4.29	multiple sugar-binding protein
SPNOXC_15100	-	-2.94	putative membrane protein
Glycerol uptake and metabolism			
SPNOXC_19270 – SPNOXC_19290	*glpF1, glpO, glpK*	-6.41 - -5.4	glycerol uptake facilitator protein 1, alpha-glycerophosphate oxidase, glycerol kinase
Thiamine metabolism			
SPNOXC_06540, SPNOXC_06560-SPNOXC-06580		-2.40 - -2.90	thiaminase, putative hydroxyethylthiazole kinase, thiamine phosphate pyrophosphorylase, phosphomethylpyrimidine kinase *** pval 0.03-0.07**
Glycogen synthesis			
SPNOXC_10270 – SNPOXC_10290	*glgA-glgC*	-3.57 - -3.41	glycogen biosynthesis proteins glucose-1-phosphate adenylyltransferase
Sialic acid utilizaion			
SPNOXC_14880	*nanA*	-2.96	sialidase A (neuraminidase A)
SPNOXC_14730	*nanH*	-3.81	putative N-acetylneuraminate lyase
SPNOXC_14810	*nanE*	-4.03	putative N-acetylmannosamine-6-phosphate 2-epimerase
Amino acid metabolism			
SPNOXC_18940-SPNOXC_18960	*arcA-arcC*	-5.40 - -5.08	arginine deiminase, ornithine carbomoyltransferase, carbamate kinase
Other metabolic genes			
SPNOXC_01030	-	-7.40	putative aldose 1-epimerase
SPNOXC_01020	*agaS*	-7.38	putative tagatose-6-phosphate aldose/ketose isomerase

SPNOXC_18880	*gcnA*	-5.82	N-acetyl-beta-D-glucosaminidase
SPNOXC_04620	-	-5.64	putative endo-beta-N-acetylglucosaminidase
SPNOXC_18970	-	-5.28	C4-dicarboxylate anaerobic carrier protein
SPNOXC_18980	-	-5.24	putative petidase
SPNOXC_18900	-	-5.15	putative glycosyl hydrolase
SPNOXC_00950	*strH*	-4.92	beta-N-acetylhexosaminidase
SPNOXC_18930	-	-4.59	putative fucosidase.
SPNOXC_15690	-	-4.48	beta-fructofuranosidase.
SPNOXC_16240	-	-4.26	thioesterase superfamily protein
SPNOXC_16650	-	-4.22	sucrose phosphorylase
SPNOXC_14790	-	-3.72	extracellular solute-binding lipoprotein
SPNOXC_03640	-	-3.71	endo-alpha-N-acetylgalactosaminidase with glycoside hydrolase activity
SPNOXC_17830	*adhE*	-3.01	aldehyde-alcohol dehydrogenase 2
SPNOXC_13570	-	-2.61	putative NADPH-dependent FMN reductase.
DNA-associated			
SPNOXC_19300	-	-2.89	putative DNA-binding protein
SPNOXC_18890	-	-5.73	ROK family protein
SPNOXC_14720	-	-3.85	ROK family protein

Table 5.9. Up- and down-regulated genes of *S. pneumoniae* strain 11 grown in mono-culture in a flow cell at 168 h compared to *S. pneumoniae* grown in mono-culture in batch culture at a pH of 7.4. Results are displayed for genes with a $\log_2$ fold change ≥ 2, and a p-value ≤ 0.05.

Upregulated Genes Locus Tag	**Gene Name**	**$\log_2$FoldChange**	**Function**
Gene class: Iron-acquisition Genes			
SPNOXC_16040-SPNOXC_16050	-	2.31	putative iron transport system
Membrane proteins			
SPNOXC_19740-SPNOXC_19750	-	5.72	putative membrane protein
Membrane Transport Proteins			
SPNOXC_03210	-	2.53	PTS system, cellobiose-specific IIC component
SPNOXC_18820	-	2.29	sugar phosphotransferase system (PTS), lactose/cellobiose-specific family, IIB subunit protein
SPNOXC_18810	-	2.29	putative sugar-specific permease, SgaT/UlaA family
SPNOXC_13130	-	2.08	putative amino acid ABC transporter, extracellular amino acid-binding protein
SPNOXC_14230	-	1.98	PTS system, fructose-specific IIA component
SPNOXC_01410	-	1.94	putative extracellular amino acid-binding protein
SPNOXC_19580	-	2.74	putative amidase
SPNOXC_10590	*nrdH*	2.82	glutaredoxin-like protein
SPNOXC_18800	-	2.49	putative transketolase subunit
SPNOXC_03590	*ugd*	2.13	UDP-glucose 6-dehydrogenase
SPNOXC_10610	-	2.18	putative ribonucleoside-diphosphate reductase beta chain
SPNOXC_13390	-	2.18	putative extracellular oligopeptide-binding protein
SPNOXC_12820	-	2.22	putative membrane protein
SPNOXC_18790	-	2.38	putative transketolase subunit
SPNOXC_18840	-	2.39	putative membrane protein
SPNOXC_01350	-	2.08	putative peptidoglycan-binding protein
SPNOXC_10930	-	2.05	putative plasmid addiction system, toxin protein
SPNOXC_18720	-	2.05	putative membrane protein
SPNOXC_16100	-	2.02	sortase
SPNOXC_05290	-	1.96	6-phospho-beta-glucosidase
SPNOXC_00080	-	1.96	putative septum formation initiator protein
SPNOXC_07160	-	1.95	putative membrane protein
DNA associated			
SPNOXC_19760	-	3.51	TetR family regulatory protein
SPNOXC_09280	-	2.61	putative regulatory protein
Downregulated Genes			
Gene class: Glycerol uptake and metabolism			
SPNOXC_19270-19290	*glpF1, glpO, glpK*	-3.56 - -3.17	glycerol uptake and glycerophospholipid metabolism genes
Lactose/galactose			

metabolism			
SPNOXC_10670-10680	*IacC2; lacD2*	-2.04 - -2.0	tagatose-6-phosphate kinase 2, tagatose 1,6-diphosphate aldolase 2
SPNOXC_00970	-	-2.32	putative beta-galactosidase**.**
SPNOXC_05930	-	-2.54	putative surface anchored beta-galactosidase
SPNOXC_16260	-	-2.31	galactokinase.
Thiamine biosynthesis			
SPNOXC_06560-06580		-2.78 - -2.3	thiamin-phosphate pyrophosphorylase, phosphomethylpyrimidine kinase, putative hydroxyethylthiazole kinase.
Membrane Transport			
SPNOXC_06530	-	-3.01	putative membrane protein
SPNOXC_17630	-	-2.83	ABC transporter ATP-binding protein
SPNOXC_16660	*msmG*	-2.49	multiple sugar-binding transport system permease protein
SPNOXC_16680	*msmE*	-2.45	multiple sugar-binding protein
SPNOXC_16670	*msmF*	-2.55	multiple sugar-binding transport system permease protein
SPNOXC_17620	-	-2.41	ABC-2 type transporter membrane protein
SPNOXC_00980	-	-2.39	PTS system sorbose subfamily transporter subunit IIB
SPNOXC_05920	-	-2.23	PTS system galactitol-specific family transporter subunit IIC
SPNOXC_01010	-	-2.20	PTS system fructose family transporter subunit IIA
SPNOXC_06520	-	-2.56	ABC transporter ATP-binding protein
SPNOXC_01190	-	-2.48	binding-protein-dependent transport system membrane protein
Metabolic			
SPNOXC_13570	-	-3.02	putative NADPH-dependent FMN reductase
SPNOXC_16650	-	-2.72	sucrose phosphorylase
SPNOXC_09660	-	-2.62	phosphonopyruvate decarboxylase
SPNOXC_19050	-	-2.47	fucolectin-rel. glycosyl hydrolase
SPNOXC_15690	-	-2.44	beta-fructofuranosidase
SPNOXC_18930	-	-2.31	putative fucosidase
SPNOXC_04620	-	-2.23	putative endo-beta-N-acetylglucosaminidase
SPNOXC_14500	*tpx*	-2.15	putative thiol peroxidase
SPNOXC_01030	-	-2.15	putative aldose 1-epimerase
SPNOXC_16250	-	-2.07	galactose-1-phosphate uridylyltransferase
SPNOXC_16640	-	-2.01	putative polysaccharide repeat unit polymerase
Gene class: Phage			
SPNOXC_00440	-	-3.94	phage portal protein * pval 0.066
Gene class: DNA-associated			
SPNOXC_19300	-	-2.78	putative DNA-binding protein

The flow cell gene expression profile included an upregulation of an iron acquisition system, (exactly correlating to observations in *H. influenzae*) (Table 5.8, Table 5.9), and supports the model of the flow cell growth having an increased requirement for iron. For *S. pneumoniae*, down-regulated genes in this environment at both 64 h and 168 h, included lactose and galactose utilisation genes, glycerol uptake and metbolism genes, and thiamine

biosynthesis genes. These findings indicate that *S. pneumoniae* adopted a different lifestyle within the flow cell system, including an altered metabolic profile.

Importantly, the differences in gene expression observed between *S. pneumoniae* in mono-culture in the flow cell system and in co-culture in the flow cell system, indicated differences in interspecies interactions on a molecular level (Table 5.10, Table 5.11).

Table 5.10: Up- and down-regulated *S. pneumoniae* strain 11 genes when grown in co-culture with *H. influenzae* in a flow cell at 64 h compared to *S. pneumoniae* grown in mono-culture in a flow cell at 64 h. Results are displayed for genes with a $\log_2$ fold change ≥ 2, and a p-value ≤ 0.05. Note: No genes were significantly downregulated in this comparison.

Upregulated genes Locus tag	**Gene Name**	**$\log_2$FoldChange**	**Function**
Gene class: Phage-associated			
SPNOXC_00280	-	9.86	hypothetical prophage antirepressor
SPNOXC_00530	-	8.36	hypothetical phage protein
SPNOXC_00510	-	8.21	phage protein
SPNOXC_00460	-	8.16	phage capsid protein
SPNOXC_00540	-	5.40	putative phage protein
Bacteriocin			
SPNOXC_01490	-	7.10	bacteriocin ABC transporter
SPNOXC_05010	*blpY*	4.55	putative bacteriocin transporter
DNA modification			
SPNOXC_07990	-	6.10	putative type I restriction-modification system S protein
SPNOXC_10660	*lacT2*	4.93	transcription antiterminator LacT 2
SPNOXC_17390	*rmuC*	1.97	DNA recombination protein
SPNOXC_13840	-	2.62	putative DNA replication protein
SPNOXC_10210	-	2.36	putative DNA binding protein
SPNOXC_14690	*recR*	1.82	recombination protein RecR
Gene class: Lactose metabolism			

SPNOXC_10640 SPNOXC_10630S PNOXC_10680 lacC2	*lacC2, lacG2,lacF, LacE2*	4.95-2.13	putative lactose-specific phosphotransferase system (PTS), IIBC component 2; lacF; PTS system lactose-specific transporter subunit IIA; lacG2 6-phospho-beta-galactosidase 2 .; tagatose-6-phosphate kinase 2
SPNOXC_01020	*agaS*	2.99	putative tagatose-6-phosphate aldose/ketose isomerase
Glycerol metabolism			
SPNOXC_19270	*glpF1*	3.14	glycerol uptake facilitator protein
SPNOXC_19280	*glpO*	2.14	alpha-glycerophosphate oxidase
SPNOXC_19290	*glpK*	1.81	glycerol kinase
Transport			
SPNOXC_02650	-	5.39	ABC transporter ATP binding protein; spermidine/putrescine
SPNOXC_01000	-	3.11	PTS system mannose/fructose/sorbose family transporter subunit IID
ISPNOXC_00990	-	3.31	PTS system sorbose-specific family transporter subunit IIC
SPNOXC_15150	-	2.33	putative sucrose-specific phosphotransferase system (PTS), IIABC component
SPNOXC_01210	-	3.62	extracellular solute binding protein; putative aldouronate transport system substrate-binding protein . ABC-type sugar transport system
Other metabolic genes			
SPNOXC_18920	-	4.21	putative alpha -1,2-mannosidase
SPNOXC_13870	-	2.86	putative methyltransferase
SPNOXC_14880	*nanA*	2.93	sialidase A (neuraminidase A

Table 5.11. Up- and down-regulated genes of *S. pneumoniae* strain 11 when grown in co-culture with *H. influenzae* in a flow cell system at 168 h compared to *S. pneumoniae* grown in mono-culture in a flow cell system at 168 h. Results are displayed for genes with a $\log_2$ fold change ≥ 2, and a p-value ≤ 0.05.

Upregulated Genes Locus tag	**Gene Name**	**$\log_2$FoldChange**	**Function**
Gene class: Transporters			
SPNOXC_03190	-	2.10	PTS system, cellobiose-specific IIA component
SPNOXC_14220	-	2.02	PTS transporter, IIB subunit
SPNOXC_03200	-	1.85	PTS transporter
SPNOXC_10650	*lacF*	1.80	PTS system lactose-specific transporter subunit IIA **(fold change 1.79)**
SPNOXC_03170	-	1.77	PTS system, cellobiose-specific IIB component **(fold change 1.77)**
SPNOXC_03150	-	1.91	6-phospho-beta-glucosidase **(foldchange 1.9)**
Downregulated genes Locus tag			
Gene class: Riboflavin synthesis			
SPNOXC_02050	-	-2.11	riboflavin synthase beta chain
SPNOXC_02060	*ribA*	-2.10	riboflavin biosynthesis protein
Trasnporters			
SPNOXC_16900	-	-2.45	ABC transporter ATP-binding protein/permease
SPNOXC_18380	-	-2.01	ABC transporter permease; phosphate transport system permease protein
SPNOXC_18390	-	-2.00	ABC transporter permease; phosphate transport system permease protein **(foldchange -1.97)**
SPNOXC_01130	-	-1.97	cell wall surface anchor family protein **(foldchange -1.96)**
SPNOXC_18410	-	-1.90	phosphate transport system protein **(foldchange -1.89)**
SPNOXC_17630	-	-1.86	ABC transporter ATP binding protein **(foldchange -1.86)**
SPNOXC_18400	*pstB3*	-1.86	phosphate import ATP-binding protein 3 **(foldchange -1.85)**
Other metabolic genes			
SPNOXC_04100	*fabE*	-2.06	biotin carboxyl carrier protein of acetyl-CoA carboxylase
DNA-associated			
SPNOXC_02030	-	-1.97	**Putative DNA-binding protein (fold change -1.96)**

At 64 h, genes up-regulated in the co-culture compared to the mono-culture included bacteriocin transport genes, phage proteins (in particular the anti-repressor) and some DNA modification proteins (Table 5.10). A large group of metabolic genes was also up-regulated, including genes involved in lactose and galactose metabolism, glycerol uptake

and metabolism, and other metabolic genes including the neuraminidase *nanA*, with no genes being significantly down-regulated (Table 5.10).

At 168 h, fewer genes were differentially expressed, but up-regulated genes included several sugar uptake proteins including *lacF* (Table 5.11). Therefore, in contrast to batch culture, where *S. pneumoniae* down-regulated metabolic genes, including lactose metabolism, glycerol import and metabolism and sugar transport in co-culture, in the flow cell, these genes were up-regulated in co-culture compared to flow cell mono-culture. It is possible that the reason for this up-regulation of metabolic genes in the flow cell co-culture was due to production of specific carbohydrates by culturable *H. influenzae* which could be utilised by the lactose/galactose utilisation systems or the PTS sugar transport systems. In contrast, in the batch co-culture model, where *H. influenzae* cells are non-culturable, many of these metabolic genes were down-regulated – which would be logical if there was some carbohydrate production by *H. influenzae* or metabolic sharing between the 2 species, which was dependent on environmental parameters (batch culture vs. flow cell). In fact, such a cross-feeding hypothesis of metabolic cooperation has previously been proposed for *S. mutans* growth in co-culture with *S. mitits*, where carbohydrate production by *S. mitis* was hypothesised to increase *S. mutans* sugar-specific PTS system expression in co-culture and increase its biofilm formation (Redanz et al. 2011). While the source of the diverse range of sugars related to the *S. pneumoniae* up-regulated PTS system genes in the flow cell is undefined, the source of some sugars is evident. It is known, for example, that *H. influenzae* LOS contains moieties of glucose, galactose and N-acetyl-glucosamine in various combinations (Swords et al. 2000). In addition, various glycoproteins of *H. influenzae* have been described, such as the HMW glycoproteins containing glucose, galactose and mannose residues (Grass et al. 2003). Therefore, galactose, and potentially other sugar moieties could be cleaved off the *H. influenzae* cell surface to be metabolized by *S. pneumoniae*. In addition, it has been shown for *A. actinomycetomcomitans* that it has the potential to metabolise L-lactate produced by *S. gordonii*, and thus enhance polymicrobial infection (Ramsey et al. 2011). Therefore, it is also possible that in the *H. influenzae/S. pneumoniae* co-culture *H. influenzae* generated metabolites that are being utilised by *S. pneumoniae*. These propositions would explain why some sugar-utilization genes would be up-regulated in the flow cell co-culture, where *H. influenzae* is viable and

culturable, and it would be logical to assume that these genes may be repressed in the batch co-culture situation where *H. influenzae* are in an altered non-culturable state. However, this is beyond the scope of the current study and future studies will determine whether such a metabolic cooperation occurs between *H. influenzae* and *S. pneumoniae*, and which specific sugars and pathways are involved

5.3. Concluding remarks

The results of this study showed that both synergy and antagonism are possible outcomes of the *H. influenzae/S. pneumoniae* interactions, which are largely dependent on the environmental conditions and on the systems functional in each species. Low pH and stationary phase of growth were shown to be non-permissive for *H. influenzae* culturability in co-culture, whereas environmental parameters dictated by the flow cell allowed co-existence. The transcriptomics results confirmed that *H. influenzae* experiences stress in the presence of *S. pneumoniae* in the batch culture model, but not in the growth phase independent flow cell. However, in addition to this result, a model of a more complex metabolic and nutrient-dependent relationship was uncovered in the transcriptomics analysis. Prior to this study, no global-scale metabolic relationship has been shown for *H. influenzae/S. pneumoniae* interactions. And, while further research needs to be performed to reveal the precise mechanisms of such a relationship, our study implies a new metabolism-related direction for future study of the *H. influenzae/S.pneumoniae* inter-species interactions.

It is important to note that within the host there are different selective pressures present that modify the inter-species interactions between *H. influenzae* and *S. pneumoniae*. For example, it has been shown that *in vivo*, in the nasopharynx of mice, *H. influenzae* is able to direct the host immune response against *S. pneumoniae* to induce its opsonophagocytosis (Lysenko et al. 2005; Lysenko et al. 2010; Lijek and Weiser 2012). However, this effect was shown to be strain-specific and largely dependent on the presence

of certain *S. pneumoniae* capsule types, some of which have a reduced or enhanced resistance to opsonophagocytosis (Lysenko et al. 2010).

In addition, it has been shown that *in vivo*, *H. influenzae* is able to enhance co-culture biofilm formation of *S. pneumoniae* in an otitis media model, and prevent the progression to systemic pneumococcal disease (Weimer et al. 2010). Hence, within the host there are additional factors pertaining to a mixed-species colonisation and infection which can facilitate or repress synergistic inter-species interactions. However, it is certain that *H. influenzae* and *S. pneumoniae* are highly adapted to the nasopharyngeal niche, where they are both present, and hence have the potential to synergistically interact even in the face of potential temporal or environmental-related antagonism. Our global *in vitro* study has shown that the outcome of the inter-species interactions may depend on a fine balance of competition and cooperation between the 2 species, which in turn is determined both by exogenous factors (such as environmental pH) and endogenous factors pertaining to the cells themselves (such as the presence of specific genes and the control of their expression). The outcome of the *H. influenzae/S. pneumoniae* interactions may in turn impact on their ability to form a complex multispecies biofilm, and hence, on the ability of both species to persist in the host and contribute to chronic OM.

Chapter 6

Nutrient source and growth dynamics determine the *Streptococcus pneumoniae* cell phenotype and the outcome of its interaction with *Haemophilus influenzae*.

Overview

In this chapter, we have shown that the outcome of the interactions between *H. influenzae* and *S. pneumoniae* is dependent on the growth media and carbon source used. We have shown that in a flow cell utilising chemically defined media with glucose as the carbon source, *S. pneumoniae* is unable to be cultured in mono-culture. In co-culture with *H. influenzae*, however, *S. pneumoniae* adopts three temporally and phenotypically distinct states – wild-type, undetected and SCV. We have analysed the transcriptome of *S. pneumoniae* in these altered states, and have identified the up-regulation of genes associated with a persister-like state in other bacterial species. We have also analysed the transcriptome of *H. influenzae* in mono-culture and in a continuous flow cell system containing CDM with glucose media, and in co-culture with *S. pneumoniae* in the same system. We have identified that *H. influenzae* does not alter its transcriptome in co-culture with *S. pneumoniae* in the undetected or SCV state, indicating the increased adaptation of *S. pneumoniae* in these states to a co-existence with *H. influenzae*. However, we have identified that the presence of *S. pneumoniae* appears to influence the transcriptomic adaptation of *H. influenzae* to different time-points during growth. Overall, the findings of this chapter present a novel observation of the development of phenotypically distinct *S. pneumoniae* cell types in co-culture with *H. influenzae* in a limited CDM media containing glucose, as well as their influence on the presence of *H. influenzae* and their multispecies interactions.

This chapter is presented in the required manuscript format for the *Journal of Bacteriology*.

6.1.1. Abstract

H. influenzae and *S. pneumoniae* are known aetiologic agents of chronic otitis media, which frequently manifests as a multispecies infection. While the molecular factors mediating *H. influenzae/S. pneumoniae* interactions are not well defined, we have previously used a transcriptomics approach to show that there are specific changes in the sugar uptake systems in *S. pneumoniae* when in co-culture (Chapter 5). We therefore have investigated this phenomenon further, and in this current study show that the outcome of the *H. influenzae*/*S. pneumoniae* interactions is indeed dependent on the nutrient source. In a growth-phase independent, continuous flow cell system containing chemically defined glucose media, *S. pneumoniae* became undetectable in mono-culture, but uniquely existed in 3 temporally and physiologically distinct states in co-culture: wild-type cells that remained present until 24 h, a dormant or "undetected" state until 336 h, and then its re-emergence as small colony variants (SCVs) from 336 h. Transcriptomic analysis of *S. pneumoniae* in these states determined that upon transition to an undetected state, *S. pneumoniae* reduced the expression of DNA replication associated genes, and up-regulated several genes associated with a bacterial persister lifestyle including a *relE* toxin/antitoxin system and a *gntR* regulator. Transcriptional changes which occurred upon transition from the wild-type state, to SCV also included up-regulation of genes associated with a persister state: including stress response genes, 2 antitoxins, and 3 transcriptional regulators: *padR*, *gntR* and *deoR*.

Transcriptomics analysis of *H. influenzae* revealed that there was no difference in the *H. influenzae* gene expression in the presence of the undetected or SCV *S. pneumoniae*, suggesting an enhanced adaptation of *H. influenzae* to *S. pneumoniae* in these states. However, *S. pneumoniae* caused subtle transcriptomics changes upon *H. influenzae* transition between time-points, suggesting *S. pneumoniae* alters *H. influenzae* adaptation between time-points.

To our knowledge, this is the first study documenting the effect of carbon source on *H. influenzae/S. pneumoniae* inter-species interactions, as well as the effect of distinct *S. pneumoniae* cell type development on these inter-species interactions.

6.1.2. Importance

Chronic otitis media (COM) is often caused by a multispecies infection. While the most common causative agents are the bacterial species *H. influenzae* and *S. pneumoniae*, little is known about their molecular interactions in disease. This is the first study documenting the development by *S. pneumoniae* of an undetected persister-like and SCV cell type in co-culture. The adoption of these lifestyles by *S. pneumoniae* was dependent on the presence of *H. influenzae* and the nutrient source used. Transcriptomics analysis has uncovered some molecular events associated with these *S. pneumoniae* lifestyles, and their effect on *H. influenzae*. Knowledge of the alternative lifestyles of *S. pneumoniae* and their relation to *H. influenzae*, enhances our understanding of COM, and may point towards regulatory pathways which can be targeted for therapeutic approaches.

6.1.3. Introduction

H. influenzae and *S. pneumoniae* are opportunistic human pathogens. Naturally, both species are found to reside in the human nasopharynx, however, they are known to transit to other anatomical sites, such as the middle ear, and cause the paediatric disease otitis media (OM) (Hall-Stoodley et al. 2006). OM can manifest as an acute, chronic or recurrent disease (Williams et al. 1993). Chronic and recurrent forms of OM (COM) are not easily cleared by the immune response, and are often recalcitrant to current therapies, including antibiotics and tympanostomy tube placement (Williams et al. 1993; Ojano-Dirain and Antonelli 2012). Recently, it has been shown that *H. influenzae* and *S. pneumoniae* form a multi-species biofilm on the middle ear, and it is this biofilm which is responsible for the chronic and recurrent forms of OM (Hall-Stoodley et al. 2006). However, while the interspecies interactions between *H. influenzae* and *S. pneumoniae* in disease are an ongoing topic of study, the specific molecular interactions between *H. influenzae* and *S. pneumoniae*, and how these contribute to disease, are currently not well defined.

In a previous published study, we investigated the interactions between *H. influenzae* and *S. pneumoniae*, in order to enhance the understanding of the inter-species events which lead to a multispecies biofilm formation (Tikhomirova et al. 2015). Previously, we have shown that there are vast transcriptomics changes in genes related to metabolism in *S. pneumoniae* in the presence of *H. influenzae* (Tikhomirova et al. 2015). These changes were dependent on the growth conditions used (the specific dynamics occurring during the growth phase dependent, closed, batch culture system versus the long term, continuous and growth phase independent flow cell growth system). Importantly, in the flow cell co-culture, *S. pneumoniae* up-regulated genes involved in lactose and galactose metabolism, as well as genes involved in sugar uptake. We proposed, that such changes indicated potential metabolic sharing between the two species, and indicated an altered metabolic lifestyle for *S. pneumoniae* in co-culture (Tikhomirova et al. 2015). However, these previous experiments were performed in a nutrient-rich HI media, therefore a more defined a nutrient limited environment was required for a deeper investigation of these findings.

To further investigate the nature of this metabolic relationship, we performed batch culture and flow cell growth experiments of *H. influenzae* and *S. pneumoniae* mono and co-cultures, using a **c**hemically **d**efined **m**edia (CDM), with a known carbon source. For these experiments, we used 2 alternative carbon sources: glucose and lactose.

Our results have shown, that specifically in a flow cell system containing CDM with either glucose or lactose as the carbon source, *S. pneumoniae* was non-detectable in mono-culture. However, the situation in co-culture was different. When lactose was used as the carbon source, *S. pneumoniae* was initially undetected in co-culture with *H. influenzae*, however, was eventually detected in co-culture after 228 h.

In co-culture with *H. influenzae*, when glucose was the carbon source utilised, *S. pneumoniae* recovered its ability to grow, but displayed several alternative growth phenotypes. *S. pneumoniae* was detectable in co-culture at 24 h displaying a wild-type phenotype, after which it entered a period of non-detection until 336 h, identified as an "undetected" state. At 336 h, *S. pneumoniae* re-emerged but with an altered **S**mall **C**olony **V**ariant (SCV) phenotype. The cells were stable in this form. We further investigated the SCV phenotype of *S. pneumoniae* by performing RNASeq of this co-culture at time-points representing all 3 phenotypes of *S. pneumoniae*. The analysis

uncovered a reduction in cell division of *S. pneumoniae* in the undetected state, and the up-regulation of genes associated with a persister cell lifestyle in both the undetected and SCV states. In addition, the transcriptomes of *H. influenzae* mono- and co-cultures were analysed at these time-points. The results uncovered that *H. influenzae* only displayed a differential gene expression between mono- and co-culture at 24 h; at 64 h and 336 h no genes were differentially expressed with any significance in *H. influenzae* between mono- and co-culture, a drastically different result to the gene expression observed in HI media (Tikhomirova et al. 2015). This indicated, that *H. influenzae* was unaffected by the presence of the undetected and SCV *S. pneumoniae*, indicating that these cell types were more optimally adapted to a co-culture environment. However, *S. pneumoniae* appeared to subtly affect the *H. influenzae* transcriptome upon transition to different time-points of growth, as well as upon the transition from HI media to CDM media growth conditions, inducing a more anaerobic growth in both cases.

To our knowledge this has been the first report documenting the effects of carbon source on *S. pneumoniae* colony-type, and the first report of the interactions of persister-like "undetected" and SCV *S. pneumoniae* colony-types with *H. influenzae* in a continuous growth flow cell environment.

6.2. Results

6.2.1. *S. pneumoniae* is unable to survive when grown in continuous culture in CDM with glucose in mono-culture, but develops distinct temporal and phenotypic states when in co-culture with *H. influenzae*.

Previously, our research has shown that the outcome of the interactions between *H. influenzae* and *S. pneumoniae* was dependent on the growth system used, with synergistic interactions occurring in a flow cell (where relative growth achieved by mono-cultures was equal to that of co-cultures), and competitive interactions in a batch culture model (whereby *S. pneumoniae* out-competed *H. influenzae*) (Tikhomirova et al. 2015). The outcome of the interactions was also associated with transcriptomic changes occurring in *S. pneumoniae*, with synergistic interactions between the two species correlating to an up-regulation of sugar transport and utilisation genes in *S. pneumoniae*. In order to further investigate the role of carbon sources in the interactions between *H. influenzae* and *S. pneumoniae*, a flow cell system was established, utilising a chemically defined (CDM) media with either glucose or lactose as the major carbon source.

The results obtained from growth in a flow cell in CDM media with glucose used as the carbon source, were vastly different to those previously obtained using HI media. For *H. influenzae*, the growth levels reached in mono-culture and in co-culture were not significantly different (Fig. 6.1). *S. pneumoniae*, however, was unable to grow in mono-culture in any of the time-points (whereas it did grow with this media in batch culture growth conditions). In co-culture, the growth of *S. pneumoniae* was dramatically different to what was observed previously with HI media – *S. pneumoniae* was able to grow at 24 h, however, after this time, point, no colony

forming units of *S. pneumoniae* were detected in co-culture until 336 h. At 336 h, 10^5 CFU/ml of *S. pneumoniae* were detected in co-culture, however, all of these colonies were small (<1mm in diameter, compared to the >3mm diameter wild-type strain 11) (Fig. 6.1; Fig. 6.2). These cells were designated (and referred to throughout this work, as small colony variants – SCVs). These SCVs were subsequently subcultured 5 times, both on HI blood agar containing gentamycin, and in broth, with no reversion to their non-SCV, wild type cell phenotype. This confirmed the stability of the SCVs in their phenotype of reduced size and non-mucoid appearance, compared to the wild-type.

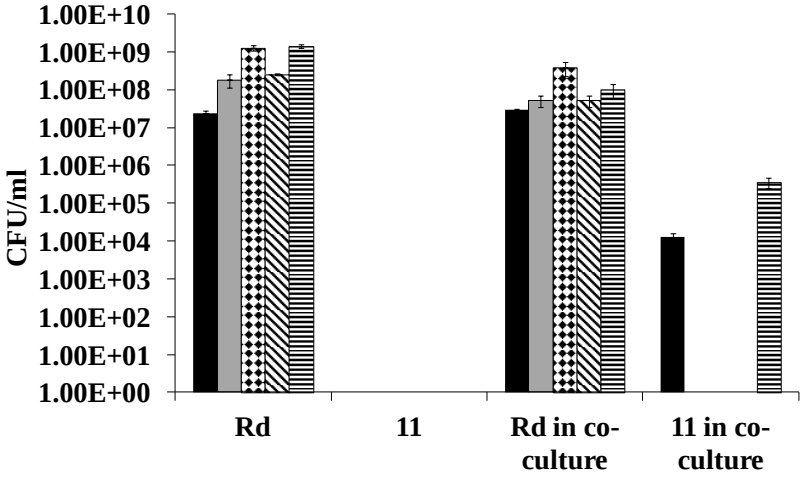

Fig. 6.1. *S. pneumoniae* strain 11 adopts 3 distinct growth phenotypes in co-culture in a flow cell containing CDM + glucose media and does not affect *H. influenzae* culturability. Planktonic growth of *H. influenzae* Rd KW20 and *S. pneumoniae* strain 11 in CDM media containing glucose, in a flow cell system is shown at 24 h (black bars), 48 h (grey bars), 64 h (checked bars), 168 h (hatched bars), and 336 h (horizontally-striped bars). *H. influenzae* was culturable in the presence of *S. pneumoniae* at all time-points. However, *S. pneumoniae* was non-culturable in mono-culture, and in co-culture it was initially culturable at 24 h, and, after a period where it was not detected, at 336 h.

A	B
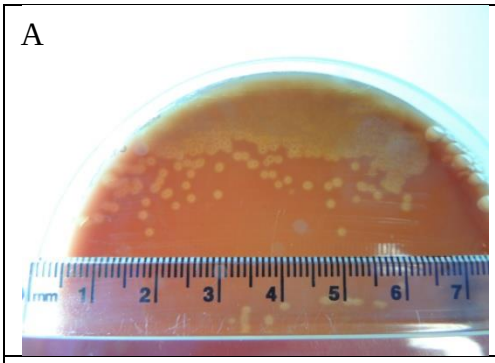	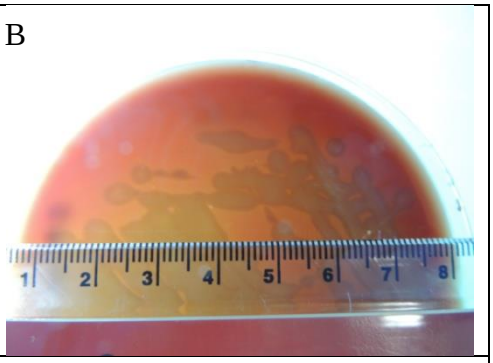
SCV strain 11 variant	Wild-type strain 11 variant

Fig. 6.2. SCV variants of *S. pneumoniae* strain 11 have a reduced size compared to wild-type *S. pneumoniae* strain 11 cells. Panel A shows SCVs of *S. pneumoniae* strain 11 obtained after growth in co-culture with *H. influenzae* in a flow cell containing CDM+glucose media. The SCVs have a diameter <1mm. Panel B shows wild-type *S. pneumoniae* strain 11 colonies with a diameter of approximately 3 mm.

The SEM results showed that the predominant cell type in the CDM+glucose flow cell co-culture was *H. influenzae*. However, phenotypically distinct *S. pneumoniae* cells appeared in the flow cell at 168 h and 336 h. Importantly, *S. pneumoniae* cells were observed in the co-culture at 168 h in SEM, even though at this time-point, *S. pneumoniae* was non-culturable (Fig. 6.3). This result suggested, that at 168 h, between an initial detection of wild-type *S. pneumoniae*, and a later detection of SCV cells, *S. pneumoniae* was present in the flow cell, but was likely in an undetectable, metabolically dormant state.

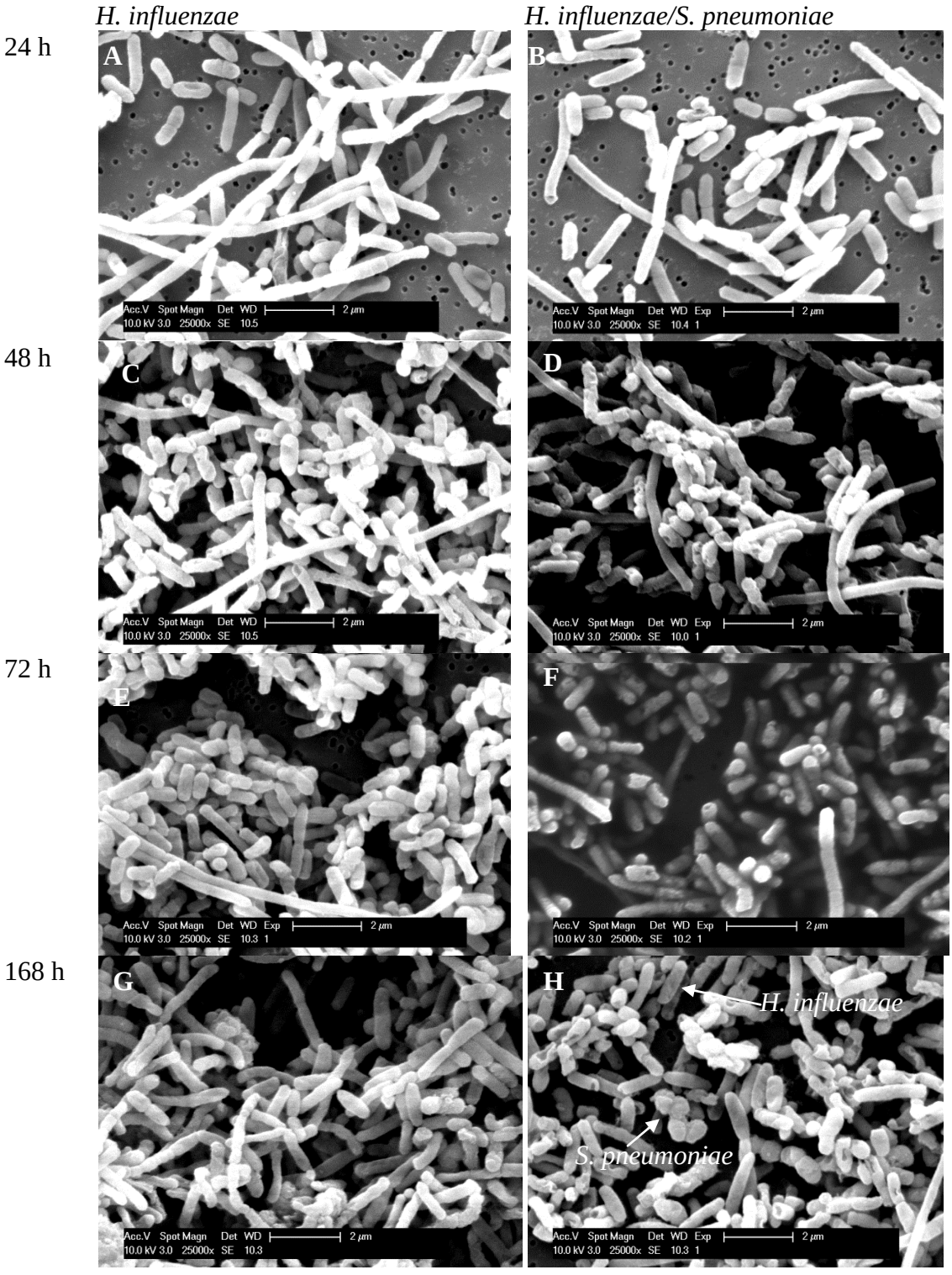
H. influenzae
H. influenzae/S. pneumoniae
24 h
48 h
72 h
168 h
A
B
C
D
E
F
G
H
H. influenzae
S. pneumoniae

336 h

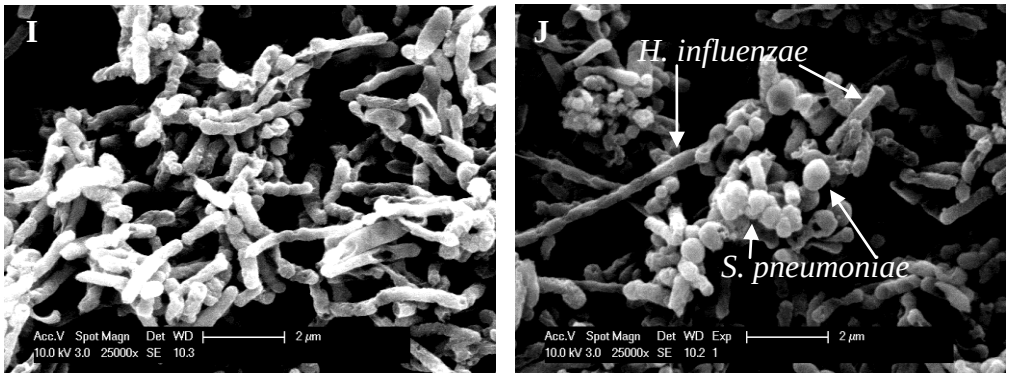

Fig 6.3. Field Emission Scanning Microscopy (SEM) of *H. influenzae* Rd KW20 mono-culture (left column) and *H. influenzae* RdKW20 and *S. pneumoniae* strain 11 co-culture (right column) grown in the flow cell system containing CDM+glucose at 24 h (A, B), 48 h (C, D), 64 h (E, F), 168 h (G, H), and 336 h (I, J). All images are shown with a magnification of 25000x. No cell-surface adhesions or EPS matrix was seen in either *H. influenzae* mono-culture or *H. influenzae/S. pneumoniae* co-culture at any time-points. In co-culture, the predominant cell-type was *H. influenzae*, however at 168 h and 336 h evident *S. pneumoniae* cells were present.

Importantly, no adhesive structures or EPS matrix were present in either the mono-culture or co-culture, suggesting that this phenomenon which we previously observed in the flow cell containing HI media, is dependent on the media and consequently on the nutrient sources (Chapter 5). We had previously reported that *H. influenzae* developed filaments when grown in a flow cell (Tikhomirova et al. 2015). Filamentous *H. influenzae* were again seen in this study and at all time-points in co-culture with these growth conditions, indicating that this phenomenon does not depend on nutrient source (Fig. 6.4).

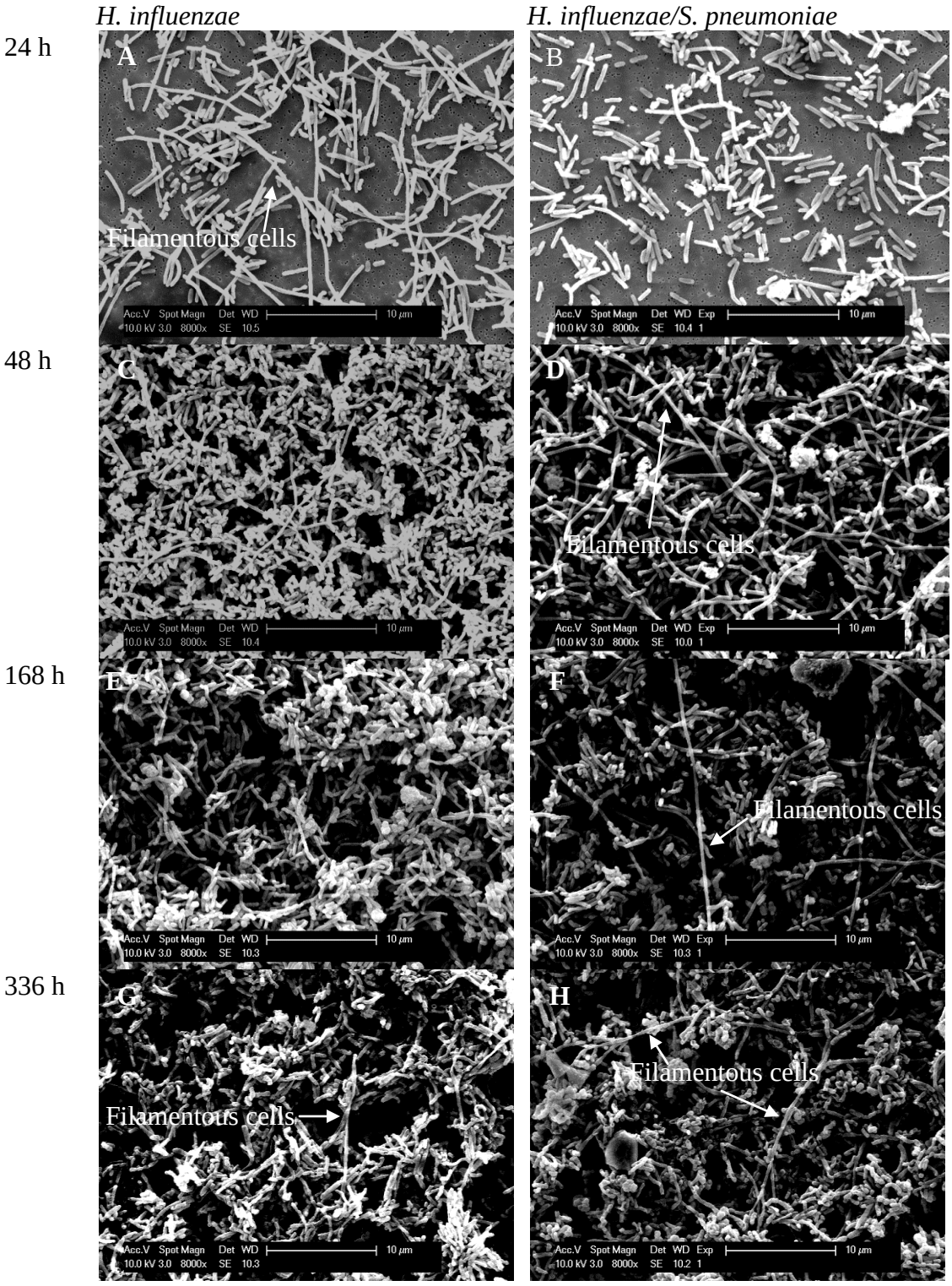

Fig 6.4 Field Emission Scanning Microscopy (SEM) of *H. influenzae* Rd KW20 mono-culture (left column) and *H. influenzae* RdKW20 and *S. pneumoniae* strain 11 co-culture

(right column) grown in the flow cell system containing CDM+glucose at 24 h (A, B), 48 h (C, D), 168 h (E, F), and 336 h (G, H). All images are shown with a magnification of 8000x to display longer filamentous cell formation of *H. influenzae*. Filamentous cells were formed in mono-culture and co-culture at all time-points apart from 24 h in co-culture, and are displayed for 24 h, 48 h, 168 h, and 336 h.

6.2.2. *S. pneumoniae* is unable to survive when grown in continuous culture in CDM with lactose in mono-culture but after 288 h forms phenotypically distinct variants in co-culture.

The results obtained for the growth of *H. influenzae* Rd KW20 and *S. pneumoniae* in the flow cell with lactose as the carbon source showed that *H. influenzae* CFU/ml was equal for growth in mono-culture, and in co-culture at all time-points up to 336 h (Fig. 6.5).

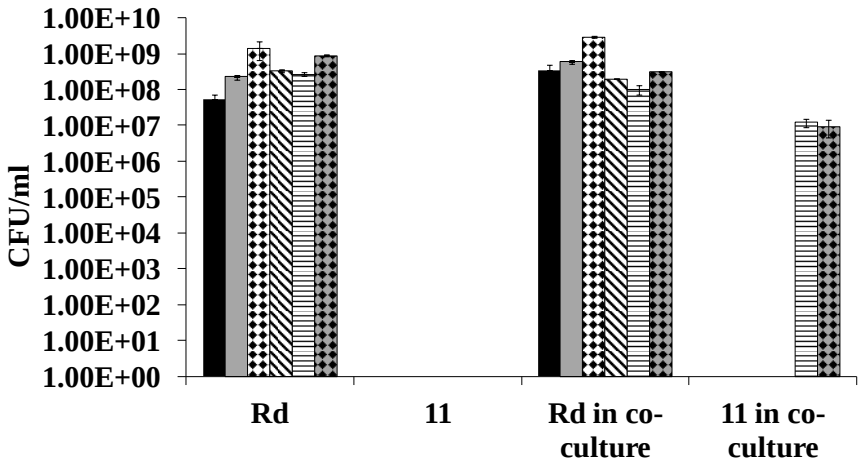

Fig. 6.5. *S. pneumoniae* adopts 2 distinct phenotypes in co-culture in a flow cell containing CDM+lactose media, and does not affect *H. influenzae* culturability. Planktonic growth of *H. influenzae* Rd KW20 and *S. pneumoniae* strain 11 in CDM media containing lactose, in a flow cell system is shown at 24 h (black bars), 48 h (grey bars), 64 h (checked bars), 168 h (hatched bars), 288 h (horizontally-striped bars), and 336 h (grey checked bars). *H. influenzae* was culturable in the presence of *S. pneumoniae* at all time-points. *S. pneumoniae* was non-culturable in mono-culture, and was not detected in co-culture until the 228 h time-point.

Importantly, *S. pneumoniae* strain 11 was unable to grow in mono-culture at any of the time points. In co-culture, *S. pneumoniae* did not produce detectable colony forming units until 288 h and 336 h. The *S. pneumoniae* cells detected at these time-points were also phenotypically distinct – these cells were able to grow on HI agar, but unable to grow on blood agar, or blood agar containing gentamycin (Fig. 6.5). While the ability to grow on blood agar and demonstrate resistance to gentamycin has previously been used to differentiate for *S. pneumoniae* in the co-culture, we regarded this phenomenon as a phenotypically distinct *S. pneumoniae* type, rather than an interfering species. Due to previous observations of *S. pneumoniae* acquiring altered phenotypes, such as the SCVs, we suggest that the flow cell environment, particularly with a limited nutrient source, such as CDM serves as a stress and stimulates the development and expression of adaptation mechanisms in *S. pneumoniae*, which subsequently may manifest as phenotypically distinct *S. pneumoniae* cells with altered traits. Nevertheless, these altered *S. pneumoniae* cells would require further study for a full characterisation. 16S DNA sequencing would provide a means for such a characterisation.

In CDM with lactose as the carbon source, the phenotype of both cell types when viewed with SEM was similar to that observed in CDM with glucose. However, the SEM results showed obviously distinguishable *S. pneumoniae* cells to appear only after 168 h (Fig. 6.6) – a phenomenon which may simply be explained by their adaptation period and subsequent slow growth at early time-points resulting in low cell numbers in co-culture compared to the dominating *H. influenzae*. It is also interesting, that surface adhesions and extracellular EPS matrix were observed in the co-culture grown in lactose media, but not in the *H. influenzae* mono-culture, indicating a role of *S. pneumoniae* – even at time-points where its growth was not detected – in the production of this extracellular material (Fig. 6.6).

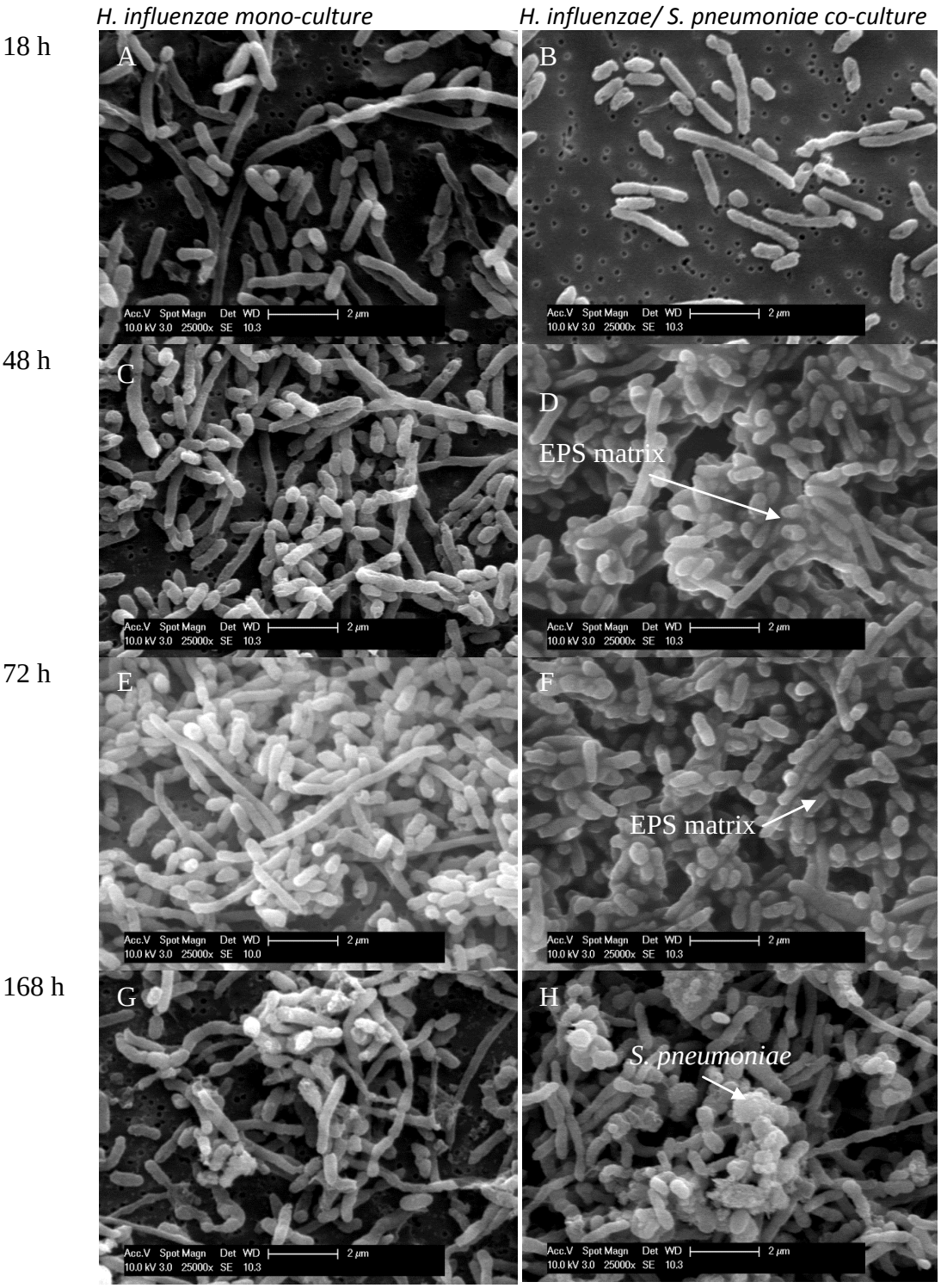
H. influenzae mono-culture
H. influenzae/ S. pneumoniae co-culture
18 h
48 h
72 h
168 h
A
B
C
D
EPS matrix
E
F
EPS matrix
G
H
S. pneumoniae
Acc.V Spot Magn Det WD 2 µm
10.0 kV 3.0 25000x SE 10.3

336 h

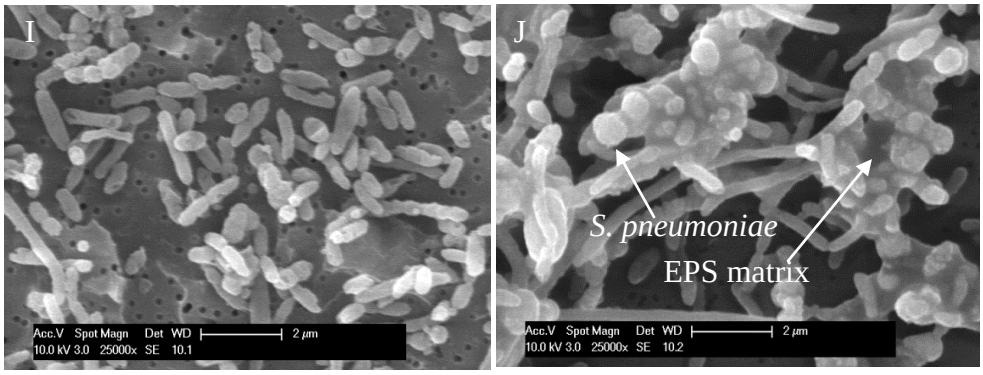

Fig. 6.6. Field Emission Scanning microscopy (SEM) imaging of *H. influenzae* Rd KW20 mono-culture (left column) and *H. influenzae* RdKW20 and *S. pneumoniae* strain 11 co-culture (right column) grown in the flow cell system containing CDM+lactose at 24 h (A, B), 48 h (C, D), 64 h (E, F), 168 h (G, H), and 336 h (I, J). All images are shown with a magnification of 25000x. Adhesins and fibrous extracellular polymeric substance matrix were observed in the co-culture at all time-points except 24 h, however no matrix was present in the *H. influenzae* mono-culture at any time-point. In the co-culture, no obvious coccus-shaped *S. pneumoniae* are observed until 168 h, although this may be due to these cells being less numerous than *H. influenzae*, and therefore being difficult to distinguish.

Interestingly, we had seen previously that the *H. influenzae* mono-culture grown in HI media produced an EPS matrix, however, the *H. influenzae* cells now grown in mono-culture with lactose media were smooth with no surface or extracellular components. Filamentous *H. influenzae* were also observed at all time-points in mono-culture, and in co-culture indicating that this phenotype was unrelated to the carbon source present (Fig. 6.7).

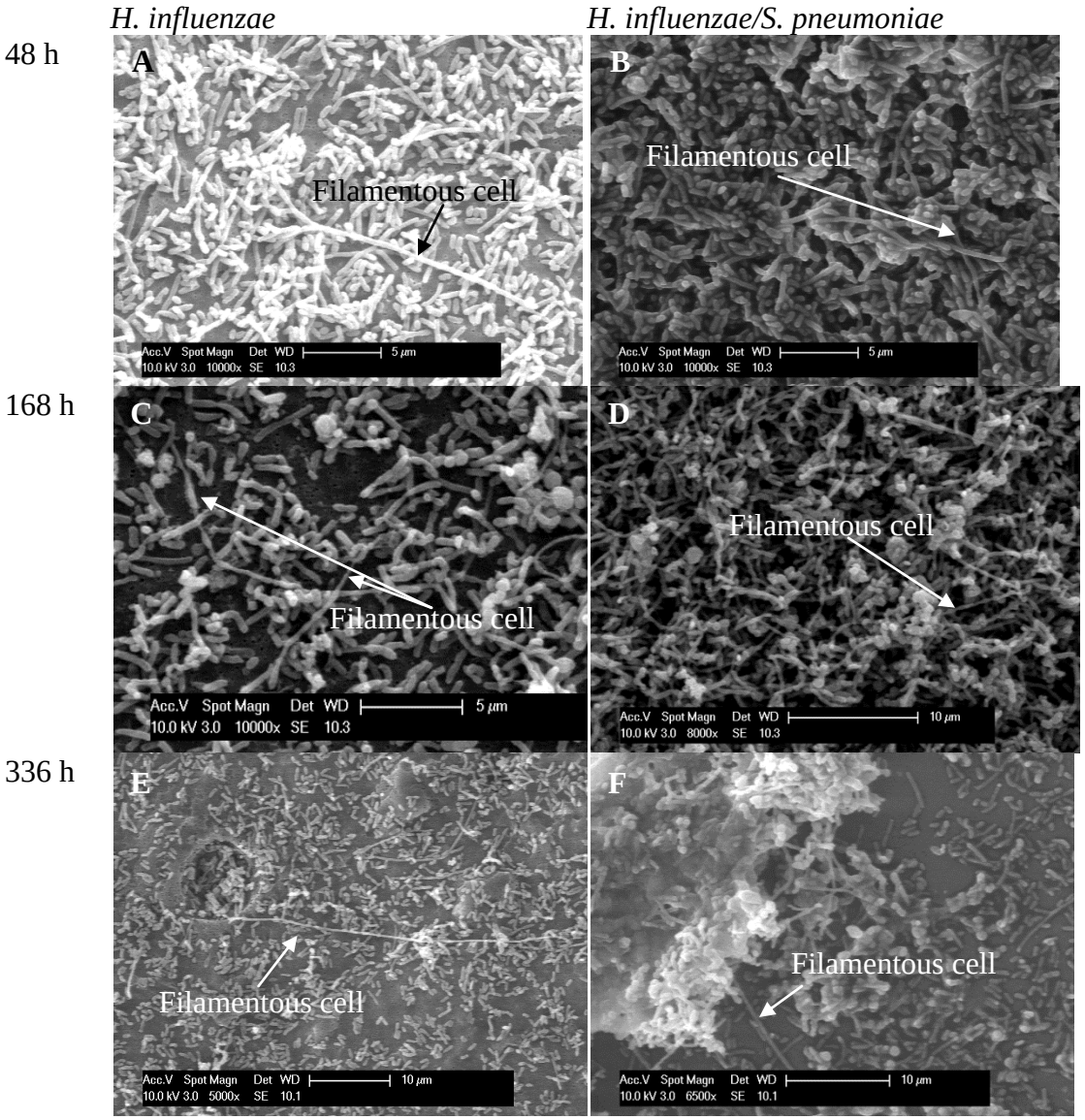

Fig. 6.7 Field Emission Scanning Microscopy (SEM) imaging of *H. influenzae* Rd KW20 mono-culture and *H. influenzae/S.pneumoniae* co-culture grown in the flow cell system containing CDM+lactose at 48 h (A,B), 168 h (C, D), and 336 h (E, F). Images A-C are shown at a magnification of 10000x, and images D, E and F are shown at 8000x, 5000x and 6500x respectively, to display optimal views of filamentous *H. influenzae* cells being formed in these conditions in mono- and co-culture.

6.2.3. *S. pneumoniae* SCVs have an improved ability to survive in a flow cell with glucose in co-culture with *H. influenzae*, and are able to grow in mono-culture.

When *H. influenzae* Rd KW20 and *S. pneumoniae* strain 11 were grown in a flow cell system with glucose as the carbon source, culturable *S. pneumoniae* cells appeared only in co-culture at 24 h, and then, after a period of non-detection, only in co-culture, and only after 336 h. (In contrast, *S. pneumoniae* was not detected in mono-culture at any time-points). These *S. pneumoniae* cells detected in co-culture at 336 h, were phenotypically distinct, with a small (<1mm) and non-mucoid morphology. This result suggested that between 24 h and 336 h, *S. pneumoniae* was present, but in a non-culturable state, and not actively dividing. Such metabolically dormant, un-dividing cells, have previously been described for other bacterial species, and are generally referred to as "persister" cells. Persister cells have been observed to form at the highest frequency during periods of nutrient limitation in stationary phase and represent an evolutionary adaptation to survival in the presence of unfavourable conditions (Lewis 2007; Lennon and Jones 2011). Hence, the period between 24 h and 336 h involved the adaptation of *S. pneumoniae* to the nutrient limited conditions in the flow cell (CDM+glucose) in co-culture, and the establishment of a more adapted cell type for growth in these parameters.

We hypothesised, that these *S. pneumoniae* SCVs were optimally adapted for growth in co-culture in the glucose-rich environment and the growth phase independent, flow cell system. To test whether the *S. pneumoniae* SCV cells were more adapted for growth in the flow cell co-culture, or even the mono-culture, a new flow cell experiment was established where *H. influenzae* Rd KW20 and *S. pneumoniae* SCV cells were inoculated into mono- and co-culture flow cells containing CDM media with glucose as the carbon source.

Importantly, the results showed that the *S. pneumoniae* SCVs were able to grow in co-culture with *H. influenzae* at all time-points, when glucose was used as the carbon source (Fig. 6.8). In

mono-culture, there was no growth of the SCVs (Fig. 6.8), until the 336 h time-point (Fig. 6.9), where it was maintained until 408 h (Fig. 6.9). *H. influenzae* also demonstrated equal culturability in mono-culture and co-culture (Fig. 6.8).

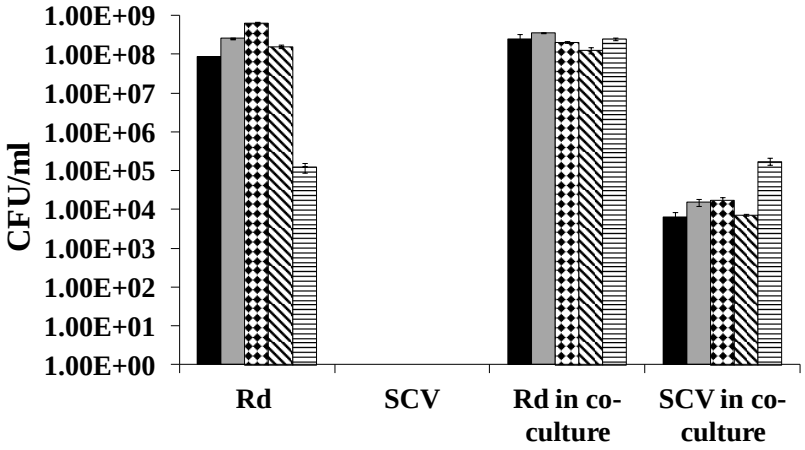

Fig. 6.8. *S. pneumoniae* SCVs are culturable in co-culture in CDM+glucose media and do not affect *H. influenzae* culturability. The planktonic growth of *H. influenzae* Rd KW20 and *S. pneumoniae* strain 11 small colony variants (SCV) in CDM media containing glucose, in a flow cell system is shown at 24 h (black bars), 48 h (grey bars), 64 h (checked bars), 168 h (hatched bars), and 312 h (horizontally striped bars). *S. pneumoniae* SCVs were not detected in mono-culture by 312 h, but were consistently observed at all time-points in co-culture, where they did not affect *H. influenzae* culturability.

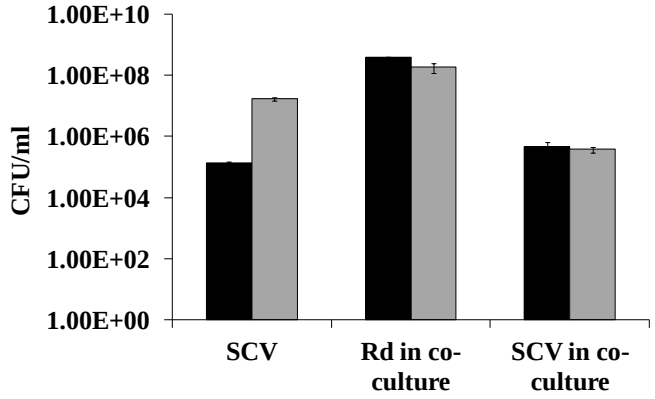

Fig. 6.9. At 336 h *S. pneumoniae* SCVs become culturable in mono-culture in a flow cell containing CDM+glucose media, and remain culturable in co-culture. Planktonic growth of *S. pneumoniae* strain 11 SCV is shown in mono-culture and co-culture , and *H. influenzae* Rd KW20 in co-culture in CDM media containing glucose, in a flow cell system at 336 h (black bars) and 408 h (grey bars).

To identify any phenotypic differences occurring in the *H. influenzae* or *S. pneumoniae* cells which could account for *S. pneumoniae* growth as a SCV with *H. influenzae* in co-culture, the co-culture of these strains was collected at 64 h, after growth with glucose and viewed with SEM. At this time-point, both *H. influenzae* and *S. pneumoniae* cells were observed, although *H. influenzae* was dominant (as expected given the large difference in CFU/ml in the co-culture). The identified *S. pneumoniae* cells did not appear phenotypically different from those previously observed in batch or flow cell experiments (Fig. 6.3). The SCVs did not express any evident adhesins and cell size appeared the same as wild type cells, although an extracellular substance matrix was observed around the SCVs and *H. influenzae* cells (Fig. 6.10). The *H. influenzae* cells in this situation also did not appear different from those observed previously such that both normal and filamentous cells were observed (Fig. 6.10).

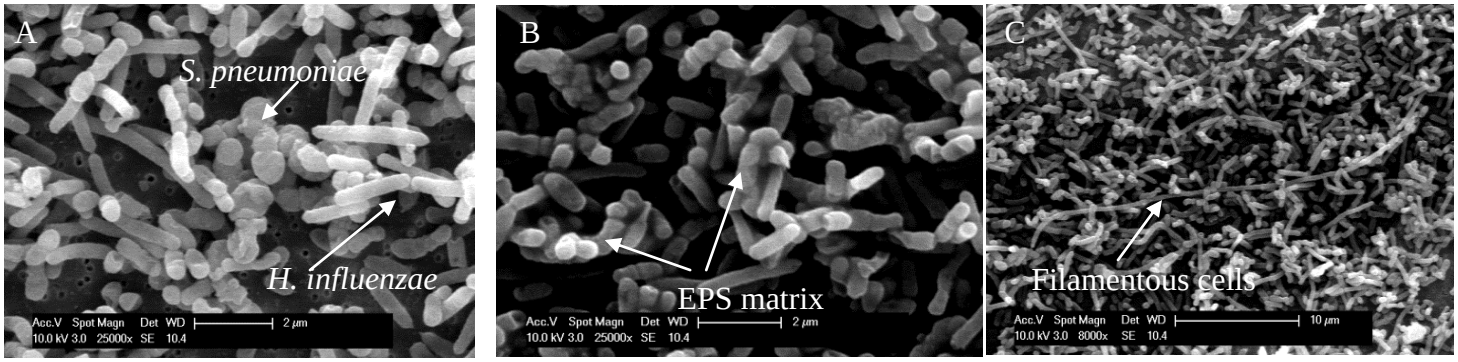

Fig. 6.10. Field Emission Scanning Microscopy (SEM) imaging of *H. influenzae* Rd KW20 and *S. pneumoniae* SCV co-culture grown in a flow cell system containing CDM+glucose media for 64 h. Images A and B show the cells with a 25000x magnification, and Image C shows a magnification of 8000x. Image A displays the phenotypically normal and easily distinguishable *S. pneumoniae* cocci and *H. influenzae* rods. Image B shows a plane of view with some obvious EPS matrix formation. Image C shows the presence of filamentous *H. influenzae* cells exceeding 10μm in length in the co-culture containing *H. influenzae* and *S. pneumoniae*.

6.2.4. In a CDM with glucose environment, *H. influenzae* alters its transcriptome in the presence of wild-type *S. pneumoniae*, but does not undergo transcriptional changes in the presence of persister and SCV *S. pneumoniae*.

To identify the whole cell transcriptional changes in both *H. influenzae* and *S. pneumoniae* when grown in the CDM+glucose flow cell, mono-cultures of *H. influenzae* and co-cultures of *H. influenzae* and *S. pneumoniae* were collected at 24 h (where *S. pneumoniae* was culturable), 64 h (where *S. pneumoniae* was undetected), and 336 h (where *S. pneumoniae* was detected in a SCV state). These samples were subsequently used to obtain mRNA and perform mRNASeq. In order to characterise the inter-species interactions occurring in this limited nutrient environment, the *H. influenzae* transcriptome was compared between the mono-culture and co-culture at 24 h, 64 h and 336 h. At 24 h, in co-culture there was an up-regulation of genes involved in defence against H_2O_2 (an alkyhydroperoxidase, catalase and peroxiredoxin), a starvation inducible DNA-binding protein and a methionine sulfoxide reductase, whereas several metabolic genes involved in amino acid biosynthesis were down-regulated, as were 2 genes related to the Mu-like phage (Table 6.1).

Table 6.1. Up- and down-regulated genes at 24 h in *H. influenzae* Rd KW20 in co-culture with *S. pneumoniae* strain 11 in a CDM flow cell with glucose compared to *H. influenzae* Rd KW20 inmono-culture, in CDM media flow cell with glucose. Results are displayed for genes with a $\log_2$ fold change ≥ 2, and a p-value ≤ 0.05.

Gene ID	Gene name	$\log_2$FoldChange	Function
Upregulated genes			
HI1053	-	2.828028	Uncharacterized conserved protein YurZ, alkylhydroperoxidase/carboxymuconolactone decarboxylase
HI1349	-	2.581637	starvation inducible DNA binding protein
HI1455	*msrA*	2.224579	bifunctional methionine sulfoxide reductase subunits A/B
HI0572	-	2.091043	peroxiredoxin hybrid Prx5
HI0928	*hktE*	1.705473	catalase
Downregulated genes			
HI0682	*ilvC*	-2.50805	ketol-acid reductoisomerase
HI1478	-	-2.37447	transposase
HI1481	*muB*	-2.3062	Mu phage associated DNA transposition protein
HI1482	-	-2.27954	hypothetical protein
HI1387	*trpE*	-1.90479	anthranilate synthase component I
HI0189	*gdhA*	-1.82087	glutamate dehydrogenase

At both 64 h and 336 h time-points, there were no differences in the *H. influenzae* transcriptome in mono-culture compared to co-culture.

6.2.5. The presence of *S. pneumoniae* causes subtle time-dependent transcriptomic events to occur in *H. influenzae* in a flow cell, in a CDM with glucose environment.

As transcriptomics differences in *H. influenzae* were not observed after comparing the mono-culture and co-culture transcriptome at individual time-points after 24 h, an analysis was performed to uncover any subtle differences occurring in *H. influenzae* between time-points. For this analysis, *H. influenzae* gene expression was compared in mono-culture, between 24 h and 64 h; and between 24h and 336 h. The same transcriptomics comparison was performed for *H. influenzae* in co-culture.

When *H. influenzae* gene expression in mono-culture at 24 h was compared to gene expression at 64 h (Table 6.2), there was an up-regulation of genes involved in iron transport, thiamine metabolism, 6 stress response genes, 4 transporter genes, and 5 metabolic genes including a cytochrome c biogenesis gene. Down-regulated genes included fatty acid biosynthesis genes, dimethylsulfoxide reductase, nitrite reductase genes related to anaerobic respiration and 2 amino acid biosynthesis genes.

Table 6.2. Up- and down-regulated genes in *H. influenzae* Rd KW20 in mono-culture in a CDM with glucose flow cell at 64 h compared to *H. influenzae* Rd KW20 in mono-culture in a CDM with glucose flow cell at 24 h. Results are displayed for genes with a $\log_2$ fold change ≥ 2, and a p-value ≤ 0.05.

Upregulated genes ID	**Gene name**	**$\log_2$FoldChange**	**Function**
Gene class: Iron-utilization			
HI-0262 - HI0264	*hxuA-hxuC*	3.413386- 4.3	heme-hemopexin utilization protein A, B, C
HI0359 - HI0362	*yfeA-yfeD*	3.906002 – 3.14	iron-chelated ABC transporter substrate-binding protein
HI0097	*hitA*	2.771525	iron-utilization periplasmic protein hFbpA
HI1217	-	2.773813	transferrin-binding protein
HI0131	*afuA*	2.488142	ferric ABC transporter protein
HI0712	-	1.958744	hemoglobin-binding protein
Gene class: Thiamine metabolism			
HI0415 – HI0147	-	2.88 - 3.100459	thiamine metabolism hydroxyethylthiazole kinase; thiamine metabolism phosphomethylpyrimidine kinase; thiamine metabolism thiamine phosphate pyrophosphorylase
HI1020	*thiP*	2.294945	thiamine transporter membrane protein thiamin ABC transporter substrate-binding protein; K02064 thiamine
HI1019	*tbpA*	3.469335	transport system substrate-binding protein
HI0357	-	3.817527	thiamine biosynthesis protein
HI0354	-	3.22884	putative hydroxymethylpyrimidine transport system ATP-binding protein
HI0355	-	3.392467	putative hydroxymethylpyrimidine transport system permease protein
Gene class: Stress Response			
HI0520	-	2.14028	putative oxidoreductase
HI1455	*msrA*	3.001927	bifunctional methionine sulfoxide reductase subunits A/B
HI1434.1	*cspD*	2.144383	cold shock-like protein
HI1349	-	2.22087	starvation-inducible DNA-binding protein
HI1602	-	2.643232	putative oxidoreductase
HI1053	-	2.853343	YurZ; Uncharacterized conserved protein YurZ, alkylhydroperoxidase/carboxymuconolactone decarboxylase family [General function prediction only]
Gene class: Regulation			

	mclA		sigma-E factor negative regulatory
HI0629		2.251627	protein RseA
	-		thiaminase (transcriptional activator
HI0358		2.367385	TenA
HI0628	*rpoE*	2.060456	RNA polymerase sigma factor RpoE
Cellular transport			
HI0502	*rbsA*	2.062835	D-ribose transporter ATP binding protein
HI0289	*sdaC*	2.774754	serine transporter
	znuA		High-affinity zinc uptake system protein
HI0119		2.154024	ZnuA
HI0418	-	2.741266	hypothetical metabolite transporter
Gene class: Other metabolic genes			
HI1649	*dld*	2.05883	D-lactate dehydrogenase
HI0288	*sdaA*	1.970889	L-serine deaminase
	-		uncharacterised protein; pyruvate
HI0521		2.009933	formate lyase or glycine radical cofactor
HI1454	-	2.624743	cytochrome c-type biogenesis protein
HI0095	-	2.411088	hypothetical methyltransferase
Gene class: Hypothetical and uncharacterised proteins			
HI1205	-	2.07175	hypothetical protein
HI1246	-	2.266225	hypothetical protein
HI1427	-	2.605547	hypothetical protein
HI1601	-	2.802975	hypothetical protein
Downregulated Genes			
Gene class: Fatty acid biosynthesis			
			fatty acid biosynthesis 3-
HI1325	*fabA*	-2.85094	hydroxydecanoyl-ACP dehydratase
HI0002	-		fatty acid biosynthesis long chain fatty
		-2.7569	acid CoA ligase
Gene class: Sulfur metabolism			
HI1045 - HI1047	*dmsA-*		anaerobic dimethyl sulfoxide reductase
	dmsC	-2.64092 - -2.9	subunit A, B, C
Anaerobic Respiration (Nitrite reductase)			
HI0643	*bisC*		
		-2.16028	biotin sulfoxide reductase
			nitrite reductase, cytochrome C type
	nrfA-		protein, nitrite reductase Fe-S protein,
HI1066 - HI1069	*nrfD*	-2.22 - - 2.48	nitrite reductase transmembrane protein
Gene class: Amino acid biosynthesis			
HI0591	*speF*		arginine and proline metabolism
		-2.56209	ornithine decarboxylase
	leuA		leucine biosynthesis 2-isopropylmalate
HI0986		-2.17035	synthase
Gene class: Transporters			
HI0590	*potE*		
		-2.29796	putrescine transporter
HI1030	-	-2.09237	hypothetical protein; putative TRAP-

			type C4-dicarboxylate transport system, small permease component [
HI0107	-	-2.06438	Mg2+/Co2+ transporter
Gene class: Other metabolic proteins			
HI1031	-	-2.5525	carbohydrate metabolism 2,3-diketo-L-gulonate reductase
Gene class: Hypothetical and uncharacterised proteins			
	-		
HI1000	-	-2.37448	hypothetical protein
HI0220.2	-	-2.28912	hypothetical protein
HI1327	-	-2.82562	uncharacterised protein
HI1326	-	-3.18613	hypothetical protein

Interestingly, when *H. influenzae* gene expression in co-culture was compared between 24 h and 64 h, (Table 6.3), while most of the genes differentially expressed were the same, some differences were observed. Notably, at 64 h, the stress response genes that were up-regulated when in mono-culture were now not differentially expressed, whereas glycerol biosynthesis genes not observed in the mono-culture analysis, were up-regulated. Importantly, the fatty acid biosynthesis genes, anaerobic respiration (nitrite reductase) associated genes and amino acid biosynthesis genes which were down-regulated in mono-culture at 64 h, were also not differentially expressed in co-culture. These results suggest, that while *H. influenzae* gene expression is similar in mono- and co-culture at individual time-points (excepting 24 h), the presence of *S. pneumoniae* does have an impact on the adaptation of *H. influenzae* to different time-points during a continuous culture growth environment.

Table 6.3. Up- and down-regulated genes in *H. influenzae* RdKW20 in co-culture at 64 h in a flow cell with CDM media with glucose compared to *H. influenzae* RdKW20 in co-culture at 24 h in a flow cell with CDM media with glucose. Results are displayed for genes with a $\log_2$ fold change ≥ 2, and a p-value ≤ 0.05.

Gene ID			
Up-regulated Genes			
Gene class: Iron acquisition	**Gene name**	**$\log_2$FoldChange**	**Function**
HI0262 -HI0264	*hxuA-hxuC*	3.517044 – 4.5	heme-hemopexin utilization protein A, B, C
HI0359-HI0362	*yfeA-yfeD*	2.84-3.08	iron (chelated) transporter ATP-binding protein complex
HI0097	*hitA*	2.884325	iron-utilization periplasmic protein
Gene class: Thiamine metabolism			
HI0354	-	3.164313	putative hydroxymethylpyrimidine transport system ATP-binding
HI0415	-	3.165685	hydroxyethylthiazole kinase
HI0417	*thiE*	2.96629	thiamine-phosphate pyrophosphorylase
HI0416	*thiD*	2.97854	phosphomethylpyrimidine kinase
HI0358	-	2.036877	thiaminase
Gene class: Transporters			
HI1019	*tbpA*	2.77606	thiamin ABC transporter substrate-binding protein
HI0355	-	3.500278	putative hydroxymethylpyrimidine transport system permease
HI0357	-	3.51023	putative hydroxymethylpyrimidine transport system substrate
HI0418	-	2.549333	putative metabolite transport protein
HI0663m	*cydD*	1.906044	ABC transporter ATP-binding protein
Gene class: Glycerol metabolism			
HI0683-HI0685		1.943712-2.67	sn-glycerol-3-phosphate

	glpA-glpC		dehydrogenase subunit A,B,C
Gene class: Metabolic			
HI0095	-	2.106361	uncharacterised putative methyltransferase
Gene class: Uncharacterised proteins and pseudogenes			
HI1427	-	1.99725	hypothetical protein
HI1369	-	2.052582	hypothetical protein
Downregulated genes			
Gene class: DMSO reductase			
HI1045-HI1047	*dmsA-dmsC*	-2.7 - -4.27469	anaerobic dimethyl sulfoxide reductase subunit A, B,C
Gene class: Metabolism			
HI1031	-	-2.89819	2,3-diketo-L-gulonate reductase
Gene class: Transport			
HI1030	-	-2.41731	TRAP-type C4-dicarboxylate transport system, small permease component
HI1029	-	-1.9792	Putative TRAP transporter large permease protein

The comparison of *H. influenzae* mono-culture gene expression between 24 h and 336 h (Table 6.4) revealed an up-regulation of iron acquisition proteins, thiamine biosynthesis genes, 4 stress response genes, ribose and serine transporters, an exinuclease and several metabolic proteins at 336 h. Down-regulated genes included 10 Mu-like phage associated genes, 5 amino acid biosynthesis genes, DMSO reductase and fatty acid biosynthesis genes, as well as several other metabolic proteins.

Table 6.4. Up– and down- regulated genes in *H. influenzae* Rd KW20 at 336 h in mono-culture in a flow cell system in CDM media with glucose, compared to *H. influenzae* Rd KW20 in mono-culture in a flow cell system with CDM media with glucose at 24 h. Results are displayed for genes with a $\log_2$ fold change ≥ 2, and a p-value ≤ 0.05.

Upregulated genes ID **Gene class: Iron-associated**	**Gene name**	**$\log_2$Fold Change**	**Function**
HI0359 – HI0362	*yfeA-yfeD*	3.15 – 3.667	iron (chelated) ABC transporter permease
HI0262 – HI0264	*hxuA-hxuC*	2.4 - 3.64437	heme-hemopexin utilization protein A, B, C
HI0712	-	2.131528	hemoglobin-binding protein
HI0097	*hitA*	2.116763	iron-utilization periplasmic protein hFbpA
HI0131	*afuA*	1.965137	ferric ABC transporter protein
HI1217	-	2.283863	transferrin-binding protein
Gene class: Thiamine metabolism			
HI1020	*thiP*	2.107778	thiamine transporter membrane protein
HI0357	-	3.294433	thiamine biosynthesis protein
HI1019	*tbpA*	3.034925	thiamine ABC transporter substrate-binding protein; K02064 thiamine transport system substrate-binding protein
HI0416	*thiD*	2.325754	phosphomethylpyrimidine kinase
HI0415	-	2.371973	hydroxyethylthiazole kinase
HI0417	*thiE*	2.40179	thiamine-phosphate pyrophosphorylase
HI0358	-	2.086198	thiaminase
Gene class: Stress Response			
HI1434.1	*cspD*	2.05265	cold shock-like protein
HI1677.1	-	2.819205	RNaseP
HI1349	-	2.872548	starvation-inducible DNA-binding protein

HI1602	-	3.047907	putative oxidoreductase
Gene class: Transporters			
HI0418	-	2.363279	putative transport protein
HI0502	*rbsA*	2.270969	D-ribose transporter ATP binding protein
HI0354	-	3.214768	putative hydroxymethylpyrimidine transport system ATP-binding protein
HI0355	-	3.465496	putative hydroxymethylpyrimidine transport system permease protein
HI0289	*sdaC*	2.569933	serine transporter
Gene class: DNA-associated			
HI0249	*uvrA*	1.974277	excinuclease ABC subunit A
Gene class: Other metabolic proteins			
HI1739.1	*lldD*	2.139505	l-lactate dehydrogenase
HI0501	*rbsD*	2.595486	D-ribose pyranase
HI1453	*purL*	2.644377	phosphoribosylformylglycinamidine synthase
HI1454	-	3.30254	cytochrome c-type biogenesis protein
HI1455	*msrA*	3.434375	bifunctional methionine sulfoxide reductase subunits A/B
Gene class: Hypothetical and uncharacterised proteins			
HI1600	-	2.232254	hypothetical protein
HI0520	-	2.380557	hypothetical protein
HI0521	-	2.38958	uncharacterised protein
HI1297	-	2.556406	hypothetical protein
HI1053	-	2.856058	hypothetical protein

HI1601	-	2.969905	hypothetical protein
HI1564	-	2.990428	hypothetical protein
HI1205	-	3.277913	hypothetical protein
Downregulated genes			
Gene classs: Mu-phage associated			
HI1481	*muB*	-1.97809	DNA transposition protein
HI1504	-	-2.74789	bacteriophage Mu I protein
HI1513	-	-2.4596	Putative bacteriophage protein
HI1518	-	-2.31265	mu phage
HI1510	-	-2.09398	flumu protein gp 38
HI1519	-	-2.02424	flumu prophage gp 46
HI1485	-	-1.92855	Mu-like prophage gene
HI1418	-	-2.01874	hypothetical prophage antirepressor
HI1511	-	-2.29983	phage sheath protein gpL
HI1483	*gam*	-2.18419	host-nuclease inhibitor protein
Gene class: Amino acid biosynthesis			
HI0986	*leuA*	-2.67493	2-isopropylmalate synthase
HI1387	*trpE*	-2.45229	biosynthesis of amino acids anthranilate synthase component I
HI0987	*leuB*	-1.9378	valine, leucine and isoleucine biosynthesis3-isopropylmalate dehydrogenase
HI0682	*ilvC*	-2.78113	ketol-acid reductoisomerase
HI0591	*speF*	-3.26457	ornithine decarboxylase
Gene class: Sulfur metabolism and DMSO reductase			

	-		twin-argninine leader-binding protein DmsD – chaperone for the folding of dimethylsulfoxide
HI1044		-2.67308	reductase
	dmsA-		anaerobic dimethyl sulfoxide
HI1045 – HI1047	*dmsC*	-3.66749 - -4.4	reductase subunitA, B, C
Gene class: Fatty acid biosynthesis			
			fatty acid biosynthesis 3-hydroxydecanoyl-ACP
HI1325	*fabA*	-2.58522	dehydratase
HI0002	-	-2.28717	long chain fatty acid CoA ligase
Gene class: Carbohydrate metabolism			
HI1031	-	-2.62891	2,3-diketo-L-gulonate reductase
Gene class: Transporters			
HI0590	*potE*	-2.86132	putrescine:ornithine antiporter
	-		TRAP C-4 dicarboxylate
HI1030		-2.26062	transport system putative
Gene class: Other metabolic proteins			
HI0643	*bisC*	-2.41535	biotin sulfoxide reductase
Gene class: Uncharacterised proteins and pseudogenes			
HI1505	-	-3.16799	hypothetical protein
HI1508	-		
		-2.82701	hypothetical protein
HI1326	-	-2.80789	hypothetical protein
HI1506	-	-2.76572	pseudogene
HI1327	-	-2.66592	hypothetical protein
HI1509	-	-2.4858	hypothetical protein
HI1512	-	-2.45645	hypothetical protein
HI0220.2	-	-2.33045	hypothetical protein
HI1482	-	-2.27581	hypothetical protein
HI1489	-	-1.96942	hypothetical protein

However, when the gene expression was analysed between *H. influenzae* at 24 h and 336 h in co-culture, several differences were observed (Table 6.5). While the up-regulated genes at 336 h were similar, including iron acquisition and thiamine biosynthesis genes, down-regulated genes in co-culture did not include any Mu-like phage genes or amino acid biosynthesis genes. In addition, 2 ferritin genes were down-regulated in co-culture, which were not differentially expressed in mono-culture.

Table 6.5. Up- and down-regulated genes in *H. influenzae* RdKW20 in a CDM with glucose flow cell in co-culture with *S. pneumoniae* strain 11 at 336 h compared to *H. influenzae* RdKW20 in co-culture with *S. pneumoniae* strain 11 at 24 h in a CDM with glucose flow cell. Results are displayed for genes with a $\log_2$ fold change ≥ 2, and a p-value ≤ 0.05.

Gene ID Up-regulated genes **Gene class: Iron acquisition**	**Gene name**	**$\log_2$Fold Change**	**Function**
HI0262 – HI0264	*hxuA-hxuC*	3.07 - 4.513959	heme-hemopexin utilization protein A, B, C
HI0359 – HI0362	*yfeA-yfeD*	2.85 – 3.68	iron (chelated) ABC transporter permease
HI0097- HI0098	*hitA, hitB*	2.6 - 2.844042	iron-utilization periplasmic protein hFbpA., iron(III) ABC transporter permease
HI1217	-	2.02322	hemoglobin/transferrin/lactoferrin receptor protein
HI0131	*afuA*	1.924069	ferric ABC transporter protein
Gene class: Ribose transport and metabolism			
HI0501	*rbsD*	2.496355	D-ribose pyranase
HI0502	*rbsA*	2.255322	D-ribose transporter ATP binding protein
Gene class: Transporters			
HI0418	-	2.412862	putative metabolite transport protein
HI0289	*sdaC*	2.146405	serine transporter
HI0354	-	3.897464	putative hydroxymethylpyrimidine transport system ATP-binding
HI0355	-	4.271972	putative hydroxymethylpyrimidine transport system permease
HI1019	*tbpA*	3.033263	thiamin ABC transporter substrate-binding protein;
HI1020	*thiP*	2.195849	thiamine transporter membrane protein
Gene class: Thiamine metabolism			
HI0358	-	1.965273	thiaminase (transcriptional activator TenA
HI0415 – HI0417	-	2.85 - 3.188105	hydroxyethylthiazole kinase; thiamine phosphate

			pyrophosphorylase
HI0357	-	3.461842	thiamine biosynthesis protein
Gene class: Metabolic			
HI0095	-	2.152375	uncharacterised protein with S-adenosylmethionine-dependent methyltransferases
HI1649	*dld*	1.967141	D-lactate dehydrogenase
HI0044	-	1.92965	hypothetical protein; K19416 modulator of FtsH protease
Gene class: Stress Response			
HI1564	-	2.477765	putative DNA repair enzyme
HI1677.1	-	2.492478	RNaseP
Gene class: Uncharacterised proteins and pseudogenes			
HI0520	-	1.98024	hypothetical protein
HI0521	-	1.911449	hypothetical protein
Gene class: Ribosomal			
HI1220	*rpsA*	1.964577	30S ribosomal protein S1
HI0857.1	-	2.153036	6S RNA
Downregulated genes			
Gene class: Stress Response			
HI0643	*bisC*	-1.92502	biotin sulfoxide reductase
Gene class: DMSO reductase			
HI1045 - HI1047	*dmsA- dmsC*	-3.17 - - 3.6259	anaerobic dimethyl sulfoxide reductase subunit A, B, C
Gene class: Iron-associated			
HI1385	*rsgA*	-2.0478	ferritin
HI1384	*rsgA*	-1.95763	ferritin like protein 1
Gene class: Fatty acid metabolism			
HI0002	-	-1.94736	long chain fatty acid CoA ligase
HI1325	*fabA*	-1.94045	fatty acid biosynthesis 3-hydroxydecanoyl-ACP dehydratase
HI0689	*glpQ*	-1.93536	lipid metabolism glpQ; glycerophosphodiester phosphodiesterase
Gene class: Carbohydrate metabolism			
HI1031	-	-3.69765	carbohydrate metabolism 2,3-diketo-L-gulonate reductase

Gene class: Uncharacterised proteins and pseudogenes			
HI1030	-	-3.4384	hypothetical protein
HI1028	-	-2.73546	hypothetical protein
HI1029	-	-2.59345	hypothetical protein
Gene class: Ribosomal			
HI0113.2	-	-2.43968	ribosomal
HI1739.7	-	-2.1469	ribosomal

6.2.6. The presence of *S. pneumoniae* causes subtle nutrient-dependent transcriptomic events to occur in *H. influenzae* in a flow cell, in a CDM with glucose environment.

The *H. influenzae* transcriptome was not significantly affected in co-culture with *S. pneumoniae* in CDM, although the presence of *S. pneumoniae* was able to cause subtle modifications to *H. influenzae* adaptation to environmental conditions over time. The relatively low level of influence of *S. pneumoniae* on *H. influenzae* gene expression was in contrast to what was observed previously in HI media (Tikhomirova et al. 2015). Therefore, in order to investigate effects of media adaptation on the transcriptome of *H. influenzae*, the gene expression in CDM at 64 h and 336 h in CDM was compared to the gene expression at 64 h and 168 h in HI media, both in mono- and co-culture respectively.

When *H. influenzae* gene expression in mono-culture at 64 h was compared to *H. influenzae* gene expression in the same conditions in HI media, in CDM conditions, *H. influenzae* displayed an up-regulation of iron-acquisition genes, molybdenum uptake, thiamine biosynthesis, as well as several others (Table 6.6). Down-regulated genes in CDM included a dimethylsulfoxide reductase, glycerol metabolism genes, genes involved in molybdenum cofactor synthesis, 5 stress response genes including an alcohol dehydrogenase, formate dehydrogenase, biotin sulfoxide reductase, *clp* protease and *dnaJ* chaperone. Three bacteriophage-associated genes were down-regulated as were 2 DNA-associated genes associated with recombination and base excision repair (recombinase and endonuclease) (Table 6.6).

Table 6.6. Up- and down-regulated genes in *H. influenzae* RdKW20 grown in a flow cell with CDM with glucose medium in mono-culture at 64 h compared to *H. influenzae* RdKW20 grown in a flow cell with HI medium in mono-culture at 64 h. Results are displayed for genes with a $\log_2$ fold change ≥ 2, and a p-value ≤ 0.05.

Gene ID		$\log_2$Fold	
Upregulated genes	**Gene name**	**Change**	**Function**
Gene class: Transporters			
HI1692 -HI1693	*modA-modC*	3.4 -5.214077	molybdenum ABC transporter complex
HI1525	-	3.170657	molybdate-binding periplasmic protein
HI1470-HI1472	-	2.30-3.28	iron chelatin ABC transporter ATP-binding protein
HI0359 -HI0362	*yfeA-yfeD*	2.29-3.557591	iron-chelated ABC transporter substrate-binding protein
HI0262 - HI0264	*hxuA-hxuC*	2.4-3.0	heme-hemopexin utilization protein A, B, C
HI1020	*thiP*	2.780493	thiamine transporter membrane protein
HI1019	*tbpA*	2.903103	thiamine ABC transporter substrate-binding protein
HI0051	-	2.597249	putative TRAP-type C4-dicarboxylate transport system, small permease component
HI0119	*znuA*	2.681236	high-affinity zinc transporter substrate-binding protein
HI1049	*merT*	2.198313	mercuric ion transport protein
HI0384	*tolR*	2.041625	colicin uptake protein TolR
HI0355	-	2.638556	putative hydroxymethylpyrimidine transport system permease protein
HI1050	*merP*	2.905463	mercuric ion scavenger protein
HI0838	-	2.044087	small protein A
HI1084	-	2.076551	phospholipid transport system substrate binding protein
HI1174	-	2.154825	opacity protein
HI0878	-	2.564036	uncharacterised transporter
Gene class: Metabolic Thiamine synthesis			
HI0416 – HI0417	*thiD-thiE*	2.422721 – 2.6	thiamine metabolism phosphomethylpyrimidine kinase; thiamine metabolism thiamine –phosphate pyrophosphorylase
HI0357	-	3.061851	thiamine biosynthesis protein
Gene class: Metabolic			

Amino acid metabolism			
HI1387	*trpE*	3.419931	anthranilate synthase component I
Gene class: Metabolic Purine biosynthesis			
HI1189	-	2.079437	hypothetical protein; SAM superfamily
Gene class: Vitamin and cofactor biosynthesis			
HI1190	-	2.912222	folate biosynthesis 6-pyruvoyl tetrahydrobiopterin synthase
Gene class: Other metabolic genes			
HI1430	-	2.207206	short chain dehydrogenase/reductase
HI0574	*fkpA*	2.06229	FKBP-type peptidyl-prolyl cis-trans isomerase
HI0236	-	2.496627	arsenate reductase
HI0366	-	2.001325	type IV pilus assembly protein PilF
Gene class: DNA associated			
HI0980	*fis*	3.451834	DNA-binding protein Fis
Gene class: Uncharacterised proteins and pseudogenes			
HI0601.1	-	3.28068	pseudogene
HI1036	-	2.82521	uncharacterised protein; Yggt family
HI1427	-	2.900347	hypothetical protein
HI0642a	-	2.424112	uncharacterised protein
HI0868	-	2.30509	hypothetical protein
HI1462.1	-	2.101984	hypothetical protein
HI0457	-	2.012517	hypothetical protein
HI1680	-	2.036723	hypothetical protein
HI1492	-	2.03853	hypothetical protein
Downregulated Genes			
Gene class: Dimethylsulfoxide reductase			
HI1045-HI1047	*dmsA-dmsC*	-3.03654 - -4.5	anaerobic dimethyl sulfoxide reductase subunit A, B, C
Gene class: glycerol metabolism			
HI0684 – HI0685	*glpA-glpB*	-3.55597 - -3.29	anaerobic glycerol-3-phosphate dehydrogenase subunit A, B
Molybdenum			

associated			
HI1673-HI1674; HI1676-HI1675	*moaE, moaD; moaA-moaC*	-2 - -2.99234	molybdopterin synthase small subunit, molubdopterin converting factor subunit 2, molybdenum cofactor biosynthesis protein A, molybdenum cofactor biosynthesis protein MoaC (anaerobic respiration and sulfur catabolism)
Gene class: Bacteriophage related			
HI1518	-	-3.07916	Mu phage hypothetical protein
HI1519	-	-2.84464	prophage hypothetical protein
HI1483	*gam*	-1.98845	host-nuclease inhibitor protein
Gene class: Stress Response			
HI0185	*adhC*	-2.64761	alcohol dehydrogenase class III
HI0007	*fdxH*	-2.29565	formate dehydrogenase subunit beta
HI0643	*bisC*	-3.42235	biotin sulfoxide reductase
HI0859	*clpB*	-2.56609	ATP-dependent Clp protease ATPase subunit
HI1238	*dnaJ*	-2.02596	chaperone protein DnaJ
Gene class: DNA-associated			
HI0991	*recF*	-2.36483	recombination protein F
HI0397	*xseA*	-1.89158	exodeoxyribonuclease VII large subunit
Gene class: Other metabolic genes			
HI0223	-	-2.31054	hypothetical chloramphenicol-sensitive protein RarD
HI0644	*yecK*	-3.19848	cytochrome C-like protein
HI1400	-	-2.09022	PHP domain containing protein

When *H. influenzae* gene expression at 64 h in co-culture in CDM was compared to the same conditions in HI media, similar genes were differentially expressed, however, additional genes were differentially expressed (Table 6.7). As in the mono-culture comparison, CDM media resulted in an up-regulation of iron acquisition and molybdate transport genes, and thiamine biosynthesis genes. However, in contrast to the mono-culture comparison, there was an up-regulation of the respiration-associated *napC*, *napD* and *napG*. Down-regulated genes included the DMSO reductase as well as several stress response and metabolic genes, as well as DNA associated *recF* and DNA polymerase, and several Mu-phage related genes.

Table 6.7. Up- and down-regulated genes in *H. influenzae* Rd KW20 when grown in co-culture with *S. pneumoniae* in a flow cell with CDM with glucose media for 64 h compared to *H. influenzae* RdKW20 grown in co-culture with *S. pneumoniae* in a flow cell with in HI media for 64 h.

Gene ID Up-regulated genes Gene class: Iron transport	**Gene name**	**log_2Fold Change**	**Function**
HI0362	*yfeA*	1.936697	iron-chelated ABC transporter substrate-binding protein
HI1471	-	2.320623	iron chelatin ABC transporter permease
HI0263	*hxuB*	1.908319	heme/hemopexin-binding protein B
HI1472	-	3.052484	iron chelatin ABC transporter substrate-binding protein
Gene class: Molybdate Transport			
HI1691	*modC*	3.059566	molybdate transporter ATP-binding protein
HI1692	*modB*	4.288166	molybdate ABC transporter permease
HI1693	*modA*	5.74453	molybdenum ABC transporter substrate-binding protein
HI1525	-	2.971829	molybdate-binding periplasmic protein
Gene class: Mercury transport			
HI0291	-	2.31066	mercury transport-like protein
HI1050	*merP*	1.990102	mercuric ion scavenger protein
Gene class: Thiamine			

biosynthesis and transport			
HI1019	*tbpA*	2.658325	thiamin ABC transporter substrate-binding protein
HI0417	*thiE*	2.446326	thiamine-phosphate pyrophosphorylase
HI0357	-	2.887793	thiamine biosynthesis protein
HI0416	*thiD*	2.736153	phosphomethylpyrimidine kinase
HI0415	-	2.258753	hydroxyethylthiazole kinase
Gene class: Electron transport/Respiration			
HI0345	*napG*	2.148029	quinol dehydrogenase periplasmic subunit
HI0343	*napD*	2.264709	nitrate reductase assembly protein NapD
HI0348	*napC*	1.911122	cytochrome C-type protein
Gene class: Other metabolic proteins			
HI0831	*mtgA*	1.938974	monofunctional biosynthetic peptidoglycan transglycosylase
HI1584	*ilvH*	2.283699	biosynthesis of amino acids acetolactate synthase 3 regulatory subunit
HI1190	-	2.53189	folate biosynthesis 6-pyruvoyl tetrahydrobiopterin synthase
Gene class: Uncharacterised proteins and pseudogenes			
HI0344	*napA*	1.95542	pseudogene
HI0418	-	2.108971	transporter
HI0878	-	2.333943	hypothetical transporter
HI1546	-	2.364985	hypothetical protein
HI0342	*napF*	2.846178	pseudogene
Down-regulated genes			
Gene class: DMSO reductase			
HI1045-HI1047	*dmsA-dmsC*	-3.0 - -4.65575	anaerobic dimethyl sulfoxide reductase subunit A, B, C
Gene class: Other metabolic proteins			
HI0643	*bisC*	-2.75984	biotin sulfoxide reductase
HI1615	*purE*	-2.37554	phosphoribosylaminoimidazole carboxylase catalytic subunit
HI1010	-	-2.23551	3-hydroxyisobutyrate dehydrogenase
HI0185	*adhC*	-2.10816	alcohol dehydrogenase class III
HI1044	-	-2.07519	twin-argninine leader-binding protein DmsD

HI1012	-	-2.0742	aldolase
HI0771	*atoB*	-2.05123	acetyl-CoA acetyltransferase
HI0644	*yecK*	-2.84629	cytochrome C-like protein
Gene class: DNA-Associated			
HI0991	*recF*	-2.62465	recombination protein F
HI1400	-	-2.03934	DNA polymerase
Gene class: Mu-phage associated			
HI1515	*muN*	-2.26981	64 kDa virion protein
HI1568	-	-2.37528	Mu-like prophage FluMu G protein
HI1516m	-	-2.36838	similar to 43 kDa tail protein; artificial frameshift
HI1416	-	-3.15721	phage holin
HI1413	-	-2.42197	uncharacterised membrane protein
HI1514	-	-2.24778	**Mu-like prophage FluMu protein gp42**
Gene class: Uncharacterised proteins and pseudogenes			
HI1565m	-	-3.14062	pseudogene
HI0043	-	-3.12336	putative membrane protein
HI1415	-	-2.81062	hypothetical protein
HI0223	-	-2.27775	chloramphenicol-sensitive protein RarD
HI1414	-	-2.16945	hypothetical protein
HI1405	-	-2.04386	hypothetical protein
Gene class: Ribosomal and trNA			
HI0601.9	-	-7.18809	5S ribosomal RNA
HI0113.2	-	-7.14627	ribosomal
HI0601.8	-	-6.61241	tRNA-Asp
HI1739.7	-	-5.84171	ribosomal
HI0621.4	-	-5.75925	ribosomal
HI0116.1	-	-5.63449	tRNA
HI0220.3	-	-5.05881	ribosomal
HI0601.4	-	-4.5595	ribosomal
HI0601.5	-	-4.46689	tRNA
HI0723.4	-	-4.43963	ribosomal
HI10044.1	-	-4.36366	tRNA
HI1154.1	-	-4.29484	4.5S RNA
HI1281.1	-	-4.1469	tRNA-Met
HI1739.6	-	-3.63024	ribosomal
HI0247.1	-	-3.62734	tRNA
HI0113.3	-	-3.6238	ribosomal
HI0220.4	-	-3.59724	ribosomal

HI1003.5	-	-3.4958	ribosomal
HI1739.3	-	-3.48523	ribosomal
HI0220.5	-	-3.4765	ribosomal
HI0723.1	-	-3.22279	ribosomal
HI0601.3	-	-3.22207	ribosomal
HI0601.2	-	-3.22024	ribosomal
HI0621.2	-	-3.21956	ribosomal
HI0621.3	-	-3.21578	ribosomal
HI0723.3	-	-3.2045	ribosomal
HI0707.1	-	-3.1851	tRNA
HI1715.1	-	-2.9117	tRNA-Gly
HI0621.5	-	-2.77794	tRNA-Glu
HI0042	-	-2.70036	tRNA pseudouridine synthase-like protein
HI1468	*rpsO*	-2.65569	30S ribosomal protein S15
HI0220.6	-	-2.37837	tRNA-Glu
HI1003.4	-	-2.19562	tRNA
HI0086.4	-	-2.11716	tRNA
HI0136.2	-	-2.04891	tRNA-Asp
HI0086.2		-1.9318	tRNA-Gly

When *H. influenzae* gene expression at 336 h in mono-culture in CDM was compared to *H. influenzae* gene expression at 168 h in mono-culture in HI media, there were several differences. In CDM, there was an up-regulation of iron and molybdate transport and thiamine biosynthesis, as well as an up-regulation of cytochrome C assembly genes, and some metabolic genes including the cell division protein *zapB* and an antitoxin of *cptA/cptB* toxin/antitoxin system, although the function of this is unclear as *H. influenzae* lacks the cognate toxin in the genome. Up-regulated genes also involved an RNAse, oxidoreductase and chaperonin, as well as elements of the *hindII* restriction-modification (RM) system, a starvation inducible DNA-binding protein and the *fis* transcriptional regulator. Down-regulated genes included a large group of phage-associated genes (predominantly belonging to the Mu-like phage), glycerol metabolism, DMSO reductase, several metabolic genes including a cytochrome C-like protein, and an RM gene and DNA polymerase (Table 6.8).

Table 6.8. Up- and down-regulated genes in *H. influenzae* Rd KW20 when grown in mono-culture in a flow cell with CDM with glucose for 336 h compared to *H. influenzae* Rd KW20 grown in a flow cell with HI media in mono-culture for 164 h.

Gene ID Up-regulated genes	Gene name	log_2Fold Change	Function
Gene class: Transport			
Gene class: Iron Transport			
HI0359-HI0362	*yfeA-yfeD*	2.084187-2.85	iron (chelated) transporter
HI1471	-	3.37901	iron chelatin ABC transporter permease
HI1472	-	3.422898	iron chelatin ABC transporter substrate-binding protein
HI1470	-	2.3681	iron chelatin ABC transporter ATP-binding protein
Gene class: Molybdate transport			
HI1691-HI1693	*modA-modC*	3.43-4.628673	molybdenum ABC transporter
HI1525	-	2.916632	molybdate-binding periplasmic protein
Gene class: Transport			
HI1050	*merP*	2.855856	mercuric ion scavenger protein
HI1079m	-	1.956312	amino acid ABC transporter permease
HI0663m	*cydD*	2.174098	ABC transporter ATP-binding protein
HI1690	-	1.982034	sodium-dependent transporter
Gene class: Thiamine Import and metabolism			
HI0355	-	1.950913	putative hydroxymethylpyrimidine transport system permease
HI1020	*thiP*	2.424204	thiamine transporter membrane protein
HI0357	-	2.385376	thiamine biosynthesis protein
HI1019	*tbpA*	2.309717	thiamin ABC transporter substrate-binding protein
HI1084	-	1.931482	phospholipid transport system substrate-binding protein
HI1607	*lolB*	1.939346	outer membrane lipoprotein LolB
Gene class: Cytochrome C assembly			
HI1091	*ccmC*	2.153217	cytochrome C protein assembly heme exporter protein C
HI1090	*ccmB*	2.16882	cytochrome c protein assembly heme exporter protein B

HI1092	*ccmD*	2.072001	heme exporter protein D
Gene class: Metabolic			
	-		acetyl-CoA:acetoacetyl-CoA transferase
HI0774		3.054457	subunit alpha
HI0044	-	2.282119	modulator of FtsH protease
HI0236	-	2.142817	arsenate reductase
	-		folate biosynthesis 6-pyruvoyl
HI1190		1.959369	tetrahydrobiopterin synthase
	-		Uncharacterised protein, antitoxin component of the CptAB toxin-antitoxin module [Posttranslational modification,
HI0627		2.028747	protein turnover, chaperones
HI0668	-	1.976319	cell division protein ZapB
HI0484	*atpE*	1.94433	F0F1 ATP synthase subunit C
Gene class: Stress Response			
HI0999	*rnpA*	2.546651	ribonuclease P
HI1602	-	2.239534	putative oxidoreductase
HI0810	*hslO*	2.001488	Hsp33-like chaperonin
Gene class: DNA associated			
HI0513	*hindIIM*	2.450057	modification methylase
	nrdA		ribonucleotide-diphosphate reductase
HI1659		2.020168	subunit alpha
HI0512	*hindIIR*	2.548371	type II restriction endonuclease
HI1349	-	3.328641	starvation-inducible DNA-binding protein
HI0980	*fis*	3.494196	Fis family transcriptional regulato
Gene class: Uncharacterised proteins and pseudogenes			
HI1036	-	3.618382	YggT family protein
HI0051	-	2.767888	hypothetical protein
HI1736	-	2.793-972	hypothetical protein
HI0862	-	2.796132	hypothetical protein
HI0601.1	-	2.5873	pseudogene
	-		
HI0878		2.744691	uncharacterised transporter
HI1680	-	2.503085	hypothetical protein
HI1546	-	2.297652	hypothetical protein
HI0420.1	-	2.277154	Uncharacterized protein
HI0120	-	2.181838	Uncharacterized integral membrane protein
HI0642a	-	2.183467	hypothetical protein

HI1297	-	2.218918	hypothetical protein
HI0342	*napF*	2.171665	pseudogene
HI1564	-	2.045301	hypothetical protein
HI1005	-	2.006786	hypothetical protein
HI1724	-	1.994719	hypothetical protein
Gene class: Ribosomal and tRNA			
HI0798.1	*rpmJ*	1.96972	50S ribosomal protein L36
HI0411	*hfq*	2.05439	RNA-binding protein Hfq
HI0577	-	2.314995	tRNA 2-thiouridine synthesizing protein B
HI0631.4	-	2.979094	tRNA Thr
HI0761.2	-	3.191112	tRNA Asn
HI1572.1	-	3.36445	tRNA Val
HI0761.1	-	4.287865	tRNA Phe
Downregulated genes			
Gene class: Mu-like phage			
HI1483	*gam*	-4.39261	Mu phage host-nuclease inhibitor protein
HI1485	-	-4.18395	**Mu-like prophage FluMu region**
HI1519	-	-4.24059	Mu phage gp 46
HI1504	-	-4.04581	bacteriophage Mu I protein
HI1518	-	-3.86491	Mu phage
HI1478	*muA*	-3.86079	Mu phage
HI1514	-	-3.65181	**Mu-like prophage FluMu protein gp42**
HI1513	-	-3.46902	Mu phage asociated
HI1481	*muB*	-3.29168	Mu phage DNA transposition protein
HI1512	-	-3.23142	Mu phage tail protein
HI1501	-	-3.16565	hypothetical protein
HI1499	-	-3.00182	**Mu-like prophage FluMu protein gp27**
HI1511	-	-2.88243	sheath protein gpL
HI1500	-	-2.86008	Mu-like prophage FluMu protein gp28
HI1515	*muN*	-2.36757	64 kDa virion protein
HI1510	-	-2.35616	**Mu-like prophage FluMu protein gp38**
HI1516m	-	-2.32276	43 kDa tail protein;
HI1505	-	-4.7607	Mu-like prophage major head subunit gpT [Mobilome: prophages, transposons]
Gene class: Glycerol metabolism			
HI0683-HI0685	*glpA-glpC*	-2.16229 - - 4.37	sn-glycerol-3-phosphate dehydrogenase subunits A, B, C

HI0691	*glpK*	-2.13364	glycerol kinase
Gene class: DMSO reductase			
	dmsA-	-3.1 - -	anaerobic dimethyl sulfoxide reductase
HI1045- HI1047	*dmsC*	5.02746	subunit A, B, C
Gene class: Metabolic			
HI1012	-	-3.05643	aldolase
HI0643	*bisC*	-3.01977	biotin sulfoxide reductase
HI1401	*pyrD*	-2.93374	dihydroorotate dehydrogenase 2
HI1010	-	-2.79986	3-hydroxyisobutyrate dehydrogenase
HI0185	*adhC*	-2.61316	alcohol dehydrogenase class III
HI1360	*glgA*	-2.41709	glycogen synthase
HI1674	*moaD*	-2.41466	molybdopterin synthase small subunit
HI0024	*citD*	-2.3919	citrate lyase subunit gamma
HI0092	-	-2.31661	gluconate:H+ symporter, GntP family
HI0595	*arcC*	-2.30672	carbamate kinase
HI1676	*moaA*	-2.23935	molybdenum cofactor biosynthesis protein A
HI0644	*yecK*	-2.22846	cytochrome C-like protein
HI0648	*mdaB*	-2.19256	modulator of drug activity B
HI0023	*citE*	-2.19212	citrate lyase subunit beta
HI0007	*fdxH*	-2.05885	formate dehydrogenase subunit beta
HI0022	*citF*	-1.93165	citrate lyase subunit alpha
HI1673	*moaE*	-1.916	molybdopterin converting factor subunit 2
HI1615	*purE*	-1.91338	phosphoribosylaminoimidazole carboxylase catalytic subunit
HI0091	-	-2.34156	glycerate kinase
Gene class: DNA-associated			
HI1056	-	-2.21212	type III restriction-modification system methyltransferase
HI1400	-	-3.34076	DNA polymerase
Gene class: Uncharacterised proteins and pseudogenes			
HI1508	-	-4.38821	hypothetical protein
HI1509	-	-4.26901	hypothetical protein
HI1497	-	-3.95558	uncharacterised protein
HI1506	-	-3.87107	pseudogene
HI1498	-	-3.76195	hypothetical protein
HI1495	-	-3.61083	uncharacterised protein
HI1488	-	-3.10372	hypothetical protein
HI1521	-	-3.08701	hypothetical protein
HI1496	-	-2.99899	hypothetical protein
HI1011	-	-2.85187	hypothetical protein

HI1489	-	-2.70167	hypothetical protein
HI1498.1	-	-2.36571	hypothetical protein
HI1486	-	-2.36139	hypothetical protein
HI0223	-	-2.31851	chloramphenicol-sensitive protein RarD
HI1729m	-	-2.22509	LamB/YcsF family protein
HI1520	-	-2.16221	ypothetical protein
HI1482	-	-2.15407	hypothetical protein
HI1161	-	-2.07271	hypothetical protein
HI1571	-	-2.05557	hypothetical protein
HI0842	-	-1.92282	pseudogene
HI1493	-	-3.33346	hypothetical Peptidoglycan recognition proteins (PGRPs) are pattern recognition receptors that bind, and in certain cases, hydrolyze peptidoglycans (PGNs) of bacterial cell walls.
Gene class: tRNA and Ribosomal			
HI0906	-	-2.03845	tRNA(adenine34) deaminase
HI0631.2	-	-2.00889	trna
HI1715.1	-	-2.00208	trna
HI0621.5	-	-1.99528	trna
HI0631.1	-	-1.93356	trna
HI0516	*rplA*	-2.15502	50S ribosomal protein L1
tRNA-Thr-2;locus_tag=HI0631.3	-	-2.17538	tRNA
HI0247.1	-	-2.65286	tRNA
HI1281.1	-	-2.72813	tRNA-Met
HI0601.5	-	-3.03273	tRNA
HI0621.4	-	-3.09131	ribosomal
HI0707.1	-	-3.12414	tRNA
tRNA-Met-1;locus_tag=HI0116.1	-	-3.63375	tRNA
HI0601.9	-	-3.71589	5S ribosomal RNA
HIrrnE5S;locus_tag=HI0113.2	-	-3.89394	ribosomal
HI10044.1	-	-4.65245	tRNA
HI1154.1	-	-6.88791	4.5S RNA
HI0601.8	-	-5.27192	tRNA-Asp

When the *H. influenzae* gene expression at 336 h in co-culture in CDM was compared to *H. influenzae* gene expression at 168 h in co-culture in HI media, in CDM there was an up-regulation of iron and molybdate transport and thiamine biosynthesis. Down-regulated genes included DMSO reductase, glycerol metabolism, stress response including chaperones, proteases

and a zinc-type alcohol dehydrogenase, as well as several metabolic genes (some related to leucine biosynthesis), and a large class of phage-associated genes (Table 6.9).

Table 6.9. Up- and down- regulated genes in *H. influenzae* Rd KW20 when grown in a flow cell with CDM with glucose in co-culture for 336 h compared to *H. influenzae* Rd KW20 grown in a flow cell with HI media in co-culture for 164 h. Results are displayed for genes with a $\log_2$ fold change ≥ 2, and a p-value ≤ 0.05.

Gene ID Up-regulated genes	**Gene name**	**$\log_2$FoldChange**	**Function**
Gene class: Iron transport			
HI1471	-	3.138869	iron chelatin ABC transporter permease
HI1472	-	3.587295	iron chelatin ABC transporter substrate-binding protein
HI1470	-	2.697821	iron chelatin ABC transporter ATP-binding protein
HI0362	*yfeA*	1.96168	iron-chelated ABC transporter substrate-binding protein
HI0360	*yfeC*	2.043177	iron (chelated) ABC transporter permease;
Gene class: Molybdate transport			
HI1525	-	2.990992	molybdate-binding periplasmic protein
HI1691-HI1693	*modA-modC*	3.108028-5.4	molybdate transporter
Hydroxymethylpyrimidine transport and thiamine biosynthesis			
HI0355	-	1.927787	putative hydroxymethylpyrimidine transport system permease protein
HI0417	*thiE*	2.25971	thiE; thiamine-phosphate pyrophosphorylase
HI0415	-	2.443157	hydroxyethylthiazole kinase
HI0416	*thiD*	2.49524	thiD; phosphomethylpyrimidine kinase
HI0357	-	2.799305	thiamine biosynthesis protein
HI1019	*tbpA*	3.152297	tbpA; thiamin ABC transporter substrate-binding protein
HI0223	-	-2.61989	chloramphenicol-sensitive protein RarD
Gene class: Uncharacterised			

proteins and pseudogenes			
HI1546	-	2.107917	hypothetical protein
HI0886	-	2.119829	hypothetical protein
HI1036	-	2.436632	hypothetical protein; K02221 YggT family protein
HI0354	-	2.677102	ABC transporter ATP-binding protein
Downregulated genes			
Gene class:Oxidoreductases			
Gene class: DMSO reductase			
HI1045-HI1047	*dmsA-dmsC*	-5.0 - -5.71069	anaerobic dimethyl sulfoxide reductase
Gene class: Oxidoreductases			
HI0643	*bisC*	-4.61901	bisC; biotin sulfoxide reductase
HI1010	-	-4.2222	3-hydroxyisobutyrate dehydrogenase
Gene class: Glycerol metabolism			
HI0683-HI0685	*glpA-glpC*	-2.18 - -2.8	sn-glycerol-3-phosphate dehydrogenase subunit A, B, C
Gene class: Stress Response			
HI0859	*clpB*	-2.84127	ATP-dependent Clp protease ATPase subunit
HI1238	*dnaJ*	-2.61373	chaperone protein DnaJ;
HI0053	-	-2.55101	zinc-type alcohol dehydrogenase
HI1237	*dnaK*	-2.13072	molecular chaperone DnaK
Gene class: Transporters			
HI1015	*gntP*	-2.513	gntP; gluconate permease
HI0590	*potE*	-2.36741	potE; putrescine transporter
Gene class: Metabolic			
HI0644	*yecK*	-4.41791	yecK; cytochrome C-like protein
HI1013	-	-3.14103	hydroxypyruvate isomerase
HI0591	*speF*	-3.088	speF; ornithine decarboxylase (arginine and proline metabolism)
HI1044	-	-2.78784	twin-argninine leader-binding protein DmsD (required for assembly of DMSO reductase
HI0986	*leuA*	-2.5886	leuA; 2-isopropylmalate synthase (valine, Leucine, Isoleucine biosynthesis)

HI1615	*purE*	-1.96326	purE; phosphoribosylaminoimidazole carboxylase catalytic subunit (puyrine metabolism)
HI0989	*leuD*	-1.95356	euD; isopropylmalate isomerase small subunit (valine, Leucine, Isoleucine biosynthesis)
HI0988	*leuC*	-2.15395	leuC; isopropylmalate isomerase large subunit
HI1012	-	-3.94346	aldolase
HI1043	*napF*	-1.97827	napF; ferredoxin-type protein
HI1729m	-	-2.05659	LamB/YcsF family protein
Gene class: Phage-associated			
HI1415	-	-2.34415	hypothetical protein; K03791 putative chitinase
HI1500	-	-2.0903	hypothetical protein
HI1514	-	-2.60972	Phage protein gp42
HI1416	-	-2.46836	phage holin hypothetical protein
HI1568	-	-2.44058	Mu-like prophage FluMu G protein
HI1515	*muN*	-2.37773	muN; 64 kDa virion protein
HI1516m	-	-2.17382	tail protein; artificial frameshift
HI1478	*muA*	-2.09842	muA; transposase
HI1411	-	-1.90202	terminase small subunit
Gene class: Uncharacterised proteins and pseudogenes			
HI1053	-	-1.90093	hypothetical protein
HI1413	-	-1.92849	hypothetical protein
HI1485	-	-1.97191	hypothetical protein
HI1493	-	-2.04951	hypothetical protein
HI1488	-	-2.02215	hypothetical protein
HI1016	-	-2.10377	hypothetical protein
HI1498	-	-2.13318	hypothetical protein
HI1498.1	-	-2.13098	hypothetical protein
HI1497	-	-2.32645	hypothetical protein
HI1499	-	-2.2735	hypothetical protein
HI1501	-	-2.25414	hypothetical protein
HI1571	-	-2.25414	hypothetical protein
HI1014	-	-2.22538	hypothetical protein
HI1521	-	-2.19958	hypothetical protein
HI0052	-	-2.19261	hypothetical protein
HI1570	-	-2.52218	pseudogene
HI1405	-	-2.92088	hypothetical protein

HI1011	-	-3.74675	hypothetical protein
HI1519	-	-2.49887	hypothetical protein
HI1518	-	-2.79542	hypothetical protein
Gene class: tRNA and Ribosomal			
HI0601.9	-	-8.81906	5S ribosomal RNA
HI0601.8	-	-8.73585	tRNA-Asp
HI0116.1	-	-8.43628	tRNA
HI1281.1	-	-7.94823	tRNA-Met; K14230 tRNA Met
HI0113.2	-	-7.52244	HIrrnE5S; 5S ribosomal RNA
HI1154.1	-	-7.20926	4.5S RNA
HI0601.5	-	-6.40916	tRNA-Trp-1
HI10044.1	-	-5.58384	tRNA-Ser
HI0621.5	-	-5.53795	tRNA-Glu
HI0707.1	-	-5.24663	tRNA-SeC(p)-1; tRNA-Sec
HI0220.6	-	-5.16431	tRNA-Glu
HI0621.4	-	-5.06927	HIrrnB5S; 5S ribosomal RNA
HI1003.4	-	-5.04797	tRNA-Glu-1
HI1715.1	-	-4.84342	tRNA-Gly
HI1739.7	-	-4.77649	HIrrnD5S; 5S ribosomal RNA
HI0723.4	-	-4.39743	HIrrnC5S; 5S ribosomal RNA
HI0220.3	-	-4.17945	HIrrnF5S; 5S ribosomal RNA
HI0601.4	-	-3.95403	HIrrnA5S; 5S ribosomal RNA
HI0247.1	-	-3.06927	tRNA-Ser-2
HI1572.1	-	-2.97372	tRNA-Val
HI0136.2	-	-2.69569	tRNA-Asp
HI1739.5	-	-2.5789	tRNA-Ala;
HI0136.1	-	-2.50265	tRNA-Asp-1
HI0273.1	-	-2.4991	tRNA-Ala-1
HI0761.2	-	-2.41748	tRNA-Asn
HI1468	*rpsO*	-2.22912	30S ribosomal protein S15
HI0601.7	-	-2.08076	tRNA-Ala; K14218 tRNA Ala
HI0857.1	-	-1.99672	6S RNA
HI0723.5	-	-1.99303	tRNA-Ala; K14218 tRNA Ala

6.2.7. There are time-dependent transcriptomic events occurring in *S. pneumoniae* during continuous culture in CDM with glucose.

In order to identify transcriptional changes occurring in *S. pneumoniae* between the 3 different time-points and the 3 different phenotypic states in the CDM+glucose flow cell, the transcriptome of *S. pneumoniae* in co-culture was compared between the 24 h, 64 h and 336 h time-points. Clearly, the alignment of the total reads obtained in co-culture to the *S. pneumoniae* serotype 3 genome OXC_141, achieved a low alignment rate given the low cell counts or indeed no culturable cells. At 24 h, of the total 41444433 reads, only 1.17% aligned to *S. pneumoniae*; at 64 h of the 42188111 reads only 0.78% aligned to *S. pneumoniae*, and at 336 h of 38339478 reads only 1.82% aligned to *S. pneumoniae*. While such an alignment is too low to obtain statistically significant data from an analysis, the *S. pneumoniae* transcriptomes were nevertheless compared, and included as provisional results.

When the *S. pneumoniae* transcriptome in co-culture at 64 h was compared to the transcriptome at 24 h, several major transcriptomics changes were observed at 64 h (Table 6.10). Up-regulated genes included transporters (including sugar transporters), an antimicrobial transporter, metabolic genes predominantly involved in carbohydrate metabolism but also pyrimidine metabolism and glycerophospholipid metabolism, *padR*, *gntR* and *argR* transcriptional regulators, transposases, competence proteins and a small group of stress response genes. In addition, there as an up-regulation of the *relE* toxin and the phage shock protein. Down-regulated genes included various transporters including cation transporters, metabolic genes, amino acid biosynthesis and folate biosynthesis, 3 stress response genes and a large class of DNA-associated genes related to chromosome replication, including topoisomerases and a DNA polymerase.

Table 6.10. Up- and down-regulated genes in *S. pneumoniae* strain 11 at 64 h (in the undetected state) in co-culture with *H. influenzae* in a CDM with glucose flow cell compared to *S. pneumoniae* strain 11 at 24 h (wild-type) in co-culture in a CDM with glucose flow cell.

Gene ID	Gene name	log_2Fold Change	Function
Up-reguated genes			
Gene class: Transport			
SPNOXC_18590	*malX*	2.298658	putative maltose/maltodextrin-binding protein precursor
SPNOXC_05560	-	2.450661	putative glutamine-binding protein precursor
SPNOXC_04370	*glnQ2*	2.77259	putative glutamine ABC transporter,
SPNOXC_17820	-	4.303104	putative lactose-specific phosphotransferase system
SPNOXC_17810	-	4.035624	putative exported PTS system protein;
SPNOXC_14860	-	3.77259	sugar transport putative ABC transport protein, solute-binding component;
SPNOXC_16060	-	3.77259	putative iron ABC transporter, solute-binding protein
SPNOXC_17800	*licC*	2.865699	PTS system, lichenan-specific IIc component;
SPNOXC_15840	-	2.77259	PTS system transporter subunit IIC
SPNOXC_18210	-	2.187627	multi antimicrobial extrusion (MATE) family transporter
SPNOXC_18610	*malD*	2.187627	putative maltose/maltodextrin ABC transport system permease protein
SPNOXC_04380	-	1.924593	glutamine ABC transporter glutamine-binding protein/permease;
SPNOXC_05550	-	1.965235	amino acid ABC transporter permease;
SPNOXC_05570	-	2.187627	putative glutamine transporter, ATP-binding protein;
SPNOXC_17460	-	1.965235	hypothetical protein; K02004 putative ABC transport system permease protein
Gene class: Metabolic			
SPNOXC_18950	*arcB*	5.725848	ornithine carbamoyltransferase
SPNOXC_03300	*idnO*	5.357552	putative gluconate 5-dehydrogenase
SPNOXC_10680	*lacC2*	4.187627	tagatose-6-phosphate kinase 2
SPNOXC_16250	*galT*	3.77259	galactose-1-phosphate uridylyltransferase
SPNOXC_17790	-	2.965235	putative beta-glucosidase
SPNOXC_12470	*nagB*	2.602665	carbohydrate metabolism glucosamine-6-phosphate isomerase
SPNOXC_10670	*lacD2*	2.450661	tagatose 1,6-diphosphate aldolase 2
SPNOXC_18580	*malQ*	2.357552	putative 4-alpha-glucanotransferase
SPNOXC_18570	*glgP*	2.124301	putative glycogen phosphorylase

SPNOXC_11060	-	2.035624	acetyltransferase (GNAT) family protein
SPNOXC_01720	-	2.187627	cetyltransferase (GNAT) family protein;
SPNOXC_02240	-	2.187627	putative cardiolipin synthetase; glycerophospholipid metabolism
SPNOXC_14810	-	2.187627	putative N-acetylmannosamine-6-phosphate 2-epimerase
SPNOXC_01710	-	2.77259	glycoprotease family protein
SPNOXC_03270	*kgdA*	3.77259	putative 4-hydroxy-2-oxoglutarate aldolase/2-dehydro-3-deoxy-phosphogluconate aldolase
SPNOXC_03350	*agaD*	3.77259	putative N-acetylgalactosamine-specific phosphotransferase system (PTS)
SPNOXC_05370	*metE*	4.77259	(cysteine and methionine metabolism); 5-methyltetrahydropteroyltriglutamate/homocysteine S-methyltransferase
SPNOXC_07460	*punA*	2.673054	purine metabolism; putative purine nucleoside phosphorylase
SPNOXC_06350	*pyrE*	3.187627	orotate phosphoribosyltransferase pyrimidine metabolism
SPNOXC_12910	-	3.506839	putative pyridoxine biosynthesis protein vitamin B6 metabolism
SPNOXC_06340	*pyrF*	2.357552	pyrimidine metabolismpyrF; orotidine 5'-phosphate decarboxylase
SPNOXC_06250	-	4.631344	BipA family GTPase
SPNOXC_10750	*lepA*	4.491689	GTP-binding protein LepA
SPNOXC_16100	-	2.187627	sortase; K13925 plasmin and fibronectin-binding protein A
SPNOXC_14330	*thrS*	3.348092	threonyl-tRNA synthetase
SPNOXC_14880	*nanA*	3.77259	sialidase A
SPNOXC_17490	-	2.77259	ribonuclease M5
Gene class: Regulation			
SPNOXC_13060	*tufA*	3.788496	elongation factor Tu
SPNOXC_01270	-	2.77259	PadR-like family regulatory protein
SPNOXC_15080	-	2.148099	GntR family transcriptional regulator
SPNOXC_09260	-	2.094518	putative RNA methyltransferase
SPNOXC_18310	*argR*	2.187627	putative arginine repressor
SPNOXC_19480	-	2.187627	sigma-54 modulation protein / S30 ribosomal protein
SPNOXC_14140	-	2.450661	NIF3 (NGG1p interacting factor 3) family protein
SPNOXC_14170	-	2.77259	IS3-Spn1 orf B
SPNOXC_13990	-	3.187627	IS3-Spn1 orf B
Gene class: Competetence			

and DNA-related			
SPNOXC_08570	*comEA*	2.77259	putative competence protein
SPNOXC_18070	*comYC*	2.77259	putative competence protein
SPNOXC_18090	-	2.77259	putative competence protein
SPNOXC_11440	*nth*	2.07215	putative endonuclease II
SPNOXC_08080	-	1.965235	putative IS1381 transposase
Gene class: Stress Response			
SPNOXC_06040	-	2.77259	putative redoxin
SPNOXC_04770	*dnaK*	4.970005	chaperone protein DnaK
SPNOXC_19810	*htrA*	2.309189	htrA; serine protease
SPNOXC_03470	*clpL*	2.116924	putative ATP-dependent protease ATP-binding subunit ClpL
Gene class: Uncharacterised proteins and pseudogenes			
SPNOXC_02020	-	2.77259	hypothetical protein
SPNOXC_04740	-	2.77259	hypothetical protein
SPNOXC_11540	-	2.77259	hypothetical protein
SPNOXC_03540	*wzg*	3.77259	pseudogene
SPNOXC_04910	-	3.77259	pseudogene
SPNOXC_09390	-	3.77259	pseudogene
SPNOXC_14120	-	3.77259	hypothetical protein
SPNOXC_00030	-	2.77259	hypothetical protein
SPNOXC_00090	-	2.77259	hypothetical protein
SPNOXC_07070	-	3.035624	hypothetical protein
SPNOXC_18700	-	3.357552	hypothetical protein
SPNOXC_17150	-	3.77259	hypothetical protein
SPNOXC_16160	-	4.77259	hypothetical protein
SPNOXC_17040	-	4.357552	hypothetical protein
SPNOXC_19220	-	2.450661	hypothetical protein
SPNOXC_07450	-	2.550197	hypothetical protein
SPNOXC_07880	-	2.450661	hypothetical protein
SPNOXC_08510	-	2.450661	hypothetical protein
SPNOXC_10860	-	2.450661	hypothetical protein
SPNOXC_18670	-	2.357552	hypothetical protein
SPNOXC_06370	-	2.187627	hypothetical protein
SPNOXC_08840	-	2.187627	pseudogene
SPNOXC_08910	-	2.187627	hypothetical protein
SPNOXC_10300	-	2.187627	pseudogene
SPNOXC_05150	-	2.187627	hypothetical protein
SPNOXC_18690	-	1.965235	hypothetical protein
SPNOXC_09250	-	2.015861	hypothetical protein

SPNOXC_09420	-	1.965235	hypothetical protein
SPNOXC_13380	-	2.07215	pseuodgene
SPNOXC_15820	-	2.187627	hypothetical protein
SPNOXC_16990	-	2.187627	hypothetical protein
Gene class: Toxin/antitoxin system			
SPNOXC_10930	*relE*	3.77259	putative plasmid addiction system, toxin protein
Gene class: Bacteriophage			
SPNOXC_09880	-	2.550197	putative phage shock protein
Gene class: tRNA and ribosomal			
SPNOXC_t40	-	2.187627	tRNA
SPNOXC_t33	-	2.77259	tRNA
SPNOXC_t28	-	3.77259	tRNA
SPNOXC_08630	*rplT*	4.627732	ribosomal protein
Downregulated genes			
Gene class: Transporters			
SPNOXC_11330	-	-3.0729	putative LicB-family membrane protein
SPNOXC_08120	-	-2.00877	putative permease
SPNOXC_01090	-	-1.95533	TrkH-family cation transport protein
SPNOXC_19400	-	-2.51281	ABC transporter substrate-binding protein
SPNOXC_11910	-	-2.4942	ABC transporter ATP-binding protein; K06147 ATP-binding cassette, subfamily B, bacterial
SPNOXC_11920	-	-2.45623	ABC transporter ATP-binding protein
SPNOXC_12840	-	-2.38728	ABC transporter permease; K02029 polar amino acid transport system permease protein
SPNOXC_17620	-	-1.95533	ABC-2 type transporter membrane protein
SPNOXC_13130	-	-2.45623	putative amino acid ABC transporter, extracellular amino acid-binding protein;
SPNOXC_09010	-	-2.2718	putative amino acid permease
SPNOXC_14480	*mtsC*	-2.12396	metal cation ABC transporter membrane protein
SPNOXC_15510	*aqpZ*	-1.92785	aquaporin Z; K06188 aquaporin Z
Gene class: Metabolic			
SPNOXC_17610	-	-2.6368	histidine sensor kinase protein; K07778 two-component system, NarL family, sensor histidine kinase DesK
SPNOXC_13670	-	-2.54934	DegV family protein

SPNOXC_15250	-	-2.75097	putative protein phosphatase
SPNOXC_15180	*mvaA*	-2.60245	3-hydroxy-3-methylglutaryl-coenzyme A reductase
SPNOXC_13330	*murC*	-2.58496	UDP-N-acetylmuramate--L-alanine ligase – amino acid metabolism
SPNOXC_08260	-	-2.54934	amino acid biosynthesissaccharopine dehydrogenase family protein
SPNOXC_13550	*aspC*	-2.31487	aspartate aminotransferase
SPNOXC_11950	*hom*	-2.24978	hom; homoserine dehydrogenase amino acid biosynthesis
SPNOXC_17350	*pflC*	-2.24978	pyruvate formate-lyase activating enzyme oxidoreductase
SPNOXC_02870	-	-2.22741	luciferase-like monooxygenase (oxidoreductase)
SPNOXC_10450	*acoL*	-2.18161	dihydrolipoamide dehydrogenase (carbohydrate metabolism)
SPNOXC_08290	-	-2.782	carbon-nitrogen hydrolase family protein (amino acid metabolism)
SPNOXC_11120	*zwf*	-2.74311	glucose-6-phosphate 1-dehydrogenase (PPP)
SPNOXC_00940	*purB*	-1.9823	adenylosuccinate lyase purine metabolism
SPNOXC_03080	*folC*	-2.08539	putative folylpolyglutamate synthase (metabolism of cofactors and vitamins; folate biosynthesis)
SPNOXC_19470	-	-1.96888	DHH family protein
SPNOXC_09900	-	-2.00877	putative GTP-binding protein
SPNOXC_03970	-	-2.07708	putative decarboxylase
SPNOXC_18130	-	-2.0729	acyltransferase family protein
SPNOXC_06100	*pabB*	-2.11005	putative chorismate binding enzyme – folate biosynthesis
Gene class: Stress Response			
SPNOXC_08520	-	-2.00877	PhoH-like protein; K06217 phosphate starvation-inducible protein PhoH and related proteins
SPNOXC_07390	*clpE*	-3.14627	putative ATP-dependent Clp protease ATP-binding subunit
SPNOXC_18480	-	-2.61973	putative peptidase
Gene class: DNA-associated			
SPNOXC_07660	*parC*	-2.22741	topoisomerase IV subunit A
SPNOXC_07760	*dnaH*	-2.31487	DNA polymerase III subunit gamma/tau
SPNOXC_07870	-	-2.33593	DNA translocase FtsK
SPNOXC_17080	*recA*	-2.70314	recombinase A
SPNOXC_16460	*scpB*	-2.18161	segregation and condensation protein B
SPNOXC_16470	*scpA*	-2.0603	segregation and condensation protein A

			hypothetical protein; K03581
SPNOXC_03900	-	-2.03477	exodeoxyribonuclease V alpha subunit
SPNOXC_11960	*mecA*	-1.95533	adapter protein MecA – negative competence regulator
Gene class: Uncharacterised proteins an pseudogenes			
SPNOXC_18190	-	-3.12223	hypothetical protein
SPNOXC_05440	-	-2.45623	leucine-rich protein
SPNOXC_02230	-	-2.20469	putative lipoprotein
SPNOXC_13160	-	-1.9823	hypothetical protein
Gene class: tRNA and ribosomal	-		
SPNOXC_18520	*tyrS*	-3.31487	putative tyrosyl-tRNA synthetase
SPNOXC_19320	-	-2.08539	putative tRNA-dihydrouridine synthase
SPNOXC_02840	*proS*	-1.92785	prolyl-tRNA synthetase

When the *S. pneumoniae* transcriptome in co-culture at 336 h was compared to the transcriptome at 24 h in co-culture, several major changes occurred at 336 h (Table 6.11). At 336 h, there was an up-regulation of PTS sugar transporters, carbohydrate utilisation genes, 2 amino acid biosynthesis genes, thiamine metabolism, 7 stress response genes predominantly involved in protein folding and degradation, 2 putative transcriptional regulators as well as the *padR*, *gntR* and *deoR* regulators, 2 putative antitoxins from the *pezA* and *yafQ/dinJ* systems, 2 purine metabolism genes, several cell-wall associated genes and a chromosome partitioning protein. Down-regulated genes included a MerR like regulator and its target genes, some metabolic genes including a cell wall degradation gene and 2 purine biosynthesis genes, several DNA-associated genes including 2 transposases and an RM system gene, and 2 genes putatively involved in a two –component regulatory system.

Table 6.11. Up- and down- regulated genes in *S. pneumoniae* strain 11 at 336 h in co-culture with *H. influenzae* in a flow cell with CDM with glucose (SCV phenotype), compared to *S. pneumoniae* strain 11 in co-culture with *H. influenzae* in a flow cell system with CDM with glucose at 24 h (wild-type phenotype).

Upregulated genes ID	Gene name	log_2Fold Change	Function
Gene class: Sugar transport			
SPNOXC_14790	-	2.080373	extracellular solute-binding lipoprotein
SPNOXC_10580	*ptsH*	2.209987	histidine-containing phosphocarrier protein
SPNOXC_18590	*malX*	3.715527	putative maltose/maltodextrin-binding protein precursor
SPNOXC_03340	*agaW*	3.176589	putative N-acetylgalactosamine-specific PTS
SPNOXC_03350	*agaD*	3.24476	putative N-acetylgalactosamine-specific PTS component
SPNOXC_13890	*msmK*	2.675565	multiple sugar-binding transport ATP-binding
SPNOXC_04370	*glnQ2*	2.703519	putative putative glutamine ABC transporter
SPNOXC_17820	-	2.511899	PTS putative lactose-specific phosphotransferase
SPNOXC_18610	*malD*	2.544321	putative maltose/maltodextrin ABC transport system permease protein
SPNOXC_17810	-	2.38428	putative exported PTS system protein
SPNOXC_07860	*fruA*	2.23362	PTS putative fructose-specific phosphotransferase
SPNOXC_15150	*scrA*	2.160992	PTS component putative sucrose-specific phosphotransferase
SPNOXC_18600	*malC*	2.192019	putative maltose/maltodextrin ABC transport
Gene class: Transport			
SPNOXC_12630	-	3.880604	putative ABC transporter
SPNOXC_15090	-	2.127517	ABC transporter ATP-binding protein
SPNOXC_16060	-	2.392317	putative iron ABC transporter, solute-binding protein
Gene class: Carbohydrate utilization/metabolism			
SPNOXC_03300	*idnO*	3.351675	putative gluconate 5-dehydrogenase (oxidoreductase in PPP)
SPNOXC_18570	*glgP*	2.824949	putative glycogen phosphorylase (starch and sucrose metabolism)

SPNOXC_16250	*galT*	2.544321	galactose-1-phosphate uridylyltransferase (galactose metabolism)
SPNOXC_18580	*malQ*	2.528661	putative 4-alpha-glucanotransferase (starch and sucrose metabolism)
SPNOXC_03270	*kgdA*	4.544321	PPP putative 4-hydroxy-2-oxoglutarate aldolase/2-dehydro-3-deoxy-phosphogluconate aldolase
SPNOXC_04430	*pfl*	2.289614	formate acetyltransferase (pyruvate metabolism)
SPNOXC_14540	*gpmA*	2.222392	2,3-bisphosphoglycerate-dependent phosphoglycerate mutase
SPNOXC_18790	-	2.129283	putative transketolase subunit
SPNOXC_18800	-	2.129283	putative transketolase subunit
SPNOXC_12470	*nagB*	1.910448	glucosamine-6-phosphate isomerase
SPNOXC_07850	*fruK*	2.010888	putative 1-phosphofructokinase
SPNOXC_03500	*dexB*	2.073574	glucan 1,6-alpha-glucosidase
Gene class: Amino acid metabolism			
SPNOXC_05370	*metE*	2.309855	5-methyltetrahydropteroyltriglutamate--homocysteine methyltransferase
SPNOXC_13370	-	2.029747	putative cystathionine beta-lyase
Gene class: Vitamin and cofactor synthesis			
SPNOXC_06490	*thiM*	1.994982	hydroxyethylthiazole kinase
SPNOXC_06500	*thiE*	2.444785	thiamine-phosphate pyrophosphorylase
Gene class: Stress Response			
SPNOXC_06040	-	2.080373	putative redoxin
SPNOXC_03470	*clpL*	2.42947	putative ATP-dependent protease ATP-binding
SPNOXC_08820	*prsA*	1.911692	foldase protein PrsA precursor
SPNOXC_17550	-	2.41879	putative universal stress protein
SPNOXC_16780	*groEL*	2.208317	chaperonin
SPNOXC_16790	*groES*	2.759199	chaperonin
SPNOXC_19810	*htrA*	3.300968	serine protease
Gene class: Regulators			
SPNOXC_09280	-	2.129283	putative regulatory protein
SPNOXC_14720	-	1.994982	ROK family protein
SPNOXC_01270	*padR*	2.176589	PadR-like family regulatory protein
SPNOXC_07840	*deoR*	2.222392	DeoR family regulatory protein
SPNOXC_15080	*gntR*	2.372689	GntR family regulatory protein
Gene class: Toxin/antitoxin system			

SPNOXC_09470	*pezA*	2.681824	putative epsilon antitoxin
SPNOXC_02930	*dinJ*	2.807355	putative plasmid stabilization system antitoxin
Gene class: Antimicrobial resistance			
SPNOXC_06980	-	1.983205	putative cyclophilin type peptidyl-prolyl cis trans isomerase
Gene class: Purine metabolism			
SPNOXC_07480	*deoD*	2.255815	putative purine nucleoside phosphorylase
SPNOXC_07460	*punA*	2.090289	putative purine nucleoside phosphorylase
Gene class: Cell-wall associated			
SPNOXC_01130	-	4.076915	cell wall surface anchor family protein
SPNOXC_01350	-	2.366188	putative peptidoglycan-binding protein
Gene class: DNA-associated			
SPNOXC_19820	*parB*	2.831571	putative chromosome partitioning protein
SPNOXC_10430	*xerC*	1.922832	tyrosine recombinase XerC
Gene class: Other Metabolic genes			
SPNOXC_14270	-	2.97728	putative acyltransferase (lpid metabolism)
SPNOXC_14880	*nanA*	2.714246	sialidase A
SPNOXC_09160	-	2.745954	putative 4-oxalocrotonate tautomerase (benzoate degradation)
Gene class: Uncharacterised genes and opseudogenes			
SPNOXC_07450	-	2.807355	conserved hypothetical protein
SPNOXC_10310;pseudo=true	-	2.807355	pseudogene
SPNOXC_03510;pseudo=true	-	2.681824	pseudogene
SPNOXC_00090	-	2.61471	conserved hypothetical protein
SPNOXC_07880	-	2.889149	putative membrane protein
SPNOXC_09400	-	2.922832	uncharacterised protein
SPNOXC_12620	-	3.24476	putative ABC transporter
SPNOXC_16160	-	3.431846	hypothetical protein
SPNOXC_09390;pseudo=true	-	4.105035	pseudogene
SPNOXC_03360	-	2.392317	putative membrane protein

SPNOXC_14320	-	2.392317	conserved hypothetical protein
SPNOXC_06830	-	2.351675	conserved hypothetical protein
SPNOXC_02950	-	2.222392	putative membrane protein
SPNOXC_09250	-	2.208525	hypothetical protein
SPNOXC_10530	-	2.080373	putative uncharacterised protein
SPNOXC_12590;pseudo=true	-	2.080373	pseudogene
SPNOXC_17310	-	1.983374	putative membrane protein
SPNOXC_09420	-	1.984893	putative uncharacterised protein
SPNOXC_01600	-	1.969626	putative membrane protei
Downregulated genes			
Gene class: MerR regulator and regulated genes			
SPNOXC_16280	-	-4.27403	zinc-binding dehydrogenase
SPNOXC_16300	-	-4.16227	cation efflux family protein
SPNOXC_16290	-	-4.09954	MerR family regulatory protein
Gene class: Metabolic			
SPNOXC_18880	*gcnA*	-2.06711	N-acetyl-beta-D-glucosaminidase (degradation of cell wall??)
SPNOXC_04620	-	-1.97353	putative endo-beta-N-acetylglucosaminidase lytB
SPNOXC_18920	-	-2	putative alpha-1,2-mannosidase
SPNOXC_01020	*agaS*	-2.36257	putative tagatose-6-phosphate aldose/ketose isomerase
SPNOXC_18900	-	-2.84472	putative glycosyl hydrolase (glycan biosynthesis and metabolism)
SPNOXC_02870	-	-2.17769	luciferase-like monooxygenase
SPNOXC_18200	-	-2.04064	putative haloacid dehalogenase-like hydrolase
SPNOXC_07910	-	-2.36257	Esterase
SPNOXC_04300	*alsS*	-2.44503	acetolactate synthase large subunit (amino acid biosynthesis)
SPNOXC_12900	-	-2.26699	SNO glutamine amidotransferase family protein (metabolism of cofactors and vitamins)
SPNOXC_00900	*purH*	-2.22507	bifunctional purine biosynthesis protein PurH
SPNOXC_00910	*purD*	-2.19265	phosphoribosylamine-glycine ligase
SPNOXC_08990	-	-2.4355	putative cytochrome c-type biogenesis protein
SPNOXC_00630	-	-2.51457	putative deaminase
SPNOXC_08020	*pepXP*	-2.4881	Xaa-Pro dipeptidyl-peptidase
SPNOXC_13280	-	-2.77761	putative acetyltransferase
SPNOXC_06050	*msrAB*	-3.57202	peptide methionine sulfoxide reductase

SPNOXC_12850	-	-2.04891	ArsC family protein
SPNOXC_05990	-	-2.23704	putative rRNA methylase
Gene class: Transporters			
SPNOXC_01200	-	-2.14018	binding-protein-dependent transport system
SPNOXC_07090	-	-2.36257	BioY family membrane protein
SPNOXC_00980	-	-2.36257	PTS sugar phosphotransferase system (PTS), sorbose
SPNOXC_16660	*msmG*	-2.04064	multiple sugar-binding transport system permease
Gene class: DNA-associated			
SPNOXC_12700	-	-2.51457	transposase
SPNOXC_08220	-	-2.55522	putative IS1239 transposase
SPNOXC_18890	-	-2.55522	ROK family protein
SPNOXC_18070	*comYC*	-2.77761	putative competence protein
SPNOXC_19740	-	-2.77761	putative membrane protein
SPNOXC_07950	-	-3.36257	putative type I RM modification enzyme
Putative elements of a Two-component Regulatory System			
SPNOXC_19770	-	-1.97025	putative response regulator protein
SPNOXC_17610	-	-1.95818	histidine sensor kinase protein
Gene class: Hypothetical proteins and pseudogenes			
SPNOXC_18910	-	-3.63559	conserved hypothetical protein
SPNOXC_16750	-	-3.36257	pseudogene
SPNOXC_17640	-	-3.36257	putative membrane protein
SPNOXC_13020	-	-3.21818	putative uncharacterized protein
SPNOXC_16910	-	-3.09954	pseudogene
SPNOXC_05120	-	-2.77761	putative membrane protein
SPNOXC_09340	-	-2.77761	pseudogene
SPNOXC_14000	-	-2.77761	pseudogene
SPNOXC_08210	-	-2.51457	pseudogene
SPNOXC_09050	*phtE*	-2.51457	pseudogene
SPNOXC_11670	-	-2.47805	pseudogene
SPNOXC_10710	-	-2.36257	pseudogene
SPNOXC_17180	-	-2.26303	putative uncharacterized protein
SPNOXC_01430	-	-2.19265	pseudogene
SPNOXC_17650	-	-2.09954	pseudogene

6.2.8. Specific transcriptomics changes pertaining to media nutrient composition in *S. pneumoniae*.

As the transcriptomics results for *H. influenzae* and *S. pneumoniae* in co-culture were different to those previously observed in the same flow cell system but utilising HI media; as indeed were the *S. pneumoniae* cell phenotypes, a transcriptional comparison was performed between *S. pneumoniae* in co-culture in HI media and CDM media at various time-points.

Overall, in CDM media co-culture at 64 h, compared to HI media co-culture 64 h, *S. pneumoniae* up-regulated several genes specifically associated with the undetected state in CDM, including the *relE* toxin and the *gntR* transcriptional regulator, and down-regulated a group of DNA associated genes pertaining to chromosomal replication, which were down-regulated in the undetected state in the CDM comparison. Similarly, when the gene expression of *S. pneumoniae* in co-culture in CDM at 336 h was compared to the gene expression of *S. pneumoniae* in co-culture in HI media at 168 h, some of the genes associated with the SCV state, such as *gntR*, remained up-regulated. This result suggests that some genes associated with both undetected and SCV *S. pneumoniae* states were specific to these lifestyles regardless of the time of cultivation or the media utilised as a baseline for comparison. However, due to the large variation in the variables compared, and the media composition differences between HI and CDM, the data for these comparisons is not described in detail.

6.2.9. Co-culture with *S. pneumoniae* SCVs does not restore *H. influenzae* culturability in a HI-media batch model.

Previously, in a batch culture system utilising HI media, we have observed competitive interactions between *S. pneumoniae* and *H. influenzae*, whereby *S. pneumoniae* is able to outcompete *H. influenzae* in co-culture at a media pH of 7.4 (Tikhomirova et al. 2015). In the flow cell system utilising CDM, we observed the development of SCV *S. pneumoniae*, specifically in co-culture with *H. influenzae*. *S. pneumoniae* SCVs were able to grow in co-culture at all time-points without reducing *H. influenzae* culturability. As these SCV cells evolved during co-culture growth with *H. influenzae*, we hypothesised that they may be especially adapted to growing in co-culture with *H. influenzae*, in a way which may facilitate their inter-species interaction synergy.

To test whether *S. pneumoniae* SCVs are more adapted to a synergistic lifestyle with *H. influenzae*, the batch co-culture experiment utilising HI media was repeated. However, co-culture with the SCVs once again caused a reduction in *H. influenzae* culturability, as was previously observed for the wild-type *S. pneumoniae* strain 11 cells (Fig. 6.11).

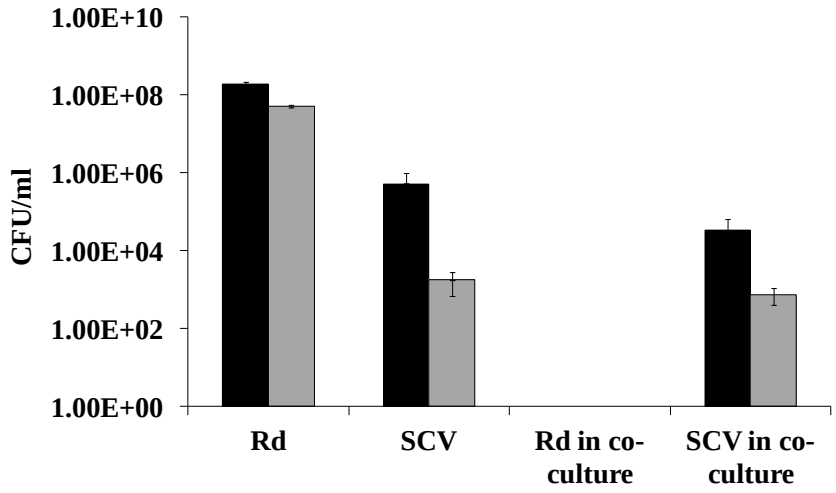

Fig. 6.11 SCVs do not restore the *H. influenzae* culturability phenotype in batch culture. The planktonic growth (black bars) and biofilm formation (grey bars) of *H. influenzae* Rd KW20 and *S. pneumoniae* strain 11 SCVs in mono- and co-culture in HI media after 14 h. *H. influenzae* was not able to grow in co-culture with SCVs in planktonic or biofilm form. However, *S. pneumoniae* SCVs were not significantly affected by the presence of *H. influenzae*.

6.2.10. *S. pneumoniae* growth in batch co-culture in CDM with lactose media does not affect *H. influenzae* culturability, but reduces *S. pneumoniae* culturability.

As the co-culture of *S. pneumoniae* and *H. influenzae* in a flow cell containing CDM+lactose medium showed a distinctive growth phenotype for *S. pneumoniae*, and suggested a co-existence of the 2 species, we tested the same co-culture in a batch culture environment to determine effects of growth phase on the outcome of these inter-species interactions in a CDM+lactose medium. The results showed that with CDM+lactose batch growth culture, *H. influenzae* remained culturable in the presence of *S. pneumoniae* in co-culture (Fig. 6.12). However, the culturability of *S. pneumoniae* was reduced in the presence of *H. influenzae*, whereby the

CFU/mL values of *S. pneumoniae* in co-culture reduced from 10^8 to 10^5 CFU/ml for planktonic cells, and no biofilm cells were detected (Fig. 6.12).

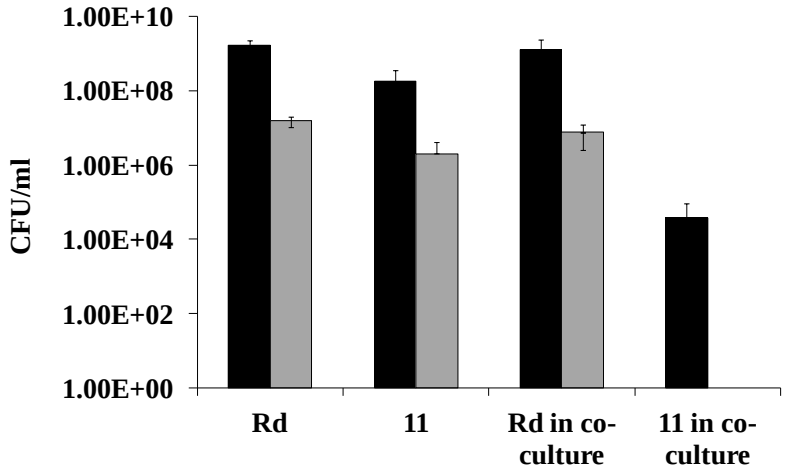

Fig. 6.12. *S. pneumoniae* strain 11 is reduced in its culturability with *H. influenzae* Rd KW20 in batch culture containing CDM+lactose media, but does not affect *H. influenzae* culturability. *H. influenzae* Rd KW20 and *S. pneumoniae* strain 11 planktonic (black bars) and biofilm (grey bars) growth is shown in batch culture in CDM+lactose media. *S. pneumoniae* strain 11 did not influence *H. influenzae* culturability, however, *S. pneumoniae* culturability in co-culture was reduced, for both the planktonic and biofilm state.

6.2.11. *S. pneumoniae* has a reduced culturability in co-culture, but enhances *H. influenzae* culturability in co-culture, in CDM with glucose batch culture.

To test the effect of growth phase on the interactions between *H. influenzae* and *S. pneumoniae* in the CDM+glucose medium, we repeated the co-culture experiment in a batch culture format. The results of this experiment were strikingly different to those obtained utilising lactose as the carbon source. In mono-culture, *H. influenzae* was only culturable in the biofilm state, however it became culturable in both the planktonic and biofilm state in co-culture (Fig. 6.13). In contrast, *S. pneumoniae* was culturable in both the planktonic and biofilm form in mono-culture (10^9 and 10^6 CFU/ml respectively), but became completely non-detectable in co-culture (Fig. 6.13).

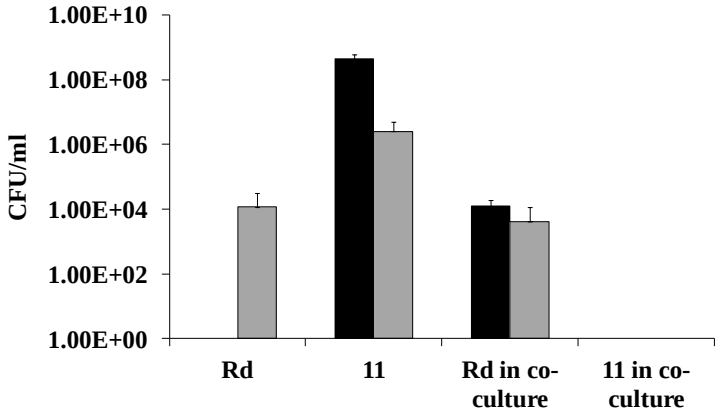

Fig. 6.13. *S. pneumoniae* strain 11 has a reduced culturability in co-culture, but enhances *H. influenzae* culturability in co-culture, in CDM+glucose medium batch culture. *H. influenzae* Rd KW20 and *S. pneumoniae* strain 11 planktonic (black bars) and biofilm (grey bars) growth is shown in CDM+glucose media. The presence of *S. pneumoniae* permitted *H. influenzae* planktonic growth in co-culture, while it was not observed in mono-culture. However, co-culture growth of *S. pneumoniae* produced no detectable CFU/ml, in contrast to what was observed in mono-culture.

6.2.12. Transcriptomics changes in *H. influenzae* and *S. pneumoniae* in the CDM+glucose flow cell - Summary.

6.10. Spn CDM co-c 72 vs Spn co-c 24
Up: ***Sugar transport and metabolism, MATE, padR, gntR, argR, comEA, comYC, endonuclease and transposase, stress response, relE phage shock protein***
Down: ***ABC transporters, stress response, Chromosomal replication: parC, dnaH, scpA-B***

CDM+glucose
FC

6.11. Spn CDM co-c 336 h vs Spn co-c 24 h
Up: ***Sugar transport and utilisation, thiM, thiE, stress response, padR, gntR, deoR, purine metabolism, pezA ,dinJ, parB***
Down: ***merR, adhC, transposases, 2 compoenent regulatory system/s***

6.6. Hi mono 64 h CDM vs Hi mono 72 HI
Up: ***yfeA-D, hxuA-C, modA-C, thiD-E***
Down: ***dmsA-C, glpA-B, modA-E, stress response, phage, xseA, recF***

6.7. Hi co-c 64 CDM vs Hi co-c 64 HI
Up: ***yfeA, hxuB, modA-C, thiD-E, merP, napC,D,G***
Down: ***dmsA-C, yecK, recF and DNA Polymerase, Mu-like phage.***

6.8. Hi mono 336 h CDM vs Hi mono 164 HI
Up: ***yfeA-D, modA-C, thiamine biosynthesis, ccmB-D, ZapB, stress response, hindII RM, starvation inducible DNA binding protein, fis***
Down: ***Mu-like phage, glpA-C,K, dmsA-C, yecK, DNA polymerase***

6.9. Hi co-c 336 f CDM vs Hi co-c 164 h HI
Up: ***yfeA, yfeC, modA-C, thiD-E***
Down: ***dmsA-C, glpA-C, yecK, stress response, Bacteriophage***

6.1. Hi mono CDM co-c 24 h vs mono 24 h
Up: ***H_2O_2 defence genes, starvation inducible DNA-binding protein, msrA***
Down: ***IlvC, trpE, gdhA Mu-like phage***
(Note: at 72 h and 336 h – no difference between *H. influenzae* mono- and co-culture)

6.2. Hi CDM mono 64 h vs *H. influenzae* mono 24 h
Up: ***hxuA-C, yfeA-D, thiamine biosynthesis, stress response, serine metabolism, cytochrome C biogenesis***
Down: ***fatty acid biosynthesis, dmsA-C ,nrfA-D, amino acid biosynthesis***

6.3.Hi CDM co-c 64 h vs Hi co-c 24 h
Up: ***hxuA-C, yfeA-D, thiamine metabolism, glpA-C***
Down: ***dmsA-C, dicarboxylate transport***

6.4.Hi CDM mono 336 h vs Hi mono 24 h
Up: ***yfeA-D, hxuA-C, thiamine biosynthesis, stress response,, cytochrome C biogenesis protein***
Down: ***Mu-like phage, amino acid biosynthesis, dmsA-C, fatty acid biosynthesis***

6.5. Hi CDM co 336 h vs Hi co 24 h
Up: ***yfeA-D, hxuA-C, thiamine metabolism,, stress response.***
Down: ***dmsA-C, fatty acid biosynthesis, rsgA***

Fig. S6.1. A summary of up- and down-regulated genes in *H. influenzae* and *S. pneumoniae* in the CDM+glucose flow cell system presented in Tables 6.1-6.11.

6.3. Discussion

Our results have shown that the growth phenotype of *H. influenzae* Rd KW20 and *S. pneumoniae* strain 11 in a flow cell are vastly different, when growth is performed in a CDM media compared to a rich HI media, and furthermore it depends on the carbon source used (glucose or lactose).

In a flow cell, when either glucose or lactose was used as the carbon source, *H. influenzae* reached identical cell numbers in mono-culture and co-culture (Fig. 6.1; 6.5). In addition, both in glucose and lactose media, *S. pneumoniae* 11 was unable to form detectable colony forming units in mono-culture (Fig. 6.1; 6.5). However, during co-culture the outcome for *S. pneumoniae* strain 11 was different. In lactose CDM, no *S. pneumoniae* was detected in co-culture until 288 h and 336 h time-points, suggesting a long lag phase of *S. pneumoniae* and adaptation to the nutrient limited co-culture environment. The cells identified at these time-points also appeared phenotypically different and were unable to grow on blood agar, or blood agar supplemented with gentamycin (Fig. 6.5). This effect may have been due to the cells existing in a biofilm lifestyle – as an extensive EPS matrix was observed in the co-culture situation in CDM+lactose media, but not in *H. influenzae* mono-culture – suggesting a potential selective switch to biofilm formation in the co-culture environment (Fig. 6.6).

In glucose containing CDM, *S. pneumoniae* strain 11 was detected in co-culture at 24 h, after which there were no viable cells until 336 h (Fig. 6.1). At 336 h, *S. pneumoniae* colonies were present and were all small and non-mucoid (Fig. 6.2), although they were haemolytic and able to grow on blood agar containing gentamycin. The complete absence of *S. pneumoniae* in mono-culture and its presence in co-culture, suggests that the presence of *H. influenzae* stimulated the growth of *S. pneumoniae* and its survival in the nutrient-limited flow cell system – both in glucose and lactose CDM. In glucose media, the time-gap between the first time-point of detectable *S. pneumoniae* in co-culture at 24 h, and the second time-point of detection at 336 h, indicates a period of adaptation of *S. pneumoniae* to growth conditions, and the establishment of an optimally adapted small colony-type. These SCV cells appeared phenotypically normal by visualisation with SEM (Fig. 6.3). We proposed, that in the "undetected" state, between 24 h and 336 h, *S. pneumoniae* was present in the co-culture, but was in a dormant, persister-cell like state in which it was adapting to the non-optimal conditions.

Testing the ability of the SCV of *S. pneumoniae* to grow in the flow cell system in mono-culture and co-culture in a CDM+glucose media flow cell, showed that the SCV was more adapted to this environment than its parental, non-SCV, wild-type counterpart. Although the SCV was unable to grow in mono-culture up to 312 h, it was stably present in co-culture at all time-points (Fig. 6.8; Fig. 6.9). This result suggests that these *S. pneumoniae* SCVs are highly adapted to growth in a glucose dominated nutrient limited environment, however, their growth is highly dependent on the presence of *H. influenzae*. This raises an intriguing consideration for prolonged co-infection by these bacteria, particularly relevant to chronic diseases such as COM. Importantly, at 336 h the SCV cells re-appeared when in mono-culture and remained present until 408 h. This is an indication of the ability of the SCVs to eventually adapt to mono-culture growth in a nutrient limited environment, however, the contrast in the time of adaptation is significant, and it is evident that although the SCVs were able to eventually adapt to a mono-culture environment, they were nevertheless, more optimally adapted to growth in co-culture in these conditions.

In order to predict molecular changes responsible for the formation of *S. pneumoniae* undetected cells and SCVs and potentially the basis for altering the interactions between *H. influenzae* and *S. pneumoniae*, several transcriptomics analyses were performed, both of *H. influenzae* in mono- and co-culture and *S. pneumoniae* in co-culture at 24 h, 64 h and 336 h.

Transcriptomic analysis of *H. influenzae* mono-culture and co-culture at 24 h, 64 h and 336 h, showed that there was an initial adaptation of *H. influenzae* to the presence of *S. pneumoniae* at 24 h (resulting mainly in an up-regulation of genes involved in protection against H_2O_2, such as alkylhydroperoxidase and catalase; Table 6.1). This result would be expected at this early time-point, as *S. pneumoniae* was in a detectable state at this time-point and would be producing H_2O_2 as a result of its metabolism. However, at 64 h and 336 h, *H. influenzae* did not significantly differentially express any genes in co-culture compared to mono-culture. One reason for this could be that the undetectable *S. pneumoniae* cells at 64 h and the SCV cells at 336 h, are more adapted to co-culture growth with *H. influenzae*, and, after an initial adaptation of *H. influenzae* to the presence of *S. pneumoniae*, both species are able to co-exist in co-culture without resulting in an alteration of the *H. influenzae* transcriptome. Conversely, lack of active growth of the *S.*

pneumoniae at 64 h and an altered growth state at 336 h, could reduce the impact of H_2O_2 stress on *H. influenzae*.

For a more in-depth analysis, the transcriptomic changes of *H. influenzae* between time-points were compared in mono-culture and co-culture. Overall, the adaptation to a longer-term growth was similar for *H. influenzae* in mono-culture and co-culture, with an up-regulation of iron acquisition genes and thiamine metabolism genes (suggesting a limitation in iron and thiamine at later growth time-points – or an increased requirement of these), and a down-regulation of dimethylsulfoxide reductase. Intriguingly, there were some differences observed in genes differentially expressed between mono-culture and co-culture. One of these differences was that nitrite reductase genes which were down-regulated in mono-culture, were no longer differentially expressed in co-culture. In contrast, metabolism associated genes including D-lactate dehydrogenase, cytochrome C biogenesis protein and pyruvate formate lyase (PFL), were up-regulated in mono-culture at 64 h, however, these too were no longer differentially expressed in the co-culture comparison (Table 6.2; Table 6.3). Nitrite reductase genes have recently been shown to be up-regulated in *H. influenzae* grown in RPMI-based CDM in anaerobic conditions, whereas D-lactate dehydrogenase and PFL were up-regulated in all levels of oxygenation (Othman et al. 2014). The observation that these genes were not differentially expressed in the co-culture time-point transition, may suggest that *S. pneumoniae* generates a more anaerobic environment for *H. influenzae* at later growth time-points (resulting in a lack of down-regulated *nrf* genes), or that it may be reducing the rate of respiration of *H. influenzae*, resulting in the lack of up-regulation of cytochrome C biogenesis protein, D-lactate dehydrogenase and pyruvate formate lyase. The up-regulation of glycerol metabolism genes in the co-culture transition, and the lack of differential expression of these genes in the mono-culture comparison, may likewise be an indication of *S. pneumoniae* modification of *H. influenzae* metabolism over time. Such subtle metabolic alteration could also account for the lack of up-regulated stress response genes in co-culture, if the metabolic changes, such as a reduced rate of respiration, did indeed account for a lowered production of reactive metabolic by-products with a potential for cellular damage.

From the 24 h to 336 h time-span, genes up-regulated in mono-culture which were not up-regulated in co-culture included several stress response genes, while genes down-regulated in mono-culture, which were not down-regulated in co-culture included Mu-like phage genes and

amino acid biosynthesis genes. While the function of the Mu-like phage in these interactions is not clear, we have previously observed it to be down-regulated in co-culture in a batch environment (Tikhomirova et al. 2015). The lack of up-regulation of stress response genes in co-culture may suggest that *S. pneumoniae* has a role in reducing the environmental stressors on *H. influenzae* which was also suggested by the transcriptomics results comparing *H. influenzae* gene expression from 24 h to 64 h. In the comparison of *H. influenzae* gene expression in co-culture between these time-points, *S. pneumoniae* affected *H. influenzae* respiration over time, and did not induce an up-regulation of *H. influenzae* stress response genes, which were observed to be up-regulated between these time-points in mono-culture. Therefore, it is possible that by modifying *H. influenzae* metabolism, *S. pneumoniae* may simultaneously be reducing reactive and damaging metabolic by-products produced inherently by *H. influenzae* during its metabolism.

In this study, the presence of *S. pneumoniae* in co-culture did not affect *H. influenzae* gene expression, and only caused subtle changes in the adaptation of *H. influenzae* over the course of different time-points. This was in contrast to what we observed previously in HI media, where *S. pneumoniae* caused significant transcriptomic changes in *H. influenzae* in co-culture (Tikhomirova et al. 2015). There could be several reasons for such a difference, including the different phenotypic and physiological states of the *S. pneumoniae* cells, as well as the difference in the media composition and its effect on metabolic systems in *H. influenzae*. Therefore, in order to investigate any potential effects of CDM media on *H. influenzae* gene expression, the *H. influenzae* transcriptome in CDM at 64 h and 336 h was compared to the transcriptomes determined from growth in HI media at 64 h and 168 h, both in mono-culture and co-culture respectively (Table 6.6-6.9). The results showed, that at 64 h in CDM media, there was a consistent up-regulation of iron and molybdenum uptake genes and thiamine biosynthesis genes, both in mono- and co-culture (Table 6.6-6.7). There was also a general consistent down-regulation of dimethylsulfoxide reductase, several phage associated genes and stress response genes. Overall, these results suggested, that in a CDM media (irrespective of the presence of *S. pneumoniae*), *H. influenzae* experienced limitations in its required levels for iron, molybdenum and thiamine. Importantly, however, some differences were uncovered. When *H. influenzae* at 64 h in CDM and HI media was compared in co-culture, there was an up-regulation of *napC, napD* and *napG* genes involved in anaerobic respiration (Smith et al. 2013). In addition, the down-

regulation of molybdenum co-factor, which was observed in the mono-culture comparison, was not present in co-culture. Hence, it is likely that when *H. influenzae* is in co-culture in CDM (compared to HI media co-culture), it adopts a more anaerobic metabolism, requiring higher expression of the nitrate reductase (*nap*) genes, as well as the molybdenum cofactor, an essential element of the functioning of the nitrate reductases (Coelho and Romão 2015). In contrast, when *H. influenzae* exists in mono-culture, its respiration in CDM and HI media is comparable.

Similarly, when *H. influenzae* in CDM at 336 h was compared to HI media at 168 h (Table 6.8-6.9), some similarities were observed between mono-culture and co-culture transcriptomics changes mediated by the change in nutrient composition of the media. In both comparisons, up-regulated genes included those involved in iron uptake, molybdate uptake and thiamine biosynthesis. In mono-culture, change from HI media to CDM caused an up-regulation of cytochrome C assembly genes, which were not up-regulated in the co-culture change from HI media growth to CDM media. This observation suggests that there are differences in *H. influenzae* respiration in HI media and CDM at later growth time-points, but also, these are related to the presence of *S. pneumoniae*. In addition, in mono-culture, there was an up-regulation of stress response and restriction modification system associated genes in CDM, which were not differentially expressed in the co-culture analysis. It is possible, that in the presence of *S. pneumoniae*, due to alterations in respiration in CDM, *H. influenzae* experiences less physiological stress, resulting in the lack of up-regulation of stress response genes and restriction endonucleases. Partially confirming this, was the down-regulation of stress response associated genes in CDM in the co-culture comparison, which were not differentially expressed in mono-culture (Table 6.2-6.5).

The analysis of the *S. pneumoniae* transcriptome in co-culture at 3 different time-points (24 h, 64 h and 336 h), enabled a detection of potential molecular factors involved in mediating the transition of *S. pneumoniae* cells from a normal state at 24 h to an undetected state at 64 h, and a SCV state at 336 h, respectively. Although the alignment of transcriptomics libraries to the *S. pneumoniae* reference genome (OXC_141) uncovered a low level of alignment, and subsequently low level of significance of the data, results presented represent an initial putative analysis, on the basis of which further research would expand, to gain a deeper and more statistically significant analysis of the *S. pneumoniae* physiological states.

Transcriptomic comparison of *S. pneumoniae* in an initial detectable state at 24 h to the undetected state at 64 h, identified global transcriptomics changes occurring which resulted in the phenotypic change from wild-type colony types to an undetectable lifestyle (Table 6.10). Interestingly, in the undetected state, a putative plasmid addiction system toxin protein was up-regulated. This up-regulation of the toxin protein *relE* of the toxin/antitoxin system is of high interest, as toxin/antitoxin systems have been implicated in persister cells. Such persister cells have previously been described to form following antibiotic treatment – while an actively growing majority of bacterial cells were susceptible to antibiotic treatment, a sub-population were not. These persister cells were identified to be resistant to antibiotics not simply due to the presence of antimicrobial resistance genes, but rather due to a dormant, non-dividing physiological state (Lewis 2007). The presence of a toxin/antitoxin system has the potential to induce the cell into a "dormant" state, in the presence of nutrient starvation or stress, as such chromosomally encoded toxin/antitoxin systems can act as regulators of growth, inducing a dormant state in non-optimal growth conditions until favourable conditions are restored (Van Melderen and Saavedra De Bast 2009; Wang and Wood 2011). Several of the up-regulated genes have also previously been described for other bacterial species to be important in the persister cell state. The *gntR* regulator has previously been identified as overexpressed in several dormant states of *Mycobacterium tuberculosis*, although its specific function in *S. pneumoniae* remains unclear (Keren et al. 2011; Zhang et al. 2012). Additionally, a suite of stress response genes that have also been associated with persister cells were up-regulated in the undetected *S. pneumoniae* state; this set included a *dnaK* chaperone, *htrA* and *clpL* proteases, as well as the phage shock protein. In a previous study of *E. coli* persister cells, SOS stress response genes, phage shock operon genes and heat- and cold-shock response genes were up-regulated in persister cells (Keren et al. 2004). Phage shock protein genes have been shown to play a role in the presence of extracytoplasmic stress, and to be important in bacterial survival in stationary phase environments. These proteins are hypothesised to maintain cell membrane integrity or the proton motive force (Darwin 2005). Importantly, a MATE (multi-antimicrobial extrusion family transporter) was also up-regulated in the undetected state. This finding is important, as persister cells are characterised by their increased tolerance to antimicrobials, and while the antimicrobial resistance of persister cells is attributed primarily to an induction of a dormant state, up-regulation of antimicrobial resistance genes in this state, cannot be excluded. Recently, it was

shown that oxidative stress induced persister cell formation and subsequent antimicrobial resistance in *E. coli* (Wu et al. 2012). Persister cells have also been reported to form at the highest frequency in stationary phase. As these undetected *S. pneumoniae* cells formed in a flow cell system representing some aspects of a stationary phase of growth, and in a nutrient-limited growth medium, which would likely present a stress on the cells, it is reasonable that the induction of intrinsic stress response mechanisms stimulate the entry into a persister cell state. It is interesting that metabolic processes did not appear to be haltered in this comparison; a similar number of metabolic proteins were down-regulated and up-regulated, with some amino acid and purine biosynthesis and a large number of carbohydrate transport and utilisation genes being up-regulated. However, a large group of DNA associated genes related to chromosome replication, including topoisomerases and a DNA polymerase, were down-regulated, clearly suggesting a drastic down-regulation of chromosomal replication in the undetected state; an observation consistent with the lack of detection of viable cells. In addition, persister cells have been associated with a generalised reduction in division rate, accompanied by reductions in cellular functions such as an inhibition of translation (mediated by the *rmf* gene) or septation (mediated by the *sulA* gene) (Lewis 2007).

At 336 h, we observed the re-emergence of *S. pneumoniae* in the co-culture flow cell, however the *S. pneumoniae* colonies had a small and non-mucoid phenotype. Previously, SCVs have been described for *S. pneumoniae*. The emergence of SCVs from a serotype 3 strain after growth in a biofilm reactor has been documented (Allegrucci and Sauer 2007). These cells had an increased adhesion, aggregation and biofilm formation, however while they were observed to be acapsular as a result of a deletion of *cps3DSU* operon, there was no further global investigation into their genome or transcriptome. An earlier study has also described the emergence of reversible acapsular serotype 3 strains in a continuous growth sorbarod reactor, and this was associated with the duplication of the capsule-related *cap3A* gene, as well as other genetic changes (Waite et al. 2001; Domenech et al. 2009). Another study investigating the small non-encapsulated variant of an 18C strain developed *in vivo*, also observed this effect to be determined by a mutation in *cpsE*, resulting in lack of capsule production; this SCV had an up-regulation of early competence genes, and an enhanced growth phenotype (Schaffner et al. 2014).

Our results suggest that there is a global transcriptomics response in the SCV phenotype, and that the development of SCVs is likely to be dependent on more factors than solely alterations in capsular genes, or an up-regulation of the competence operon.

When the transcriptome of the *S. pneumoniae* SCVs at 336 h was compared to that of the parental cells of *S. pneumoniae* from 24 h, several major transcriptomics changes were observed (Table 6.11). At 336 h, there was an up-regulation of PTS sugar transporters and carbohydrate utilisation genes, 2 amino acid synthesis genes and thiamine metabolism genes, and purine degradation genes. This was expected, as the cell numbers in the SCV state, exceeded those observed at 24 h, indicating an increased rate of cell division. It is interesting, however, that many of these genes were also up-regulated in the undetected state; this suggests that a differential expression of sugar uptake and utilisation may be generally associated with both an undetected and SCV state, and is not necessarily related to metabolic rate. However, an up-regulation of a chromosome partitioning protein, indicating an increased rate of cell division and chromosome replication at 336 h, did suggest a potentially elevated replication rate. In addition, in the SCV state, there was an up-regulation of 7 stress-response genes (predominantly proteases and chaperones) including *groES, groEL, htrA, prsA* and *clpL*, as well as a universal stress response protein. Also up-regulated in the SCV state were 2 putative transcriptional regulators as well as the *gntR, padR* and *deoR* transcriptional regulators. It is interesting that the *gntR* regulator was also up-regulated in the undetected state, which suggests that this regulator may have several roles pertaining to altered physiological states – both undetected and SCV physiologies. Also noteworthy was that a recombinase was up-regulated at the 336 h time-point, whereas a restriction endonuclease was up-regulated at the 64 h time-point; it has recently been shown that in *E. coli*, adaptation to H_2O_2 oxidative stress, resulted in adaptation mediated by increase in mutation rate mediated by DNA repair pathways, and subsequent formation of SCV (Painter et al. 2015). Therefore, there is a possibility that genetic, as well as transcriptomic events occurred at an increased frequency between 64 h and 336 h, resulting in the SCV phenotype, and that these events may be continuing at 336 h, to provide an optimal potential for genetic adaptation to non-optimal conditions.

In addition, 2 putative antitoxins were up-regulated in the SCV state; specifically the *pezA* antitoxin of the *pezAT* system and *dinJ* of the *yafQ/dinJ* system. While the toxin genes,

putatively on the same operon, were not up-regulated (which may be a function of the low read numbers obtained in this study), the expression of the toxin/antitoxin system would suggest the potential for regulating the rate of cell division. Typically, the up-regulation of a toxin/antitoxin system is hypothesised to maintain bacteriostasis in the presence of stress or starvation. While the SCVs, in contrast to the *S. pneumoniae* cells in the undetected state, were actively dividing, the expression of the toxin/antitoxin system, and the potential homeostasis of toxin neutralisation by the antitoxin, could provide a means to control the rate of cell division, without actively inducing complete bacteriostasis.

In order to confirm that the gene expression observed in *S. pneumoniae* at 64 h, in the undetected state, and at 336 h, in the SCV state was truly relevant to the cell state, and not solely the time of culture in the flow cell system, we performed a parallel analysis of *S. pneumoniae* grown in co-culture with *H. influenzae* in HI media to the *S. pneumoniae* grown in co-culture with *H. influenzae* in CDM (obtained in the current experiment). This analysis ensured that similar time-points were compared, and allowed for an analysis of nutrient-dependent pathways differentially expressed at the same time-point, but between different nutrient (and cell phenotype) conditions.

When the *S. pneumoniae* transcriptome in co-culture at 64 h in HI media was compared to the *S. pneumoniae* transcriptome in the same conditions in CDM, there was a down-regulation of genes involved in DNA replication, as well as an up-regulation of genes associated with the undetected state in CDM including the *relE* toxin and the *gntR* transcriptional regulator (data not shown). It is interesting to note that likewise when the transcriptome of *S. pneumoniae* grown in co-culture in CDM media for 336 h was compared to the transcriptome of *S. pneumoniae* grown in HI media for 168 h (data not shown), some of the up-regulated genes, such as *gntR*, were the same as those previously associated with the SCV state in CDM. Overall, these results suggest that some of the genes which were differentially expressed in the undetected or SCV states of *S. pneumoniae* were specifically associated with the adoption of an alternate lifestyle, and not directly related to the transition to a different time-point of growth, or specifically to the transition to CDM.

Importantly, the results observed in the flow cell appeared to be highly dependent on this growth system, and consequently the growth phase; replication of the co-culture experiment using CDM with glucose/lactose media in batch culture showed strikingly different results compared to the

flow cell experiments. In CDM with lactose batch culture, *S. pneumoniae* culturability was reduced in co-culture, both in the planktonic and biofilm state, whereas *H. influenzae* culturability was unaffected. In CDM with glucose batch culture, *H. influenzae* culturability increased in co-culture (while it was non-culturable in mono-culture), whereas *S. pneumoniae* culturability decreased. Hence, it appears that firstly, *H. influenzae* had different abilities to survive in glucose media compared to lactose media, and secondly that depending on the media used, *S. pneumoniae* could increase the culturability of *H. influenzae*, but did not decrease it in either media. In contrast, *S. pneumoniae* culturability reduced in batch co-culture, both in glucose and lactose media. Therefore, the results observed in the flow cell system (including the non-culturability of *S. pneumoniae* in mono-culture), were very specific not only to the carbon source, but also to the growth system and growth phase.

As the SCVs developed specifically in a co-culture environment, and did not reduce *H. influenzae* culturability, we hypothesised that these strains might be more adapted to a synergistic co-culture environment lifestyle. We have previously seen that co-culture of *H. influenzae* with *S. pneumoniae* strain 11 in a batch culture model of growth utilising HI media causes a reduction in *H. influenzae* culturability (Tikhomirova et al. 2015). However, if these SCVs were indeed more adapted to a synergistic co-culture lifestyle, any genetic or physiological changes could potentially allow for an increased synergy between the species, and *H. influenzae* survival even in a batch culture setting. However, the results showed that *H. influenzae* was still not able to survive in co-culture with SCVs in batch culture in HI media. This indicates that while the SCVs were adapted to co-culture growth in a flow cell, where CDM media with glucose was used, they still retained the potential to reduce *H. influenzae* culturability when in batch growth culture.

In conclusion, our study has uncovered the development of novel physiological states of *S. pneumoniae* in a limited nutrient environment flow cell containing glucose, specifically in the presence of *H. influenzae*. These physiological states are specifically the "dormant" state where *S. pneumoniae* is undetected (at 64 h) and the SCV state at 336 h. The acquisition of these physiological states by *S. pneumoniae* did not affect the gene expression of *H. influenzae* in co-culture, but appeared to affect the *H. influenzae* transcriptome with time, as well as the *H. influenzae* transcriptome upon transition from an HI media to CDM. Both in the case of *H.*

influenzae adaptation over time, and *H. influenzae* transition from HI media to CDM, the presence of *S. pneumoniae* appeared to induce subtle changes in the expression of respiration-related genes pertaining to a more anaerobic metabolism. Importantly, a subset of genes putatively involved in the formation of the dormant and SCV state of *S. pneumoniae* was documented, with many genes correlating to previously documented molecular mechanisms known to play a role in the development of persister cells in other bacterial species. Importantly, the SCV *S. pneumoniae* did not have an interaction of increased synergy with *H. influenzae* in a batch culture model, although the SCV *S. pneumoniae* appeared to be optimally adapted to *H. influenzae* presence in a flow cell environment. Indeed, the outcome of *H. influenzae* and *S. pneumoniae* interactions, both when SCV or wild-type *S. pneumoniae* were used, appeared to be heavily influenced by the environmental conditions (batch or flow cell), nutrient composition of growth media (HI or CDM), and carbon source (glucose or lactose).

Chapter 7

Discussion and Conclusions

Overview

In this chapter, we summarise the major findings explored in this thesis. Overall, the work described in this thesis has shown that *H. influenzae* is highly sensitive to environmental conditions, and is able to adopt diverse lifestyles and accordingly regulate gene expression patterns in order to adapt to changing environmental conditions. However, more importantly, this thesis has shown that the environmental conditions pertaining to the *H. influenzae* lifestyle are complex, and are not only dependent on physical and chemical parameters but other species present in the microenvironment, including *S. pneumoniae*. Importantly, this study has shown that the environmental conditions in a multispecies environment exist in a state of fluctuation, and that depending on the specifics of the environment, each species is able to influence the other, either by inducing an altered physiological state, stimulating a co-existence, or enhancing the other species' adaptation potential.

7.1 The *H. influenzae* biofilm formation is a complex response to environmental factors.

In this thesis we have described both molecular, genetic, transcriptomic and environmental elements which influence the *H. influenzae* lifestyle. It has long been known that *H. influenzae* is capable of forming biofilm, and that its biofilm formation is vital in its colonisation of host-surfaces and in chronic disease. However, the environmental conditions pertaining to this, as well as the strain-specificity of this phenomenon, have not been well described. We have shown that the ability of *H. influenzae* to form biofilm is strain-specific, and greatly influenced by the nutritional composition of the media (rich HI media vs CDM). This strain- and nutrient-dependence, was also related to the presence of ROS or RCS stress present. For some strains the presence of stress induced biofilm formation, while for others, there was no change in biofilm formation, or even a repression of biofilm formation. While these results have shown both a dependence on strain-specific and environmental factors in the *H. influenzae* biofilm formation, further studies would render a deeper insight into the molecular mechanisms responsible for determining such a strain-specific response.

In addition, we have specifically shown the role of nickel in the biofilm formation response of *H. influenzae*. Previously, we have identified the nickel uptake system *(nikKLMQO* and its regulator *nimR*) in the *H. influenzae* laboratory strain Rd KW20. It was shown that in Rd KW20, the deletion of *nikQ* caused significant phenotypic changes. These changes included an increased hydrophobicity of the cells, as well as a more electronegative charge, and an increased aggregation and biofilm formation. In this study we have shown that these changes are accompanied by a global transcriptomics response. Overall, the *nikQ* mutant displayed an up-regulation of genes related to surface structures including LOS biosynthesis, sialic acid metabolism and type IV pili, as well as an up-regulation iron uptake genes associated with biofilm formation. In contrast, down-regulated genes included genes involved with anaerobic metabolism (*nrfDC*, *napG*), and central

metabolism (*gdhA*, *mdh*, *fumC*, *pfl*, *gapDH*, and *gpmA)*. Overall, the transcriptomics analysis suggested, that in the *nikQ* mutant of Rd KW20, there was an up-regulation of genes associated with the modification of cell-surface elements, and a down-regulation of genes associated with anaerobic respiration, and central metabolism. As biofilm cells have previously been reported to have a more reduced metabolic rate compared to their planktonic counterparts, these results indicate that in the environmental absence of nickel, *H. influenzae* induce global transcriptomics changes, assuming a more dormant metabolic state, and altering cell surface structures, which is reflected as a change in electronegativity and aggregation, as well as a resultant increase in biofilm formation. Therefore, the biofilm formation of *H. influenzae* is specifically a response to nickel levels in the environment. While nickel levels are not the only factor influencing *H. influenzae* biofilm formation, knowledge of their effect on *H. influenzae* adaptation to microenvironments is essential in understanding the *H. influenzae* biofilm formation response to multifactorial environmental conditions. We have also shown that the absence of the nickel uptake system component *nikQ* in the otitis media isolate, strain 86-028NP, also has an impact on surface charge, aggregation and biofilm formation, while at the same time reducing twitching motility. This finding indicates that in clinical strains associated with biofilm formation, nickel levels also play a role in determining the biofilm formation phenotype, as well as influencing twitching motility and inducing a more sessile biofilm existence. As strain 86-028NP is an otitis media isolate, and known to form a biofilm, this result indicates the role of low nickel levels in the biofilm formation in a more clinically relevant model, and suggests that this result is relevant across multiple *H. influenzae* strains, particularly those with a biofilm-associated lifestyle in disease.

While we have shown that nickel levels influence *H. influenzae* surface structures and thus induce biofilm formation, we have also identified the role of other EPS matrix components in the *H. influenzae* biofilm. Specifically, eDNA was shown to play a role in the biofilm formation of *H. influenzae*, and DNAse I treatment reduced biofilm formation for some biofilm-forming *H. influenzae* strains. However, the role of eDNA appeared to be varying in importance, and depended on the *H. influenzae* strains used, as well as on the media used for the assay (HI media or CDM). This finding indicates, that the biofilm formation dynamics of *H. influenzae* strains, and the EPS matrix components involved, may differ, in

different microenvironments. We have also identified the presence of the *pilA* gene, encoding for the major subunit of the type IV pilus in the majority of non-biofilm forming strains tested. While the scope of this study did not allow a more in-depth analysis of the presence and functionality of the type IV pilus in the *H. influenzae* biofilm, the finding suggests that the EPS matrix, as a complex structure comprised of various macromolecules, does not depend exclusively of the type IV pilus, and therefore, that the presence of this structure may not alone determine the biofilm formation of a strain.

7.2. There are subtle transcriptomics and genetic elements affecting *H. influenzae* adaptation to environmental conditions.

In order to obtain a better understanding of the biofilm formation response, we performed an in-depth analysis of the biofilm formation response of 2 *H. influenzae* clinical isolates obtained from different disease sources; one was a blood isolate (Eagan), and the other an otitis media isolate obtained from a healthy child (strain R3264). In this analysis, the blood isolate Eagan was not found to form a biofilm, whereas R3264 formed a biofilm, and increased biofilm formation at a more basic pH of 8.0. Transcriptomic analysis of R3264 revealed that at pH 8.0, where there was a higher level of biofilm formation, this strain displayed an up-regulation of iron acquisition genes. Given the role of iron in biofilm formation of many bacterial species, including *H. influenzae*, this was not unexpected. However, the transcriptomics of strain Eagan, displayed an up-regulation of 2 gluconate:H+ symporters, and associated gluconate (or sugar acid) metabolic genes. Some of these genes were found to be homologues to those involved in initial steps of the PPP, indicating the potential of these pathways to regulate intracellular pH, as well as induce energy-generating pathways, which could facilitate for planktonic growth at a more basic pH. While the precise pH of different sites of the human body is methodologically difficult

to precisely measure, and is known to vary between individuals and in different states of disease, it is generally accepted that the pH range of the blood is more acidic, whereas the pH range of the middle ear effusion during chronic otitis media covers a more basic range (pH 7.4-9). Therefore, these results have shown that isolates obtained from different sites (and disease states), do have adaptation mechanisms optimised to their niche, however, these are expressed as lifestyle and transcriptomic changes.

Importantly, this adaptation was a response to subtle changes in the environmental pH, whereas some more significant environmental changes caused a ubiquitous response among *H. influenzae* strains. Specifically, the co-culture of various strains with *S. pneumoniae* at pH 7.4 caused a reduction in environmental pH to pH 5.3, and a ubiquitous transition of *H. influenzae* to a non-culturable state (which we have further described as a viable but non-culturable VBNC state). While an environmental pH of 8.0, allowed for *H. influenzae* to be co-cultured with *S. pneumoniae* in a batch model, we utilised a higher pH of 8.6 to analyse the growth of a broader range of *H. influenzae* clinical isolates with *S. pneumoniae*.

At pH 8.6, there were differences in the abilities of *H. influenzae* isolates to grow in co-culture. All strains tested reduced their survival in co-culture with *S. pneumoniae* (although CFU/ml were still detected), except strains BS139 and strain BS171, which showed only a slight reduction in culturability. The biofilm formation of all strains tested, except strain BS139, also reduced in co-culture with *S. pneumoniae*. The altered phenotypes of strains BS139 and strain BS171 suggest that these strains may have an altered growth rate, resulting in being less affected by the presence of *S. pneumoniae*, and its production of acidic by-products. While these strains are predicted to lack a functional type IV pilus, their genome has not been fully sequenced, and therefore a multitude of additional factors which may affect their growth and lifestyle in co-culture was not determined. However, a future transcriptomics and genomic analysis would potentially uncover the factors responsible for the altered lifestyle in co-culture of these strains. It is noteworthy that in these studies, strain Eagan was found to form biofilm at pH 8.6, but not at pH 8.0. While the reason for this in not clear, and was not further investigated, it is possible that Eagan is able to form biofilm in specific defined environmental conditions, and that there may be a

threshold to its growth ensuring for planktonic growth at pH 7.4 and 8.0, but driving a switch to biofilm formation at pH 8.6, perhaps relevant as this higher pH is more characteristic of the pH encountered in chronic OM.

It is important that while we have previously identified the role of the nickel import system *nikKLMQO* and *nimR* in the response of *H. influenzae* to pH via the function of nickel as a co-factor for the urease enzyme involved in maintaining intracellular pH, we have also identified the requirement of this system in co-culture survival with *S. pneumoniae*. As we have shown the presence of *S. pneumoniae* to reduce acidity in co-culture, the inability of the *nikQ* mutant to remain culturable with *S. pneumoniae* even at pH 8.0 (where the wild-type was culturable), it is likely that this observation was directly linked to the lack of urease function in the absence of nickel. This result highlights the importance of nickel in the co-culture environment, and indicates for the importance of nickel and other environmental factors to be investigated in influencing *H. influenzae/S. pneumoniae* inter-species interactions and their role in chronic disease.

7.3. The outcome of *H. influenzae* and *S. pneumoniae* inter-species interactions depends on pH, nutrient availability and growth phase.

We have shown that the environmental conditions, presence of ROS and RCS induces *H. influenzae* adaptation to such environments, resulting in transcriptomic changes, which enable for a survival in such environments. Such an adaptive response can also be associated with evident changes in lifestyle, such as the induction of a biofilm existence.

We have also shown, that the presence of the opportunistic respiratory pathogen *S. pneumoniae*, alters the environmental conditions, and likewise induces the adaptation of *H. influenzae*. We have demonstrated that in a batch culture environment, *S. pneumoniae* was

able to induce *H. influenzae* to a VBNC state by increasing the acidity of the growth medium by stationary phase. However, in the same model, *H. influenzae* culturability could be restored to near-normal levels by utilising a higher pH of the growth medium. By performing RNASeq, we demonstrated that during co-culture with *S. pneumoniae* in a batch culture model in permissive conditions, *H. influenzae* alters its transcriptome, inducing the expression of a suite of genes related to stress response and bacteriophage. We have also demonstrated that in non-permissive conditions, at pH 7.4 in batch culture, *S. pneumoniae* causes the inhibition of *H. influenzae* culturability of *H. influenzae* by inducing *H. influenzae* into a VBNC state. In this state, *H. influenzae* up-regulated a large class of stress response genes, as well as several genes associated with metabolic processes, suggesting that *H. influenzae* experiences a large degree of physiological stress in this environment, but also indicating some metabolic changes in this state. We have also shown *S. pneumoniae* to undergo significant transcriptional changes in co-culture when inducing *H. influenzae* into a non-culturable state; specifically, in batch co-culture *S. pneumoniae* displayed an up-regulation of bacteriocin and phage associated genes as well as glycerol metabolism genes, and down-regulated a vast class of sugar transport and utilisation genes, including lactose utilisation genes. Importantly, these results were novel in demonstrating a potential metabolic link between *H. influenzae* and *S. pneumoniae* in co-culture.

We have also shown that in addition to pH, growth phase plays a vital role in determining the outcome of the inter-species interactions between *H. influenzae* and *S. pneumoniae*. Specifically, in a continuous flow cell system, independent of growth phase, *H. influenzae* was able to survive in the presence of *S. pneumoniae*, without entering a VBNC state.

We have shown, that in the flow cell system, *H. influenzae* and *S. pneumoniae* alter their mono-culture transcriptomes compared to the observed gene expression in a batch system.

During the transition from batch culture to flow cell growth, both at 64 h and 168 h of growth in the flow cell, *H. influenzae* up-regulated iron acquisition genes, glycerol metabolism genes and thiamine metabolism genes, compared to growth in a batch culture system. These results indicated an altered lifestyle in the flow cell system, which was supported by the novel observation of *H. influenzae* forming filamentous cells in the flow

cell environment (both in mono-culture and in co-culture), as well as by the production of an extensive EPS matrix substance in the flow cell.

Importantly, in co-culture with *S. pneumoniae*, *H. influenzae* also displayed differential gene expression compared to mono-culture growth, however, these changes were time-point specific. At 64 h, *H. influenzae* predominantly up-regulated φ-Flu bacteriophage associated genes, which were likely an early response to the presence of *S. pneumoniae*. At 168 h in co-culture, *H. influenzae* up-regulated genes involved with the transport of carbon sources and DNA synthesis, suggesting a potential enhancement of cell division at 168 h in co-culture.

S. pneumoniae was also shown to display differential gene expression from the transition from a batch culture growth to a flow cell environment. These changes included an up-regulation of iron-acquisition genes in the flow cell environment, as well as a down-regulation of glycerol metabolism genes, thiamine metabolism genes and lactose and galactose utilisation genes. Hence, the flow cell environment caused alterations in the *S. pneumoniae* lifestyle in the flow cell environment.

However, our results have further shown that the presence of *H. influenzae* in the flow cell environment, also cause changes in *S. pneumoniae* relative to its mono-culture growth. Importantly, at 64 h in co-culture, *S. pneumoniae* up-regulated several phage and bacteriocin-associated genes, as well as a large group of sugar utilisation genes, including lactose and galactose utilisation genes. At 168 h, up-regulated genes also included several sugar utilisation genes.

Overall, these results have demonstrated that the environmental conditions greatly impact the outcome of the *H. influenzae* and *S. pneumoniae* interactions. In unfavourable conditions (at low pH and in a growth phase dependent system), *S. pneumoniae* is able to reduce environmental pH, causing stress on the *H. influenzae* cells and inducing them to a VBNC state. However, in a permissive system, such as the growth phase independent flow cell, *S. pneumoniae* is able to co-exist with *H. influenzae* without any reductions in *H. influenzae* cell numbers. We have shown that in this continuous culture system, both *H. influenzae* and *S. pneumoniae* produced EPS material and appeared to be entering a

biofilm-like lifestyle. By RNASeq, we have also shown that in these conditions, *H. influenzae* does not experience cellular stress, and induces a time-specific expression of specific genes. We have also demonstrated, that in conditions where *H. influenzae* is in a VBNC state and cannot be cultured, *S. pneumoniae* down-regulated the expression of sugar utilisation genes. However, when *H. influenzae* is culturable in a flow cell system, *S. pneumoniae* up-regulates sugar utilisation genes. This is an indication of a potential metabolic-dependent relationship between *H. influenzae* and *S. pneumoniae*, which has not been demonstrated previously, and which may indicate an added complexity to the environmental-dependence of *S. pneumoniae* and *H. influenzae* inter-species interactions.

7.4. Nutrient source and growth dynamics determine the *Streptococcus pneumoniae* cell phenotype, and outcome of its interaction with *H. influenzae.*

While we had observed the differential expression of sugar transport and utilisation genes in *S. pneumoniae* to be associated with the lifestyle of *H. influenzae* (culturable vs VBNC), we hypothesised that there may be a nutrient-dependent metabolic relationship between the two species. To investigate this phenomenon further, we performed co-culture growth experiments of *H. influenzae* and *S. pneumoniae* in a flow cell environment, this time using a CDM media with a defined single carbohydrate as the carbon source (glucose or lactose).

Intriguingly, we found that the growth dynamics of *H. influenzae* and *S. pneumoniae* in a CDM environment were vastly different to the result previously obtained using HI media. In a flow cell containing CDM, when either glucose or lactose were used as a carbon source, *H. influenzae* reached identical numbers in mono-culture and co-culture. *S. pneumoniae*, however, was unable to grow in mono-culture, and in co-culture displayed a

different growth dynamic, depending on the carbon source used. When lactose was used as the carbon source, *S. pneumoniae* was undetectable in co-culture until 228 h.

When glucose was used as the carbon source, *S. pneumoniae* was initially detected in co-culture at 24 h in the wild-type state. Subsequently, it entered a period of non-detection until 336 h, where it was detected to be present, but in a small, non-mucoid colony state (SCV). Analysis of the *H. influenzae* and *S. pneumoniae* transcriptomes obtained from the flow cells containing CDM and glucose as the carbon source, showed that the transcriptional events occurring in *S. pneumoniae* in the 3 alternate physiological states are different to those observed in the wild-type cells.

In the undetectable state (compared to the wild-type), *S. pneumoniae* was shown to down-regulate genes associated with chromosomal replication processes, indicating a down-regulation of cell division. However, cells in this state were also shown to up-regulate genes involved with persister cell formation in other bacterial species. These included a suite of stress response proteins associated with protein folding as well as a phage shock protein, the *relE* toxin of a toxin/antitoxin system, as well as an antimicrobial transport protein and the *gntR* regulator previously associated with various states of persister *M. tuberculosis*. It is interesting that although cell division appeared to be reduced in this state, sugar utilisation genes were still up-regulated, indicating the continuation of metabolic processes.

In the SCV state (compared to the wild-type), *S. pneumoniae* up-regulated several gene classes which were also up-regulated in the undetected state. Up-regulated genes included those associated with sugar transport and utilisation, stress response (predominantly proteases and chaperones), *pezA* and *dinJ* antitoxins of toxin/antitoxin systems, and transcriptional regulators (*gntR*, *padR* and *deoR*). In addition, in the SCV state there was an up-regulation of a chromosome partitioning protein, suggesting a possible enhancement of cell division in this state. Hence, it appeared that overall, the transcriptomes of the undetectable and SCV state of *S. pneumoniae* displayed a similar (although not identical) transcriptional profile classified by an up-regulation of carbohydrate metabolism, stress response and toxin/antitoxin system induction. However, primarily, the undetectable state

displays a unique characteristic of a reduction in chromosomal replication and cell division.

We have also indentified that *H. influenzae* only experiences transcriptomic changes in co-culture with *S. pneumoniae* at 24 h, when *S. pneumoniae* is in the wild-type state. These changes were subtle, and predominantly related to the defence against *S. pneumoniae*-generated H_2O_2. However, when *H. influenzae* was co-cultured with *S. pneumoniae* in the undetected or SCV state, no transcriptomics differences occurred in *H. influenzae* compared to mono-culture growth. This suggests that in the undetected and SCV states, *S. pneumoniae* may be more adapted to the presence of *H. influenzae*, and its presence may therefore not affect *H. influenzae* or cause it to adapt to *S. pneumoniae* by altering its gene expression patterns. Such an optimal adaptation of SCV *S. pneumoniae* to *H. influenzae* is also supported by the observation that re-inoculated SCV cells were able to survive with *H. influenzae* in a flow cell at all time-points, without the requirement of an adaptation period, whereas these cells did require an adaptation period in order to adapt to mono-culture flow cell growth conditions.

Interestingly, however, we identified that *H. influenzae* changes alters its transcriptome in the CDM+glucose flow cell environment over time. Major changes at both 72 h and 336 h, included an up-regulation of iron-acquisition genes, thiamine metabolism and a down-regulation of DMSO reductase. Importantly, however, while these changes were observed between time-points both in mono-culture and in co-culture, co-culture comparison identified the potential for the adoption of a more anaerobic respiration by *H. influenzae* in the presence of both undetected and SCV *S. pneumoniae* cells. Therefore, there is the potential that *S. pneumoniae*, while not directly affecting *H. influenzae* gene expression in co-culture, was subtly modifying *H. influenzae* adaptation to growth in a flow cell over time.

While SCV *S. pneumoniae* cells have been previously characterised, this is the first time that *S. pneumoniae* SCVs have been identified in the context of a co-culture with *H. influenzae*. This is also the first documentation of transcriptomics events occurring in *S. pneumoniae* cells adapting to limiting conditions (in the undetected state), and those which have adapted and assumed an SCV phenotype in co-culture. Likewise, this is the first

documentation of the effects of undetected and SCV *S. pneumoniae* on the transcriptome of *H. influenzae*. Certainly this data provides interesting information about these bacteria during persistence and chronic infections, which are frequently caused by a mixed-species infection of both *H. influenzae* and *S. pneumoniae*.

7.5. Conclusions

In this thesis, we have identified the impact of environmental elements pertaining to the *H. influenzae* niches within the host on the *H. influenzae* lifestyle. We have observed that the presence of ROS and RCS relevant to both the nasopharyngeal microbiome metabolism and the host immune response, has the potential to induce biofilm formation in *H. influenzae* as a protective stress response. However, we have shown that this biofilm formation response is also linked to the nutrient sources present, and therefore, associated with the *H. influenzae* metabolism. In addition, we have shown that low nickel levels, also linked to the host immune function, likewise induce *H. influenzae* biofilm formation. This biofilm formation response in the absence of nickel was accompanied by a global transcriptomics response inducing the expression of cell surface structures and iron acquisition genes, and down-regulating anaerobic and central metabolic pathways, indicating a more dormant lifestyle characteristic of biofilm cells.

We have also identified the complex impact of pH on the *H. influenzae* lifestyle. These findings were particularly important in view of the documented difference in pH observed in different disease states; in chronic forms of otitis media with effusion, the middle ear fluid was observed to have a more basic pH ranging from pH 7.4-9.0, while the pH of blood is generally accepted as being close to neutral pH. We have interestingly observed differences in the response of two different strains (obtained from different disease states), to pH. Both strains Eagan, a blood isolate, and R3264, a middle ear isolate, displayed equal planktonic growth at pH 6.8 and 8.0. However, strain R3264 formed biofilm at both pH conditions, increasing biofilm formation at pH 8.0, whereas Eagan was unable to form a biofilm in either pH condition. We also identified, that the adaptation response of each strain from pH 6.8 to pH 8.0, was different. Strain R3264 induced the expression of iron

uptake genes, associated with a potential induction of a biofilm formation lifestyle. Eagan, however, induced the expression of gluconate:H+ symporters, as well as genes known to be involved in the ED and pentose phosphate energy production pathways. Therefore, it appears that strain Eagan, induced pathways enabling the maintenance of intracellular pH, while at the same time providing a means for energy production and planktonic growth at a more basic pH condition. This finding uniquely suggested that the response of different strains to pH (as well as potentially the response to a broader range of environmental conditions), can be mediated by subtle transcriptomics changes, and can be strain-specific.

We have also shown that pH has a broader effect on *H. influenzae* in the multispecies microbiome environment. We have shown that *S. pneumoniae* is able to lower the environmental pH of the growth media, inducing the expression of stress response pathways in *H. influenzae*. We have also shown that, if a higher pH of 8.0 is used for the growth media, *H. influenzae* is able to survive in co-culture in stationary phase, whereas if a lower pH of 7.4 is used, *H. influenzae* enters a VBNC state in which it continues gene expression, but cannot be detected by standard culture techniques. It is also important to note, that the lowering of the media pH by *S. pneumoniae* was also related to growth phase; at pH 7.4 in co-culture, *H. influenzae* was still culturable in late log phase, and at all time-points when growth was performed in a growth phase independent flow cell. This is the first report of the inter-species interactions in a flow cell environment. Importantly, while we have shown transcriptomics changes in both *H. influenzae* and *S. pneumoniae* in co-culture, one of the most notable changes was the differential expression of sugar acquisition and utilisation genes in *S. pneumoniae* when in co-culture. Importantly, these sugar utilisation genes were up-regulated in co-culture in the flow cell system, when *H. influenzae* was in a culturable state, however in the batch system co-culture, when *H. influenzae* was in a VBNC state, these genes were down-regulated. This finding suggested that there may be a more complex metabolic relationship between the two species, and that their interactions exist on a deeper level than simply co-existence which is influenced by pH.

We subsequently found, that indeed, the nutrient composition of growth media is able to influence the interactions between *H. influenzae* and *S. pneumoniae*, as well as their

lifestyle in this environment. In a flow cell containing a chemically defined medium, the dynamics observed between *H. influenzae* and *S. pneumoniae* were different, and dependent on the carbon source. When lactose was used as a carbon source, *S. pneumoniae* was not observed in mono-culture, and appeared in co-culture only after 288 h, in an altered state, whereas *H. influenzae* was observed in mono- and co-culture at all time-points.

When glucose was used as a carbon source, the inter-species dynamics differed yet again. *H. influenzae* was present in mono- and co-culture at all time-points. *S. pneumoniae* however, was not able to grow in the mono-culture environment. In co-culture, *S. pneumoniae* also displayed a different growth phenotype; while it was observed in a wild-type state at 24 h, it subsequently entered an undetected state until 336 h where it was observed in a SCV state. Interestingly, we observed that in the undetected and the SCV state, *S. pneumoniae* did not cause significant transcriptomics changes in *H. influenzae*, suggesting an optimal adaptation of *S. pneumoniae* to *H. influenzae* in these growth conditions. Upon re-inoculation into such a flow cell environment, the SCV *S. pneumoniae* were able to grow (and were culturable), in co-culture with *H. influenzae* at all time-points, indicating an optimally adapted cell type for co-existence with *H. influenzae*. We also observed that while *S. pneumoniae* did not appear to affect the *H. influenzae* transcriptome at individual time-points, it did appear to subtly modify *H. influenzae* gene expression upon its adaptation to different time-points, inducing a more anaerobic gene expression in *H. influenzae*. In addition, while the transcriptomic analysis of the *S. pneumoniae* undetected and SCV cells could only be obtained as a preliminary result, the results suggested that both in the undetected and in the SCV state, *S. pneumoniae* induced the expression of genes potentially associated with the dormant persister cell state as described in other bacterial species. In both of these altered states, it is interesting that *S. pneumoniae* did not specifically reduce the expression of metabolic genes, suggesting that such altered states may not be associated with a reduction in metabolic activity in *S. pneumoniae*, although the undetected state did display an evident down-regulation of genes associated specifically with chromosomal replication, suggesting a reduction in cell division processes.

Overall, the studies incorporated in this thesis have shown that the *H. influenzae* lifestyle in highly dependent on a multitude of environmental factors. We have also shown that *H. influenzae* is able to adapt to environmental conditions not only by inducing a biofilm formation, but also by inducing an altered VBNC state, and that the adaptation to different environmental conditions, and acquisition of altered lifestyles is governed by specific molecular factors involved in a complex transcriptomics response. In addition, we have demonstrated that in a multispecies *H. influenzae/S. pneumoniae* environment, the environmental conditions are in a dynamic state, and, while the presence of *S. pneumoniae* affects *H. influenzae*, it is also true that the presence of *H. influenzae* affects *S. pneumoniae*, and that their interactions and adaptation to each other are in a constant dynamic state. For the first time, we have described the complex transcriptomics response of *H. influenzae* and *S. pneumoniae* to a co-culture environment in both a standard batch culture and a growth phase independent flow cell environment. We have identified a potential metabolic relationship between *H. influenzae* and *S. pneumoniae*, which would require further study, and which suggests that there are more environmental factors involved in these multispecies relationships, which are in a process of constant change. We have further shown that indeed, the nutrient media and carbon source have a large effect on the *H. influenzae/S. pneumoniae* inter-species interactions, and that *H. influenzae* facilitates *S. pneumoniae* adaptation to a nutrient-limited glucose environment, where *S. pneumoniae* adopts an adaptive undetected and SCV state. Overall, our findings suggest that while individual factors significantly impact on the *H. influenzae* lifestyle, it is rather a combination of environmental factors, and the constant dynamic process of their modification, which impacts not only on *H. influenzae*, but indeed on the multi-strain and multispecies environment of the host otorhinolaryngological niches.

The studies included in this thesis have, overall, contributed to expanding the field of knowledge on the molecular and bacteriological factors involved in COM disease pathogenesis. While these studies were performed in vitro, future studies aimed at expending the findings presented in this thesis could be transferred to an environment more representative of the human host, such as on the platform of human nasopharyngeal cells or human middle ear epithelial cells. The analysis of molecular factors involved in *H. infuenzae* biofilm formation or the maintenance of *H. influenzae/ S. pneumoniae* inter-species interaction in these environments, would consolidate the

results obtained in this thesis. In addition, the analysis of global transcriptomic changes in a broader range of clinical isolates of *H. influenzae* and *S. pnemoniae* could further identify common or strain-dependent molecular factors in forming biofilm and maintatining inter-species communities. In the future, the identified molecular factors could be used as targets for novel antimicrobial therapies, or at therapies aimed to disrupt or disperse the biofilm, or the inter-species interactions within the multispecies environment.

Chapter 8

Appendix 1

Overview

This Chapter presents figures supplementary to Chapter 3. Specifically, it includes the complete list of genes differentially expressed in Rd KW20 *nikQ*- relative to the wild-type. In addition, results of the aggregation, biofilm formation and oxidative stress response assays in a *nikQ*- strain of a naturally urease negative *H. influenzae* strain R2866 are presented.

Table S1 The complete list of genes differentially expressed in Rd KW20 *nikQ*$^{-}$ compared to Rd KW20 listed in order of the values of the fold change.

Gene (locus, annotated function)	log_2 Fold Change	P-value (p_{val})	FDR (p_{adj})
HI1047, *dmsA*	-7.16627756	0.000469468	0.04060209
HI1570; HP	-6.805632358	0.000750756	0.060060458
HI1049, *merT*	-4.588040923	0.024788659	0.69250857
HI1046, *dmsB*	-4.068666764	0.09129814	1
HI1502; Mu phage	-3.96913109	0.032710751	0.872286703
HI0109; HP	-3.746738669	0.36219236	1
HI1154; Sodium:dicarboxylate symporter family	-3.675802762	0.037775489	0.981092819
HI1080; PAAT ABC uptake	-3.495820549	0.048140171	1
HI1066, *nrfD*	-3.381454205	0.061221754	1
HI1693, *modA*	-3.345776355	0.065294708	1
HI0857; Z-ring protein ZapA	-3.331701169	0.293752571	1
HI0967	-3.331701169	0.491688554	1
HI1618; *nikO*	-3.331701169	0.491688554	1
HI0643, *bisC*	-3.208642773	0.071834893	1
HI0685, *glpA*	-3.18195405	0.071719401	1
HI0684, *glpB*	-3.054860964	0.103613344	1
HI0832, *frdD*	-2.905436415	0.105407095	1
HI0998, *rpmH*	-2.877983202	0.109127944	1
HI0853, *dppA*	-2.835547936	0.100353322	1
HI0154, *acpP*	-2.752407419	0.112178756	1
HI0495m, *aphA*	-2.746738669	0.683705834	1
HI0548, *infA*	-2.746738669	0.210962623	1
HI1079; PAAT transporter	-2.746738669	0.153016107	1
HI1493	-2.746738669	0.308102783	1
HI1500; Mu protein, gp28	-2.746738669	0.132496388	1
HI1320, *rplT*	-2.651291883	0.11999499	1
HI1519; FluMu gp46	-2.626444435	0.159086176	1
HI0189, *gdhA*	-2.600190005	0.135661554	1
HI0381, Pal OMP P6	-2.566011286	0.132459497	1
HI0082; oxidoreducatse	-2.554093591	0.362656328	1
HI1518; FluMu gp45	-2.492982076	0.174396506	1
HI0093; sugar diacid regulator	-2.483704263	0.447396303	1
HI0439, *comA*	-2.483704263	0.447396303	1
HI1319m, *rpmI*	-2.4748669	0.146387212	1
HI1356, *malQ*	-2.454972544	0.160992339	1
HI1445, *bioD*	-2.453007466	0.160274948	1
HI1095, *dsbE*	-2.438616373	0.233467098	1
HI1520; FluMu	-2.438616373	0.191285418	1
HI1067, *nrfC*	-2.36401889	0.171243639	1
HI1505, FluMu	-2.361307631	0.165645021	1
HI0228, HP	-2.331701169	0.604626777	1
HI0297, *pilC*	-2.331701169	0.604626777	1
HI0742	-2.331701169	0.251996216	1
HI1205; IM protein	-2.331701169	0.265710805	1

HI1390, *hybG*	-2.331701169	0.604626777	1
HI0745, *ansB*	-2.296425695	0.189460583	1
HI1506; FluMu	-2.250312843	0.195777111	1
HI0501, *rbsD*	-2.232165496	0.416755859	1
HI1045, *dmsC*	-2.232165496	0.416755859	1
HI0180; *pfl*	-2.205168763	0.188783539	1
HI1523; HP	-2.182837783	0.272472068	1
HI0035; RCK, potassium uptake	-2.170546378	0.20495006	1
HI0345, *napG*	-2.168439898	0.20249923	1
HI1210, *mdh*	-2.164842471	0.200376316	1
HI1398, *fumC*	-2.157022638	0.205343206	1
HI0597; HAD-like hydrolase	-2.148101231	0.225244208	1
HI1078; PAAT ABC transporter	-2.142667345	0.237234422	1
HI1522; FluMu	-2.136685187	0.25030457	1
HI0571, *oxyR*	-2.130067308	0.217199303	1
HI0001, *gapdH*	-2.117472941	0.205218429	1
HI1510; FluMu	-2.109308748	0.275511337	1
HI0757, *gpmA*	-2.097235916	0.216908183	1
HI0644, *yecK*	-2.09668114	0.237555528	1
HI0631, *coaA*	-2.068666764	0.33511158	1
HI1298; TM protein	-2.068666764	0.33511158	1
HI1508; FluMu	-2.059896554	0.230857757	1
HI0758, *rpmE*	-2.046298951	0.22879057	1
HI1676, *moaA*	-2.022373111	0.26512546	1
HI0830, *trpR*	-2.009773075	0.488251251	1
HI1370, *mopI*	-2.009773075	0.328797	1
HI0150, *hflC*	2.005823781	0.265342404	1
HI0239, *secF*	2.008148833	0.323721078	1
HI0043	2.025850835	0.446612477	1
HI1481, *muB*	2.025850835	0.346446922	1
HI0252, *exbD*	2.047677198	0.312085782	1
HI0431	2.060616253	0.434864724	1
HI0828	2.060616253	0.434864724	1
HI1173, *sprT*	2.060616253	0.518499877	1
HI1436	2.060616253	0.518499877	1
HI1684, *rnfB*	2.060616253	0.518499877	1
HI0633, membrane protein/channel	2.160151927	0.669570121	1
HI1029, TRAP, *dctM*	2.160151927	0.356109499	1
HI1480	2.160151927	0.402005004	1
HI1605	2.160151927	0.669570121	1
HI1640, *sapC*	2.160151927	0.669570121	1
HI1344, *potD*	2.164072296	0.209844784	1
HI1464, *folP-2*	2.172124569	0.277211292	1
HI0894, RND efflux pump Protein	2.183998669	0.274024401	1
HI1427	2.219045616	0.264761812	1

HI0151, *hflK*	2.238844559	0.19508015	1
HI1253, TM protein	2.253261331	0.452412833	1
HI0789, *rplX*	2.265606522	0.178939489	1
HI0144, *nanK*	2.340724173	0.234270838	1
HI0152, acyl carrier, fatty acid biosynthesis	2.340724173	0.60692834	1
HI1082, *bolA*	2.340724173	0.226309944	1
HI1281	2.340724173	0.60692834	1
HI0793, *rplF*	2.385640262	0.154893888	1
HI0573, *slyX* homolog	2.423186333	0.578389265	1
HI1695, LOS biosynthesis	2.423186333	0.397013527	1
HI1259, DegQ/htrA	2.426188821	0.152709293	1
HI1279, *neuA*	2.462714697	0.384588532	1
HI0513, *hindIIM*	2.501188845	0.372677	1
HI1375	2.501188845	0.551544309	1
HI1085	2.53866355	0.210622833	1
HI1282	2.542767949	0.182453832	1
HI0095	2.575189426	0.526281565	1
HI0242	2.575189426	0.526281565	1
HI1401, *pyrD*	2.575189426	0.350293743	1
HI1619	2.575189426	0.241689834	1
HI1624, *nikK*	2.578620332	0.144805662	1
HI1622, *nikL*	2.593111334	0.159400512	1
HI0512, *hindIIR*	2.610813336	0.339775199	1
HI1697, LOS biosynthesis	2.645578754	0.502495934	1
HI0792, *rpsH*	2.681290851	0.110572922	1
HI0240, *secD*	2.809464839	0.112113063	1
HI1283, *nusA*	2.831882305	0.109110507	1
HI1334, *rrmJ*	2.897117521	0.133109668	1
HI1479	2.925686673	0.254662336	1
HI0420 – RHH Family regulator	3.008148833	0.385730686	1
HI1010	3.008148833	0.385730686	1
HI1251, *vapA*	3.008148833	0.385730686	1
HI0417, *thiE*	3.060616253	0.222764734	1
HI0098, *hitB*	3.086151345	0.21704619	1
HI0214, *prlC*	3.137533624	0.069331909	1
HI0859, *clpB*	3.188166303	0.071396581	1
HI1621, *nikM*	3.222887682	0.141451485	1
HI1286, *hsdS*	3.275629144	0.177772067	1
HI1456, TM protein	3.275629144	0.177772067	1
HI0357, Nmt1, thiamine biosynthesis	3.423186333	0.269630584	1
HI1285, *hsdR*	3.737077109	0.061922582	1
HI0243, HHE, heme binding domain	3.867971175	0.172062369	1
HI0543, *groEL*	3.968376204	0.020518699	0.607190347
HI0497, *hslU*	4.164517119	0.021064884	0.607190347
HI1287, *hsdM*	4.207457642	0.057099089	1

HI0542, *groES*	4.727520368	0.009198035	0.337261276
HI0496, *hslV*	5.382544348	0.010443371	0.354069976
HI1237, *dnaK*	5.529385737	0.002236003	0.135702261
HI1238, *dnaJ*	5.529385737	0.003234272	0.167421132
HI0104, *htpG*	6.054161231	0.008778905	0.328741964

Fold change represent $\log_2$ fold change. Negative values are down-regulated in *nikQ* mutant compared to wild type. Annotations with TM – transmembrane protein and HP – hypothetical protein.

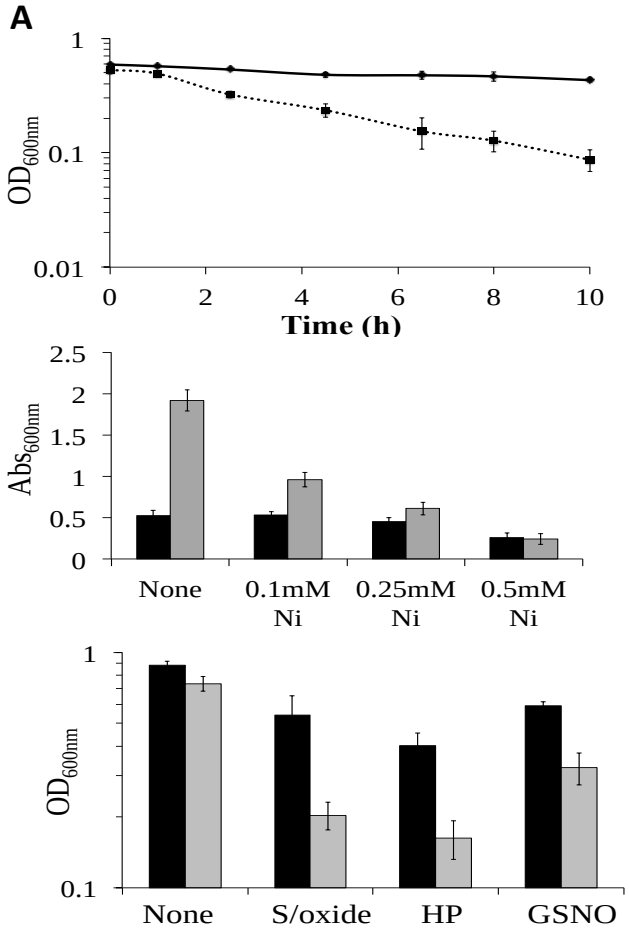

Fig. S1 Nickel limitation in the urease negative *H. influenzae* R2866 strain effects lifestyle. (A) The wild type cells (solid line) did not aggregate (the y-axis shows the OD_{600nm}) compared to a *nikQ* mutant (dotted line) and this translated to a (B) nickel dependent biofilm formation. Biofilm assays (Abs_{600nm}; y-axis) revealed an increased biofilm in the *nikQ* mutant (grey bars) compared to the wild type (black bars) and this was removed by addition of nickel. (C) The R2866 *nikQ* mutant (grey bars) were more sensitive to the presence of oxidative stress (S/oxide, superoxide, menadione; HP, hydrogen peroxide; GSNO, S-nitrosoglutathione at concentrations described in the Materials and methods) than the wild type cells (black bars). The values represent an average (OD_{600nm}) of replicates as described in the Materials and methods and the error bars are the standard deviation.

Chapter 8

Appendix 2

Overview

This Chapter presents additional and supplementary figures to Chapter 4. In particular, this Chapter presents an in-depth summary of planktonic and biofilm growth of 11 *H. influenzae* strains at different pH, as well as their relative growth rates in different pH conditions. In addition, scatter plots obtained from DESeq analysis in R, of differentially expressed genes in strains Eagan and R3264 at pH 8.0 compared to pH 6.8 are presented.

A

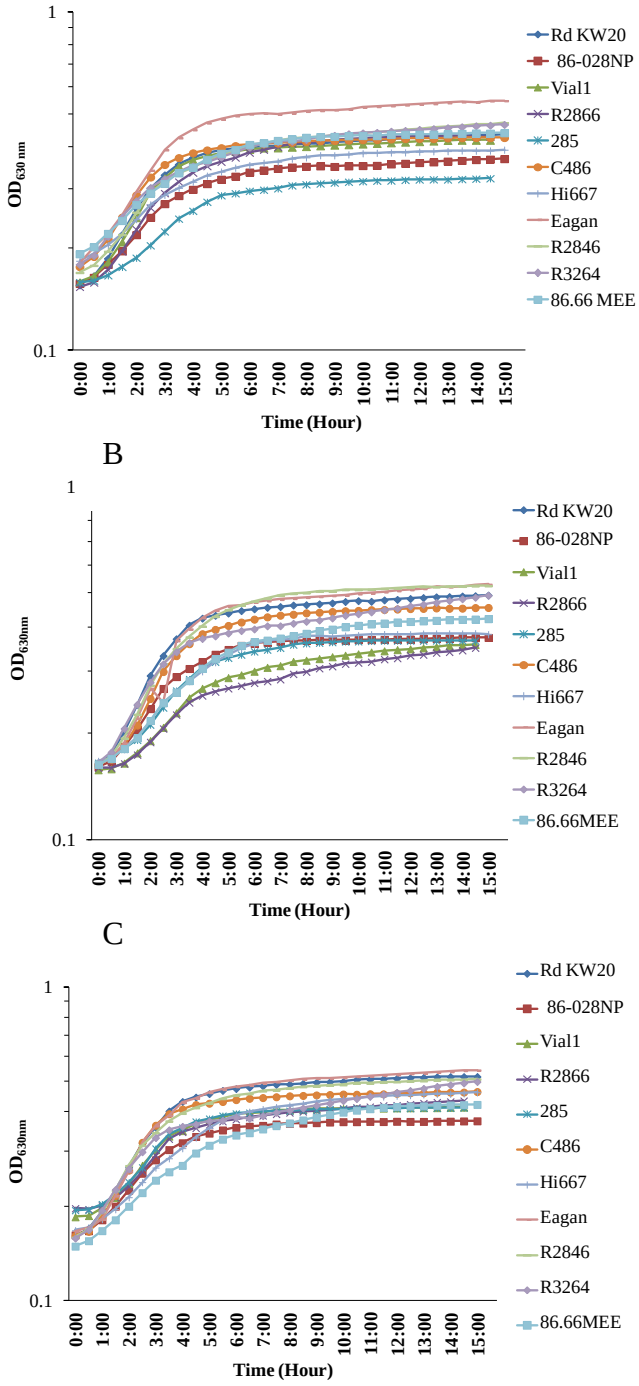

Fig. S 2.1. Plantkonic growth of *H. influenzae* at pH 6.8 (A), 7.4 (B) and 8.0 (C) is comparable for 11 *H. influenzae* isolates. Growth curves displaying planktonic growth of 11 *H. influenzae* isolates were similar, with slight inter-strain differences observed.

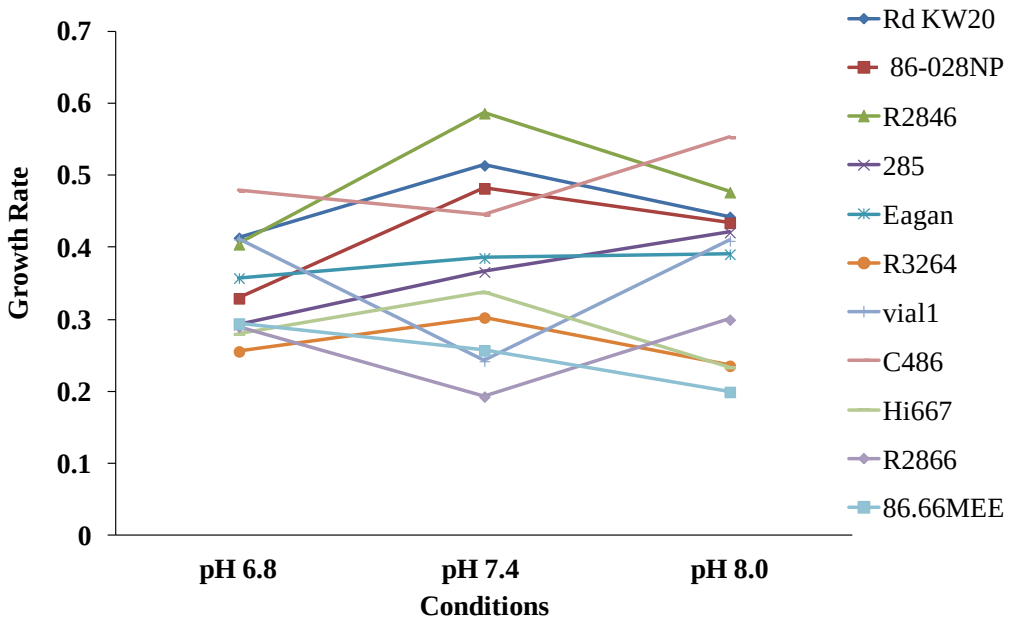

Fig. S 2.2. The growth rates of *H. influenzae* strains under different pH. The growth rates were calculated from Fig S1 and plotted.

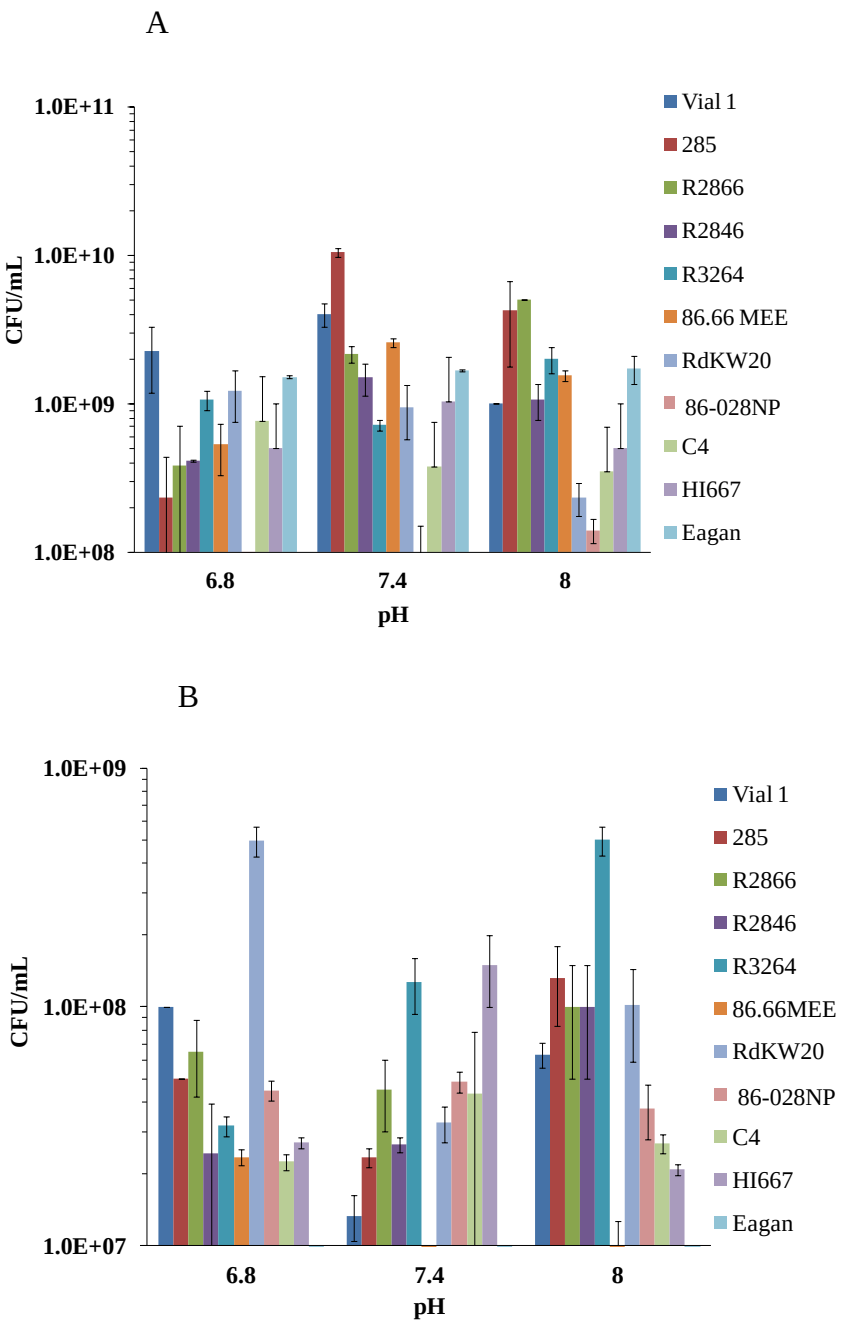

Fig. S2.3. Viable cell counts of different *H. influenzae* strains grown under pH 6.8, 7.4 and 8.0. The isolates were grown and viable cells counted for the (A) planktonic cell number (CFU/ml) and concurrently the (B) biofilm cell number.

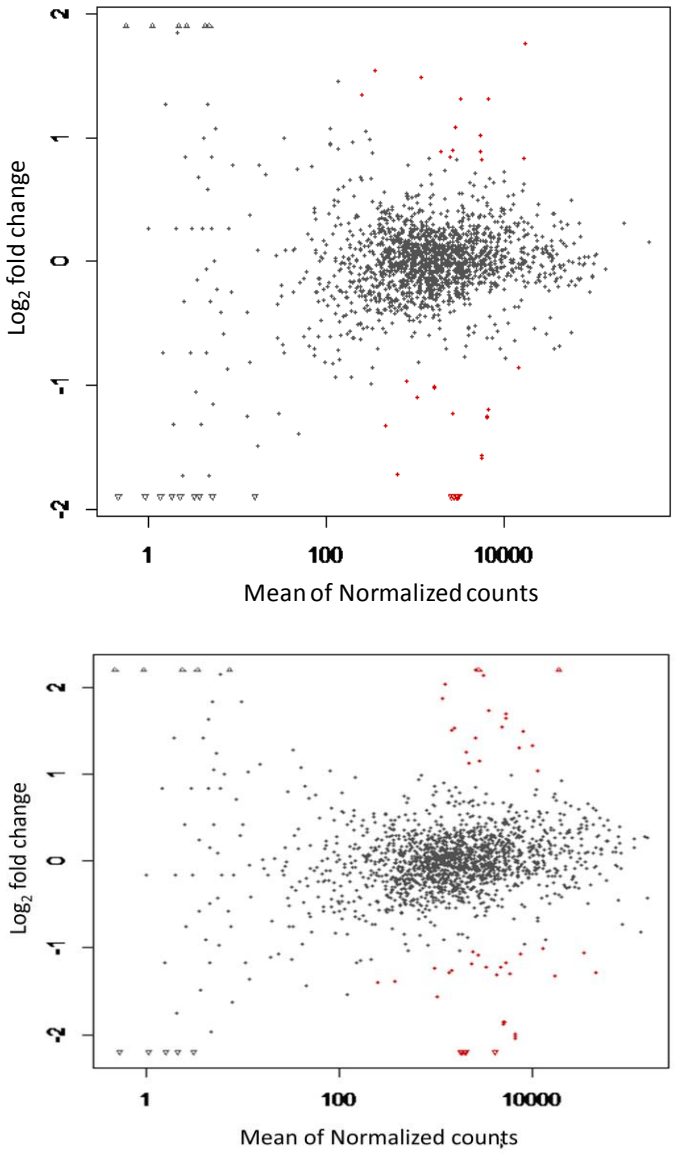

Fig. S2.4 Scatter plots of log_2 fold change against normalized counts for each of the genes identified from mRNAseq. Each dot represents a gene identified from the RNA sequencing library and then compared for counts in the library from pH 8.0 compared to pH 6.8 for (A) R3264 and then for (B) Eagan. The dots that red are those genes determined as being significantly differentially expressed with p-value<0.05 and FDR<10%.

Table S2.1. Growth rates of *H. influenzae* isolates grown at different pH values.

Strain		***pH 6.8***	***pH 7.0***	***pH 8.0***
Rd KW20	Serotype d, non-capsular	0.414 ± 0.08*	0.515 ± 0.10	0.443 ± 0.12
86-028NP	NTHi, OM	0.330 ± 0.09	0.483 ± 0.05	0.435 ± 0.04
R2846	NTHi, OM	0.405 ± 0.11	0.587 ± 0.04	0.477 ± 0.09
NTHi-1	NTHi, lung	0.412 ± 0.07	0.243 ± 0.01	0.410 ± 0.08
R2866	NTHi, blood	0.291 ± 0.04	0.194 ± 0.01	0.300 ± 0.05
285	NTHi, OM	0.293 ± 0.05	0.367 ± 0.07	0.422 ± 0.10
C486	NTHi, OM	0.480 ± 0.03	0.446 ± 0.04	0.554 ± 0.05
Hi667	NTHi, OM	0.281 ± 0.04	0.338 ± 0.01	0.234 ± 0.02
Eagan	Serotype b, CSF	0.358 ± 0.03	0.386 ± 0.07	0.391 ± 0.08
R3264	NTHi, middle ear of healthy child	0.256 ± 0.04	0.303 ± 0.03	0.236 ± 0.06
86-66MEE	NTHi, OM	0.295 ± 0.04	0.258 ± 0.02	0.200 ± 0.04

List of References:

Aas FE, Wolfgang M, *et al*. (2002). Competence for natural transformation in *Neisseria gonorrhoeae*: components of DNA binding and uptake linked to type IV pilus expression. *Mol Microbiol* 46*:* 749–760.

Adam H, Richardson S, *et al*. (2010). Changing epidemiology of invasive *Haemophilus influenzae* in Ontario, Canada: evidence for herd effects and strain replacement due to Hib vaccination. *Vaccine* 28(24): 4073-4078.

Adams WG, Deaver KA, *et al.* (1993). Decline of childhood *Haemophilus influenzae* type b (hib) disease in the hib vaccine era. *JAMA* 269*:* 221–226.

Adderson, EE, Byington CL, *et al*. (2001). Invasive Serotype a *Haemophilus influenzae* infections with a virulence genotype resembling *Haemophilus influenzae* type b: emerging pathogen in the vaccine era? *Pediatrics* 108(1): e18-e18.

Åhman H, Kayhty H *et al*. (1998). *Streptococcus pneumoniae* capsular polysaccharide-diphtheria toxoid conjugate vaccine is immunogenic in early infancy and able to induce immunologic memory. *Pediatr Infect Dis J*17: 211–216.

Allesen-Holm M, Barken KB, *et al*. (2006). A characterization of DNA release in *Pseudomonas aeruginosa* cultures and biofilms. *Mol Microbiol* 59: 1114–1128.
Direct Link:

Alonso M, Marimon JM, Ercibengoa M, *et al*. (2013). Dynamics of *Streptococcus pneumoniae* serotypes causing acute otitis media isolated from children with spontaneous middle-ear drainage over a 12-year period (1999–2010) in a region of northern Spain. *PLoS One* 8: e54333.

Allegrucci, M. and K. Sauer (2007). Characterization of colony morphology variants isolated from *Streptococcus pneumoniae* biofilms. *J Bacteriol* 189(5): 2030-2038.

Anderson, KW, Kingsley LA, *et al*. (1998). Comparative evaluation of culture and PCR for the detection and determination of persistence of bacterial strains and DNAs in the *Chinchilla laniger* model of otitis media. *Ann Otol Rhinol Laryngol* 107(6): 508-513.

Andrews JS, Rolfe SA, *et al*. (2010). Biofilm formation in environmental bacteria is influenced by different macromolecules depending on genus and species. *Environ Microbiol* 12(9): 2496-2507.

Antelmann, H. and Helmann JD. (2011). Thiol-based redox switches and gene regulation. *Antioxid Redox Signal* 14(6): 1049-1063.

Armbruster CE, Hong W *et al*. (2009). LuxS promotes biofilm maturation and persistence of nontypeable *Haemophilus influenzae in vivo* via modulation of lipooligosaccharides on the bacterial surface. *Infect Immun* 77: 4081–4091.

Armbruster CE, Hong W, *et al*. (2010). Indirect pathogenicity of *Haemophilus influenzae* and *Moraxella catarrhalis* in polymicrobial otitis media occurs via interspecies quorum signaling. *MBio* 1. e00102–10.

Armbruster CE, Pang B, *et al*. (2011). RbsB (NTHI_0632) mediates quorum signal uptake in nontypeable *Haemophilus influenzae* strain 86-028NP. *Mol Microbiol* 82: 836–850.

Bakaletz LO, Baker BD, *et al*. (2005). Demonstration of Type IV Pilus expression and a twitching phenotype by *Haemophilus influenza*e. *Infect Immun* 73: 1635–1643.

Balachandran P, Hollingshead SK, et al. (2001). The autolytic enzyme LytA of *Streptococcus pneumoniae* is not responsible for releasing pneumolysin. *J Bacteriol* 183(10): 3108-3116.

Barenkamp SJ and St Geme JW. (1994). Genes encoding high-molecular-weight adhesion proteins of nontypeable *Haemophilus influenzae* are part of gene clusters. *Infect Immun* 62: 3320–3328.

Barken, KB, Pamp SJ, *et al*. (2008). Roles of type IV pili, flagellum-mediated motility and extracellular DNA in the formation of mature multicellular structures in *Pseudomonas aeruginosa* biofilms. *Environ Microbiol* 10(9): 2331-2343.

Becker P, Hufnagle W, *et al*. (2001). Detection of differential gene expression in biofilm-forming versus planktonic populations of *Staphylococcus aureus* using micro-representational difference analysis. *Appl Environ Microbiol* 67: 2958–2965.

Beenken KE, Dunman PM, *et al*. (2004). Global gene expression in *Staphylococcus aureus* biofilms. *J Bacteriol* 186:4665–4684.

Berk SL, Holtsclaw SA, *et al*. (1982). Nontypeable *Haemophilus influenzae* in the elderly. *Arch Intern Med* 142:537–539.

Berman, S. (1995). Otitis media in children. *New Engl J Med* 332(23): 1560-1565.

Besnard V, Federighi M, *et al*. (2000). Evidence of viable but non-culturable state in *Listeria monocytogenes* by direct viable count and CTC-DAPI double staining. *Food Microbiol* 17(6): 697-704.

Bogaert D, van Belkum A, *et al*. (2004). Colonisation by *Streptococcus pneumoniae* and *Staphylococcus aureus* in healthy children. *Lancet* 363(9424): 1871-1872.

Bonifait L, Gottschalk M, *et al*. (2010). Cell surface characteristics of nontypeable isolates of *Streptococcus suis*. *FEMS Microbiol Lett* 311(2): 160-166.

Bouchet V, Hood DW, *et al*. (2003). Host-derived sialic acid is incorporated into *Haemophilus influenzae* lipopolysaccharide and is a major virulence factor in experimental otitis media. *Proc Natl Acad Sci* 100(15): 8898-8903.

Branda S, Vik S, *et al*. (2005) Biofilms: the matrix revisited. *Trends Microbiol* 13: 20–26.

Bresser P, Out TA, *et al*. (2000) Airway inflammation in nonobstructive and obstructive chronic bronchitis with chronic *Haemophilus influenzae* airway infection: comparison with noninfected patients with chronic obstructive pulmonary disease. *Am J Respir Crit Care Med* 162: 947–952.

Brinkmann V, Reichard U, *et al*. (2004). Neutrophil extracellular traps kill bacteria. *Science* 303: 1532–1535.

Buckwalter CM. and King SJ. (2012). Pneumococcal carbohydrate transport: food for thought. *Trends Microbiol* 20(11): 517-522.

Bui LMG, Turnidge JD, *et al*. (2015). The induction of *Staphylococcus aureus* biofilm formation or Small Colony Variants is a strain-specific response to host-generated chemical stresses. *Microb Infect* 17(1): 77-82.

Bylander-Groth A and Stenström C. (1998). Eustachian tube function and otitis media in children. *Ear Nose Throat J* 77: 762–769.

Cabiscol E, Tamarit J, *et al*. (2010). Oxidative stress in bacteria and protein damage by reactive oxygen species. *Int Microbiol* 3(1): 3-8.

Carrolo M, Frias MJ, *et al*. (2010). Prophage spontaneous activation promotes DNA release enhancing biofilm formation in *Streptococcus pneumoniae*. *PLoS ONE* 5(12): e15678.

Carruthers MD, Tracy EN, *et al*. (2012). Biological roles of nontypeable *Haemophilus influenzae* type IV pilus proteins encoded by the *pil* and *com* operons. *J Bacteriol* 194: 1927–1933.

Carvalho SM, Farshchi Andisi V, *et al*. (2013). Pyruvate oxidase influences the sugar utilization pattern and capsule production in *Streptococcus pneumoniae*. *PLoS ONE* 8(7): e68277.

Chakrabarti SK, Bai C, *et al*. (2001). DNA–protein crosslinks induced by nickel compounds in isolated rat lymphocytes: role of reactive oxygen species and specific amino acids. *Toxicol Appl Pharm* 170(3): 153-165.

Chang A, Kaur R, *et al*. (2011). *Haemophilus influenzae* vaccine candidate outer membrane protein P6 is not conserved in all strains. *Hum Vaccin* 7: 102–105.

Chhibber S, Nag D, *et al*. (2013). Inhibiting biofilm formation by *Klebsiella pneumoniae* B5055 using an iron antagonizing molecule and a bacteriophage. *BMC Microbiol* 13(1): 174.

Chiang SM and Schellhorn HE. (2012). Regulators of oxidative stress response genes in *Escherichia coli* and their functional conservation in bacteria. *Arch Biochem Biophys* 525(2): 161-169.

Clarisse B, Laurent AM, *et al*. (2003). Indoor aldehydes: measurement of contamination levels and identification of their determinants in Paris dwellings. *Environ Res* 92(3): 245-253.

Coleman HN, Daines DA, *et al*. (2003). Chemically defined media for growth of *Haemophilus influenzae* strains. *J Clin Microbiol* 41(9): 4408-4410.

Coelho, C. and M. J. Romão (2015). Structural and mechanistic insights on nitrate reductases. *Prot Sci* n/a-n/a.

Cohen SS. (1951). Gluconokinase and the oxidative path of glucose-6-phosphate utilization. *J Biol Chem* 189(2): 617-628.

Cope, EK, Goldstein-Daruech N, *et al*. (2011). Regulation of virulence gene expression resulting from *Streptococcus pneumoniae* and nontypeable *Haemophilus influenzae* interactions in chronic disease. *PLoS ONE* 6(12): e28523.

Cornu C, Yzèbe D, *et al.* (2001). Efficacy of pneumococcal polysaccharide vaccine in immunocompetent adults: a meta-analysis of randomized trials. *Vaccine* 19: 4780–4790.

Coutard F, Pommepuy M, *et al*. (2005). mRNA detection by reverse transcription–PCR for monitoring viability and potential virulence in a pathogenic strain of *Vibrio parahaemolyticus* in viable but nonculturable state. *J Appl Microbiol* 98(4): 951-961.

Cundell DR, Gerard NP, *et al*. (1995). *Streptococcus pneumoniae* anchor to activated human cells by the receptor for platelet-activating factor. *Nature* 377: 435–438.

Dahl AR and Hadley WM. (1983). Formaldehyde production promoted by rat nasal cytochrome P-450-dependent monooxygenases with nasal decongestants, essences, solvents, air pollutants, nicotine, and cocaine as substrates. *Toxicol Appl Pharm* 67(2): 200-205.

Dahlgren C and Karlsson A. (1999). Respiratory burst in human neutrophils. *J Immunol Methods* 232(1–2): 3-14.

Daines DA, Bothwell M, *et al*. (2005). *Haemophilus influenzae luxS* mutants form a biofilm and have increased virulence. *Microb Pathog* 39(3): 87-96.

Danese PN, Pratt LA, *et al*. (2000). The outer membrane protein, Antigen 43, mediates cell-to-cell interactions within *Escherichia coli* biofilms. *Mol Microbiol* 37(2): 424-432.

Darwin AJ. (2005). The phage-shock-protein response. *Mol Microbiol* 57(3): 621-628.

Das T, Sharma PK, *et al*. (2010). Role of extracellular DNA in initial bacterial adhesion and surface aggregation. *Appl Environ Microbiol* 76(10): 3405-3408.

Davies D. (2003). Understanding biofilm resistance to antibacterial agents. *Nat Rev Drug Discov* 2(2): 114-122.

de Bernonville TD, Noël LD, *et al*. (2014). Transcriptional reprogramming and phenotypical changes associated with growth of *Xanthomonas campestris pv. campestris* in cabbage xylem sap. *FEMS Microbiol Ecol* 89(3): 527-541.

del Mar Lleò M, Pierobon S, *et al*. (2000). mRNA detection by reverse transcription-PCR for monitoring viability over time in an *Enterococcus faecalis* viable but nonculturable population maintained in a laboratory microcosm. *Appl Environ Microbiol* 66(10): 4564-4567.

del Mar Lleo M, Tafi MC, *et al*. (1998). Nonculturable *Enterococcus faecalis* cells are metabolically active and capable of resuming active growth. *Syst Appl Microbiol* 21(3): 333-339.

Domenech M, García E, *et al*. (2013). Insight into the composition of the intercellular matrix of *Streptococcus pneumoniae* biofilms. *Environ Microbiol* 15: 502–516.

Domenech M, Ramos-Sevillano E, *et al*. (2013). Biofilm formation avoids complement immunity and phagocytosis of *Streptococcus pneumoniae*. *Infect Immun*. 81: 2606–2615.

Domenech M, García E, *et al*. (2009). Versatility of the capsular genes during biofilm formation by *Streptococcus pneumoniae*. *Environ Microbiol* 11(10): 2542-2555.

Dowell SF, Butler JC, Giebink GS, *et al*. (1999). Acute otitis media: management and surveillance in an era of pneumococcal resistance - a report from the drug-resistant *Streptococcus pneumoniae* Therapeutic Working Group. *Pediatr Infect Dis J* 18: 1–9.

Earl CS, Keong TW, *et al*. (2015). *Haemophilus influenzae* responds to glucocorticoids used in asthma therapy by modulation of biofilm formation and antibiotic resistance. *EMBO Mol Med* 7(11):1385-1502.

Egere U, Townend J, *et al*. (2012). Indirect effect of 7-valent pneumococcal conjugate vaccine on pneumococcal carriage in newborns in rural Gambia: a randomised controlled trial. *PLoS One* 7: e49143.

Ehrlich GD, Ahmed A, *et al*. (2010). The distributed genome hypothesis as a rubric for understanding evolution in situ during chronic bacterial biofilm infectious processes. *FEMS Immunol Med Mic* 59(3): 269-279.

Ehrlich GD, Veeh R, *et al*. (2002). Mucosal biofilm formation on middle-ear mucosa in the chinchilla model of otitis media. *JAMA* 287(13): 1710-1715.

Eisenberg RC and Dobrogosz WJ. (1967). Gluconate metabolism in *Escherichia coli*. *J Bacteriol* 93(3): 941-949.

Engel J, Mahler E, *et al* .(2001). Why are NICU infants at risk for chronic otitis media with effusion? *Int J Pediatr Otorhinolaryngol* 57: 137–144.

Faden H. (2001). The microbiologic and immunologic basis for recurrent otitis media in children. *Eur J Pediatr* 160: 407–413.

Falla TJ, Crook DWM, Kraak WAG *et al*. (1993). Population-based study of non-typable *Haemophilus influenzae* invasive disease in children and neonates. *Lancet* 341: 851–854.

Fenoll A, Granizo J, *et al*. (2009). Temporal trends of invasive *Streptococcus pneumoniae* serotypes and antimicrobial resistance patterns in Spain from 1979 to 2007. *J Clin Microbiol* 47(4): 1012-1020.

Ferguson GP, Tötemeyer S, *et al.* (1998). Methylglyoxal production in bacteria: suicide or survival? *Arch Microbiol* 170(4): 209-218.

Ferrero RL and Lee A. (1991). The importance of urease in acid protection for the gastric-colonising bacteria *Helicobacter pylori* and *Helicobacter felis* sp. nov. *Microb Ecol Health Dis* 4: 121–134.

Filloux A. and Ramos JL. (2014). Pseudomonas Methods and Protocols, Springer.

Fink DL and St. Geme JW III. (2003). Chromosomal expression of the *Haemophilus influenzae* Hap autotransporter allows fine-tuned regulation of adhesive potential via inhibition of intermolecular autoproteolysis. *J Bacteriol* 185: 1608–1615.

Flemming HC & Wingender J. (2010). The biofilm matrix. *Nat Rev Microbiol* 8: 623–633.
Frey RL, He L, *et al*. (2010). Reaction of N-acylhomoserine lactones with hydroxyl radicals: rates, products, and effects on signaling activity. *Environ Scie Technol* 44(19): 7465-7469.

Frunzke J, Engels V, *et al*. (2008). Co-ordinated regulation of gluconate catabolism and glucose uptake in Corynebacterium glutamicum by two functionally equivalent transcriptional regulators, GntR1 and GntR2. *Mol Microbiol* 67(2): 305-322.

Gallaher T, Wu S, *et al*. (2006). Identification of biofilm proteins in non-typeable *Haemophilus influenzae*. *BMC Microbiol* 6: 65.

García-Cobos S, Moscoso M, *et al*. (2014). Frequent carriage of resistance mechanisms to β-lactams and biofilm formation in *Haemophilus influenzae* causing treatment failure and recurrent otitis media in young children. *J Antimicrob Chemother* 70 (11).

Gebhart DE. (1981). Tympanostomy tubes in the otitis media prone child. *Laryngoscope* 91: 849–866.

Geier H, Mostowy S, *et al*. (2008). Autoinducer-2 triggers the oxidative stress response in *Mycobacterium avium*, leading to biofilm formation. *Appl Environ Microbiol* 74(6): 1798-1804.

Georges S, Lepoutre A, *et al*. (2013). Impact of *Haemophilus influenzae* type b vaccination on the incidence of invasive *Haemophilus influenzae* disease in France, 15 years after its introduction. *Epidemiol Infect* 141: 1787–1796.

Gloag ES, Turnbull L, *et al*. (2013). Self-organization of bacterial biofilms is facilitated by extracellular DNA. *Proc Natl Acad Scie* 110(28): 11541-11546.

Goetghebuer T, West TE, *et al*. (2000). Outcome of meningitis caused by *Streptococcus pneumoniae* and *Haemophilus influenzae* type b in children in the Gambia. *Trop Med Int Health* 5: 207–213.

González Barrios AF, Zuo R, *et al*. (2006) Autoinducer 2 controls biofilm formation in *Escherichia coli* through a novel motility quorum-sensing regulator (MqsR, B3022). *J Bacteriol* 188: 305–316.

Grande R, Nistico L, *et al*. (2014). Temporal expression of *agrB*, *cidA*, and *alsS* in the early development of *Staphylococcus aureus* UAMS-1 biofilm formation and the structural role of extracellular DNA and carbohydrates. *Pathog Dis* 70(3): 414-422.

Grass S, Buscher AZ, *et al*. (2003). The *Haemophilus influenzae* HMW1 adhesin is glycosylated in a process that requires HMW1C and phosphoglucomutase, an enzyme involved in lipooligosaccharide biosynthesis. *Mol Microbiol* 48(3): 737-751.

Greiner L, Watanabe H, *et al*. (2004). Nontypeable *Haemophilus influenzae* strain 2019 produces a biofilm containing N-acetylneuraminic acid that may mimic sialylated O-linked glycans. *Infect Immun* 72(7): 4249-4260.

Hall-Stoodley L, Hu FZ, *et al*. (2006). Direct detection of bacterial biofilms on the middle-ear mucosa of children with chronic otitis media. *JAMA* 296(2): 202-211.

Hall-Stoodley L, Nistico L, Sambanthamoorthy K *et al*. (2008). Characterization of biofilm matrix, degradation by DNase treatment and evidence of capsule downregulation in *Streptococcus pneumoniae* clinical isolates. *BMC Microbiol* 8: 173.

Hammer BK and Bassler BL. (2003). Quorum sensing controls biofilm formation in *Vibrio cholerae*. *Mol Microbiol* 50(1): 101-104.

Hampton MB, Kettle AJ, *et al*. (1998). Inside the Neutrophil Phagosome: Oxidants, Myeloperoxidase, and Bacterial Killing. *Am Soc Hematology*. 92(9): 3007-3017.

Harrison A, Santana EA, *et al*. (2013). Ferric uptake regulator and its role in the pathogenesis of nontypeable *Haemophilus influenzae*. *Infect Immun* 81(4): 1221-1233.

Harrison A, Ray WC, *et al*. (2007). The OxyR regulon in nontypeable *Haemophilus influenzae. J Bacteriol* 189(3): 1004-1012.

Harrison A, Dyer DW, *et al*. (2005). Genomic sequence of an otitis media isolate of nontypeable *Haemophilus influenzae*: comparative study with *H. influenzae* serotype d, strain KW20. *J Bacteriol* 187(13): 4627-4636.

Harvey H, Habash M, *et al*. (2009). Single-residue changes in the C-terminal disulfide-bonded loop of the *Pseudomonas aeruginosa* type IV pilin influence pilus assembly and twitching motility. *J Bacteriol* 191(21): 6513-6524.

Heijstra BD,. Pichler FB, *et al*. (2009). Extracellular DNA and Type IV pili mediate surface attachment by *Acidovorax temperans*. *A van Leeuw* 95(4): 343-349.

Ho PL, Chiu SS, *et al*. (2011). Serotypes and antimicrobial susceptibilities of invasive *Streptococcus pneumoniae* before and after introduction of 7-valent pneumococcal conjugate vaccine, Hong Kong, 1995–2009. *Vaccine* 29(17): 3270-3275.

Hoa M, Syamal M, *et al*. (2010). Biofilms and chronic otitis media: an initial exploration into the role of biofilms in the pathogenesis of chronic otitis media. *Am J Otolaryngol* 31: 241–245.

Hogg JS, Hu FZ, *et al*. (2007). Characterization and modeling of the *Haemophilus influenzae* core and supragenomes based on the complete genomic sequences of Rd and 12 clinical nontypeable strains. *Genome Biol* 8(6): R103.

Høiby N, Bjarnsholt T, *et al*. (2010). Antibiotic resistance of bacterial biofilms. *Int J Antimicrob Agents* 35:322–332.

Hong W, Juneau RA, *et al*. (2009). Survival of bacterial biofilms within neutrophil extracellular traps promotes nontypeable *Haemophilus influenzae* persistence in the chinchilla model for otitis media. *J Innate Immun* 1: 215–224.

Hong W, Khampang P, *et al*. (2014). Nontypeable *Haemophilus influenzae* inhibits autolysis and fratricide of *Streptococcus pneumoniae* in vitro. *Microb Infect* 16(3): 203-213.

Horton R M, Ho S, *et al*. (1992). Gene splicing by overlap extension. *Methods Enzymol* 217: 270-279.

Huang S-H & Jong A (2009) Evolving role of laminin receptors in microbial pathogenesis and therapeutics of CNS infection. *Future Microbiol* 4: 959–962.

Hunter LL, Margolis RH, *et al*. (1996) High frequency hearing loss associated with otitis media. *Ear Hear* 17: 1–11.

Irino K, Grimont F, *et al*. (1988). rRNA gene restriction patterns of *Haemophilus influenzae* biogroup aegyptius strains associated with Brazilian purpuric fever. *J Clin Microbiol* 26(8): 1535-1538.

Isaacman D J, McIntosh ED, *et al*. (2010). Burden of invasive pneumococcal disease and serotype distribution among *Streptococcus pneumoniae* isolates in young children in Europe: impact of the 7-valent pneumococcal conjugate vaccine and considerations for future conjugate vaccines. *Int J Infect Dis*14(3): e197-e209.

Izu H, Adachi O, *et al*. (1997). Gene organization and transcriptional regulation of the *gntRKU* operon involved in gluconate uptake and catabolism of *Escherichia coli*. *J Mol Biol* 267(4): 778-793.

Jones PA, Samuels NM, *et al*. (2002). *Haemophilus influenzae* type b strain A2 has multiple sialyltransferases involved in lipooligosaccharide sialylation. *J Biol Chem* 277: 14598–14611.

Jones EA, McGillivary G and Bakaletz LO. (2013). Extracellular DNA within a nontypeable *Haemophilus influenzae*-induced biofilm binds human beta defensin-3 and reduces its antimicrobial activity. *J Innate Immun* 5: 24–38.

Juneau RA, Pang B, *et al*. (2011). Nontypeable *Haemophilus influenzae* initiates formation of neutrophil extracellular traps. *Infect Immun* 79: 431–438.

Jurcisek JA and Bakaletz LO. (2007). Biofilms formed by nontypeable *Haemophilus influenzae in vivo* contain both double-stranded DNA and type IV pilin protein. *J Bacteriol* 189: 3868–3875.

Jurcisek J, Greiner L, *et al.* (2005). Role of sialic acid and complex carbohydrate biosynthesis in biofilm formation by nontypeable *Haemophilus influenzae* in the chinchilla middle ear. *Infect Immun* 73:3210–3218.

Jurcisek JA, Bookwalter JE, *et al.* (2007). The PilA protein of non-typeable *Haemophilus influenzae* plays a role in biofilm formation, adherence to epithelial cells and colonization of the mammalian upper respiratory tract. *Mol Microbiol* 65: 1288–1299.

Keren I, Minami S, *et al*. (2011). Characterization and transcriptome analysis of *Mycobacterium tuberculosis* persisters. *mBio* 2(3):e00100-11.

Keren I, Shah D, *et al*. (2004). Specialized persister cells and the mechanism of multidrug tolerance in *Escherichia coli*. *J Bacteriol* 186(24): 8172-8180.

Kidd SPK, Djoko Y, *et al*. (2011). A novel nickel responsive MerR-like regulator, NimR, from *Haemophilus influenzae*. *Metallomics* 3(10): 1009-1018.

Kim J, Hahn JS, *et al*. (2009). Tolerance of dormant and active cells in *Pseudomonas aeruginosa* PA01 biofilm to antimicrobial agents. *J Antimicrob Chemother* 63(1): 129-135. Direct Link:

Kim JO and Weiser JN. (1998). Association of intrastrain phase variation in quantity of capsular polysaccharide and teichoic acid with the virulence of *Streptococcus pneumoniae*. *J Infect Dis* 177: 368–377.

Kim JO, Romero-Steiner S, *et al*. (1999). Relationship between cell surface carbohydrates and intrastrain variation on opsonophagocytosis of *Streptococcus pneumoniae*. *Infect Immun* 67:2327–2333.

Klein G, Müller-Loennies S, *et al.* (2013). Molecular and structural basis of inner core lipopolysaccharide alterations in *Escherichia coli* incorporation of glucouronic acid and phosphoethanolamine in the heptose region. *J Biol Chem* 288(12): 8111-8127.

Klein G, Lindner B, *et al*. (2011). Molecular basis of lipopolysaccharide heterogeneity in *Escherichia coli* envelope stress-responsive regulators control the incorporation of glycoforms with a third 3-deoxy-α-d-manno-oct-2-ulosonic acid and rhamnose. *Jof Biol Chem* 286(50): 42787-42807.

Klein JO. (2000). The burden of otitis media. *Vaccine* 19 (Suppl 1): S2–S8.

Krishnamurthy A and Kyd J. (2014). The roles of epithelial cell contact, respiratory bacterial interactions and phosphorylcholine in promoting biofilm formation by *Streptococcus pneumoniae* and nontypeable *Haemophilus influenzae*. *Microb Infect*16(8): 640-647.

Kulkarni R, Antala S, *et al*. (2012). Cigarette smoke increases *Staphylococcus aureus* biofilm formation via oxidative stress. *Infect Immun* 80(11): 3804-3811.

LaCross NC, Marrs CF, *et al*. (2013). Population structure in nontypeable *Haemophilus influenzae*. *Infect, Genet Evol* 14: 125-136.

Lennon JT and Jones SE. (2011). Microbial seed banks: the ecological and evolutionary implications of dormancy. *Nat Rev Micro* 9(2): 119-130.

Leroy M, Cabral H, *et al*. (2007). Multiple consecutive lavage samplings reveal greater burden of disease and provide direct access to the nontypeable *Haemophilus influenzae* biofilm in experimental otitis media. *Infect Immun* 75(8): 4158-4172.

Letek M, Valbuena N, *et al*. (2006). Characterization and use of catabolite-repressed promoters from gluconate genes in *Corynebacterium glutamicum*. *J Bacteriol* 188(2): 409-423.

Leung B, Taylor S, *et al*. (2012). *Haemophilus influenzae* type b disease in Auckland children during the Hib vaccination era: 1995–2009. *N Z Med J* 125: 21–29.

Lewis K. (2007). Persister cells, dormancy and infectious disease. *Nat Rev Microbiol* 5(1): 48-56.

Li L, Mendis N, *et al*. (2014). The importance of the viable but non-culturable state in human bacterial pathogens. *Front Microbiol* 5:258.

Lijek RS and Weiser JN. (2012). Co-infection subverts mucosal immunity in the upper respiratory tract. *Curr Opin Immunol* 24(4): 417-423.

Lysenko ES, Lijek RS, *et al*. (2010). Within-host competition drives selection for the capsule virulence determinant of *Streptococcus pneumoniae*. *Curr Biol* 20(13): 1222-1226.
Lysenko ES, Ratner AJ, *et al*. (2005). The role of innate immune responses in the outcome of interspecies competition for colonization of mucosal surfaces. *PLoS Pathog* 1(1): e1.

Mah TFC and O'Toole GA. (2001). Mechanisms of biofilm resistance to antimicrobial agents. *Trends Microbiol* 9: 34–39.

Mahdi, L. K., H. Wang, *et al*. (2012). Identification of a novel pneumococcal vaccine antigen preferentially expressed during meningitis in mice. *J Clin Invest* 122(6): 2208-2220.

Marks LR, Reddinger RM and Hakansson AP. (2012). High levels of genetic recombination during nasopharyngeal carriage and biofilm formation in *Streptococcus pneumoniae*. *MBio* 3.

Marks LR, Reddinger RM and Hakansson AP. (2012). High levels of genetic recombination during nasopharyngeal carriage and biofilm formation in *Streptococcus pneumoniae*. *MBio* 3.

Margolis E, Yates A and Levin B .(2010). The ecology of nasal colonization of *Streptococcus pneumoniae, Haemophilus influenzae* and *Staphylococcus aureus*: the role of competition and interactions with host's immune response. *BMC Microbiol* 10: 59.

Martín-Galiano AJ, Overweg K, *et al*. (2005). Transcriptional analysis of the acid tolerance response in *Streptococcus pneumoniae*. *Microbiol* 151(12): 3935-3946.

Mason KM, Munson RS, *et al*. (2005). A mutation in the sap operon attenuates survival of nontypeable *Haemophilus influenzae* in a chinchilla model of otitis media. *Infect Immun* 73(1): 599-608.

Mason KM, Munson RS Jr and Bakaletz LO. (2003). Nontypeable *Haemophilus influenzae* gene expression induced *in vivo* in a chinchilla model of otitis media. *Infect Immun* 71: 3454–3462.

Melegaro A and Edmunds WJ. (2004). The 23-valent pneumococcal polysaccharide vaccine. Part I. Efficacy of PPV in the elderly: a comparison of meta-analyses. *Eur J Epidemiol* 19: 353–363.

Merritt J, Qi F, *et al*. (2003) Mutation of *luxS* affects biofilm formation in *Streptococcus mutans*. *Infect Immun* 71: 1972–1979.

Mobley HL, Island MD and Hausinger RP. (1995). Molecular biology of microbial ureases. *Microbiol Rev* 59: 451–480.

Mole B, Habibi S, *et al*. (2010). Gluconate metabolism is required for virulence of the soft-rot pathogen *Pectobacterium carotovorum*. *Mol Plant Microb In* 23(10): 1335-1344.

Mori Y, Yamaguchi M, *et al*. (2012). α-enolase of *Streptococcus pneumoniae* induces formation of neutrophil extracellular traps. *J Biol Chem* 287: 10472–10481.

Moscoso M and Claverys JP. (2004). Release of DNA into the medium by competent *Streptococcus pneumoniae*: kinetics, mechanism and stability of the liberated DNA. *Mol Microbiol* 54: 783–794.
Direct Link:

Moscoso M, García E and López R. (2006). Biofilm formation by *Streptococcus pneumoniae*: role of choline, extracellular DNA, and capsular polysaccharide in microbial accretion. *J Bacteriol* 188: 7785–7795.

Muñoz-Elías EJ, Marcano J and Camilli A. (2008). Isolation of *Streptococcus pneumoniae* biofilm mutants and their characterization during nasopharyngeal colonization. *Infect Immun* 76: 5049–5061.

Munson RS, Harrison A, *et al*. (2004). Partial analysis of the genomes of two nontypeable *Haemophilus influenzae* otitis media isolates. *Infect Immun* 72(5): 3002-3010.

Murphy T and Brauer A. (2011). Expression of urease by *Haemophilus influenzae* during human respiratory tract infection and role in survival in an acid environment. *BMC Microbiol* 11: 183.

Murphy TF, Sethi S, *et al*. (1999). Simultaneous respiratory tract colonization by multiple strains of nontypeable *Haemophilus influenzae* in chronic obstructive pulmonary disease: implications for antibiotic therapy. *J Infect Dis* 180: 404–409.

Mutepe ND, Cockeran R, *et al*. (2013). Effects of cigarette smoke condensate on pneumococcal biofilm formation and pneumolysin. *Eur Respir J* 41: 392–395.

Ng J and Kidd SP. (2013). The concentration of intracellular nickel in *Haemophilus influenzae* is linked to its surface properties and cell–cell aggregation and biofilm formation. *Int J Med Microbiol* 303: 150–157.

Nuorti JP & Whitney CG. (2010). Prevention of pneumococcal disease among infants and children: use of 13-valent pneumococcal conjugate vaccine and 23-valent pneumococcal polysaccharide vaccine: recommendations of the advisory committee on immunization practices (ACIP). Department of Health and Human Services, Centers for Disease Control and Prevention.

Nuutinen J, Torkkeli T and Penttilä I. (1993). The pH of secretions in sinusitis and otitis media. *J Otolaryngol* 22: 79.

Obaid NA, Jacobson GA, *et al*. (2015). Relationship between clinical site of isolation and ability to form biofilms in vitro in nontypeable *Haemophilus influenzae*. *Can J of Microbiol* 61(3): 243-245.

Ojano-Dirain C and Antonelli PJ. (2012). Tympanostomy tube in vitro biofilm potential of common otopathogens. *Otolaryngol-Head Neck Surg* 146(5): 816-822.

Osgood R, Salamone F, *et al*. (2015). Effect of pH and oxygen on biofilm formation in acute otitis media associated NTHi clinical isolates. *Laryngoscope*: n/a-n/a.

Othman DS, Schirra H, *et al*. (2014). Metabolic versatility in *Haemophilus influenzae*: a metabolomic and genomic analysis. *Front Microbiol* 5: 69.

O'Toole GA. Gibbs KA, *et al*. (2000). The global carbon metabolism regulator Crc is a component of a signal transduction pathway required for biofilm development by *Pseudomonas aeruginosa*. *J Bacteriol* 182(2): 425-431.

O'Toole GA and Kolter R. (1998). Initiation of biofilm formation in *Pseudomonas fluorescens* WCS365 proceeds via multiple, convergent signalling pathways: a genetic analysis. *Mol Microbiol* 28(3): 449-461.

Painter KL, Strange E, *et al*. (2015). *Staphylococcus aureus* adapts to oxidative stress by producing H_2O_2-resistant small-colony variants via the SOS response. *Infect Immun* 83(5): 1830-1844.

Palchevskiy V and. Finkel SE. (2006). *Escherichia coli* competence gene homologs are essential for competitive fitness and the use of DNA as a nutrient. *J Bacteriol* 188(11): 3902-3910.

Patra T, Koley H, *et al*. (2012). The Entner-Doudoroff pathway is obligatory for gluconate utilization and contributes to the pathogenicity of *Vibrio cholerae*. *J Bacteriol* 194(13): 3377-3385.

Peekhaus N, Tong S, *et al*. (1997). Characterization of a novel transporter family that includes multiple *Escherichia coli* gluconate transporters and their homologues. *FEMS microbiol lett* 147(2): 233-238.

Peltola H. (2000). Worldwide *Haemophilus influenzae* type b disease at the beginning of the 21st century: global analysis of the disease burden 25 years after the use of the polysaccharide vaccine and a decade after the advent of conjugates. *Clin Microbiol Rev* 13(2): 302-317.

Pericone C D, Overweg K, *et al*. (2000). Inhibitory and bactericidal effects of hydrogen peroxide production by *Streptococcus pneumoniae* on other inhabitants of the upper respiratory tract. *Infect Immun* 68(7): 3990-3997.

Poortinga AT, Bos R, *et al*. (2002). Electric double layer interactions in bacterial adhesion to surfaces. *Surf Sci Rep* 47(1): 1-32

Porco A, Peekhaus N, *et al*. (1997). Molecular genetic characterization of the *Escherichia coli gntT* gene of GntI, the main system for gluconate metabolism. *J Bacteriol* 179(5): 1584-1590.

Post DM, Held JM, *et al*. (2014). Comparative analyses of proteins from *Haemophilus influenzae* biofilm and planktonic populations using metabolic labeling and mass spectrometry. *BMC Microbiol* 14(1): 329.

Post JC. (2001). Candidate's Thesis: direct evidence of bacterial biofilms in otitis media. *Laryngoscope* 111: 2083–2094.

Poulsen K, Reinholdt J and Kilian M. (1992). A comparative genetic study of serologically distinct *Haemophilus influenzae* type 1 immunoglobulin A1 proteases. *J Bacteriol* 174: 2913–2921.

Price CE, Zeyniyev A, *et al*. (2012). From meadows to milk to mucosa–adaptation of *Streptococcus* and *Lactococcus* species to their nutritional environments. *FEMS Microbiol Rev* 36(5): 949-971.

Priftis KN, Litt D, Manglani S *et al*. (2013). Bacterial bronchitis caused by *Streptococcus pneumoniae* and nontypable *Haemophilus influenzae* in children. *Chest* 143: 152–157.

Prigent-Combaret C, Vidal O, *et al*. (1999) Abiotic surface sensing and biofilm-dependent regulation of gene expression in *Escherichia coli*. *J Bacteriol* 181: 5993–6002.

Prouty AM and Gunn JS. (2003). Comparative analysis of *Salmonella enterica* serovar *Typhimurium* biofilm formation on gallstones and on glass. *Infect and Immun* 71(12): 7154-7158.

Qin L, Kida Y, *et al*. (2013) Impaired capsular polysaccharide is relevant to enhanced biofilm formation and lower virulence in *Streptococcus pneumoniae*. *J Infect Chemother* 19: 261–271.

Rachid S, Ohlsen K, *et al*. (2000). Effect of subinhibitory antibiotic concentrations on polysaccharide intercellular adhesin expression in biofilm-forming *Staphylococcus epidermidis*. *Antimicrob Agents Ch* 44(12): 3357-3363.

Ramsey MM, Rumbaugh KP, *et al*. (2011). Metabolite cross-feeding enhances virulence in a model polymicrobial infection. *PLoS Pathog* 7(3): e1002012.

Redanz S, Standar K, *et al*. (2011). A five-species transcriptome array for oral mixed-biofilm studies. *PLoS ONE* 6(12): e27827.

Reid SD, Hong W, Dew KE *et al*. (2009). *Streptococcus pneumoniae* forms surface-attached communities in the middle ear of experimentally infected chinchillas. *J Infect Dis* 199: 786–794.

Resch A, Leicht S, *et al*. (2006). Comparative proteome analysis of *Staphylococcus aureus* biofilm and planktonic cells and correlation with transcriptome profiling. *Proteomics* 6(6): 1867-1877.

Resch A, Rosenstein R, *et al*. (2005). Differential gene expression profiling of *Staphylococcus aureus* cultivated under biofilm and planktonic conditions. *Appl Environ Microbiol* 71(5): 2663-2676.

Rezzonico F and Duffy B (2008) Lack of genomic evidence of AI-2 receptors suggests a non-quorum sensing role for *lux*S in most bacteria. *BMC Microbiol* 8: 154.

Ribeiro GS, Reis JN, *et al*. (2003). Prevention of *Haemophilus influenzae* type b (Hib) meningitis and emergence of serotype replacement with type a strains after introduction of Hib immunization in Brazil. *J Infect Dis* 187: 109–116.

Rijnaarts HH, Norde W, *et al*. (1999). DLVO and steric contributions to bacterial deposition in media of different ionic strengths. *Colloid Surface B* 14(1): 179-195.

Romao S, Memmi G, *et al* (2006) LuxS impacts on LytA-dependent autolysis and on competence in *Streptococcus pneumoniae*. *Microbiol* 152: 333–341.

Rosenberg M. (2006). Microbial adhesion to hydrocarbons: twenty-five years of doing MATH. *FEMS Microbiology Lett* 262(2): 129-134.

Rothfork JM, Timmins GS, *et al*. (2004). Inactivation of a bacterial virulence pheromone by phagocyte-derived oxidants: new role for the NADPH oxidase in host defense. *Proc Natl Acad Sci* 101(38): 13867-13872.

Rovers MM, Glasziou P, Appelman CL *et al*. (2006) Antibiotics for acute otitis media: a meta-analysis with individual patient data. *Lancet* 368: 1429–1435.

Rumbo-Feal S, Gómez MJ, *et al*. (2013). Whole transcriptome analysis of *Acinetobacter baumannii* assessed by RNA-sequencing reveals different mRNA expression profiles in biofilm compared to planktonic cells. *PLoS ONE* 8(8): e72968.

Safadi R A, Abu-Ali GS, *et al*. (2012). Correlation between in vivo biofilm formation and virulence gene expression in *Escherichia coli* O104:H4. *PLoS ONE* 7(7): e41628.

Sanchez CJ, Kumar N, Lizcano A, *et al*. (2011). *Streptococcus pneumoniae* in biofilms are unable to cause invasive disease due to altered virulence determinant production. *PLoS One* 6: e28738.

Sanderson AR, Leid JG, *et al*. (2006). Bacterial biofilms on the sinus mucosa of human subjects with chronic rhinosinusitis. *Laryngoscope* 116(7): 1121-1126.

Sandrini S, Alghofaili F, *et al*. (2014). Host stress hormone norepinephrine stimulates pneumococcal growth, biofilm formation and virulence gene expression. *BMC Microbiol* 14(1): 180.

.

Sauer K. (2003). The genomics and proteomics of biofilm formation. *Genome Biol* 4(6): 219.

Sauer K and Camper AK. (2001). Characterization of phenotypic changes in *Pseudomonas putida* in response to surface-associated growth. *J Bacteriol* 183: 6579–6589.

Sauer K, Camper AK, *et al*. (2002) *Pseudomonas aeruginosa* displays multiple phenotypes during development as a biofilm. *J Bacteriol* 184: 1140–1154.

Schaffner TO, Hinds J, *et al*. (2014). A point mutation in *cpsE* renders *Streptococcus pneumoniae* nonencapsulated and enhances its growth, adherence and competence. *BMC Microbiol* 14(1): 210.

Schembri MA, Kjærgaard K and Klemm P. (2003). Global gene expression in *Escherichia coli* biofilms. *Mol Microbiol* 48: 253–267.

Schembri MA, Givskov M, *et al*. (2002). An attractive surface: gram-negative bacterial biofilms. *Sci STKE* 132: RE6.

Scott DR, Weeks D, *et al*. (1998). The role of internal urease in acid resistance of Helicobacter pylori. *Gastroenterology* 114(1): 58-70.

Segal N, Leibovitz E, *et al*. (2005). Acute otitis media-diagnosis and treatment in the era of antibiotic resistant organisms: updated clinical practice guidelines. *Int J Pediatr Otorhinolaryngol* 69: 1311–1319.

Selinger DW, Saxena RM, *et al*. (2003). Global RNA half-life analysis in *Escherichia coli* reveals positional patterns of transcript degradation. *Genome Res* 13(2): 216-223.

Shakhnovich EA, King SJ, *et al*. (2002). Neuraminidase expressed by *Streptococcus pneumoniae* desialylates the lipopolysaccharide of *Neisseria meningitidis* and *Haemophilus influenzae*: a paradigm for interbacterial competition among pathogens of the human respiratory tract. *Infect and Immun* 70(12): 7161-7164.

Shapiro ED, Berg AT, Austrian R *et al*. (1991). The protective efficacy of polyvalent pneumococcal polysaccharide vaccine. *N Engl J Med* 325: 1453–1460.

Shivshankar P, Sanchez C, *et al*. (2009). The *Streptococcus pneumoniae* adhesin PsrP binds to keratin 10 on lung cells. *Mol Microbiol* 73: 663–679.

Shriberg LD, Friel-Patti S, *et al* (2000) Otitis media, fluctuant hearing loss, and speech-language outcomes: a preliminary structural equation model. *J Speech Lang Hear Res* 43: 100–120.

Smith HK, Nelson KL, *et al*. (2013). Effect of anaerobiosis on the antibiotic susceptibility of *H. influenzae*. *BMC Res Notes* 6(1): 241.

Spellerberg B, Cundell DR, *et al*. (1996). Pyruvate oxidase, as a determinant of virulence in *Streptococcus pneumoniae*. *Mol Microbiol* 19: 803–813.

Spinola SM, Peacock J, *et al*. (1986). Epidemiology of colonization by nontypable *Haemophilus influenzae* in children: a longitudinal study. *J Infect Dis* 154: 100–109

Steinmoen H, Knutsen E, *et al*. (2002). Induction of natural competence in *Streptococcus pneumoniae* triggers lysis and DNA release from a subfraction of the cell population. *Proc Natl Acad Sci* 99(11): 7681-7686.

Stenström C, Bylander-Groth A and Ingvarsson L. (1991). Eustachian tube function in otitis-prone and healthy children. *Int J Pediatr Otorhinolaryngol* 21: 127–138.

Stewart, P. S. and M. J. Franklin (2008). Physiological heterogeneity in biofilms. *Nat Rev Micro* 6(3): 199-210.

Stingl K, Altendorf K and Bakker EP. (2002). Acid survival of *Helicobacter pylori*: how does urease activity trigger cytoplasmic pH homeostasis? *Trends Microbiol* 10: 70–74.

Sutherland IW. (2001). The biofilm matrix – an immobilized but dynamic microbial environment. *Trends Microbiol* 9: 222–227.

Sweeney NJ, Klemm P, *et al*. (1996). The *Escherichia coli* K-12 *gntP* gene allows *E. coli* F-18 to occupy a distinct nutritional niche in the streptomycin-treated mouse large intestine. *Infect Immun* 64(9): 3497-3503.

Sweeney NJ, Laux DC, *et al*. (1996). *Escherichia coli* F-18 and *E. coli* K-12 *eda* mutants do not colonize the streptomycin-treated mouse large intestine. *Infect Immun* 64(9): 3504-3511.

Swords WE, Moore ML, *et al*. (2004). Sialylation of lipooligosaccharides promotes biofilm formation by nontypeable *Haemophilus influenzae*. *Infect Immun* 72: 106–113.

Swords WE, Buscher BA, *et al*. (2000). Non-typeable *Haemophilus influenzae* adhere to and invade human bronchial epithelial cells via an interaction of lipooligosaccharide with the PAF receptor. *Mol Microbiol* 37(1): 13-27.

Szelestey BR, Heimlich DR, *et al.* (2013). *Haemophilus* responses to nutritional immunity: epigenetic and morphological contribution to biofilm architecture, invasion, persistence and disease severity. *PLoS Pathog* 9: e1003709.

Taira M, Sasaki M, *et al*. (2008). Dose-dependent effects of Ni (II) ions on production of three inflammatory cytokines (TNF-α, IL-1β and IL-6), superoxide dismutase (SOD) and free radical NO by murine macrophage-like RAW264 cells with or without LPS-stimulation. *J Mater Sci: Mater Med* 19(5): 2173-2178.

Tashiro Y, Ichikawa S, *et al*. (2010). Variation of physiochemical properties and cell association activity of membrane vesicles with growth phase in *Pseudomonas aeruginosa*. *Appl Environ Microbiol* 76(11): 3732-3739.

Teele DW, Klein JO, *et al*. (1989). Epidemiology of otitis media during the first seven years of life in children in greater Boston: a prospective, cohort study. *J Infect Dis* 160: 83–94.

Thornton R, Rigby P, *et al*. (2011). Multi-species bacterial biofilm and intracellular infection in otitis media. *BMC Pediatr*11: 94.

Tikhomirova A, Trappetti C, *et al*. (2015). The outcome of *H. influenzae* and *S. pneumoniae* inter-species interactions depends on pH, nutrient availability and growth phase. *Int J Med Microbiol.*

Tikhomirova A, Jiang D, *et al*. (2015). A new insight into the role of intracellular nickel levels for the stress response, surface properties and twitching motility by *Haemophilus influenzae*. *Metallomics* 7(4): 650-661.

Tikhomirova A and Kidd SP. (2013). *Haemophilus influenzae* and *Streptococcus pneumoniae*: living together in a biofilm. *Pathog Dis* 69(2): 114-126.

Trappetti C, Potter AJ, *et al*. (2011). LuxS mediates iron-dependent biofilm formation, competence, and fratricide in *Streptococcus pneumoniae*. *Infect Immun* 79: 4550–4558.

Tseng BS, Zhang W, *et al*. (2013). The extracellular matrix protects *Pseudomonas aeruginosa* biofilms by limiting the penetration of tobramycin. *Environ Microbiol* 15(10): 2865-2878.

Ünal CM, Singh B, *et al*. (2012). QseC controls biofilm formation of non-typeable *Haemophilus influenzae* in addition to an AI-2-dependent mechanism. *Int J Med Microbiol* 302: 261–269.

Urwin G, Krohn JA, *et al.* (1996). Invasive disease due to *Haemophilus influenzae*serotype f: clinical and epidemiologic characteristics in the *H. influenzae* serotype b vaccine era. *Clin Infect Dis* 22: 1069–1076.

Utz CB, Nguyen AB, *et al*. (2004). GntP is the *Escherichia coli* fructuronic acid transporter and belongs to the UxuR regulon. *J Bacteriol* 186(22): 7690-7696.

Van der Linden M, Winkel N, *et al*. (2013). Epidemiology of *Streptococcus pneumoniae* serogroup 6 isolates from IPD in children and adults in Germany. *PLoS One* 8: e60848.

Van Melderen L and Saavedra De Bast M. (2009). Bacterial toxin-antitoxin systems: more than selfish entities. *PLoS Genet* 5(3): e1000437.

Van Merode AE, van der Mei HC, *et al*. (2006). Influence of culture heterogeneity in cell surface charge on adhesion and biofilm formation by *Enterococcus faecalis*. *J Bacteriol* 188(7): 2421-2426.

Van Schaik EJ, Giltner CL, *et al*. (2005). DNA binding: a novel function of *Pseudomonas aeruginosa* type IV pili. *J Bacteriol* 187(4): 1455-1464.

Verhaegh SJC, Flores AR, *et al*. (2013). Differential virulence gene expression of group A *Streptococcus* serotype M3 in response to co-culture with *Moraxella catarrhalis*. *PLoS ONE* 8(4): e62549.

Vidal JE, Ludewick HP, *et al*. (2011). The LuxS-dependent quorum-sensing system regulates early biofilm formation by *Streptococcus pneumoniae* strain D39. *Infect Immun* 79: 4050–4060.

Vidal JE, Howery KE, *et al*. (2013). Quorum-sensing systems LuxS/Autoinducer 2 and Com regulate *Streptococcus pneumoniae* biofilms in a bioreactor with living cultures of human respiratory cells. *Infect Immun* 81: 1341–1353.

Vogel AR, Szelestey BR, *et al*. (2012). SapF-mediated heme-iron utilization enhances persistence and coordinates biofilm architecture of *Haemophilus*. *Front Cell Infect Microbiol* 2: 42.

Voulgaridou GP, Anestopoulos I, *et al*. (2011). DNA damage induced by endogenous aldehydes: current state of knowledge. *Mut Res/Fund Mol M* 711(1–2): 13-27.

Waggoner-Fountain LA, Hendley JO, *et al*. (1995). The emergence of *Haemophilus influenzae* types e and f as significant pathogens. *Clin Infect Dis* 21(5): 1322-1324.

Waite RD, Papakonstantinopoulou A, *et al*. (2005). Transcriptome analysis of *Pseudomonas aeruginosa* growth: comparison of gene expression in planktonic cultures and developing and mature biofilms. *J Bacteriol* 187(18): 6571-6576.

Waite RD, Struthers JK, *et al*. (2001). Spontaneous sequence duplication within an open reading frame of the pneumococcal type 3 capsule locus causes high-frequency phase variation. *Mol Microbiol* 42(5): 1223-1232.

Walters M, Sircili MP and Sperandio V. (2006). AI-3 synthesis is not dependent on *lux*S in *Escherichia coli*. *J Bacteriol* 188: 5668–5681.

Wang X and Wood TK. (2011). Toxin-antitoxin systems influence biofilm and persister cell formation and the general stress response. *Appl Environ Microbiol* 77(16): 5577-5583.

Wang H, Ayala JC, *et al*. (2014). The LuxR-type regulator VpsT negatively controls the transcription of *rpoS*, encoding the general stress response regulator, in *Vibrio cholerae* biofilms. *J Bacteriol* 196(5): 1020-1030.

Wang IN, Smith DL, *et al*. (2000). Holins: the protein clocks of bacteriophage infections. *Annu Rev Microbiol* 54(1): 799-825.

Webb DC and Cripps AW. (1998). Secondary structure and molecular analysis of interstrain variability in the P5 outer-membrane protein of non-typable *Haemophilus influenzae* isolated from diverse anatomical sites. *J Med Microbiol* 47: 1059–1067.

Webster P, Wu S, *et al*. (2006) Distribution of bacterial proteins in biofilms formed by non-typeable *Haemophilus influenzae*. *J Histochem Cytochem* 54: 829–842.

Weimer KE, Armbruster CE, *et al*. (2010). Coinfection with *Haemophilus influenzae* promotes pneumococcal biofilm formation during experimental otitis media and impedes the progression of pneumococcal disease. *J Infect Dis* 202(7): 1068-1075.

Weimer KED, Juneau RA, *et al*. (2011). Divergent mechanisms for passive Pneumococcal resistance to β-Lactam antibiotics in the presence of *Haemophilus influenzae*. *J Infect Dis* 203(4): 549-555.

Weiser JN, Shchepetov M and Chong ST. (1997). Decoration of lipopolysaccharide with phosphorylcholine: a phase-variable characteristic of *Haemophilus influenzae*. *Infect Immun* 65: 943–950.

Weiss K, Low DE, *et al*. (2004). Clinical characteristics at initial presentation and impact of dual therapy on the outcome of bacteremic *Streptococcus pneumoniae* pneumonia in adults. *Can Respir J* 11: 589–593.

West-Barnette S, Rockel A and Swords WE. (2006). Biofilm growth increases phosphorylcholine content and decreases potency of nontypeable *Haemophilus influenzae* endotoxins. *Infect Immun* 74: 1828–1836.

Wezyk M and Makowski A. (2000). pH of fluid collected from middle ear in the course of otitis media in children. *Otolaryngol Pol.* 54(2): 131.

Williams CJ and Jacobs AM. (2009). The impact of otitis media on cognitive and educational outcomes. *Med J Aust* 191: S69–S72.

Williams RL, Chalmers TC, *et al*. (1993). Use of antibiotics in preventing recurrent acute otitis media and in treating otitis media with effusion: a meta-analytic attempt to resolve the brouhaha. *JAMA* 270(11): 1344-1351.

Wu S, Baum MM, *et al*. (2014). Biofilm-specific extracellular matrix proteins of nontypeable *Haemophilus influenzae*. *Pathog Dis* 72(3): 143-160.

Wu S, Li X, *et al*. (2014). Beta- lactam antibiotics stimulate biofilm formation in non-typeable *Haemophilus influenzae* by up-regulating carbohydrate metabolism. *PLoS ONE* 9(7): e99204.

Wu Y, Vulić M, *et al*. (2012). Role of oxidative stress in persister tolerance. *Antimicrob Agents Chemother* 56(9): 4922-4926.

Yoshida A, Ansai T, Takehara T & Kuramitsu HK. (2005). LuxS-based signaling affects *Streptococcus mutans* biofilm formation. *Appl Environ Microbiol* 71: 2372–2380.

Young R, Wang IN, *et al*. (2000). Phages will out: strategies of host cell lysis. *Trends Microbiol* 8(3): 120-128.

Young GM, Amid D, *et al*. (1996). A bifunctional urease enhances survival of pathogenic Yersinia enterocolitica and Morganella morganii at low pH. *J Bacteriol* 178(22): 6487-6495.

Yousefi S, Mihalache C, *et al*. (2009). Viable neutrophils release mitochondrial DNA to form neutrophil extracellular traps. *Cell Death Differ* 16: 1438–1444.

Zhang JR, Idanpaan-Heikkila I, *et al*. (1999). Pneumococcal *lic*D2 gene is involved in phosphorylcholine metabolism. *Mol Microbiol* 31: 1477–1488.

Zhang L, Patel M, *et al*. (2013). Urease operon and urease activity in commensal and disease-causing nontypeable *Haemophilus influenzae*. *J Clin Microbiol* 51: 653–655.

Zhang Y, Yew WW, *et al*. (2012). Targeting Persisters for Tuberculosis Control. *Antimicrob Agents Chemother* 56(5): 2223-2230.